



UNIVERSITY
of
GREENWICH

Greenwich Academic Literature Archive (GALA)
– the University of Greenwich open access repository
<http://gala.gre.ac.uk>

Citation:

[Balasubramaniam, Anuluxshy \(2012\) Root adaptive responses of tall fescue \(*Festuca arundinacea*\) growing in sand treated with petroleum hydrocarbon contamination. PhD thesis, University of Greenwich.](#)

Please note that the full text version provided on GALA is the final published version awarded by the university. “I certify that this work has not been accepted in substance for any degree, and is not concurrently being submitted for any degree other than that of (name of research degree) being studied at the University of Greenwich. I also declare that this work is the result of my own investigations except where otherwise identified by references and that I have not plagiarised the work of others”.

*Balasubramaniam, Anuluxshy (2012) Root adaptive responses of tall fescue (*Festuca arundinacea*) growing in sand treated with petroleum hydrocarbon contamination. ##thesis type##, ##institution##*

Available at: <http://gala.gre.ac.uk/9147/>

Contact: gala@gre.ac.uk

**Root adaptive responses of tall fescue (*Festuca arundinacea*)
growing in sand treated with petroleum hydrocarbon
contamination**

By

Anuluxshy Balasubramaniyam (B.Sc., M.Sc.)

**A thesis submitted to the University of Greenwich in partial
fulfilment of the requirements for the degree of Doctor of
Philosophy**

March 2012

School of Science

University of Greenwich, Medway Campus

Chatham Maritime

Kent, ME4 4TB, UK



the
UNIVERSITY
of
GREENWICH

DECLARATION

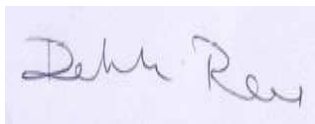
I certify that this work has not been accepted in substance for any degree, and is not concurrently being submitted for any degree other than that of Doctor of Philosophy (PhD) being studied at the University of Greenwich. I also declare that this work is the result of my own investigations except where otherwise identified by references and that I have not plagiarised the work of others.

(Ms Anuluxshy Balasubramaniam) (Candidate)

Ph.D. Supervisors



(Professor Patricia J. Harvey) (1st supervisor)



(Dr. Debbie Rees) (2nd supervisor)

18.06.2012

DEDICATION

This thesis is dedicated to the loving memory of my grandparents Mr. & Mrs. S. Thinagaranpillai, whose love and guidance I still feel surrounded by, and whose upbringing gave me wonderful childhood memories.

ACKNOWLEDGEMENTS

First of all, I would like to acknowledge the excellent guidance and support given by my first supervisor Professor Patricia J. Harvey. I would like to thank her for giving me the drive to conduct my research to the best of my ability, too. Thanks, Pat. Secondly, I would like to acknowledge the excellent support and guidance received from my second supervisor Dr. Debbie Rees. I would like to express my warmest thanks to Dr. Mark M. Chapman I feel privileged being closely and gently guided by for the past three years and who has brought a note of joy into my research. Thanks also to Dr. John E. Orchard for his occasional, yet really good advice and help. A particular appreciation is felt for Dr. Puy Robello and Dr. Christian E. Scheer who helped me through my first steps into this research journey. I appreciate very much the excellent guidance given by Professor Anthony I. Mallet on mass spectrometry. I would like to thank Professor Francis S. Pullen for his great guidance and help regarding my metabolomic work. I would like to thank Dr. Kai Law for his help with GC-MS method development. An appreciation is felt for Dr. Richard Blackburn and Dr. Ian Slipper for their great guidance on scanning electron microscopy. I would like to acknowledge the excellent guidance and help given by Dr. Stephen Young on my statistical interpretation. I am grateful to Mrs. Atiya Raza, Mrs. Deviyani Amin, Mr. Steven Williams, Mr. Dudley I. Farman, Mrs. Natalie Morley, Mr. Cristian Laphorn, Miss. Rachel Nice, Dr. Florence Lowry and my colleague Mr. Aminu Abubakar for their excellent practical help and support. I would like to acknowledge the helpful advice and support given by Professor Babur Chowdhry and Mrs. Julie C. Boyer. I would like to acknowledge the helpful editorial suggestions provided by my PhD examiners, Professor Philip C. Stevenson and Dr. Chris D. Collins. I am also grateful to my family and friends for supporting and encouraging me through tough, challenging as well as good times.

ABSTRACT

Root adaptive responses of tall fescue (*Festuca arundinacea*) growing in sand treated with petroleum hydrocarbon contamination

Phytoremediation is a green technique used to restore polluted sites through plant-initiated biochemical processes. Its effectiveness, however, depends on the successful establishment of plants in the contaminated soil. Soils that are contaminated with polycyclic aromatic hydrocarbons (PAHs), especially low molecular weight, mobile PAHs such as naphthalene pose a significant challenge to this. Plant roots growing in these soils exhibit changes to their structure, physiology and growth patterns.

Tall fescue (*Festuca arundinacea*) roots grown in sand contaminated with either petroleum crude oil (10.8g total extractable hydrocarbons kg⁻¹ sand dw) or naphthalene (0.8g kg⁻¹ sand dw) exhibited a temporary inhibition in elongation with accelerated lateral growth ($p < 0.01$), whilst also showing a deviation from the normal root orientation responses to gravity. Scanning electron micrographs (SEM) revealed that the stele in the contaminated roots was located much further away from the root epidermis, because the cortex was larger ($p < 0.001$) due to the cells being more isodiametric in shape. Once past the initial acclimatisation period of 2.5-3.0 months, no visual differences were observed between control and treated plants, but the root ultrastructural modifications persisted.

The fluorescent hydrophobic probe 'Nile red' was applied to the epidermis of a living root to mimic and visualise the uptake of naphthalene into the root through the transpiration stream. The root sections were also stained with 0.1% (w/v) berberine hemisulphate in order to stain Casparian bands. Overlaying images obtained with the use of Texas red HYQ filter (wavelength 589-615nm) and UV illumination (wavelength 345-458nm) revealed the presence of passage cells in the endodermis and uptake of Nile red into protoxylem vessels beyond the endodermis of control roots. On the other hand, the path of Nile red was blocked at the endodermis of naphthalene- treated roots. The cell walls in the endodermis of naphthalene-treated roots were prominently thickened ($p < 0.001$) and lacked passage cells. The treated roots also possessed a well-formed exodermis ($p < 0.01$). The results suggest that the

well-formed endodermis lacking passage cells, the well-formed exodermis as well as the increased cortex zone provided an effective barrier to the flux of hydrophobic xenobiotics towards the inner core of the roots, if previously exposed to the contaminants.

The SEM images of naphthalene-treated as well as crude oil-treated roots showed partial collapse in the cortex zone, presumably due to water stress, but the treated plants withstood drought stress better than the control plants.

The underlying physiological changes responsible for the adaptive responses of tall fescue to the exposure to naphthalene contamination were studied through metabolic profiling of plant roots and shoots. The results indicated synergistic interactions between sugars or sugar- like compounds and phenolic compounds may assist to create an integrated redox system and contribute to stress tolerance in naphthalene-treated tall fescue. The signal for a compound speculated to be indole acetic acid (IAA) was either subdued or absent in the tissues of naphthalene-treated tall fescue, suggesting the existence of a detoxification mechanism/ defence pathway in the treated plants. The ultra-structural and molecular modifications, resulting from PAH stress enabled tall fescue to resist tougher challenges.

Anuluxshy Balasubramaniam [B.Sc., M.Sc.]

TABLE OF CONTENTS

TITLE PAGE..	i
DECLARATION.....	ii
DEDICATION.....	iii
ACKNOWLEDGMENTS.....	iv
ABSTRACT.....	v
TABLE OF CONTENTS.....	vii
LIST OF FIGURES.....	xv
LIST OF TABLES.....	xxiii
LIST OF ABBREVIATIONS.....	xxvi

Chapter 1: Introduction: Impacts of petroleum hydrocarbon-contamination on plants used in phytoremediation.....1

1.1: Petroleum hydrocarbon contamination in our environment and the importance of remediation.....	1
1.2 Uptake of organic pollutants by plants	6
1.2 a. Abiotic factors.....	6
Properties of the organic pollutant.....	6
Soil composition.....	6
1.2 b. Biotic factors: Roots.....	9
1.2 b1.Root systems.....	11
1.2 b2.Root growth and root structures.....	14
The effect of transpiration on transport of organic contaminants from soil pore water across the root.....	24
The effect of root lipids content on root uptake of petroleum hydrocarbons....	27
The effect of enzyme complements on catabolism of hydrocarbons within the root tissues.....	33
Root Exudates.....	38
Growth dilution due to phytostimulation or rhizo-biodegradation.....	40
1.3 Influence of plants in restoring soils contaminated with petroleum hydrocarbons.....	45

1.4 Contaminant exposure pathways and entry of contaminants into wildlife food chain.....	46
1.5 Impacts of petroleum hydrocarbon contamination on plants.....	46
1.6 Summary.....	55
1.7 Research questions.....	56
1.8 Project lay-out.....	57
Chapter 2: Materials and Methods.....	59
2.1 Introduction.....	59
2.2 Soil water.....	59
2.2.1 Determination of soil water-holding capacity.....	59
2.2.2 Determination of soil moisture content.....	60
2.2.3 Determination of soil water potential.....	60
2.3 Preparing treatment soil for contaminated treatments.....	61
2.3.1 Spiking soils with polycyclic aromatic hydrocarbons (PAHs).....	61
2.3.2 Mixing clean sand with petroleum crude oil-contaminated sand.....	62
2.4 Setting up rhizo-boxes.....	63
2.5 Seeding.....	64
2.6 Experimental designs, plant material and growth conditions.....	64
2.6.1 Experimental designs, plant material and growth conditions used in chapter 3.....	64
2.6.2 Experimental designs, plant material and growth conditions used in chapter 4.....	66
2.6.3 Experimental designs, plant material and growth conditions used in chapter 5.....	67
2.7 Recording root shoot development and root hair analysis.....	67
2.8 Root shoots biomass analysis.....	68
2.9 Scanning Electron Microscopy (SEM).....	68
2.9.1 Preparation of fixatives.....	68
2.9.2 Fixation steps.....	69

2.9.3 Dehydration steps.....	69
2.9.4 Mounting and viewing root sections with a scanning electron microscope (SEM).....	70
2.10 Epi-fluorescence Microscopy	71
2.10.1 Procedure for staining Casparian band structures for epi-fluorescence microscopy.....	71
2.10.2 Microscopic settings and obtaining images of roots stained with berberine hemisulphate.....	71
2.10.3 Nile red stain preparation.....	71
2.10.4 Procedure for staining vital roots with Nile red	72
2.10.5 Root preparation and fixing.....	72
2.10.6 Sectioning the roots.....	72
2.10.7 Microscopic settings and obtaining images of roots stained with Nile red	73
2.10.8 Overlaying images using microscopic imaging software.....	73
2.11 Gas chromatography-mass spectrometry (GC-MS)	73
2.11.1 Sampling.....	73
2.11.2 Sample preparation.....	74
2.11.3 Extraction and derivatization.....	74
2.11.4 Gas chromatography- mass spectrometry (GC-MS) analysis.....	76
2.11.5 Data analysis.....	76
2.12 Quantification of naphthalene in root shoot tissues of tall fescue using gas chromatography-flame ionisation detection (GC-FID) technique.....	77
2.12.1 Sampling.....	77
2.12.2 Sample preparation.....	77
2.12.3 Extraction and analysis.....	77
2.13 Statistical analysis.....	78
2.14 Quality assurance and control.....	78
2.14.1 Introduction.....	78
2.14.2 Labelling systems.....	78

2.14.3 Calibration and controlling parameters.....	78
2.13.4 Homogenization.....	78
2.13.5 Replication.....	79
Chapter 3: Changes in root growth patterns and root ultra-structure arising from growth in sand contaminated with petroleum crude oil.....	80
3.1 Introduction.....	80
3.2 Results.....	81
a. Sensitivity of three different plant species that possess tap root system (parsnip, carrot and beetroot) to the exposure to crude oil contamination.....	81
b. Deviations in growth patterns of a grass mixture that possesses fibrous root system due to the exposure to crude oil contamination.....	86
b1. Differences in growth patterns of tall fescue (<i>Festuca arundinacea</i>) arising from growth in crude oil-treated sand.....	88
b1-1. Growth differences when exposed to a higher concentration of contaminants [16.5 g total extractable hydrocarbons kg ⁻¹ sand (dw)] and periodical monitoring of root shoot elongation.....	88
b1-2. Growth differences when exposed to a lower concentration of contaminants [10.8 g total extractable hydrocarbons kg ⁻¹ sand (dw)].....	90
b2. Differences in growth patterns of brown top bent (<i>Agrostis capillaries</i> L.) arising from growth in crude oil-treated sand.....	92
c. Root ultrastructural differences arising from growth in crude oil-treated sand (10.8 g total extractable hydrocarbons kg ⁻¹ sand dw).....	94
c1. Ultrastructural modifications illustrated by beetroot (<i>Beta vulgaris</i>) roots.....	95
c2. Ultrastructural modifications illustrated by tall fescue (<i>Festuca arundinacea</i>) roots.....	95
d. A biphasic dose response illustrated by crude oil-treated tall fescue (<i>Festuca arundinacea</i>) to enhanced drought conditions.....	99
3.3 Discussion.....	99
Chapter 4: Responses of tall fescue (<i>Festuca arundinacea</i>) to growth in naphthalene-contaminated sand: xenobiotic stress versus water stress.....	106
4.1 Introduction.....	106

4.2 Materials and Methods.....	110
4.2.1 Spiking sand with polycyclic aromatic hydrocarbons (PAHs).....	110
4.2.2 An initial gradient rhizo-box experiment to examine the effect of naphthalene, fluoranthene, and benzo (a) pyrene [B(a)P] on seed germination and plant development.....	111
4.2.3 Experimental protocol to test the effect of exposure to anthracene at the concentration of 1000mg kg ⁻¹ sand dw on seed germination and plant development.....	112
4.2.4 Experimental protocol to test the effect of exposure to naphthalene at the concentration of 800mg kg ⁻¹ sand dw on tall fescue: Seed germination in rockwool cubes.....	112
4.2.5 Experimental protocol to test the impacts of naphthalene contamination on seed germination and plant growth patterns: Direct sowing in sand medium.....	112
4.2.6 Watering and nutrition.....	113
4.2.7 Determination of water potential of naphthalene-treated and clean sand.....	113
4.2.8 Determination of soil moisture content of naphthalene-treated and clean sand.....	114
4.2.10 Scanning Electron Microscopy (SEM).....	115
4.2.11 Epi-fluorescent microscopy.....	115
4.2.11a. Staining Casparian band structures.....	115
4.2.11b. Nile red as a tool to probe the uptake of hydrophobic xenobiotics from soil into roots.....	116
4.2.11c. Further staining with berberine hemisulphate and overlaying images using microscopic imaging software.....	118
4.2.12 Statistical analysis.....	118
4.3 Results.....	110
a. Impacts of exposure to polycyclic aromatic hydrocarbons (PAHs) on plants: A preliminary investigation.....	119
a1. The effect of naphthalene, fluoranthene, and benzo (a) pyrene [B(a)P] on seed germination and plant development: An initial gradient rhizo-box experiment.....	119
a2. Effect of exposure to anthracene at the concentration of 1000mg kg ⁻¹ sand dw on seed germination and plant development.....	119
a2-1. Effect of exposure to anthracene on tall fescue.....	119

a2-2. Effect of exposure to anthracene on brown top bent	122
a3. Effect of exposure to naphthalene at the concentration of 800mg kg ⁻¹ sand dw on tall fescue: Seed germination in rockwool cubes.....	122
b. Impacts of naphthalene contamination on seed germination, plant growth patterns and the abundance of Casparian strip.....	124
b1. Effect of naphthalene contamination on the germination of tall fescue seeds.....	124
b2. Effect of naphthalene contamination on the initial root growth of tall fescue.....	124
b3. Differences in root growth patterns during the acclimatisation period due to exposure to naphthalene contamination.....	125
b4. Effect of growth in naphthalene-contaminated sand on biomass and moisture content of plant tissues during the acclimatisation period.....	127
b5. Root growth patterns and root ultrastructural modifications of naphthalene-treated tall fescue beyond the acclimatisation period of 3 months: Major emphasis on Casparian strip.....	129
c. Effect of growth in naphthalene- contaminated sand on plants' resilience to drought.....	132
c1. Differences in the onset of wilting.....	132
c2. Examination of root ultrastructural features of tall fescue exposed to water stress for 4 days: A short exposure to drought.....	133
c3. Examinations of root shoot growth parameters of tall fescue exposed to severe water stress.....	134
c4. Examination of root ultrastructural features of tall fescue exposed to severe water stress: A long exposure to drought.....	135
d. Soil-water relations.....	137
d1. The effect of naphthalene on the water status of the treated sand.....	137
e. Resistances to the uptake of hydrophobic xenobiotic solutes across the root tissues of tall fescue grown in naphthalene-treated sand: Nile red as a hydrophobic molecular probe.....	142
e1. Nile red as a tool to probe the uptake of hydrophobic organic xenobiotics from soil into roots: Result of the preliminary investigation.....	142

e2. Uptake of xenobiotic solutes into protoxylem vessels exemplified by the path of Nile red.....	145
4.4 Discussion.....	150
4.5 Conclusions.....	161
References.....	162
Chapter 5: Differences in hydrophilic metabolome of tall fescue (<i>Festuca arundinacea</i>), grown in naphthalene-treated sand reflects plant adaptive responses to stress: a gas chromatography-mass spectrometric study.....	166
5.1 Introduction.....	166
5.2 Materials and Methods.....	167
5.2.1 Plant materials and growth conditions.....	167
5.2.2 Sampling.....	167
5.2.3 Sample preparation.....	167
5.2.4 Extraction and derivatization.....	167
5.2.5 Gas chromatography- mass spectrometry (GC-MS) analysis.....	168
5.2.6 Selection criteria for the identification of compounds.....	169
5.2.7 Data analysis.....	170
5.2.8 Statistical analysis.....	170
5.3 Results.....	170
5.3.1 Identification of compounds.....	170
5.3.2 Differential abundances of polar compounds in the leaves and roots of tall fescue grown in naphthalene-contaminated sand in comparison to the controls.....	180
5.4 Discussion.....	188
5.5 Conclusions.....	196
References.....	197
Chapter 6: Discussion.....	200
Research implications.....	220
Further work recommendations.....	221

References.....	222
Appendix 1: Spectrum interpretation and identification of compounds.....	241
Appendix 2: Entry of Xenobiotics into xylem vessels of plant roots exemplified by Nile red penetration.....	252
Appendix 3: Quantification of naphthalene in the root, shoot tissues of tall fescue (Festuca arundinacea) grown in naphthalene-treated sand (0.8g kg⁻¹ sand dw) for 6 months using GC-FID technique.....	254

LIST OF FIGURES

Chapter 1

Fig.1.1: Relationship between the octanol: water partition coefficient ($\log K_{OW}$) and uptake of organic compounds by roots cultivated in hydroponic conditions (Adapted from Briggs et al., 1983).....	7
Fig.1.2: Influence of the weight fraction of organic carbon (F_{OC}) in soil on uptake of organic compounds by roots cultivated in soil (Adapted from Ryan et al., 1988).....	8
Fig.1.3: Schematic diagram of the primary root system showing acropetal branching (Adapted from Pages et al., 2000).....	12
Fig 1.4: Schematic diagram of the adventitious root system.....	13
Fig. 1.5: a: Scanning electron micrograph of tall fescue root (<i>Festuca arundinacea</i>) showing root cap. b: Epi-fluorescent micrograph of tall fescue root stained with Nile red (a lipid fluorescent stain) and viewed through Texas red HYQ filter and UV illumination (images were overlaid using microscopic imaging software), showing root cap as well as root hairs. c: Schematic diagram for a longitudinal view of a growing root, illustrating different growth zones and root structures (Adapted from Wild et al., 2005). d: Schematic diagram for a cross sectional view of a growing root sectioned through root hair zone, illustrating different root structures. e: Schematic diagram for part of a cross sectional view of a root sectioned through root hair zone (Adapted from Brundrett, 2008, 1999).....	16
Figure 1.6: Structure of the plant cuticle. (a) Diagrammatic structure of epidermis and cuticle. (b) Ultrastructure of the cuticle of the leaf epidermis of <i>Arabidopsis</i> plants (presented directly as in Molina, 2010).....	17
Fig. 1.7: A hypothetical arrangement of monomers that could be found in a ω -hydroxy fatty acid-rich cutin. R: aliphatic polyester (Presented directly as in Molina, 2010).....	18
Fig.1.8: Lignin structure.....	21
Fig.1.9: A diagram showing apoplastic and symplastic flow of water and solutes through adjacent cells (Adapted from: Brett and Waldron, 1996).....	25
Fig. 1.10: Partial cross sections showing, A (above): a root with a mature endodermis and immature or absent exodermis; D (below): a root with mature endodermis and exodermis, illustrating the movement of apoplastic ions (red) within roots (After Enstone et al., 2003).....	26
Fig. 1.11: Structure of Nile red.....	26
Fig. 1.12: Chicory root cells (a1)-Bright field and (a2)- fluorescence using standard DAPI filter set. No fluorescence was detected in lipid bodies of the control in comparison to cultures grown in the presence of PAH (Directly presented as in Verdin et al., 2006).....	28
Fig. 1.13: Root concentrations of phenanthrene (dw) for plants growing in spiked soils (soil pH 5.05, organic matter 1.45%) with initial phenanthrene concentration of 133mg kg^{-1} , after 45 days of exposure to the PAH (Adapted from: Gao et al., 2004).....	30
Fig.1.14: Root concentrations of pyrene (dw) for plants growing in spiked soils (soil pH 5.05, organic matter 1.45%) with initial pyrene concentration of 172mg kg^{-1} , after 45 days of exposure to the PAH (Adapted from: Gao et al., 2004).....	31
Fig.1.15: Light microscopic observations of crude oil ($16.5\text{g total extractable hydrocarbons kg}^{-1}$ sand dw)-contaminated tall fescue root fragment. Scale: $400\mu\text{m}$ (After Scheer, 2006).....	32

Fig.1.16: Laser scanning microscopic images (Z-series) of the root fragments of tall fescue grown in petroleum crude oil-contaminated sand (16.5g total extractable hydrocarbons kg⁻¹ sand dw), at the depths of
a) 0µm b) 19.2µm c) 28µm and d) 48µm (After Scheer, 2006).....32

Fig. 1.17: The pathway of oxidation of n-alkanes to primary alcohols via cytochrome P₄₅₀ system (Adapted from: Jenkins, 1992).....36

Fig. 1.18: Pathway showing subsequent oxidation of primary alcohols to the corresponding monocarboxylic acid (Adapted from: Jenkins, 1992).....36

Fig.1.19: Accumulation of anthracene into fungal hyphae (b) and fungal spore (c) of an AM fungus *Glomus caledonium* that was colonizing chicory roots grown on anthracene supplemented medium (×100 objective lens). 1. Bright field and 2. Fluorescence using standard DAPI filter set (Directly presented as in Verdin et al., 2006).....44

Fig.1.20: Principal pathways for plant uptake of PAHs (Adapted from Collins et al., 2006).....46

Fig.1.21: Two year old poplar root excavated from Heath, Ohio, phytoremediation site, showing 0.8m of root penetration, which stopped short of the smear zone (1.0m depth) (Presented directly as in Rentz et al., 2003).....48

Fig.1.22: Germination rates (%) of different grasses exposed to varying concentrations of diesel oil, measured 14 days after planting at 20^o C (Adapted from: Adam and Duncan, 1999).....52

Fig.1.23: Germination rates (%) of different herbs and legumes exposed to varying concentrations of diesel oil, measured 14 days after planting at 20^o C (Adapted from: Adam and Duncan, 1999).....53

Fig.1.24: Germination rates (%) of different commercial crops exposed to varying concentrations of diesel oil, measured 14 days after planting at 20^o C (Adapted from: Adam and Duncan, 1999).....53

Chapter 2

Fig. 2.1: Rhizo-box set up.....63

Fig.2.2: Rhizo-boxes kept at an angle of 35^o from vertical.....64

Fig. 2.3: An example of oximation (Adapted from Dettmer et al., 2007).....75

Fig. 2.4: An example of silylation (Adapted from Dettmer et al., 2007).....75

Chapter 3

Fig.3.1: Shoot development of carrot during the first 3 weeks.....82

Fig.3.2: Carrot grown in clean sand (left) and HC-contaminated sand (right) for 3 months.....82

Fig.3.3: Shoot development of beetroot during the first 3 weeks.....84

Fig. 3.4: Photograph of beetroot plants growing in HC-contaminated (left) and clean sand (right) for 2.5 months.....84

Fig.3.5: Beetroot grown in clean sand (left) and HC-contaminated sand (right) for 3 months.....85

Fig. 3.6: Root growth characteristics of a grass mixture (tall fescue, perennial ryegrass and brown top bent) grown in clean sand (a), HC-treated sand without compost addition (b) and HC-treated sand with compost addition (c) for 3 months.....87

Fig. 3.7: Tall fescue grown in clean sand (a) and HC-treated sand [16.5g total extractable hydrocarbons kg ⁻¹ sand (dw)] (b) for ~2months.....	88
Fig. 3.8: Line graph showing the shoot elongation of 3 selected plants from each different treatment.....	89
Fig.3.9: Line graph showing the root elongation of 3 selected plants from each different treatment....	89
Fig. 3.10: Bar graph showing the difference in number of root hairs as well as the number of vital root hairs per cm segment of roots of 2 months old tall fescue demonstrated by a light microscopic study.....	90
Fig. 3.11: Scanning electron micrographs of control (a) and HC-treated (b) tall fescue showing fragments of roots of 2 months old plants sectioned at one third as a fraction of root length above the root tip.....	90
Fig.3.12: Root shape of tall fescue after growing in clean (a) and HC-treated (b) sand for 14 months.....	91
Fig.3.13: Scanning electron micrographs of control (a) and HC-treated (b) tall fescue showing cross sections of roots of 14 months old plants sectioned at one third as a fraction of root length above the root tip.....	92
Fig.3.14: Brown top bent grown in clean sand (a) and HC-treated sand [16.5g total extractable hydrocarbons kg ⁻¹ sand (dw)] (b) for ~2months.....	93
Fig. 3.15: Scanning electron micrographs of roots of tall fescue (<i>Festuca arundinacea</i>) grown in clean (a) and HC-contaminated sand at the concentration of 10.8g TEH kg ⁻¹ sand dw (b), showing transversal sections, taken at one third (a) and one fourth (b) as a fraction of root length above the root tip.....	94
Fig.3.16: Scanning electron micrographs of 3 months old control (a) and HC-treated (b) beetroot showing transversal root sections at 1/3 as a fraction of root length above the root tip.....	95
Fig.3.17: Scanning electron micrographs of tall fescue roots grown in clean sand (a), HC-treated sand (b) and HC-treated sand that had compost added to it (c), for 3 months, showing transversal root sections at the position of 1/3 as a fraction of root length above the root tip.....	96
Fig. 3.18: Scanning electron micrographs of control (a) and HC-treated (b) tall fescue plants showing transversal root sections at 1/3 as a fraction of root length above the root tip. Age of plants: 6 months....	96
Fig. 3.19: Scanning electron micrographs of 14 months old control (a, b) and HC-treated (c, d) tall fescue showing cross sections of roots sectioned at one third as a fraction of root length above the root tip.....	98
Fig.3.20: The relationship between metaxylem wall thickness and total metaxylem area in control and HC-treated, 14 months old tall fescue plant roots at the position of one third as a fraction of root length above the root tip.....	99
Fig.3.21: Photograph showing water staying on top of the HC-contaminated soil matrix, before quickly running through the holes at the bottom of the pot.....	100

Chapter 4

Fig.4.1: Illustration of saturation, field capacity and wilting point (Apart from labelling A, B and C, the figure is directly presented as in Dept of Agriculture Bulletin, 462, 1960).....	108
Fig.4.2: Rhizo-box set up showing the different layers consisting of different concentrations of PAH (e.g. fluoranthene).....	111

Fig.4.3: Line graph showing the shoot elongation of tall fescue plants from control (blue) and anthracene (brown) (1000mg kg^{-1} sand dw)-treatment for a period of 66-days.....	120
Fig.4.4: Line graph showing the root elongation of tall fescue plants from control (blue) and anthracene (brown) (1000mg kg^{-1} sand dw)-treatment for a period of 66 days.....	120
Fig.4.5: Scanning electron micrographs of tall fescue root fragments grown in clean sand (left) and in anthracene-treated (1000mg kg^{-1} sand dw) sand (right) for ~2 months.....	121
Fig.4.6: Scanning electron micrograph of tall fescue grown in anthracene-treated (1000mg kg^{-1} sand dw) sand for 66 days, showing transversal root section sectioned at 1/3 as a fraction of root length above the root tip.	121
Fig.4.7: Brown top bent grown in clean sand (A) and anthracene-treated [1000mg kg^{-1} sand (dw)] sand (B) for ~2months.....	122
Fig.4.8: Tall fescue showing resistance to growth in sand contaminated with naphthalene at the concentration of 800mg kg^{-1} sand (dw). Tall fescue plants from control (left) and naphthalene (right) - treatment, after 55 days (A) and 136 days (B) of growth.....	123
Fig.4.9: Line graph showing the differences in the percentage of germination of tall fescue seeds between control and naphthalene-treatments on day 4, 8 and 12 since sowing.....	124
Fig.4.10: (A) Bar graph showing differences in initial shoot and root development between tall fescue grown in clean sand and sand contaminated with naphthalene. The age of the plants: 3 weeks. Photographs of 3 weeks old tall fescue grown in (B) clean sand and (C) sand contaminated with naphthalene.....	125
Fig. 4.11: Bar graph showing the root lengths of tall fescue grown in clean sand and sand treated with naphthalene.....	126
Fig.4.12: Bar graph showing the differences in root diameter ($p<0.01$ as determined by Student's t-test) and distance from root epidermis to root stele ($p<0.001$ as determined by Student's t-test) between tall fescue grown in clean sand and sand treated with naphthalene.....	127
Fig.4.13: Differences in shoot and root dry weight between control and naphthalene-treated tall fescue after growth of 78 days in respective treatments.....	128
Fig.4.14: Bar graph showing the dry weight percentage of root and shoot tissues of tall fescue grown in clean sand and naphthalene-treated sand for 78 days.....	128
Fig. 4.15: Tall fescue grown in clean sand (A) and naphthalene-treated sand (B) for 14 weeks.....	130
Fig.4.16: Fluorescent (A1, B1) and superimposed (A2, B2) images of control (A1, A2) and naphthalene-treated (B1, B2) 6 months old tall fescue roots stained with berberine hemisulphate, counterstained with aniline blue and viewed with UV illumination (excitation at 345 nm; emission at 458 nm), showing cross sections at the position of one third as a fraction of root length above the root tip.....	131
Fig.4.17: Tall fescue grown in clean sand (A) and naphthalene-treated sand (B) for 3 months, after left without watering for 4 days.....	132
Fig.4.18: Scanning electron micrographs of transversal sections of roots of tall fescue grown in clean sand (A) and naphthalene-treated sand (B) for 3 months and exposed to water stress for 4 days, sectioned at one third as a fraction of root length above the root tip.....	133
Fig.4.19: Differences in shoot and root dry weight between control and naphthalene-treated tall fescue	

at the age of 94 days, after exposed to severe water stress.....	134
Fig.4.20: Bar graph showing the dry weight percentage of root and shoot tissues of tall fescue grown in clean sand and naphthalene-treated sand for 94 days, after exposed to severe water stress.....	135
Fig.4.21: Scanning electron micrographs of control (A) and naphthalene-treated (B) tall fescue showing cross sections of roots of 94 days old plants at plant wilt point state, sectioned at one third as a fraction of root length above the root tip.....	136
Fig. 4.22: Bar graph showing the values for distance between root epidermis and root stele and root diameter of 94 days old control and naphthalene-treated tall fescue, exposed to severe water stress...	136
Fig. 4.23: Bar graph showing the values for endodermis thickness of 94 days old control and naphthalene-treated tall fescue, exposed to severe water stress.....	137
Fig.4.24: Bar graph showing the difference in (A) moisture content % (N=15; NS; Student's t-test) and (B) matrix potential (N=4; p<0.001; two-sample t-test in GenStat) between clean and naphthalene-contaminated sand at field capacity (saturated conditions).....	138
Fig.4.25: Bar graph showing the differences in (A) moisture content % in top, mid and bottom portions of the potted sand [N=5 (control)+ 8 (treated) ; p<0.01 for mid layer as determined by Student's t-test) and (B) matrix potential (N=2;NS; Student's t-test) between unplanted treatments at unsaturated, water-deficit conditions.....	139
Fig. 4.26: Line graph showing the matrix potential readings over time under regular watering regime in representative planted pots.....	140
Fig.4.27: Bar graph showing the difference in (A) moisture content % (N=6; NS; Student's t-test) and (B) matrix potential (N=2; NS; Student's t-test) between control and naphthalene treatment at plant wilt point.....	142
Fig.4.28: A: Epi fluorescent micrograph of a cross section of a tall fescue root painted with Nile red in its vital state, sectioned at two third as a fraction of root length above the root tip and viewed through UV-2A filter (excitation at 345nm; emission at 458nm), FITC filter block (excitation at 494nm; emission at 518nm) and Texas red HYQ filter cube (excitation at 589nm; emission at 615nm).....	144-145
Fig.4.29: Fluorescent (A1, B1) and superimposed (A2, B2) images of control (A1, A2) and naphthalene-treated (B1, B2) 3 months old tall fescue roots painted with Nile red in their vital state and viewed through Texas red HYQ filter (excitation at 589nm; emission at 615nm), showing cross sections at one third as a fraction of root length above the root tip.....	146
Fig.4.30: Epi-fluorescent micrographs of control (A1-A3) and naphthalene-treated (B1-B3) 6 months old tall fescue, showing parts of transversal root sections at one third as a fraction of root length above the root tip, viewed through Texas red HYQ filter (excitation at 589nm; emission at 615nm) (A2, B2) and UV illumination (excitation at 345nm; emission at 458nm) (A3, B3).....	148
Fig.4.31: Fluorescent (A1, B1) and superimposed (A2, B2) images of control (A1, A2) and naphthalene-treated (B1, B2) 6 months old tall fescue, showing transversal root sections at one third as a fraction of root length above the root tip.....	149
Fig.4.32: A hypothetical schematic diagram showing the reduced width of meniscus of soil pore water and water repellence in naphthalene-treated sand in comparison to the clean sand.....	152
Fig.4.33: Schematic diagram of the water and solute transportation pathways across root tissues.....	160

Chapter 5

- Fig.5.1: Overlaid EI positive total ion chromatograms for polar compounds extracted from leaf tissues of tall fescue grown in clean sand (green) and sand contaminated with naphthalene (red).....171
- Fig.5.2: Overlaid EI positive total ion chromatograms for polar compounds extracted from root tissues of tall fescue grown in clean sand (green) and sand contaminated with naphthalene (red).....171
- Fig.5.3: Representative EI positive total ion chromatogram for reagents used in the extraction and derivatization of plant tissues.....172
- Fig.5.4: Zoomed part of EI positive total ion chromatogram for the compounds extracted from root tissues of tall fescue grown in naphthalene-contaminated sand. Inset: The extracted mass spectrum for the compound eluting at 10.72 minutes. RI: Retention Index.....173
- Fig.5.5: Zoomed part of EI positive total ion chromatogram for the compounds extracted from root tissues of tall fescue grown in clean sand. Inset: The extracted mass spectrum for the compound eluting at 10.73 minutes. RI: Retention Index.....174
- Fig.5.6: EI positive total ion chromatogram for 1-naphthol dissolved in chloroform (GC-grade). Inset: The extracted mass spectrum for 1-Naphthol. RI: Retention Index.....174
- Fig.5.7: EI positive total ion chromatogram for silylated 1-naphthol. Inset: The extracted mass spectrum for silylated 1-Naphthol. RI: Retention Index.....175
- Fig.5.8: EI positive total ion chromatogram for the trimethylsilylated 3-Indole acetic acid and mass spectra for compounds RT 26.78 min (A) and RT 27.63 min (B) corresponding to 1 TMS Indole acetic acid and 2 TMS Indole acetic acid respectively from reference to the mass spectral database library.....177
- Fig.5.9: Overlaid EI positive total ion chromatograms for polar compounds extracted from shoot tissues of tall fescue grown in clean sand (green) and sand contaminated with naphthalene (red), showing the retention time region between 22.00-26.00 minutes.....181
- Fig.5.10: Overlaid EI positive total ion chromatograms for polar compounds extracted from root tissues of tall fescue grown in clean sand (green) and sand contaminated with naphthalene (red), showing the retention time region between 22.00-26.00 minutes.....181
- Fig. 5.11: Bar graph showing the differences in the abundance of polar compounds in shoots (A) and roots (B) of tall fescue between control (green) and naphthalene-contaminated (red) treatments.....183
- Fig.5.12: XY scatter graph showing the mean values for the abundances of simple sugars and the nucleotide sugar UDP-Glucose in the root (indicated by squares) and shoot (indicated by diamonds) tissues of tall fescue grown in clean sand (left) and sand contaminated with naphthalene (right; differentiated by filled shapes).....184
- Fig. 5.13: Box and whisker plot showing the differences in the abundance of the putative IAA in the root ($p<0.05$; $N=4$, t-test) and shoot tissues ($p<0.001$; t-test; $N=4$) of tall fescue grown in clean sand (abbreviated as con.) and sand contaminated with naphthalene (abbreviated as treat.).....185
- Fig. 5.14: Bar graph showing the difference in the ratio between root and foliar (shoot) pools of phosphoenol pyruvic acid/ phosphoenolpyruvate (PEP) between treatments ($p<0.01$; t-test; $N=4$)...187
- Fig.5.15: Overlaid EI positive total ion chromatograms for polar compounds extracted from shoot tissues of tall fescue grown in clean sand (green) and sand contaminated with naphthalene (red), showing the retention time region between 46.00-51.50 minutes. Inset: Magnified ($\times 124$) part of the

chromatogram for compounds extracted from treated shoots showing the presence of signal for fructans (retention time 50.67 minutes) (indicated by red arrow).....187

Chapter 6

Fig.6.1: (E) Leaf of a plant grown continuously on 0.5 mM phenanthrene for 60 d before staining with trypan blue. Dark blue spots indicate dye accumulation in dead cells. (F) Ion leakage (as the percentage of total ion content) into distilled water during 20 h of incubation at room temperature in 26-d-old plants grown on 0–0.5 mM phenanthrene (Presented directly as in Alkio et al., 2005).....210

Fig.6.2: Schematic diagram of the xenobiotic uptake models for control and naphthalene-treated tall fescue roots, based on both general and initial results.....213

Fig.6.3: Dose response models used in toxicology (Source: Mattson and Calabrese, 2008).....216

Appendix 1

Fig. A1-1: The extracted mass spectrum for the compound tentatively identified as further oxidised or glycosylated/ malonylated naphthol (RT 10.72 min) from treated root extract.....241

Fig. A1-2: The extracted mass spectrum for the compound tentatively identified as IAA (RT 10.73 min) from control root extract.....242

Fig. A1-3: The extracted mass spectrum for the compound identified as malic acid (RT 15.63 min) from control shoot extract.....243

Fig. A1-4: The extracted mass spectrum for the compound identified as erythritol (RT 16.10 min) from control shoot extract.....244

Fig. A1-5: The extracted mass spectrum for the compound identified as isocitric acid (RT 16.51 min) from control shoot extract.....244

Fig. A1-6: The extracted mass spectrum for the internal standard, ribitol (RT 21.04 min) extracted together with control shoots.....245

Fig. A1-7: The extracted mass spectrum for the compound identified as ribose (RT 23.00 min) from control shoot extract.....246

Fig. A1-8: The extracted mass spectrum for the compound identified as phosphoenolpyruvic acid (RT 23.86 min) from control shoot extracts.....246

Fig. A1-9: The extracted mass spectrum for the compound identified as fructose (RT 24.17 min) from control shoot extract.....247

Fig. A1-10: The extracted mass spectrum for the compound identified as UDP-glucose (RT 24.36 min) from control shoot extract.....248

Fig. A1-11: The extracted mass spectrum for the compound identified as glucose (RT 24.64 min) from control shoot extract.....248

Fig. A1-12: The extracted mass spectrum for the compound identified as galactose (RT 24.97 min) from control shoot extract.....249

Fig. A1-13: The extracted mass spectrum for the compound identified as sucrose (RT 37.56 min) from control shoot extract.....250

Fig. A1-14: The extracted mass spectrum for the compound identified as fructan (RT 50.68 min) from

treated shoot extract.....	250
Fig. A1-15: The extracted mass spectrum for the compound identified as trehalose (RT 50.96 min) from control shoot extract.....	251

Appendix 2

Fig. A2-1: Epi-fluorescent micrographs of transversal sections of 3 months old carrot (<i>Daucus carota</i>) roots stained with Nile red and viewed through Texas red HYQ filter cube (excitation at 589 nm; emission at 615 nm). a: The plant was grown in clean sand b: The plant was grown in fluoranthene-treated sand (1g kg^{-1} sand dw).....	252
--	-----

Fig. A2-2: Epi-fluorescent micrographs of transversal sections of 3 months old white clover (<i>Trifolium repens</i>) roots stained with Nile red and viewed through Texas red HYQ filter cube (excitation at 589 nm; emission at 615 nm). a: The plant was grown in clean sand b: The plant was grown in naphthalene-treated sand (0.8g kg^{-1} sand dw).....	253
--	-----

LIST OF TABLES

Chapter 1

Table 1.1: Principal components of petroleum crude oil and their impacts on human health....	1
Table 1.2: 16 EPA PAHs and their significant physico-chemical characteristics	3
Table 1.3: Compositional comparison between cutin and suberin.....	19
Table 1.4: Prevalence of soil bacteria that contained genes involved in HC-degradation.....	42
Table 1.5: Effect of PAH contamination on germination and subsequent growth	51
Table 1.6: Effect of diesel contamination on the subsequent growth of specific plants.....	54

Chapter 2

Table 2.1: The different categories of petroleum hydrocarbons of a soil that had soaked liquid petroleum leaked from a petroleum storage tank and their concentrations and percentages as a fraction of total dichloromethane (DCM)-extractable petroleum hydrocarbons (TEH).....	62
Table 2.2: Experimental design used in chapter 3.....	65
Table 2.3: Experimental design used in chapter 4, section 4.3a.....	66
Table 2.4: Experimental design showing number of replicates established for the water balance study described in chapter 4 (Chapter 4; Section 4.3 b-4.3 d).....	67
Table 2.5: Concentrations of ethanol (EtOH) and duration of soaking plant tissues in EtOH during dehydration.....	70

Chapter 3

Table 3.1: Plant growth parameters of carrot grown in clean and HC-treated sand for 3 months.....	83
Table 3.2: Plant growth parameters of beetroot grown in clean and HC-treated sand for 3 months.....	85
Table 3.3: Plant growth parameters of a grass mixture containing tall fescue, brown top bent and perennial ryegrass grown in clean sand and HC-treated sand that is either amended or not amended with compost, for 3 months.....	87
Table 3.4: Plant growth parameters of brown top bent grown in clean and HC-treated sand [16.5g total extractable hydrocarbons kg ⁻¹ sand (dw)] for ~2 months.....	93
Table 3.5: Descriptive statistics for root ultra-structural parameters of 14 months old tall fescue roots at the position of 1/3 as a fraction of root length above the root tip.....	98

Chapter 4

Table 4.1: Physico-chemical parameters of naphthalene, fluoranthene, anthracene and benzo (a) pyrene [B(a)P].....	107
---	-----

Table 4.2: PAH concentrations used in the different layers in the gradient rhizo-box experiment.....	111
Table 4.3: Descriptive statistics for plant parameters of 66 days old brown top bent from control and anthracene (1000mg kg ⁻¹ sand dw) –treatment.....	122
Table 4.4: Descriptive statistics for structural and ultrastructural parameters (root hair, xylem vessel and endodermis wall thickness) of tall fescue roots grown in clean sand and naphthalene-treated (800mg kg ⁻¹ sand dw) sand for 2.5 months, at the position of 1/3 as a fraction of root length above the root tip.....	123
Table 4.5: Differences in fresh weight and moisture content % of plant tissues between treatments during plant acclimatisation period.....	129
Table 4.6: Contingency table showing the difference in the abundance of exodermal Casparian bands at one third as a fraction of root length of tall fescue grown in clean (Control) and naphthalene-treated (Treated) sand.....	132
Table 4.7: Differences in fresh weight and moisture content % of plant tissues between treatments, after exposed to severe water stress.....	135
Table 4.8: Differences in matrix potential at 18.00 pm on day 70, after the plants were subjected to water stress during 62-70 days of plant growth in clean and naphthalene-treated sand.....	141
Table 4.9: Contingency table showing the difference in the uptake of Nile red into protoxylem vessels, at one third as a fraction of root length of tall fescue grown in clean (Control) and naphthalene-treated (Treated) sand.....	146
Table 4.13: Differences in matrix potential at 18.00 pm on day 70, after the plants were subjected to water stress during 62-70 days of plant growth in clean and naphthalene-treated sand.....	137
Table 4.14: Differences in moisture content % and matrix potential between treatments at 14.00 pm on day 94, at plant wilt point state.....	138
 Chapter 5	
Table 5.1: Comparison of spectra of a peak at RT 10.73 min in plant samples with silylated authentic indole acetic acid. Similar ion abundance in spectra is indicated by ^a	176
Table 5.2: List of 14 metabolites tentatively identified from mass spectra analysis and database inspection in the shoots and roots of tall fescue grown in clean sand and sand contaminated with naphthalene for 6 months plus the internal standard (differentiated by the italic font).....	178
Table 5.3: Descriptive statistics for normalised integrated signals of peak areas for the polar compounds extracted from the shoots and roots of tall fescue grown in clean sand and sand contaminated with naphthalene (0.08% w/w) for 6 months.....	182
Table 5.4: Descriptive statistics for the ratios between root and foliar (shoot) pools of sugars extracted from tall fescue grown in clean sand and sand contaminated with naphthalene for 6 months.....	186

Appendix 3

Table A3-1: Concentration of naphthalene detected in plant tissues grown in naphthalene-treated sand (0.8 g kg^{-1} sand dw) for 6 months.....	254
---	-----

LIST OF ABBREVIATIONS

- ADP:** adenosine di-Phosphate
ATP: adenosine tri-Phosphate
AM: arbuscular mycorrhizae
AMDIS: Automated Mass Spectral Deconvolution and Identification System
Ant: anthracene
~: approximately
APS: apparent photosynthesis
ARE: artificial root exudates
B(a)P: benzo (a) pyrene
BCF: soil-crop bio concentration factor
C: carbon
C: Celsius
Ca: calcium
Cd: cadmium
cm: centimetre
Cl⁻:chloride
CO₂:carbon dioxide
CPD: critical point dryer
m³: cube
d: day
Da: dalton
DAB: diaminobenzidine
DAPI: 4',6-diamidino-2-phenylindole
DCM: dichloromethane
°: degree
dH₂O: distilled water
DMF: dimethyl formamide
DNA: deoxyribonucleic acid
DOM: dissolved organic matter
dw: dry weight
e.g.: for example
EI: Electron Ionization
EPA: Environmental Protection Agency
etc: etcetera
EtOH: ethanol

eV: electron volt
FAD: Flavin Adenine Dinucleotide
Fe: iron
FeCl₃: ferric chloride
FID: flame ionisation detection
FITC: fluorescein isothiocyanate
Fig.: figure
Flt: fluoranthene
F_{oc}: weight fraction of organic carbon in soil
fru: fructose
g: gram
gal: galactose
GC: gas chromatography
GC-FID: gas chromatography-flame ionisation detection
GC-MS: gas chromatography-mass spectrometry
glc: glucose
GRP: glycine-rich cell wall protein
H: Henry's law constant
HC: crude oil
HCl: hydrochloric acid
HMW: high molecular weight
HPLC: high performance liquid chromatography
H₂O: water
H₂O₂: hydrogen peroxide
IAA: indole acetic acid
i.e.: that is (to say)
K: potassium
KCl: potassium chloride
kg: kilogram
KH₂PO₄: potassium phosphate
kV: kilo volt
<: larger
L: litre
LD₅₀: Lethal Dose, 50%
LMW: low molecular weight
log K_{ow}: octanol :water partition coefficient
LSD: least significance difference

µg: microgram
µl: micro litre
µm: micro metre
m: metre
M: molarity
mal: malic acid
mbar: millibar
M.C: moisture content
Mg: magnesium
mg: milligram
min: minutes
ml: millilitre
mm: millimetre
mM: millimolar
Mn: manganese
mol: mole
MS: mass spectrometry
MS: Murashige and Skoog medium
MSTFA: N-methyl-N-trimethylsilyl-trifluoroacetamide
mTorr: millitorr
m/z: mass-to- charge ratio
N: nitrogen
Na⁺:sodium ion
Na (CH₃)₂ AsO₂.3H₂O: sodium cacodylate
NaCl: sodium chloride
NAD: Nicotinamide Adinine Dinucleotide
NADH: Nicotinamide Adinine Dinucleotide plus Hydrogen
NADPH: Nicotinamide Adinine Dinucleotide Phosphate
Na₂HPO₄: sodium biphosphate
NaOH: sodium hydroxide
Nap/ nap: naphthalene/ naphthol/ naphthalene epoxide
ND: Not Detected
nm: nanometre
ng: nano gram
No.: number
ns: not significant
NSOS: Nitrogen, Sulphur, Oxygen compounds

ω-hydroxy acids: omega hydroxy acids
O₂: oxygen
OCP: organochlorine pesticide
OM: organic matter
/: or
OsO₄: osmium tetroxide
P: phosphorous
⁻¹: per
%: percentage
p: probability
Pa: Pascal
PAH: polycyclic aromatic hydrocarbon
PAR: photosynthetically active radiation
PBS: phosphate buffered saline
PCB: polychlorinated biphenyl
PEP: phosphor enol pyruvate
PFA: paraformaldehyde
ppm: parts per million
psi: pounds per square inch
QA/QC: quality assurance / quality control
rep: replicate(s)
rib: ribose
RNA: ribonucleic acid
ROS: reactive oxygen species
rpm: rotation per minute
RT: Reverse Transcription
s: second
S: sulphur
SA: salicylic acid
SAR: Systemic Acquired Resistance
SD: standard deviation
SEM: scanning electron microscope/ scanning electron microscopy
>: smaller
SO₄²⁻: sulphate
SOM: soil organic matter
²: square
suc: sucrose

Σ : sum/ total

TCA: Tri-Carboxylic acid cycle

TEH: total dichloromethane extractable petroleum hydrocarbons

TRITC: tetramethyl rhodamine isothiocyanate

TIC: Total Ion Chromatogram

Torr: unit of measure for the pressure exerted by 1 mm of mercury equal to 1/760th of standard atmospheric pressure; used to measure pressure in vacuum systems

TPEM: two-photon excitation microscopy

tre: trehalose

UDP: uridine diphosphate

UDP-glc: uridine diphosphate glucose

UK: United Kingdom

U.S. or US: United States

UV: ultra violet

v: version

vs.: versus

V: volt

v/v: volume: volume ratio

W: watt

WC: soil water content/ soil moisture content

WHC: soil-water holding capacity

WS: water soluble

w/v: weight: volume ratio

ww: wet weight

w/w: weight: weight ratio

CHAPTER 1

Introduction: Impacts of petroleum hydrocarbon-contamination on plants used in phytoremediation

1.1 Petroleum hydrocarbon contamination in our environment and the importance of remediation

Industrial activities such as gasification/ liquefaction of fossil fuels (gasworks sites), coke production, asphalt production, coal tar production, wood treatment processes, wood preservative production and fuel processing result in soils contaminated with petroleum hydrocarbons. There are at least 350 000 contaminated sites in Western Europe (Vandevivere and Verstraete, 2001), and the largest part of this contamination is due to petroleum hydrocarbon-based products (Troquet et al., 2003). Petroleum crude oil is composed of a complex mixture of hydrocarbons and other organic compounds. These are categorised in table 1.1. Many of its chemical components are toxic, mobile and environmentally persistent (Farrell-Jones, 2003).

Table 1.1: Principal components of petroleum crude oil and their impacts on human health

Category	Characteristics	Examples	Impact on human health
Naphthenes (Cycloparaffins/ cycloalkanes)	Ring structures	Cyclopentane, cyclohexane	Contact with skin and eye causes irritation; ingestion of this product or subsequent vomiting can result in aspiration of light hydrocarbon liquid which can cause pneumonitis. Prolonged breathing of vapours can cause central nervous system effects
Normal paraffins/ normal alkanes	Straight chain structures; readily biodegradable; occur as homologous series in most crude oils (C1-C4: gases; C5-C16: liquids; >C17:solids at ambient temperature); forms a major component of crude oil	n-Octane	Affects central nervous system at high concentrations ($<0.8\text{mg L}^{-1}$)
Iso paraffins/ iso alkanes	Often associated with single carbon atom (methyl) branches; from C9 upwards, most iso-paraffins are isoprenoids.	Pristane, phytane	Affects central nervous system at high concentrations ($<0.8\text{mg L}^{-1}$)

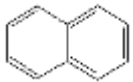
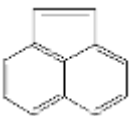
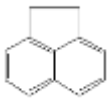
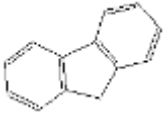
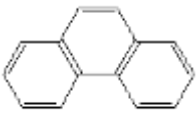
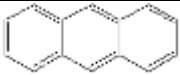
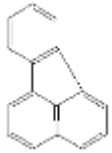
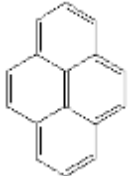
Aromatics	Occur as a series of isomers; simple aromatics contain only one aromatic ring, and may be either mono-, di-, or tri-substituted; multiple ring aromatic compounds are commonly referred to as polycyclic aromatic hydrocarbons (PAHs).	Methyl benzene, Anthracene	PAH burdens via inhalation, ingestion and dermal absorption cause cancer and genetic disorders via interactions with DNA. Systemic effects have been observed and the respiratory tract is thought to be the predominant target site.
Nitrogen, Sulphur, Oxygen compounds (NSOs)	Typically defined as non-hydrocarbons	Pyrrrole, Benzofuran	Affects lung function at high concentrations(<0.8mg L ⁻¹)
Asphaltics	High molecular weight and resinous compounds.		Considered cancer-causing because they contain PAHs

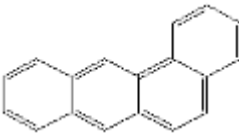
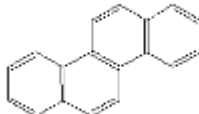
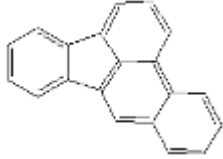
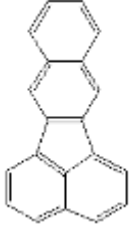
Source of category, characteristics and examples: Farrell-Jones (2003). For Stoddard solvent that contains a mixture of straight and branched-chain paraffins, naphthenes and aromatic hydrocarbons, the acute dermal LD50 >0.3g kg⁻¹, acute oral LD50>0.5g kg⁻¹, acute inhalation toxicity <10mg L⁻¹ within 7.5 hours of exposure. Source of impact on human health: U.S. Department of health and human services (2010).

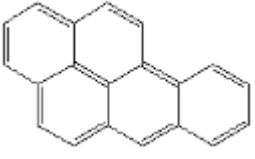
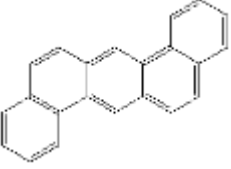
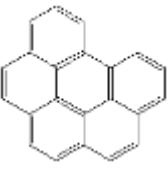
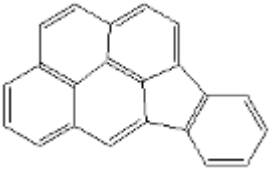
Of the various petroleum hydrocarbons, polycyclic aromatic hydrocarbons (PAHs) are considered significant environmental pollutants because of their carcinogenic and/ or mutagenic potential, ubiquity and persistence, and the occurrence of these components in food is a human health concern (Janska et al., 2006). Over 53 000 tonnes of polycyclic aromatic hydrocarbons (PAHs) (sum of 12 individual compounds) are estimated to reside in the UK environment, with soil being the major repository (Wild and Jones, 1994). UK soil Σ PAH concentrations generally fall into the concentration range of 100-54, 500 $\mu\text{g kg}^{-1}$ (Jones et al., 1989). Heavy urban traffic and residential and communal heating heavily affect the deposition of PAHs in soil (Crnkovic' et al., 2006). PAH concentrations are found to be higher in urban soils and roadside soils whilst very high concentrations have been reported for contaminated sites such as old gas works sites (Wild and Jones, 1994).

The US Environmental Protection Agency (EPA) has classified 16 PAHs as priority pollutants (Table 1.2).

Table 1.2: 16 EPA PAHs and their significant physico-chemical characteristics

PAH	No. of aromatic rings	Molecular weight (g mol ⁻¹)	Octanol water partition coefficient (log K _{ow})	Solubility in water (mg L ⁻¹)
Naphthalene 	2	128.2	3.37	31
Acenaphthylene 	2	152.2	4.07	3.9
Acenaphthene 	2	154.2	4.33	3.8
Fluorene 	2	166.2	4.18	1.9
Phenanthrene 	3	178.2	4.57	1.1
Anthracene 	3	178.2	4.54	0.045
Fluoranthene 	3	202.3	5.22	0.26
Pyrene 	4	202.3	5.18	0.132

Benzo [a] anthracene 	4	228.3	6.75	0.011
Chrysene 	4	228.3	5.75	0.002
Benzo [b] fluoranthene 	4	252.3	6.57	0.001
Benzo [k] fluoranthene 	4	252.3	6.84	0.0005

Benzo [a] pyrene 	5	252.3	6.04	0.004
Dibenz [a,h,] anthracene 	5	278.4	6.75	0.0006
Benzo [g,h,i] perylene 	5	276.3	7.23	0.003
Indeno [1,2,3-cd] pyrene 	5	276.3	7.66	0.06

Source of K_{ow} & solubility in water: Farrell-Jones (2003).

1.2 Uptake of organic pollutants by plants

Collins et al. (2006) documented that uptake of organic pollutants by plants from contaminated soils depends on many factors:

- Abiotic
 - Properties of the molecule, ie. $\log K_{ow}$ and molecular weight
 - Soil components (clays, iron oxides, organic matter)
- Biotic
 - Transpiration rates
 - Types and amounts of lipids in root cells
 - Enzyme complement
 - Root exudates
 - Growth dilution

1.2 a. ABIOTIC FACTORS

Properties of the organic pollutant

The hydrophobicity of a molecule is measured and classified according to its octanol-water partition coefficient ($\log K_{OW}$), which describes its capacity to dissolve into an organic solvent (i.e. octanol) relative to an aqueous solvent (i.e. water). Generally, the hydrophobicity and environmental stability of a PAH molecule rises with an increase in size and the number of aromatic rings it possesses (Kanaly and Harayama, 2000). PAHs with more than three rings are often referred to as high molecular weight (HMW) PAHs, and those with three or less as low molecular weight (LMW) PAHs. Some PAHs are regarded as mobile pollutants, i.e., contaminants that can be leached with water (UNEP, 2008). Apart from naphthalene, a 2-aromatic ring, linear PAH, PAHs are practically insoluble in water and are very slow to degrade (Smith et al., 2006; Aprill and Sims, 1990). Naphthalene does not persist, and degrades rapidly to simpler, generally non-toxic compounds (Smith et al., 2006).

Soil composition

Organic chemicals such as PAHs can be sorbed or bound to several components in soil such as clays, iron oxides, and especially organic matter. Competitive sorption between plant lipids and soil organic carbon results in less bioavailability of the organic chemicals for plant roots at a higher soil organic matter (SOM) content

(Collins et al., 2006 and references therein). Briggs et al. (1983) for example examined the uptake of organic compounds by roots cultivated in hydroponic conditions and showed that molecules with a high log K_{ow} were taken out of solution by binding to roots (see Fig.1.1 below)

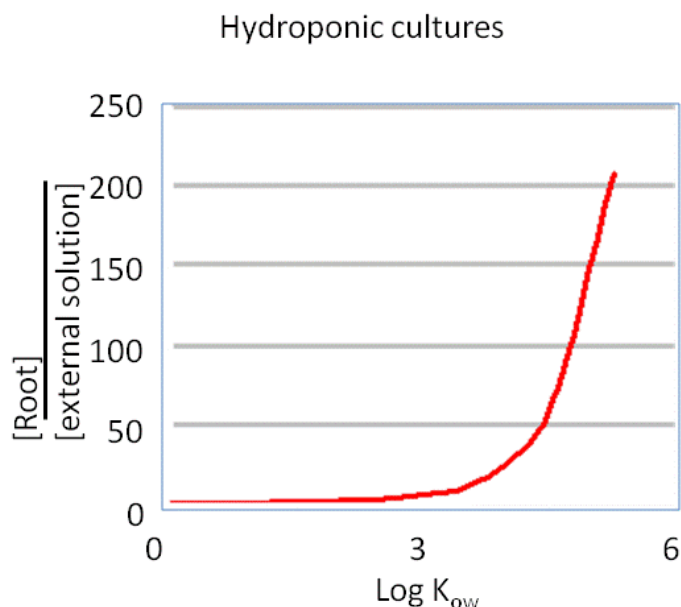


Fig.1.1: Relationship between the octanol water partition coefficient ($\log K_{ow}$) and uptake of organic compounds by roots cultivated in hydroponic conditions (Adapted from Briggs et al., 1983)

Soil-plant transfer of persistent organic chemical residues like PAHs also depends on soil moisture content (Beck et al., 1996). Normally, PAH uptake by crops is favoured under moist conditions in soils with low organic matter content. In dry soils with high organic matter content, chemical residues are strongly bound by soil, retarding uptake by plant roots (Zohair et al., 2006).

An increase in $\log K_{ow}$ of the organic contaminant retards the uptake of organic chemicals by crops growing in soil (Collins et al., 2006 and references therein) (see Fig.1.2). Soil-crop bio concentration factors (BCFs) were reported to decrease with increasing $\log K_{ow}$ for PAHs up to about 4.5 (above this $\log K_{ow}$ value no changes were discernible). Here, BCF was measured by dividing contaminant concentration in peel and core of the roots by contaminant concentration in soil (Zohair et al., 2006). Several researchers including Karickhoff (1981) have found empirical relationships between the lipophilicity of a chemical and its affinity to sorb to soil organic matter. Non-mobile PAHs with a high $\log K_{ow}$ [e.g. benzo (a) pyrene-a 5 aromatic ring, branched PAH molecule] tend to partition in the organic humic phase (Binet et al.,

2000; Wild and Jones, 1992), or are retained in the soil as a result of sorption, cation exchange, or precipitation processes, and are thus far less bio available to soil organisms and plants. On the other hand, more water-soluble and more volatile low molecular weight compounds such as acenaphthene, fluorine and phenanthrene are more susceptible to crop uptake (Zohair et al., 2006). It should however be noted that, stable PAHs originating from decades of industrial pollution will have a far lower bioavailability as a result of sorption to soil organic matter for long periods of time compared to those added experimentally (Joner et al., 2006; Alexander et al., 1995). Hence, when predicting uptake of experimentally added PAHs and evaluating their bio-phytoremediation aspect, a correction factor for sorption of PAHs to soil organic matter needs to be considered. On the other hand, in sand and water media, the PAH molecules are readily bio available, due to the absence of SOM that PAHs preferentially bind to, in these media.

Influence of weight fraction of organic carbon (F_{oc}) in soil

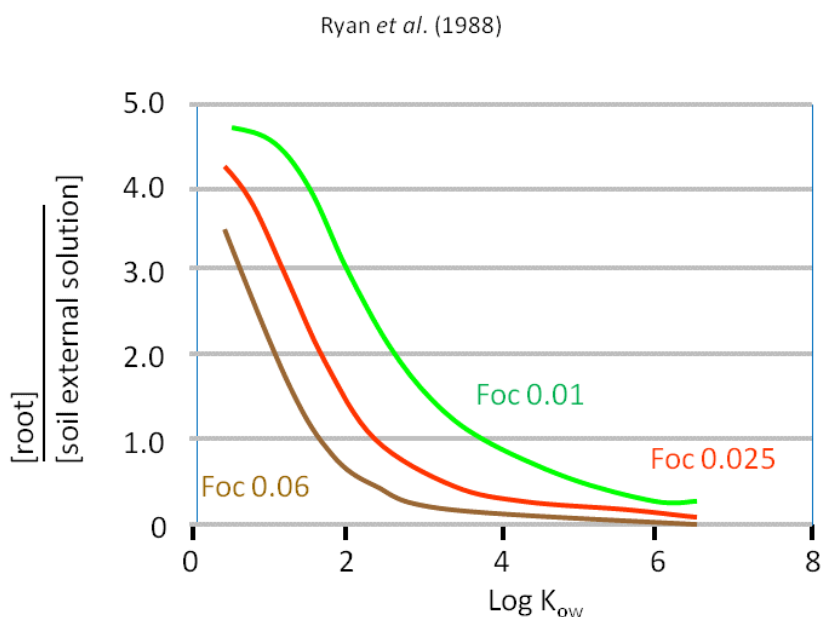


Fig.1.2: Influence of the weight fraction of organic carbon (F_{oc}) in soil on uptake of organic compounds by roots cultivated in soil (Adapted from Ryan et al., 1988).

Remediation of old industrial sites becomes necessary in meeting the demand for urban housing, office and leisure space (Smith et al., 2006). Remediation of polluted soils and waters is desirable as the polluted sites present a potential resource to solve the food and /or fuel shortages of the world. Also, following ingestion by organisms, PAHs can be metabolically transformed into mutagenic, carcinogenic and teratogenic agents such as dihydrodiol epoxides at the site of entry. These metabolites bind to

and disrupt DNA and RNA, leading the way to tumour formation. Benzofluoranthenes, benzo (a) pyrene, benzo (a) anthracene, dibenzo (a, h) anthracene and indeno (1, 2, 3-cd) pyrene are the most potent carcinogens among the PAHs (Wild and Jones, 1994 and references therein) and should therefore be targeted on this basis. But, their lower bioavailability means that they actually present less of a danger than the more mobile pollutants (i.e. contaminants with lower K_{OW}). So, it is beneficial to the wider environment to reduce these toxic hazards caused by PAHs, especially LMW PAHs (Smith et al., 2006).

Engineering techniques based on physical, chemical and thermal processes have been used for remediation purposes, but these methods are very expensive and not always effective (Okoh et al., 2006; Frick et al., 1999). Another option is landfilling of contaminated soil, but this is also expensive and becomes an increasingly greater problem as landfill sites are now in short supply and apart from this, it is not deemed a sustainable approach to solving the problem. Biological techniques such as phytoremediation are considered attractive due to their cost effectiveness and the benefit of pollutant mineralization to carbon dioxide and water (Okoh et al., 2006; Smith et al., 2006). Phytoremediation is a low input biotechnology approach: it relies on the knowledge that natural attenuation by biodegradation and physicochemical mechanisms will decrease the pollutant concentration, and is particularly beneficial where sowing seeds may be the only intervention (Smith et al., 2006). Planting PAH-contaminated sites gives other important benefits such as protection against wind erosion, reduction of surface water run-off, reinforcement of soil by roots and aesthetically pleasing impacts on the area (Smith et al., 2006): it can also maintain the livelihoods of the communities living in these environments.

1.2 b. BIOTIC FACTORS: **Roots**

The root is an important feature in phytoremediation, because plant roots are in direct contact with the contaminants in their surrounding soil. The presence of hydrocarbon contaminants modifies the soil structure (Merkl et al., 2005) and soil structure influences root growth (Passioura, 1991). Roots modify biological activity, structure, water status and mineral constituents of the surrounding soil (Neergaard et al., 2000; Atkinson, 2000), but will also be modified themselves by the contaminants. Unlike

animals, higher plants, cannot escape from their surroundings, as they are sessile, thereby the interactions of their roots with the soil which presents many abiotic stress factors such as water deficiency and toxicity due to the presence of organic contaminants and how the plants respond to the stress conditions are critical. In order to grow in contaminated soils, plants need to adapt themselves to their growth environment that exposes them to stress factors, through a series of molecular responses to cope with the adverse conditions. The integration of many transduced events into a comprehensive network of signalling pathways forms the basis of the physiological processes for the molecular responses, which enable the plants to adapt to the adverse conditions. Plant hormones may act in conjunction with other signals to regulate cellular processes such as division, elongation and differentiation. Since stress factors are also major ecological factors influencing the terrestrial ecosystem, the mutual concerted relationship between plant roots and the environment which presents the cues or stimuli for the plants to evolve molecular mechanisms of stress signalling pathways is fundamental. The plant signalling pathways and sensor network as adaptive mechanisms to environmental stress are crucial in the contexts of agricultural environment and sustainable development (Wu et al., 2007). Plant roots have several functions in the terrestrial ecosystem such as:

- a. feeding soil organisms with carbon substrates and contributing to soil organic matter through root exudation and root death
- b. providing a habitat for mycorrhizal fungi and rhizosphere organisms including PAH-degrading bacteria
- c. changing soil pH , and concentrating rare elements as well as toxic PAHs within the rhizosphere
- d. regulating plant growth via sensor-networking, predominantly due to plant hormones playing a central role in sensor network (Wu et al., 2007) frequently in conjunction with other signalling molecules such as sugars and sugar-like compounds (Bolouri-Moghaddam et al., 2010 and references therein)
- e. absorbing soil resources comprised of water and nutrients, whilst promoting formations of hydraulic conduits and redistributions of soil water and nutrients within the root growth zone
- f. strengthening the soil via humification and stabilisation; preventing soil erosion by forming a vegetative cover

- g. providing mechanical support for the plants which are essential for keeping a stable environment, by regulating the global climate as well as promoting the sustainability of their surroundings in several ways at different levels such as molecular, cellular, organ, individual, community, regional, ecosystem and global ecosystem levels (Wu et al., 2007).
- h. playing a vital role in sustaining the agricultural environment during times of stress, via production of higher root mass: higher amounts of photosynthetic sugars are translocated to the roots under stress conditions (Taiz and Zeiger, 1998). The roots of some crops such as carrot and beetroot are also storage organs, providing food for humans and other animals

1.2 b1. ROOT SYSTEMS

The pattern of development of a root system is termed root architecture. The recognition of different types of root architecture is important in phytoremediation as these root morphological variations will influence the capacities of roots to stimulate the proliferation of PAH-degrading micro organisms within the rhizosphere as well as to survive adverse conditions. Most plants produce one or more orders of lateral root branches that vary in branching patterns. These higher order lateral roots are generally thinner, shorter and do not live as long as those of lower orders (Brundrett, 2008, 1999). Root axes which originate directly from the shoot system are called axile roots or order 1 axes. Two main types of root system are distinguished according to the methods of root emergence (Pages et al., 2000).

(1) Primary root systems:

Primary root systems originate entirely from a single root called a radicle, which emerges soon after germination. Nodal roots successively form on the plant stem and these are called axile roots. With respect to the root system of mature plants for example in mature maize (*Zea mays* L.), the primary root is a minor constituent (Ober and Sharp, 2007).

Radicles give rise to 2nd and 3rd order lateral roots. Most roots in the primary root systems originate from the branching process. Together with their initial direction, the

description of the branching process in root architecture also specifies the locations and times of appearance of branches on the mother root, which is the primary root. Acropetal branching is the predominant type of root branching in many species, and it takes place on young parts of the root (see Fig.1.3). This typically results in a branching front which follows the apex of the mother root at a more or less definite distance (generally some centimetres). However, other types of branch roots may appear out of the acropetal sequence in some species. The geometrical pattern of root branching is much less clear than the arrangement of leaves on the stem (Pages et al., 2000). The primary root and its branches constitute the tap root system or primary root system, as seen in the mustard plant.

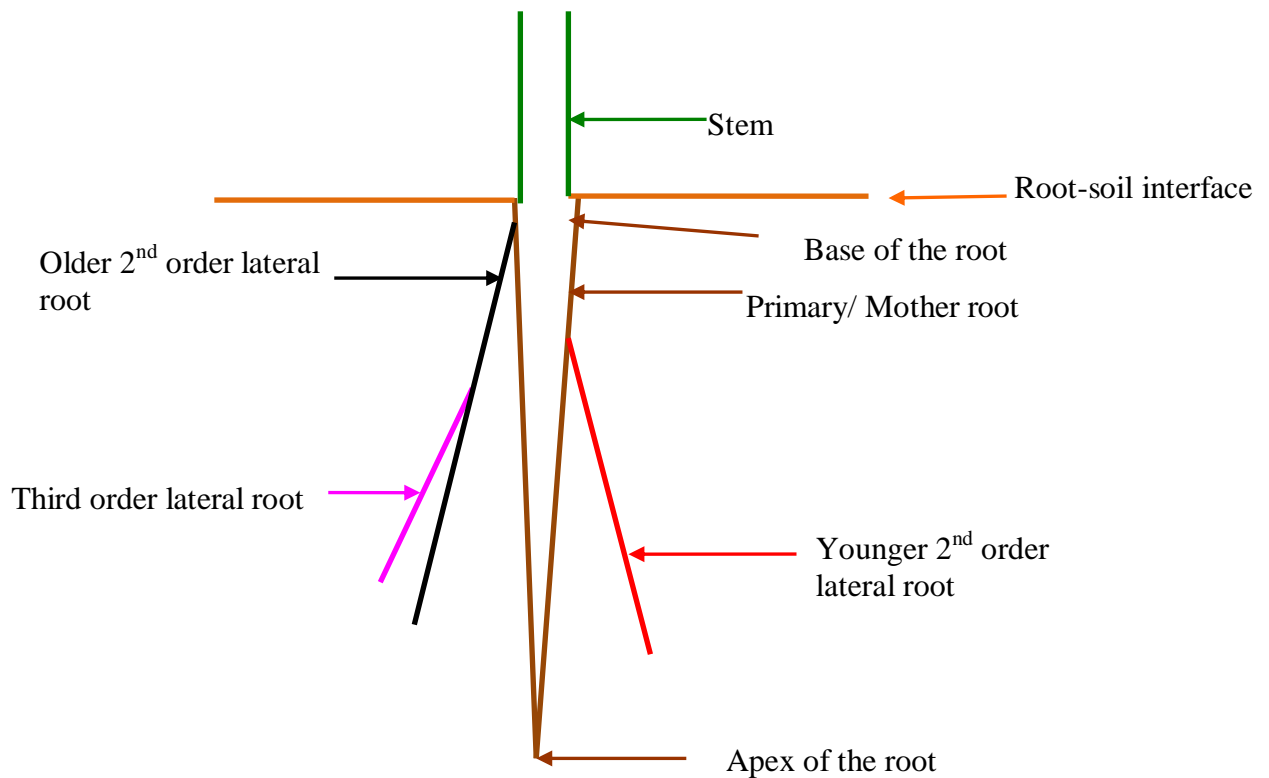


Fig.1.3: Schematic diagram of the primary root system showing acropetal branching (Adapted from Pages et al., 2000).

Eudicotyledons/ eudicots (eg. poplar, willow, apple) possess primary root system which also shows secondary growth, giving way to mature, thicker “woody” roots with bark and additional vascular tissue. They produce coarse roots that may live for a long time and have important roles in transport and mechanical support. The root architecture of eudicotyledons can be referred to as coarse and woody.

(ii) Adventitious root systems:

In these systems, several axile roots are generated from the stem throughout plant development (Fig.1.4). This type of root system is typical of grasses (Pages et al., 2000). The root architecture of grasses is referred to as fibrous and is comprised of fine roots.

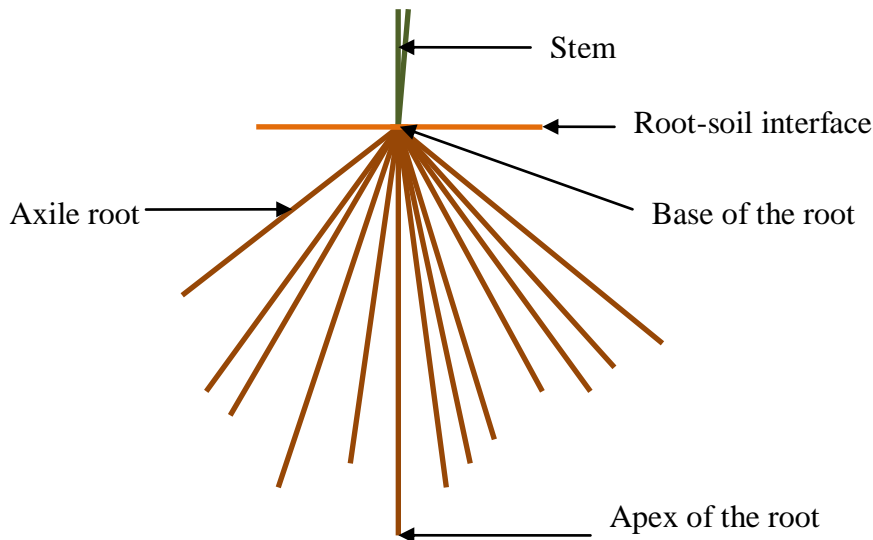


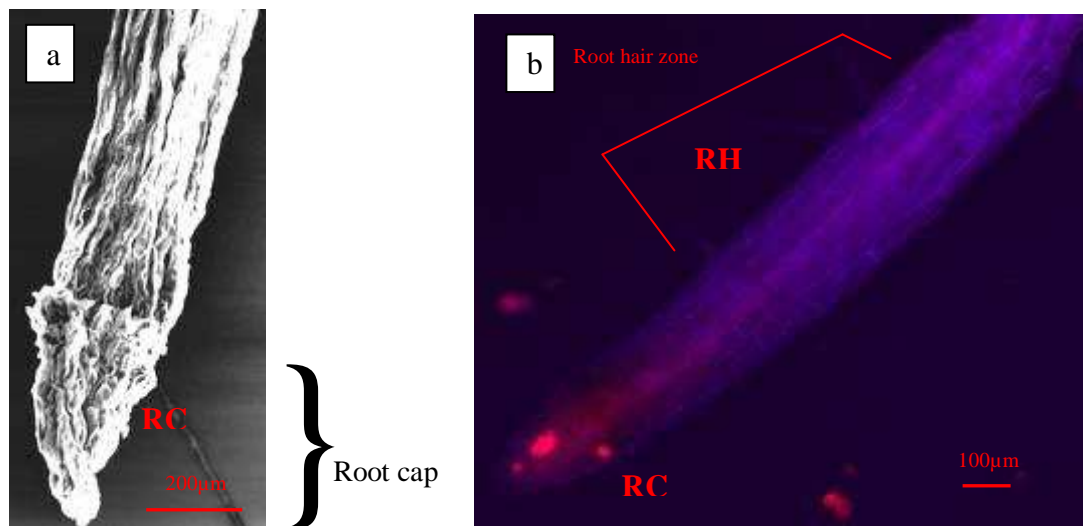
Fig 1.4: Schematic diagram of the adventitious root system

In plant-initiated remediation of PAHs or other organic contaminants, maximising root-soil contact is an important attribute. A high specific root length (SRL, length per unit mass) implies an effective and maximised root-soil contact. SRL varies between species. Generally, SRL is lower in the eudicots having coarse, woody root architecture (eg. for apple tree, SRL is 5m g^{-1}), than in grasses possessing fibrous root architecture (eg. for ryegrass, SRL is 750m g^{-1}) (Atkinson, 2000). The amount of root in the soil and root length density (RLD), also vary among species and are generally higher for grasses as seems evident for SRL (Atkinson, 2000). Grasses also show fast growth which is a favourable feature for phytoremediation. Grasses are favoured in the remediation of surface contamination (Brandt et al., 2006; Smith et al., 2006), but deep rooted plants such as poplar are required to access contaminants found deep in the soil profile (Rentz et al., 2003).

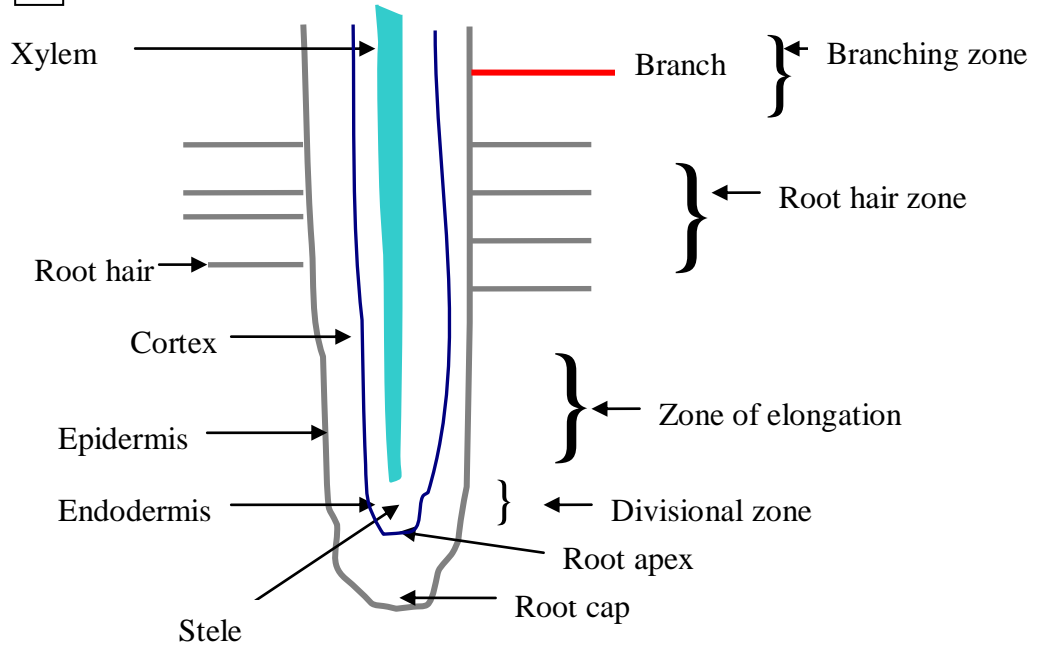
In root system architecture, the growth direction of the roots is an important component. The main guidance system that operates in the young root of the germinating seed is that which senses gravity and this ensures that the root is directed downwards (Wilkins, 1999). This guidance system constitutes both sensing and response mechanisms with which deviations from the preferred direction of growth can be corrected (Wilkins, 1999). Some of the long roots have very specific behaviours such as vertical or horizontal growth, depending on the environmental characteristics, and this strongly determines the overall shape of the system, including such important characteristics as overall width and depth (Coutts, 1989). At a smaller scale, roots generally exhibit some convolutions in response to the mechanical constraints and unfavourable factors which they experience (Pages et al., 2000). As petroleum hydrocarbon-contamination presents adverse conditions for the growth of plant roots (Merkl et al., 2005), it is of interest to study how growth in contaminated soil affects the growth direction of plant roots that possess different architecture.

1.2 b2. ROOT GROWTH AND ROOT STRUCTURES

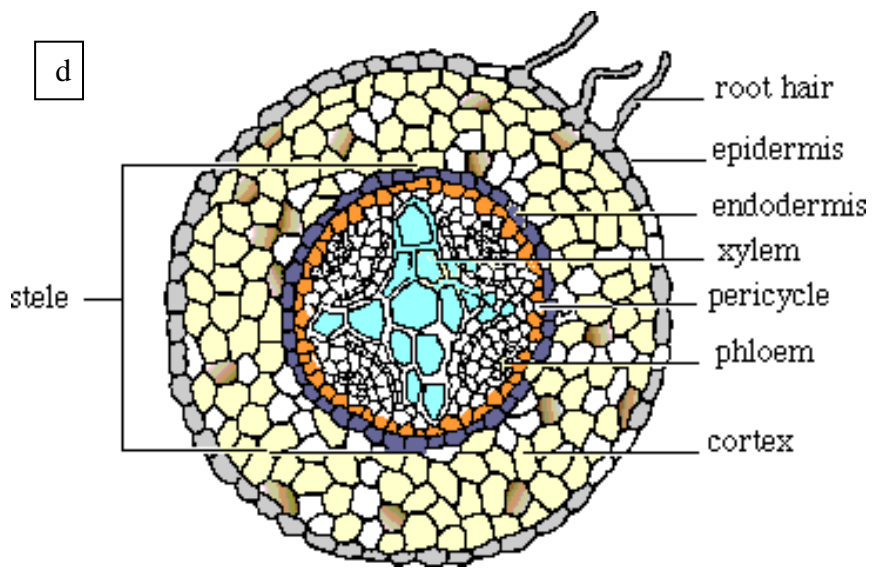
Plant roots grow deeper into the soil, exploring new volumes of soil in order to acquire nutrients and water. Root tissues are produced by cell division in the root apex and cell expansion in sub apical regions (Fig. 1.5 c). The apical meristem produces new root cap cells (Fig. 1.5 a & b) in an outward direction and new root cells in an inward direction. A growing root can be divided into divisional zone (meristematic zone), elongation zone, root hair zone and branching zone (Fig. 1.5 c).



c



d



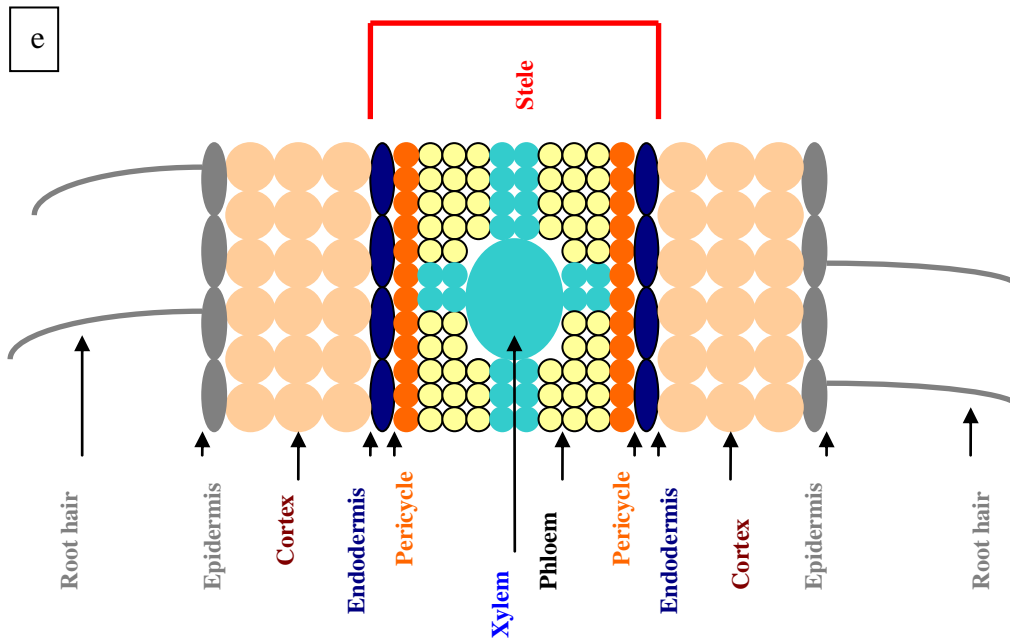


Fig. 1.5: a: Scanning electron micrograph of tall fescue root (*Festuca arundinacea*) showing root cap. Key: RC: root cap; Scale: 200 μm . b: Epi-fluorescent micrograph of tall fescue root stained with Nile red (a lipid fluorescent stain) and viewed through Texas red HYQ filter and UV illumination (images were overlaid using microscopic imaging software), showing root cap as well as root hairs. Key: RC: root cap; RH: root hair; Scale: 100 μm . c: Schematic diagram for a longitudinal view of a growing root, illustrating different growth zones and root structures (Adapted from Wild et al., 2005). d: Schematic diagram for a cross sectional view of a growing root sectioned through root hair zone, illustrating different root structures. e: Schematic diagram for part of a cross sectional view of a root sectioned through root hair zone (Adapted from Brundrett, 2008, 1999).

Root tip

The growing tip of roots is protected by a root cap (see Fig. 1.5 a-c) consisting of concentric layers of cells surrounding the apical meristem where new root cells are produced. The surface of the root cap of growing roots is often covered by a thick layer of mucilage (Rougi er and Chaboud, 1985).

The epidermis and root hairs

The epidermis is the outermost layer of roots that functions as the interface between plants and the soil. Epidermal cells may contain cutin, an insoluble, complex, protective lipid which is composed of glycerol and fatty acid derivatives with a range of oxygen-containing functional groups and may be adhered by a thin layer of pectin, continuous with the pectin which glues the epidermal cells together to the outer cell walls (Schulz, 2008; Forbes and Watson, 1992). Cutin constitutes the structural component of the cuticle, an outer hydrophobic skin that protects cells and organs

from desiccation and acts as a mechanical barrier against pathogens. The major hydrophobic constituents of the plant cuticle are the insoluble polymers, cutin and cutan, and a mixture of chloroform-soluble epicuticular and intracuticular lipids, collectively called waxes. Cuticles have several layers, which are defined on the basis of their position and chemical composition: the cuticular layer, attached to the cell wall, and contains polymers, waxes, and polysaccharides that extend from the underlying cell wall; the cuticle proper, comprised of cutin and intracuticular waxes; and epicuticular waxes covering the cuticle proper (Fig.1.6 a). The thickness of these layers and their composition depend on the species, anatomical location and developmental stage. The cuticle usually has an amorphous appearance when observed by electron microscopy (Fig. 1.6 b), but in some plants it presents a lamellar ultrastructure (Molina, 2010).

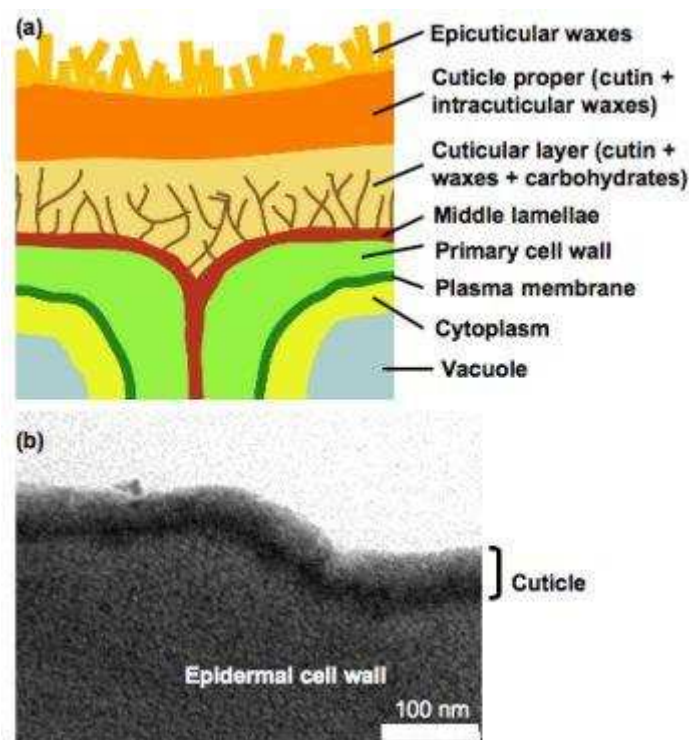


Fig.1.6: Structure of the plant cuticle. (a) Diagrammatic structure of epidermis and cuticle. (b) Ultrastructure of the cuticle of the leaf epidermis of *Arabidopsis* plants (presented directly as in Molina, 2010).

Cutin is polyester of C16 and C18 oxygenated fatty acids and glycerol. Monomers released after chemical cleavage of ester bonds usually include ω -hydroxy and ω -hydroxy-epoxy fatty acids, which are derived from C16 saturated and C18 unsaturated fatty acids. Minor amounts of hydroxycinnamic acids have been also reported as

structural components. Cutan is another structural polymer that remains as a non-depolymerizable fraction after ester-bond hydrolysis of cutin; it is possibly composed of cutin monomers mostly linked by ether and C-C bonds. Cuticular waxes include very long chain alkanes and substituted derivatives such as fatty acids, primary and secondary alcohols, aldehydes and ketones. Cutin monomers are esterified to each other by their primary hydroxyl groups (Fig.1.7) forming a linear polyester. In addition, esters formed between the carboxyl group of one fatty acid and a hydroxyl group of glycerol or a secondary hydroxyl group of another fatty acid allow a branched structure such as cross-linked and dendrimeric arrangements. However, the three-dimensional structure of cutin remains unresolved. It is also unclear if the insolubility of the polyester is a consequence of covalent linkage to the cell wall or cutan, or of the high molecular weight of the polymer (Molina, 2010).

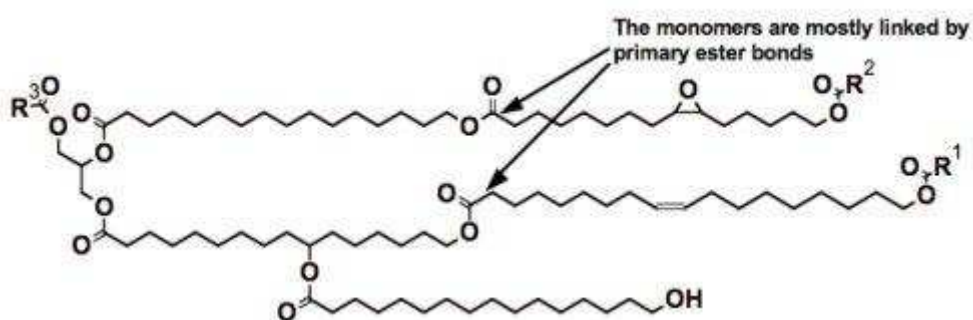
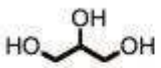
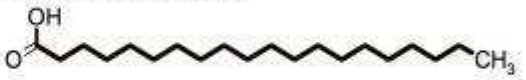


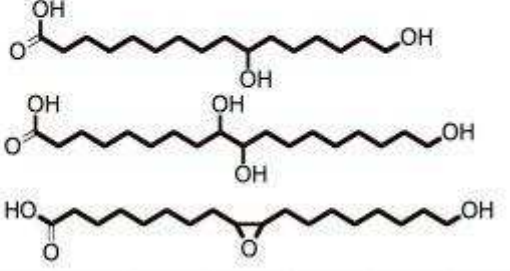

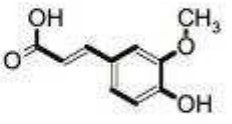


Fig. 1.7: A hypothetical arrangement of monomers that could be found in a ω -hydroxy fatty acid-rich cutin. R: aliphatic polyester (Presented directly as in Molina, 2010)

Cutin is similar to suberin in structure and function, but can be distinguished by its chemical composition (see Table 1.3 below) and deposition sites.

Table 1.3: Compositional comparison between cutin and suberin^a (Source: Molina, 2010)

Monomer	Cutin	Suberin
Glycerol 	Substantial	Substantial
Unsubstituted acids 	Minor (C ₁₆ -C ₁₈)	Minor (C ₁₆ -C ₂₆)
α,ω-Dicarboxylic acids (C₁₆-C₂₆) 	Minor ^b	Common and substantial
ω-hydroxy acids 	Major (C ₁₆ -C ₁₈)	Common and substantial (C ₁₆ -C ₂₆)
Substituted ω-hydroxy acids (C₁₆-C₁₈) 	Major	Minor ^c
Fatty alcohols 	Rare and minor (C ₁₆ -C ₁₈)	Common and Substantial (C ₁₈ -C ₂₂)
Ferulate 	Low	High

^aAdapted from Kolattukudy (2001)

^bC₁₆-C₁₈ dicarboxylates are major monomers in *Arabidopsis* and *Brassica napus* cutin (>50%).

^cIn some cases is substantial. Substituted dicarboxylic acids and α,ω -diols are also frequently found in suberins.

The outer-facing wall of epidermal cells in the leaves and stems contain some waterproofing, due to the presence of cuticle. Since young roots must be able to absorb water, their epidermal cells do not generally possess cuticle, but a very rudimentary cuticle composed of cutin may occur in the outer epidermal cells of some roots (Forbes and Watson, 1992). PAHs may be adhered by non-polar hydrophobic

interaction to the walls of the root epidermal cells due to the hydrophobic character of cutin.

Root hairs are microscopic extensions of root epidermal cells and they greatly increase the surface area of the root (see Fig. 1.5 b-d). They provide greater capacity for absorption of soil ions and, to a lesser extent, soil pore water. Water enters the root most readily in the apical part of the root which includes the root hair zone (Taiz and Zeiger, 1998). Studies carried out by Jones et al. (1995) on *Limnobium* root hairs using a vibrating microelectrode highlight the importance of root hair number for calcium ion (Ca^{2+}) uptake and root hair length for potassium ion (K^+) uptake (Neergaard et al., 2000). Another study carried out by Gahoonia and Nielsen (1998) using radioactive phosphorous (P^{3+}) provided direct evidence on the substantial participation of root hairs in the uptake of phosphorous from soil.

Ample moisture and a good oxygen supply are necessary to promote abundant development of root hairs, whereas a very concentrated soil solution and extremes of temperature retard root hair development (Weaver, 1926). As regards hydrophobic pollutants, a study carried out by Alkio et al. (2005) on *Arabidopsis thaliana* grown on phenanthrene-containing growth medium, showed a drastic inhibition of root hair development. Possibly the presence of hydrophobic petroleum hydrocarbons may act as a water-impermeable barrier in soil and interfere with the movement of water in soil pores, and this consequently will affect the supply of water and oxygen to root hairs in contaminated soil matrix. Additionally, PAHs possess darker, solar radiation absorbing properties and may raise the soil temperature to unfavourable degrees (Merkl et al., 2005). The aspects will be further considered in the present work.

Root cortex

The zone between epidermis and endodermis, consisting of many layers of cells is termed cortex. The cortex is the largest organ of primary roots and is important for storage and transport (Brundrett, 2008, 1999). Barcelo et al. (1988) have shown an increase in the cortical zone due to differences in the arrangement and shape of cortex cells in bush bean stems exposed to cadmium (Cd) toxicity. As PAHs could impose toxic effects on plant roots (Merkl et al., 2005), it is of interest to study the differences in root cortex due to exposure to PAH contamination.

Endodermis

The endodermis is the innermost boundary of the cortex. It executes a major function in regulating nutrient transfer and solute uptake into root stele. Endodermis is considered as the plant's 'physiological sheath', a structurally specialised layer, which also protects the plants against stress (Enstone et al., 2003). The primary cell wall of all root cells is composed of cellulose microfibrils embedded in a highly hydrated, amorphous matrix, consisting of two major groups of polysaccharides called hemicelluloses and pectins, plus a small amount of structural proteins (Taiz and Zeiger, 1998). Endodermis has lignin and to a lesser extent suberin incrustated into the framework of the primary wall (Shreiber 1996; Shreiber et al., 1994), forming a well-characterised feature in the anticlinal walls of its cells, termed Casparian strip (Enstone et al., 2003). Both lignin and suberin are highly hydrophobic, preventing the ready passage of water (and ions) into the root, but differ in chemical composition: Lignin (see Fig.1.8) is a highly heterogeneous biopolymer comprised of phenylpropanoid residues covalently linked by non-specific oxidation reactions triggered by peroxidase, Suberin (see Table 1.3) is a protective lipid composed of glycerol esterified to fatty acids but enriched in carboxyl and hydroxyl groups (Schulz, 2008).

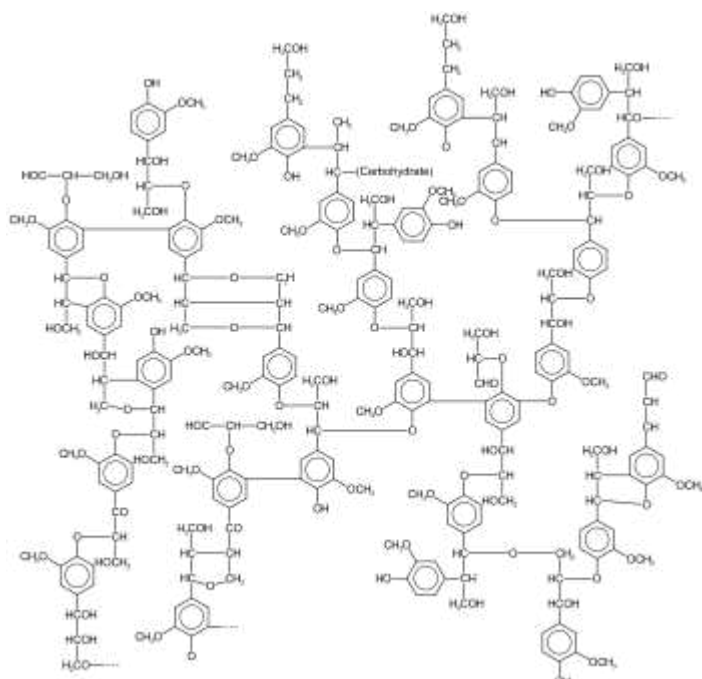


Fig.1.8: Lignin structure

Several investigators have shown that the endodermis Casparian band blocks the passage of various ions, heavy metals and fluorescent dyes from entering the stele, beginning with the classic work of de Rufz de Lavison in 1910 (Enstone et al., 2003). In many plants, suberin lamellae, the major biopolymers of which are suberin and, in lower amounts, lignin (Zeier, 1999), are deposited as secondary walls in the mature endodermis (Enstone et al., 2003), mostly in the inner walls (Schulz, 2008). Suberin lamellae are hypothesised to consist of a suberin poly aliphatic domain and a suberin poly phenolic domain (Bernards, 2002). Suberin lamellae form a hydrophobic covering around the cell, except in those regions occupied by plasmodesmata. Suberin lamellae protect against pathogen invasion and possibly root drying during times of stress (Enstone et al., 2003). Although many species, particularly woody eudicotyledons, do not develop cell wall modifications beyond suberin lamellae in their endodermis, most grasses and a few eudicotyledons develop thick, tertiary layers (Enstone et al., 2003). This tertiary cell wall thickening is generally asymmetrical, being thinner on the outer tangential wall than on other walls (Esau, 1965). The major component of tertiary walls is cellulose, which may be impregnated with lignin (Esau, 1953), but lignin can be the major component of last-deposited tertiary wall materials (Scott and Peterson, 1979). Suberin is frequently absent or present in extremely low levels in tertiary walls (Zeier et al., 1999; Zeier and Schreiber, 1998). Tertiary walls have been assumed to aid in protecting roots against the tension, perhaps due to water stress (Enstone et al., 2003). Due to the presence of suberin and lignin, the absorption of water to the cell walls is limited, whereas absorption of hydrophobic substances may be favoured, in the mature endodermis.

Enstone et al. (2003) and Soukup et al. (2004) have reported an accelerated maturation of endodermis when plants are exposed to stress conditions such as salinity and drought. The presence of petroleum hydrocarbons in soil presents many stress factors including water stress for the growth of plant roots (Merkl et al., 2005). Hence, understanding how the exposure to petroleum hydrocarbon-contamination influences this root ultrastructure could shed light on the practical applications in plant resistance to the contaminated environment. Key structural components of root cells, such as cellulose, proteins, hemicellulose, lignin, pectin, and suberin, differ in proportion/ volume along a developing root. It is hypothesised that the progressional changes in cellular structure from the root tip to the branching zone is likely to affect

the uptake of organic chemicals including PAHs (Wild et al., 2005). So, a study on the endodermis of plant roots exposed to the petroleum contaminants also merits attention in the context of uptake of the toxic PAHs by plant roots.

Stele

The centre of the root is called the vascular cylinder or stele and is enclosed by the endodermis. Conducting elements, consisting of xylem and phloem are located within the vascular cylinder. The phloem transports photosynthetic sugars from the leaves to other plant organs such as roots. The xylem vessels function in the long-distance transport of water, various nutrients, and signaling molecules throughout the life of the plants (Raven et al., 1999). Two types of xylem vessels are distinguished in a plant root, according to the time of their maturity: (a) protoxylem vessels and (b) metaxylem vessels. Protoxylem vessels mature before the surrounding structures such as xylem parenchyma, pericycle and endodermis have elongated. Mature protoxylem vessels transport water and solute from the root towards the shoot during a period of intense longitudinal growth of the surrounding root tissues (e.g. endodermis). The primary cell walls of protoxylem vessels are not lignified but as they mature, secondary walls are deposited in the form of lignified annular, helical, or reticulate thickenings, allowing the functioning of the protoxylem for some time during a period of passive stretching (Barnett, 1981). The protoxylem vessels are frequently destroyed by the extension of the surrounding tissues. Riser and Keller (1992) have demonstrated localisation of a glycine-rich cell wall protein (GRP 1.8) in the unlignified primary cell walls of the oldest protoxylem elements and also in the corners of the proto- and metaxylem elements of French bean hypocotyls. Riser and Keller (1992) suggested that this GRP 1.8 protein is synthesised by xylem parenchyma cells and secreted into the walls of the adjacent xylem vessels and that this protein fulfils a repair or “filling-in” function for the primary walls of the dead protoxylem vessels that were subjected to intense passive stretching. The metaxylem vessels usually have reticulate and pitted thickenings and mature after the surrounding organs complete their growth. In contrast to protoxylem vessels, they are not destroyed, and constitute the water-conducting tubes of the mature plant (Esau, 1977).

Kubo et al. (2005) reported that the formation of protoxylem and metaxylem vessels is controlled by transcription factors, suggesting a genetic control over the production

of xylem vessels in plants. Environmental influences could have impacts on the expression of genes of an organism. Barcelo et al. (1988) have shown that smaller xylem vessels were produced in bush bean stems exposed to Cd-toxicity, whereas Huang et al. (1991) demonstrated smaller and fewer metaxylem vessels in seminal wheat roots exposed to higher temperature (40°C). Both Barcelo et al. (1988) and Huang et al. (1991) also suggested that water economy of these plants containing smaller or fewer metaxylem vessels was affected or modified. It would be interesting to investigate into the differences in the size and number of the xylem vessels in the roots of the plants grown in soils contaminated with petroleum hydrocarbons.

The effect of transpiration on transport of organic contaminants from soil pore water across the root

The transport of water within the plant, which is known as translocation, is the major mechanism for the movement of nutrients and other components from soil pore water to plant (Bell, 1992). Water and solutes are transported upward from the root into other plant parts through the xylem by mass flow resulting from a pressure gradient. This driving force is created during transpiration, where water is drawn in through the root system by capillary action to replace evaporative losses from stomata within the leaves (McFarlane, 1995).

Chemical transfers from the soil into the root are primarily mediated by the uptake of soil pore water during transpiration where contaminants can move from the root system to stems, leaves, and storage organs through the transpiration stream (McFarlane, 1995). In order for chemicals to be taken up into plant roots to reach the xylem, they must first penetrate a number of plant tissues: the epidermis, the cortex, endodermis and pericycle, and need to be dragged along the water transportation pathway (Collins et al., 2006 and references therein; Enstone et al., 2003).

Water is transported into the conducting xylem vessels via apoplastic fluxes or the symplastic stream. In the apoplastic pathway, water and molecules diffuse between cell walls and through intercellular air spaces whilst the symplastic pathway allows entry of molecules into the root cell cytosol after transport across the cell membrane or plasmodesmata (Fig.1.9) (Wild et al., 2005).

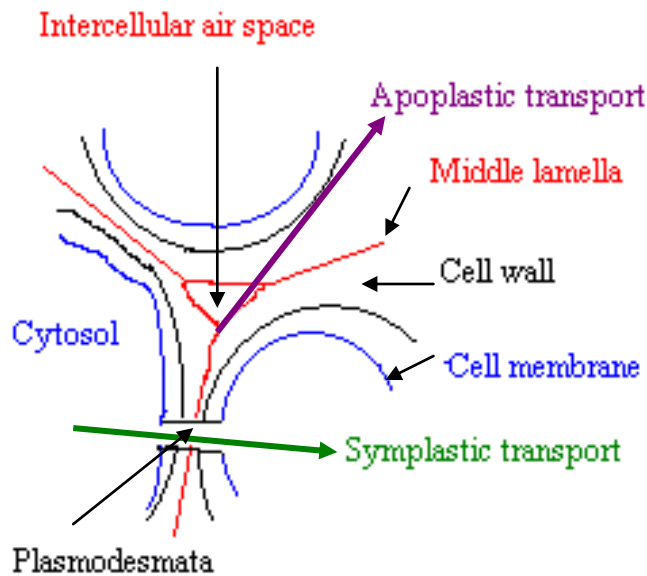


Fig.1.9: A diagram showing apoplastic and symplastic flow of water and solutes through adjacent cells (Adapted from: Brett and Waldron, 1996).

At the endodermis, which is a layer of cells packed with no intercellular space, separating the cortex from the central cylinder (Esau, 1977), molecules in symplastic stream are shunted from the symplastic pathway into apoplastic stream (Wild et al., 2005; Enstone et al., 2003). The endodermis effectively functions as an apoplastic transport barrier and subjects further solute uptake from the soil in the symplast to a cytoplasmic control (Esau, 1977). Molecules in the apoplastic stream or symplastic pathway can be blocked from entering the stele by the Casparian bands in the endodermis (see Fig. 1.10 A). However, not all endodermal cells develop Casparian bands or suberin lamellae and these cells are called passage cells. Passage cells, if present, are generally situated opposite to the proto xylem poles, and solutes and water could enter the vessel elements unimpeded via the passage cells (Enstone et al., 2003). Lateral roots generally appearing on a defined number of ranks on the mother root also face the internal xylem poles of the primary root (Pages et al., 2000). If Casparian bands are formed in the hypodermis, i.e. the cortex layer just beneath the epidermis, it is called exodermis (see Fig. 1.10 D). If exodermal Casparian band structures are present in a plant root, the restrictions on the apoplastic inflow of solutes occurs near the root surface (see Fig. 1.10 D) (Enstone et al., 2003).

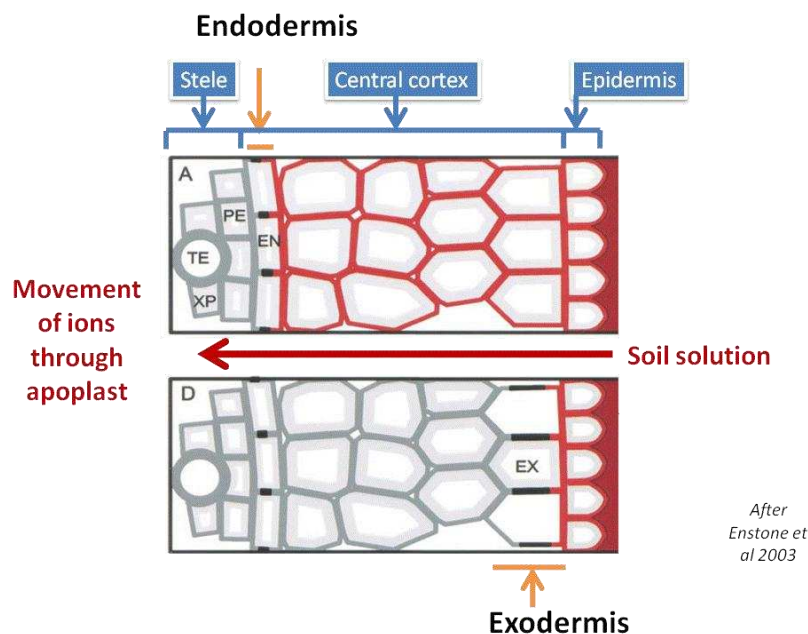


Fig. 1.10: Partial cross sections showing, A (above): a root with a mature endodermis and immature or absent exodermis; D (below): a root with mature endodermis and exodermis, illustrating the movement of apoplastic ions (red) within roots. Intensity of red signifies ion concentrations. Key: EN: endodermis; EX: exodermis; PE: pericycle; TE: tracheary element; XP: xylem parenchyma. Casparian bands are indicated by black areas in the walls (After Enstone et al., 2003).

Nile red as a vital, hydrophobic probe in modelling the passage of hydrophobic xenobiotics such as PAHs

Nile red (9-diethylamino-5H-benzo[α] phenoxazine-5-one) (Fig. 1.11) is a fluorescent dye with a hydrophobic character.

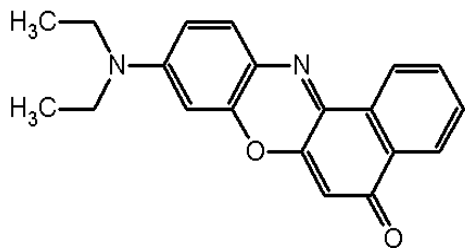


Fig. 1.11: Structure of Nile red

Nile red is poorly soluble in water, and the fluorescence of the dye is quenched in water. It is strongly fluorescent, but only in the presence of a hydrophobic environment. It dissolves in a variety of organic solvents. Partition coefficients of Nile red relative to water are ~200 (Greenspan and Fowler, 1985). The dye is very soluble in the lipids it is intended to show, but does not dissolve the lipids it is supposed to reveal (Greenspan et al., 1985). Furthermore, Nile red stains living cells, being highly membrane-permeable and not acutely toxic to living cells at nanomolar

concentrations (Diaz et al., 2008). These characteristics make Nile red as an excellent hydrophobic probe as well as a vital stain (Diaz et al., 2008; Greenspan et al., 1985).

A study carried out by Greenspan et al. (1985) on cytoplasmic lipid overloading of cultured aortic smooth muscle cells and peritoneal macrophages showed that, when measured at excitation wavelengths of 487-489nm and emission wavelengths of 530-550nm, the fluorescence intensity observed in the presence of very low density lipoprotein was 10-to 20- fold greater than in the presence of hepatic microsomal membranes and was 200-to 400-fold greater than that found with defatted albumin. Nile red is also characterised by a shift of emission from red to yellow according to the degree of hydrophobicity of lipophilic substances. Polar lipids (i.e., phospholipids) which are mostly present in membranes are stained in red whereas neutral lipids (esterified cholesterol and triglycerides) which are present in lipid droplets are stained in yellow (Diaz et al., 2008 and references therein). Diaz et al. (2008) showed a good linear relationship of red and green emissions for reference lipids (free cholesterol, oleyl cholesteryl ester, triolein, oleic acid, monoolein and phosphatidylcholine) stained with Nile red. The study by Diaz et al. (2008) demonstrated that red/yellow emission ratios ranged from 1.9 for cholesterol ester to 82.1 for monoolein and that the ratios were highly discriminated for all lipids tested. Additionally, Nile red emission is virtually absent in the blue region, so that Nile red may be used in combination with other important blue-emitting probes such as DAPI (Diaz et al., 2008). The affinity of Nile Red to bind to hydrophobic molecules suggested that it might be used as a tool to probe the passage of uptake of organic pollutants by roots.

The effect of root lipids content on root uptake of petroleum hydrocarbons

Organic contaminants such as PAHs can be absorbed by the roots for subsequent storage, metabolism or translocation via the transpiration stream (Fismes et al., 2002; U.S.EPA, 1999; Wenzel et al., 1999), and this is termed phytoextraction. Phytoextraction is considered as a minor phytoremediation pathway in the remediation of petroleum hydrocarbons (Merkl et al., 2005). Several investigators such as Verdin et al. (2006), Wild et al. (2005), Alkio et al. (2005) and Gao et al. (2004) have documented root absorption and uptake of PAHs. Alkio et al. (2005)

have shown internalisation of phenanthrene in the root and leaf tissues of *Arabidopsis thaliana* with the use of gas chromatography-mass spectrometry (GC-MS) and fluorescence spectrometric techniques. Here plants were grown on Murashige and Skoog (MS) medium supplemented with 0.5 and 0.75 mM of phenanthrene (Alkio et al., 2005). Similarly, Verdin et al. (2006) have shown intracellular accumulation of the low molecular weight PAH, anthracene, in the root cell lipid bodies of chicory (*Chicorium itybus*) grown on nutrient medium containing 140mg L⁻¹ anthracene (Fig.1.12). However, it is important to note that the plants were grown hydroponically in nutrient medium in both studies, so that no competitive sorption could have occurred between PAHs and the organic carbon, as would have been the case had they been grown in soil. Hence, a correction factor for sorption of the PAHs to SOM may need to be applied when predicting PAH uptake in field conditions, when using the results of these studies.

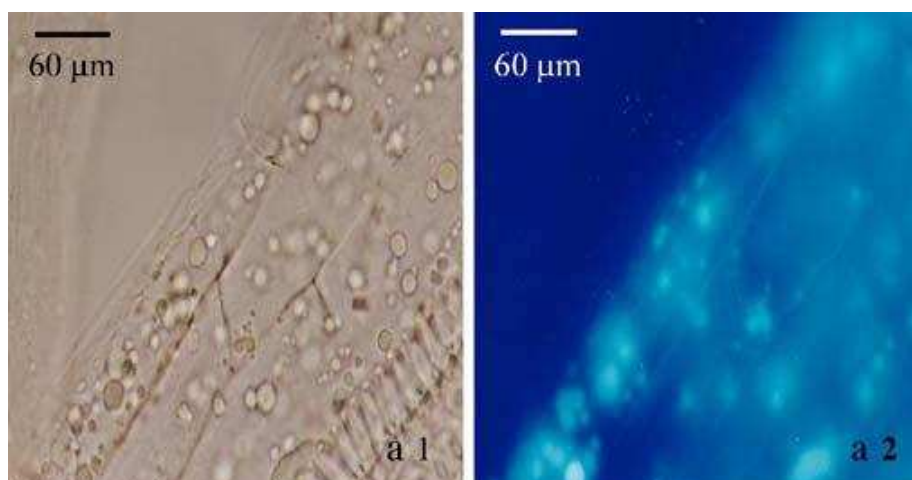


Fig. 1.12: Chicory root cells (a1)-Bright field and (a2)- fluorescence using standard DAPI filter set. No fluorescence was detected in lipid bodies of the control in comparison to cultures grown in the presence of PAH (Directly presented as in Verdin et al., 2006)

Another study carried out by Gao et al. (2004) in which 12 different species of plants were grown in phenanthrene or pyrene-spiked soil, containing 1.45% of organic matter (w/w), revealed that PAHs accumulated in the roots, with pyrene levels being higher than those of phenanthrene. Higher log K_{OW} values denote a higher degree of hydrophobicity. Since highly hydrophobic substances can be adsorbed to lipophilic plant components easily, this is likely to have resulted from the higher log K_{OW} values of pyrene than that of phenanthrene (Gao et al., 2004). This finding is however, contradictory to the results of the study carried out by Zohair et al. (2006),

where PAH burden in potatoes and carrots was dominated by low molecular weight compounds, and BCFs (soil-crop bio concentration factors) were shown to decrease with increasing log K_{ow} . The facts that the soil was experimentally spiked with PAHs and had only 1.45% of organic matter in the study by Gao et al. (2004), whereas the crops were grown in organic farm soil with organic matter content ranging from 3% to 5% in the study by Zohair et al. (2006) could explain the differences between the two results.

The study by Gao et al. (2004) showed that different concentrations of phenanthrene and pyrene occurred between different plant species (Fig. 1.13 & 1.14). These differences were positively correlated ($p < 0.05$) with root lipid contents of the plants (Phenanthrene $R^2 = 0.79$; Pyrene $R^2 = 0.86$; $N = 12$) (Gao et al., 2004). The contribution from plant uptake to soil PAH removal was negligible ($< 0.01\%$ for phenanthrene and 0.24% for pyrene) in the study by Gao et al. (2004). Still, this study was suggestive of translocation from root to shoot as the major pathway of shoot accumulation of PAHs.

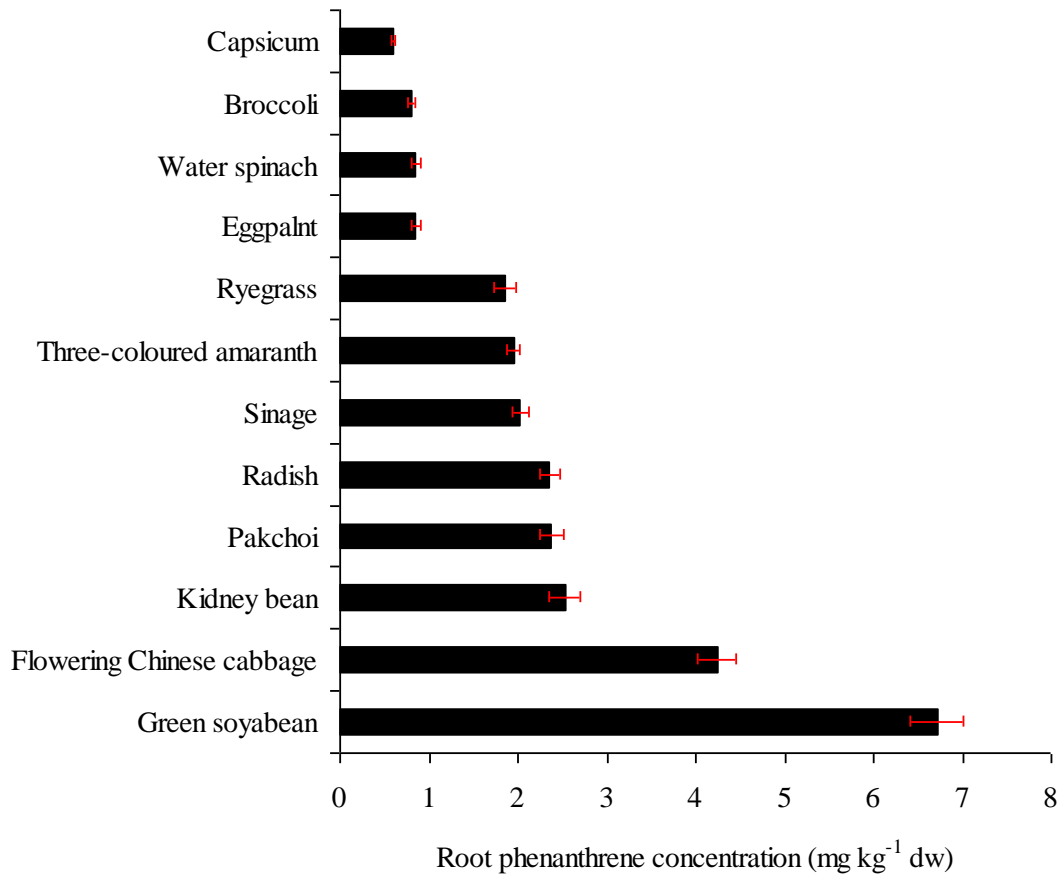


Fig. 1.13: Root concentrations of phenanthrene (dw) for plants growing in spiked soils (soil pH 5.05, organic matter 1.45%) with initial phenanthrene concentration of 133mg kg^{-1} , after 45 days of exposure to the PAH. Bars show standard error of the mean (Adapted from: Gao et al., 2004)

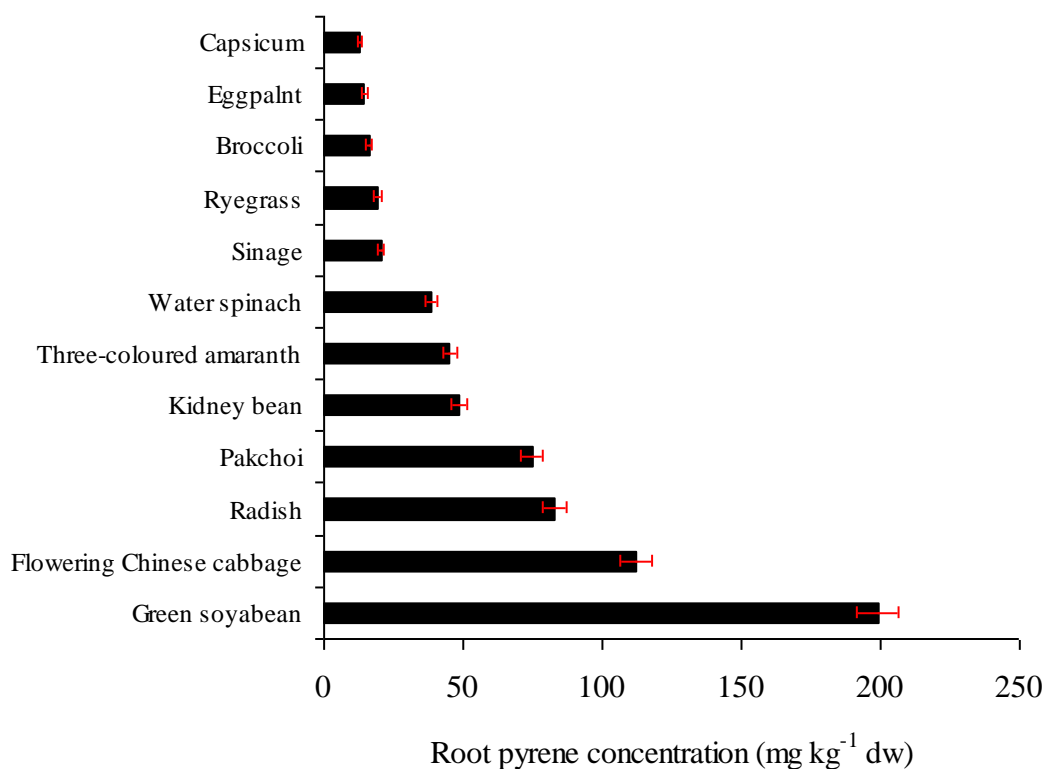


Fig.1.14: Root concentrations of pyrene (dw) for plants growing in spiked soils (soil pH 5.05, organic matter 1.45%) with initial pyrene concentration of 172mg kg⁻¹, after 45 days of exposure to the PAH. Bars show standard error of the mean (Adapted from: Gao et al., 2004).

Chiou et al. (2001) also suggested that plant lipids are a major factor in causing differences in plant uptake of lipophilic contaminants. Additionally, peeling carrots and potatoes removed 55.9-100% of PAH residues, depending on crop variety and contaminant properties (Zohair et al., 2006). Here, the higher lipid content in peels than that in their corresponding cores could explain the removal of organic pollutant residues by peeling (Fismes et al., 2002; Chiou et al., 2001). Even though there was no correlation for PAHs with either carrots or potatoes, stronger correlations of polychlorinated biphenyls (PCBs) and organochlorine pesticides (OCPs) in soil and their uptake by carrots than potatoes were found (Zohair et al., 2006), and this could be due to the presence of oil channels in carrots (Kipopoulou et al., 1999; WHO, 1998). Here oil channels refer to secreting ducts that secrete and store essential oils and can be found either on the surface of plants or within the plant tissue (Glisic et al., 2007).

Moreover, a light and laser scanning microscopic study carried out by Scheer (2006) using 405nm as the excitation wavelength on petroleum crude oil (16.5g total extractable hydrocarbons kg^{-1} sand dw)-treated tall fescue root fragments revealed oily droplets on the surfaces of the treated roots (Fig.1.15), but strong fluorescence associated with petroleum hydrocarbon molecules was not detected beyond the depth of 48 μm (Fig.1.16).

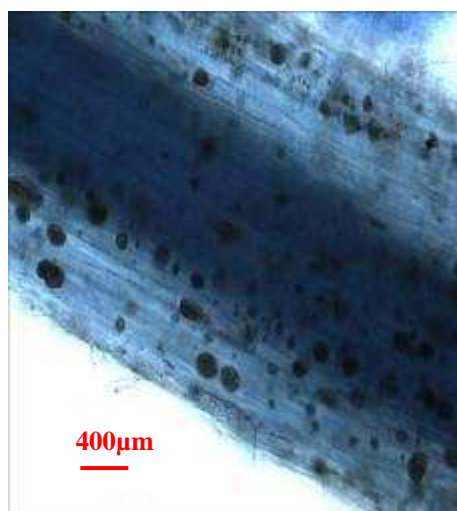


Fig.1.15: Light microscopic observations of crude oil (16.5g total extractable hydrocarbons kg^{-1} sand dw)-contaminated tall fescue root fragment. Scale: 400 μm (After Scheer, 2006).

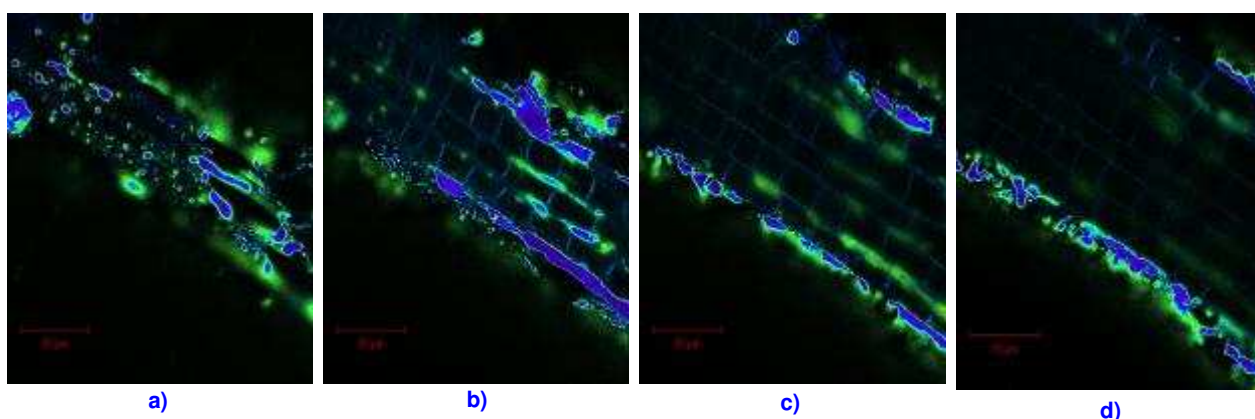


Fig.1.16: Laser scanning microscopic images (Z-series) of the root fragments of tall fescue grown in petroleum crude oil-contaminated sand (16.5g total extractable hydrocarbons kg^{-1} sand dw), at the depths of
a) 0 μm b) 19.2 μm c) 28 μm and d) 48 μm (After Scheer, 2006).

These microscopic observations by Scheer (2006) suggest that hydrocarbon molecules were adsorbed onto the root surfaces, but penetration of these xenobiotic compounds into the central cylinder where conducting vessels are located, may not have occurred in tall fescue roots growing in petroleum hydrocarbon-contaminated sand. It has been assumed that mobile pollutants are drawn into the rhizosphere via transpiration stream, and that a limited amount of PAH uptake by plants takes place (Harvey et al., 2001), but the xenobiotic compounds may not reach the xylem vessels which represent the predominant route for the long distance transportation towards the shoots. Hence, the PAHs taken up by plant roots may not reach the shoots.

Similarly, Wild et al. (2005) demonstrated that the radial movement of anthracene and phenanthrene did not extend beyond the cortex cells of the roots of maize and wheat grown in a contaminated sand medium, over a 56-day growth period. Wild et al. (2005) have shown highly focussed streaming of the xenobiotic compounds within the cortex of the plant roots, but also demonstrated that the xenobiotic compounds did not pass beyond the base of the roots into the stems. Additionally, the uptake and movement of anthracene within maize cell walls was approximately 3 times slower than that of phenanthrene, presumably reflecting differences in the solubility of the PAHs tested. Also, the uptake of both anthracene and phenanthrene were approximately 3 times slower in wheat than in maize, perhaps due to differences in lipid composition of the cell walls between the two plant species (Wild et al., 2005). Furthermore, similarly as Harms (1996), Wild et al., (2005) reported that anthracene was located predominantly within the cell walls. Meagher (2000) suggested that the plants isolate toxic xenobiotic compounds from the metabolic powerhouse of the cytoplasm, by sequestering them in either cell walls or vacuoles, presumably as a protective mechanism. Hence, the passage of PAHs across the root tissues could be predominantly apoplastic.

The effect of enzyme complements on catabolism of hydrocarbons within the root tissues

The metabolic breakdown of complex molecules into simpler ones, often resulting in a release of energy is termed catabolism. Catabolism of petroleum hydrocarbons within a biological system helps to achieve complete mineralization of the compounds

to non-toxic end products such as CO₂ and H₂O and is typically undertaken by rhizospheric heterotrophic micro organisms. Plants which are phototrophic do not need to catabolize/ mineralise these compounds for energy extraction purposes, but appear nevertheless to catabolize them to non-toxic intermediates that are then stored in vacuoles or excreted into the cell wall. Since hydrocarbons are virtually insoluble in water, more highly reduced than cellular molecules, and chemically unreactive, they require specialised enzymes for their initial oxidation which is an essential prerequisite before they can be incorporated into cellular material or metabolised. Oxidation often means the removal of hydrogen atoms or electrons from the substrate, however, in the case of plant oxidation of hydrocarbons, the initial step of hydrocarbon oxidation usually requires the addition of an oxygen atom from atmospheric oxygen. There are two classes of direct oxidation:

- a. those in which both atoms of a molecule of O₂ are added to the hydrocarbon, catalysed by dioxygenases &
- b. those in which only one atom of O₂ is added, catalysed by mono-oxygenases (Jenkins, 1992).

The addition of an oxygen atom increases both the solubility and the chemical reactivity of the hydrocarbon (Meulenberg et al., 1997; Wilson and Jones, 1993; Sutherland, 1992). However, plants must carry the genes which code for the synthesis of these enzymes required for the oxidation of hydrocarbons. Oxidation of hydrocarbons within plant tissues depends both on the genetic composition of the plant and the type of hydrocarbon molecules (Phillips et al., 2006; Siciliano et al., 2003; Jenkins, 1992).

Short-chain n-alkanes (<C₉) are soluble in water and can be found in higher concentrations in water, therefore they are toxic to organisms. They bind to membrane lipids and proteins and thereby cause disorganisation of the plasma membrane. n-Alkanes of the C₁₀ – C₂₂ range are usually readily metabolised, but higher molecular weight alkanes tend to be solid waxes and are not readily biodegraded. Unsaturated compounds and branched-chain compounds are also less readily biodegraded. Monocyclic aromatic hydrocarbons can be toxic, but in low concentration can be metabolised. Polycyclic aromatic hydrocarbons (PAHs) with two to four rings are biodegraded at the rates that decrease with increase in the

number of rings the PAH possesses. PAHs with five or more fused rings resist biodegradation. At low concentrations, cycloalkanes are degraded at moderate rates, but highly condensed cycloalkanes are resistant to biodegradation (Farrell-Jones, 2003; Jenkins, 1992).

Adhesion between the cell and a hydrocarbon droplet followed by solubilisation of the droplet by specific agents may promote the entry of the droplet into the cell. Once inside a biological system, hydrocarbons, especially n-alkanes ($>C_9$ or $C_{10} - C_{22}$) are initially oxidised to the corresponding alcohol (n-alcohol) via the mono-oxygenase class of enzymes (Jenkins, 1992). Metabolic studies have shown that a reducing agent such as NADH or NADPH has to be present, and is oxidised concurrently with the hydrocarbon molecule. Sufficient activation of the rather stable O_2 molecule to be split into two atoms is achieved by linking the mono-oxygenase enzymes to one or more of several different electron-carrier systems such as cytochrome P_{450} (Harvey et al., 2001 and references therein). Pairs of electrons are transferred from NADPH or NADH via electron-carrier proteins to the mono-oxygenase. The enzyme then adds a single atom from molecular oxygen to the hydrocarbon and forms the corresponding alcohol and water (Fig. 1.17). The mono-oxygenases are termed hydroxylases since a hydroxyl group is formed. They are also called mixed function oxidases as they oxidise a wide variety of substrates (Jenkins, 1992).

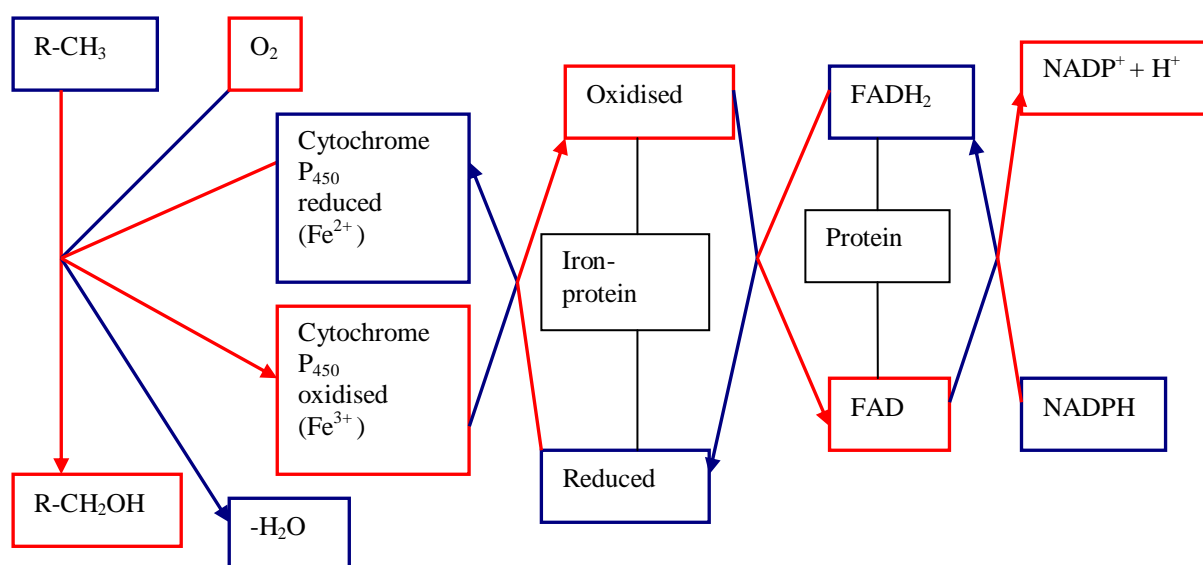


Fig. 1.17: The pathway of oxidation of n-alkanes to primary alcohols via cytochrome P_{450} system. Blue textboxes/ lines/ arrows indicate reduced molecules/ reduction path; Red textboxes/ lines/ arrows indicate oxidised molecules/ oxidation path (Adapted from: Jenkins, 1992).

Further oxidation of primary alcohols proceeds via the aldehyde to the corresponding monocarboxylic acid (fatty acid), catalysed by the enzyme called dehydrogenase that removes hydrogen atoms from the hydrocarbons (Jenkins, 1992) (Fig. 1.18).

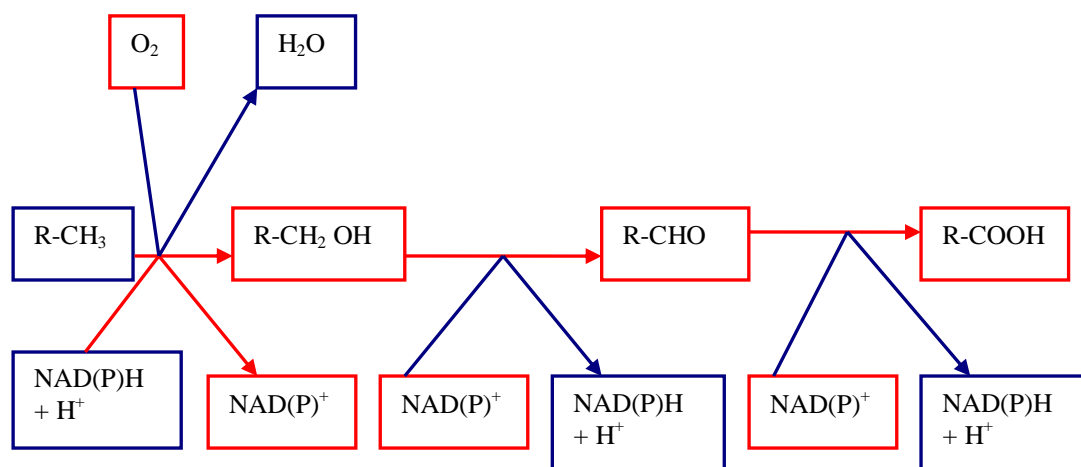


Fig. 1.18: Pathway showing subsequent oxidation of primary alcohols to the corresponding monocarboxylic acid. Blue textboxes/ lines/ arrows indicate reduced molecules/ reduction path; Red textboxes/ lines/ arrows indicate oxidised molecules/ oxidation path (Adapted from: Jenkins, 1992).

Subsequent metabolism of fatty acids could occur following the same pathway as that involved in lipid metabolism, such as β -oxidation pathway. This could lead to the

generation of acetyl CoA, succinyl CoA and pyruvate molecules and eventually produce CO₂ and H₂O (Meagher, 2000; Jenkins, 1992).

The ability of plants to catabolise hydrocarbons, especially aromatic hydrocarbons, is extremely limited, perhaps due to the inadequacy of the enzyme systems required for PAH-degradation within plant tissues (Harvey et al., 2001 and references therein; Jenkins, 1992). Furthermore, plants do not require these compounds as a source of carbon and energy as micro organisms do. Nevertheless, metabolism of PAHs inside the plant root tissues may occur, depending on several factors such as the growth medium, the genetic composition of the plant, the concentration and physico chemical characteristics of the PAH. Wild et al. (2005) have shown degradation of anthracene to the partial breakdown products anthrone, anthraquinone, and hydroxyanthraquinone in the zones of root elongation and branching of maize root, through in situ visualisation of the movement of these xenobiotic compounds that chemically auto-fluoresce inside living plant tissues, using two-photon excitation microscopy (TPEM). It has been suggested that the activity of most enzymes and enzyme systems change in different growth zones of the root and that the enzymatic activity is relatively high in the mature zones. The cells in the zone of elongation possess a complete profile of enzyme systems and the activity of some enzymes including those associated with PAH uptake and assimilation increase after elongation (Kolek and Kozinka, 1991). Anthracene degradation was principally observed in the mature region of the root, presumably because the enzymes involved in PAH-degradation were sufficiently developed in the mature zone of the plant roots (Wild et al., 2005).

Furthermore, investigations carried out by Kolb and Harms, 2000, Huckelhoven et al., 1997, Sandermann, 1994 and Harms et al., 1977 on fluoranthene, pyrene and benzo (a) pyrene in plant cell suspensions demonstrated biotransformation of the PAHs into hydroxyl-PAHs or PAH-quinones. These PAH metabolites are often considered to be conjugated with glucose, glucuronic acid or other cell wall components via the mono-oxygenase pathways (Meudec et al., 2006 and references therein; Harvey et al., 2001 and references therein; Kolb and Harms, 2000). According to Schnoor et al. (1995), remediation can occur by the direct uptake of the contaminant into vegetative tissues,

resulting in transformation by plant enzymes, sequestration within the plant, or transpiration through leaves.

Root Exudates

Roots may modify the physical, chemical and biochemical characteristics of the soil in their vicinity (rhizosphere) by not only absorbing nutrients and other components in soil pore water, but also by releasing different compounds such as root border cells and root exudates (Grayston et al., 1996). Synthesizing, accumulating and secreting a diverse array of compounds are specialized processes mediated by roots in the rhizosphere. The chemicals secreted by roots into the soil are broadly classified as root exudates. Nearly 5% to 21% of all photosynthetically fixed carbon is transferred to the rhizosphere through root exudates, representing a significant carbon cost to the plant (Walker et al., 2003). Root exudates have been traditionally classified into low- and high-molecular weight compounds. Low-molecular weight compounds such as amino acids, sugars, organic acids and phenolics comprise the majority of root exudates. Micro organisms can modify and degrade low molecular weight exudates like citric acid and phenolic compounds (Engels et al., 2000). High-molecular weight compounds primarily include mucilage and proteins. Root exudates act as chemical messengers that communicate and initiate biological and physical interactions between roots and soil organisms, and participate in regulating the soil microbial community in the rhizosphere (Walker et al., 2003). Therefore this remarkable metabolic feature of plant roots is important in plant-promoted biodegradation of organic compounds.

Roots of specific plants may demonstrate diurnal rhythms and localization of enhanced exudation as adaptations to particular environmental conditions (Engels et al., 2000). For example, enhanced release of organic acids in phosphorous-deficient rape (Hoffland et al., 1989) or of phytosiderophores in iron-deficient maize (Romheld, 1991) is largely confined to the root tip (apical cm), and this is expected to increase the efficiency of exudates in mobilizing phosphorous and iron in the rhizosphere as the density of micro organisms which may catabolize exudates is higher in basal root zones than in the apical region (Uren and Reisenauer, 1988). Moreover, the distinct diurnal rhythm exhibited by iron-deficient plants (Marschner et

al., 1986) for the release of phytosiderophores, may increase the probability that phytosiderophores mobilize iron in the rhizosphere before being degraded by microorganisms (Engels et al., 2000).

Root exudation patterns of plant roots can also influence the redox state of the rhizosphere. For example, the release of reducing substances (Marschner et al., 1986) such as phenolic acids or carboxylic acids (Dinkelaker et al., 1996, 1993; Hether et al., 1984) can increase the availability of Fe and Mn through the reduction of Fe or Mn oxides, especially in soils of neutral or alkaline pH (Cairney and Ashford, 1989). Contrastingly, excessive uptake of reduced Fe, Mn and sulphides is avoided by an increase in the redox potential of the rhizosphere of marsh plants such as rice, by diffusion of oxygen from the shoot to the roots and subsequent release into the rhizosphere (Trolldenier, 1988).

The presence of petroleum hydrocarbons in soil changes the rhizosphere environment of plant roots. Survival of any plant species in a particular growth environment depends chiefly on the ability of the plant to perceive changes in the local environment that require an adaptive response. Upon encountering a challenge, roots typically respond by secreting root exudates (Stintzi and Browse, 2000; Stotz et al., 2000) which participate in root-soil contact as well as positive or negative communication with other plant roots and soil organisms (Walker et al., 2003). The pattern of root exudates is not homogeneous between plant species, under different environmental conditions or along the root axis of a plant root (Walker et al., 2003).

An investigation conducted by Gao et al. (2010) on the impact of root exudates on desorption of phenanthrene and pyrene in soils, revealed that the addition of Artificial Root Exudates (ARE) positively influenced the desorption of phenanthrene and pyrene in test soils. Gao et al. (2010) reported that desorption of phenanthrene and pyrene increased with ARE concentration, and particularly higher with the addition of citric and oxalic acid, but decreased with higher soil organic matter (SOM). They attributed the increased desorption of phenanthrene and pyrene in the presence of AREs to the increased dissolved organic matter (DOM) in solution and decreased SOM, and indicated the dominant influence of organic acids on the desorption of the PAHs. They also reported that ageing of the PAHs had a negative impact on

desorption of the compounds. Gao et al. (2010) implied that root exudates conditionally promote the release of PAHs from the soil, enhancing the bioavailability of the PAHs with effects varying with the concentration of root exudates in soil and ageing of the PAHs. Root exudation processes may contribute to improving plant fitness from the point of phytoremediation, because, the presence of particular root exudates can stimulate the proliferation of PAH-degrading micro organisms within the rhizosphere (Phillips et al., 2006; Siciliano et al., 2003). Also some root exudates can keep soils hydrated under drought and drying conditions (Walker et al., 2003) and can soften hard, resistant soils to facilitate root growth (Morel et al., 1991). Since crude oil may impose mechanical impedance and water scarcity on plant roots (Merkl et al., 2005), these features of root exudates could be useful in facilitating the root growth of plants in petroleum hydrocarbon-contaminated soils.

Growth dilution due to phytostimulation or rhizo-biodegradation

As plants grow and their biomass increase over the growing season, the chemical concentration within plant tissues relative to the flux of chemical uptake would be diluted (Collins et al., 2006 and references therein). Growth dilution could also be referred to dilution of PAH-concentration within the dynamic region of the rhizosphere due to increased microbial activities as the root which is important in promoting phytostimulation increases in terms of mass, surface area, length and excretion of root exudates over the growing season, and is of importance in the successful establishment of plants in PAH-contaminated soils. It has been suggested that plants accumulate hydrophobic compounds such as PAHs in the rhizosphere after facilitating their transport toward the roots (Harvey et al., 2001; Liste and Alexander, 2000 b). Remediation predominantly occurs by the rhizosphere-stimulated microbial biodegradation of organic pollutants (Phillips et al., 2006; Gao et al., 2004; Siciliano et al., 2003; Yang et al., 2001; Schnoor et al., 1995). It has been demonstrated that when grown in hydrocarbon-contaminated soil, plants increase the catabolic potential of rhizospheric soil (soil within 1mm of plant roots) by altering the composition of the indigenous microbial communities and proliferating the PAH-degrading micro organisms within the dynamic region of the rhizosphere (Siciliano et al., 2003). Here microbial catabolic potential relates to several parameters such as substrate

specificity, inducer specificity, number of catabolic routes and kinetics of catabolic enzymes (Watanabe et al., 2002).

Certain micro organisms such as bacteria (eg. some species of the genus *Pseudomonas*), filamentous fungi (eg. some species of the genus *Cladosporium*) and yeast (eg. some species of the genus *Candida*) use petroleum hydrocarbons as their sole source of carbon and energy. Additionally, several species of micro organisms are capable of degrading the hydrocarbons including the aromatic hydrocarbons, bringing them back into the carbon cycle and degrading them. Similar to plants, micro organisms also possess electron-carrier systems to facilitate hydrocarbon-degradation, perhaps to a greater extent. In addition to cytochrome P₄₅₀, rubredoxin systems are also found in bacteria. Rubredoxin is quite different from the cytochrome P₄₅₀ system, and only uses NADH as reductant, but produces the same end-products, the corresponding primary alcohol and water. The hydrocarbons are finally degraded to CO₂ and H₂O by micro organisms, as they convert these hydrocarbons into the chemical constituents of the cell (Jenkins, 1992).

Depending on the chemical nature of the individual hydrocarbons, some compounds are utilised readily by many micro organisms, whereas some other compounds resist microbial attack and can be utilised by only a few microbial species. Some micro organisms are not able to assimilate certain hydrocarbons, but they can oxidise these molecules. In mixed communities of micro organisms such as soils, the partially-oxidised hydrocarbon produced by one type of micro organism can serve as a growth substrate for another, leading way to co-metabolism. Here, the presence of one micro organism influencing positively the activity of another is referred to as co-metabolism. Furthermore, the presence of a hydrocarbon molecule may induce the synthesis of two sets of enzymes-one set capable of metabolising the substrate and another capable of metabolising another substrate. This is also an example of co-metabolism (Jenkins, 1992).

The rhizosphere contains a rich organic mixture of root exudates, leaked and secreted compounds, mucilage, and sloughed dead cells, allowing for the proliferation of soil micro organisms (Rentz et al., 2003; Lynch, 1990). An increase of rhizosphere microbial populations over nonrhizosphere populations on the order of 4 to 100 times

has been documented (Chaineau et al., 2000; Jordahl et al., 1997; Crowley et al., 1996).

In an investigation carried out by Liste and Alexander (2000 a, b), the rhizosphere of several plant species including tall fescue and wheat, grown in soil contaminated with phenanthrene and pyrene, temporarily contained appreciably more phenanthrene or pyrene than the unplanted soils, but the PAHs in the rhizosphere were degraded with time. Liste and Alexander (2000 a, b) suggested that the degradation of pyrene and phenanthrene in the rhizosphere was due to the catabolic activities of the rhizospheric micro organisms. Additionally, in a study conducted by Siciliano et al. (2003) the number of soil bacteria that contained genes involved in hydrocarbon degradation were found to be higher in planted treatments composed of a mixture of grasses (Bromus hordeaceus, Festuca arundinacea, Bromus carinatus , Elymus glaucus, Festuca ruba, Hordeum californicum, Leymus triticoides, and Nassella pulchra) and legumes (Trefoil fragiferum, Trifolium hirtum, and Vulpia microstachys) when compared to the unplanted control ($p < 0.05$) (Table 1.4).

Table 1.4: Prevalence of soil bacteria that contained genes involved in HC-degradation: alkB (gene encoding alkane mono-oxygenase), ndoB (naphthalene dioxygenase), and xylE (catechol-2, 3-dioxygenase), isolated on YTS 250 medium from planted and unplanted treatments; averaged over all the sampling points

Treatments	log colony forming units (cfu) g ⁻¹ soil		
	alkB positive bacteria	ndoB positive bacteria	xylE positive bacteria
Planted	6.5	6.5	6.5
Unplanted	5.5	<6	5.5

Source: Siciliano et al., (2003)

Degradation of contaminants is principally based on the catabolic activities of micro organisms and their enzymes (Okoh et al., 2006; Anderson et al., 1993). It has been reported that changes in exudate patterns of plant roots, which are induced by the presence of petroleum hydrocarbons in the rhizosphere, can cause alteration in the number and diversity of rhizospheric micro organisms (Phillips et al., 2006; Walton et al., 1994), with a positive impact on contaminant degradation. The input of easily degradable root exudates such as organic acids improves physical and chemical soil conditions and increases humification and adsorption of pollutants in the rhizosphere.

The root exudates also facilitate desorption of the PAHs, promoting their bio-availability (Gao et al., 2010). The root exudates contribute to the enhanced microbial degradation of PAHs in the rhizosphere because they support larger microbial populations of PAH degraders (Gao et al., 2004; Harvey et al., 2001 and references therein).

Siciliano et al. (2003) reported that mineralization of naphthalene was higher in the rhizosphere of tall fescue (*Festuca arundinacea*) grown in contaminated soil, than it was in the bulk soil ($p < 0.05$). In contrast to this, growing rose clover (*Trifolium hirtum*) resulted in lower PAH-degradation activity in the rhizosphere compared to that in bulk soil ($p < 0.05$) (Siciliano et al., 2003). Other investigators have also reported a strong species dependence on the ability of phytoremediation systems to promote PAH-degradation. This may be attributed to root exudate patterns but also to differences in the root architecture of the plants in question (Siciliano et al., 2003).

In a study carried out on benzo (a) pyrene [B(a)P] degradation using ryegrass (*Lolium perenne* L.), the extractable B(a)P concentration in the planted soil was found to be significantly lower than that in the unplanted control soil at the concentration of 50 mg B(a)P kg⁻¹, suggesting a potential of ryegrass to remediate B(a)P contaminated soil at this concentration (Xing et al., 2006). Similarly, it was observed that the concentration of B(a)P in soil in which alfalfa (*Medicago sativa*) was grown over a period of 90 days, was significantly lower ($p < 0.05$) than in unplanted soil (Liu et al., 2004). In addition to that, Reilley et al. (1996) demonstrated enhanced degradation of anthracene and pyrene by fescue (*Festuca* spp.) and alfalfa (*Medicago sativa*).

Also, it has been observed that PAH-degradation rates increased when alfalfa was inoculated with the arbuscular mycorrhizal fungus *Glomus caledonium* (Liu et al., 2004). Moreover, anthracene degradation has been reported in the presence of chicory plants, and it was found that the degradation was higher when the roots were colonised by the arbuscular mycorrhizae, *Glomus intraradices* (Verdin et al. 2006). Studies by Binet et al. (2001) also show the degradation of anthracene was greater in the presence of mycorrhizal ryegrass roots than in the absence of mycorrhizal colonisation.

Positive contribution of arbuscular mycorrhizal (AM) fungus in phytoremediation is possible through improved root growth by facilitating water and nutrient acquisition - important limiting factors in PAH-contaminated soil. Extra radical mycelium extending from root system can influence PAH degradation, through mycorrhiza-associated PAH degrading micro flora (Joner and Leyal, 2001), but the AM fungus may also participate in the PAH-degradation more directly (Fig.1.19) (Verdin et al., 2006).

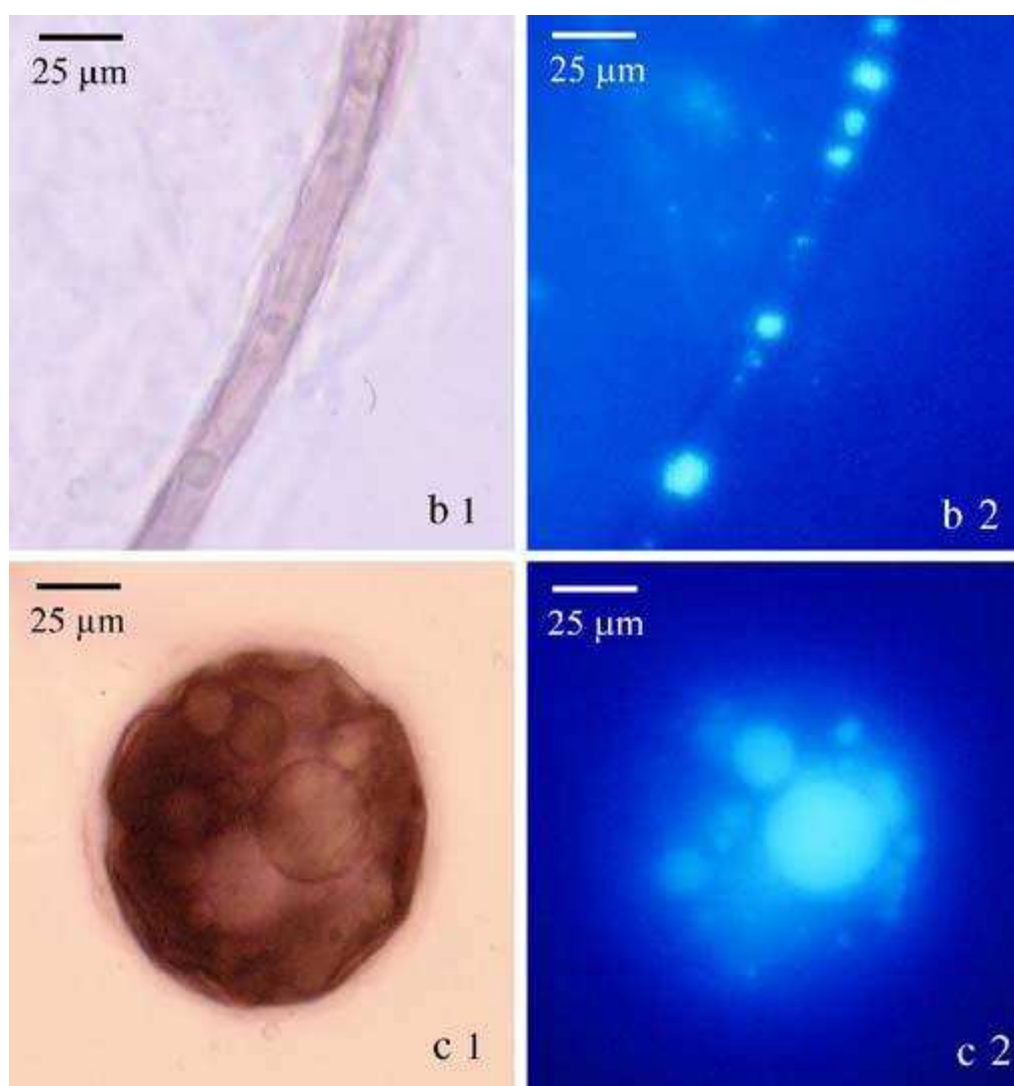


Fig.1.19: Accumulation of anthracene into fungal hyphae (b) and fungal spore (c) of an AM fungus *Glomus caledonium* that was colonizing chicory roots grown on anthracene supplemented medium ($\times 100$ objective lens). 1. Bright field and 2. Fluorescence using standard DAPI filter set (Directly presented as in Verdin et al., 2006).

The degree of hydrocarbon-degradation was found to be greater in the rhizosphere of grasses, possibly due to the differences in cell wall components and root exudate patterns (Merkl et al., 2005; Shann and Boyle, 1994; Anderson et al., 1993).

However, not all grasses contribute positively to remediation, and the fact that a plant is unaffected by contamination is not to be attributed to higher degradation of contaminants. In a study carried out by Merkl et al. (2005 a), soils planted with *Brachiaria brizantha* and *Cyperus aggregatus*, that both showed morphological changes in contaminated compared to uncontaminated soil, had a higher degradation of petroleum than unplanted soil. On the other hand, no significant difference was found in the decrease of petroleum concentrations between a soil planted with *Eleusine indica*, which was unaffected by growth in contaminated soil, and its control. The reason why *Eleusine indica* did not have a significant impact on degradation is perhaps due to its small root surface area, being in itself not large enough to promote the proliferation of hydrocarbon-degrading micro organisms (Merkl et al., 2005 a). The characteristics of soil, the type and amount of oil contaminants, the species of plants and their root architecture, the indigenous micro flora in the soil and the environmental conditions (i.e. temperature, rainfall) all limit the effectiveness of phytoremediation (Brandt et al., 2006; Siciliano et al , 2003), which essentially depends on rhizobiodegradation promoting growth dilution in the rhizosphere

1.3 Influence of plants in restoring soils contaminated with petroleum hydrocarbons

Plants enhance the degradation of petroleum hydrocarbons in soil by supporting higher hydrocarbon-degrading microbial populations in the rhizosphere than are found in the bulk soil, (Siciliano et al., 2003), increasing the bioavailability of PAHs, by influencing desorption of PAHs from the soil (Gao et al., 2010), and stabilisation of organic pollutants by polymerisation actions such as humification (Harvey et al., 2001; Walton et al., 1994), whilst also allowing a limited amount of uptake into their cell walls and vacuoles (Wild et al., 2005; Harvey et al., 2001 and references therein). The main pathway of phytoremediation is phytostimulation or rhizo biodegradation, in which the remediation of organic pollutants occurs mainly due to the catabolic activities of micro organisms proliferated by the presence of plant roots within the dynamic region of the rhizosphere (Wild et al., 2005 and references therein; Siciliano et al., 2003). Root architecture, root exudate patterns, cell wall components and genetic composition of the plant in question may give some plants better potential for phytoremediation (Phillips et al., 2006; Siciliano et al., 2003).

1.9 Contaminant exposure pathways and entry of contaminants into wildlife food chain

Plants growing in PAH-contaminated soils can potentially take up PAHs via i) uptake of PAHs in the soil solution through root tissues, ii) absorption of PAHs to the root surfaces, iii) foliar uptake of PAHs which have volatilised from the soil surface, and iv) absorption of PAHs from the atmosphere to leaf surfaces (Collins et al., 2006; Wild and Jones, 1991) (Fig.1.20).

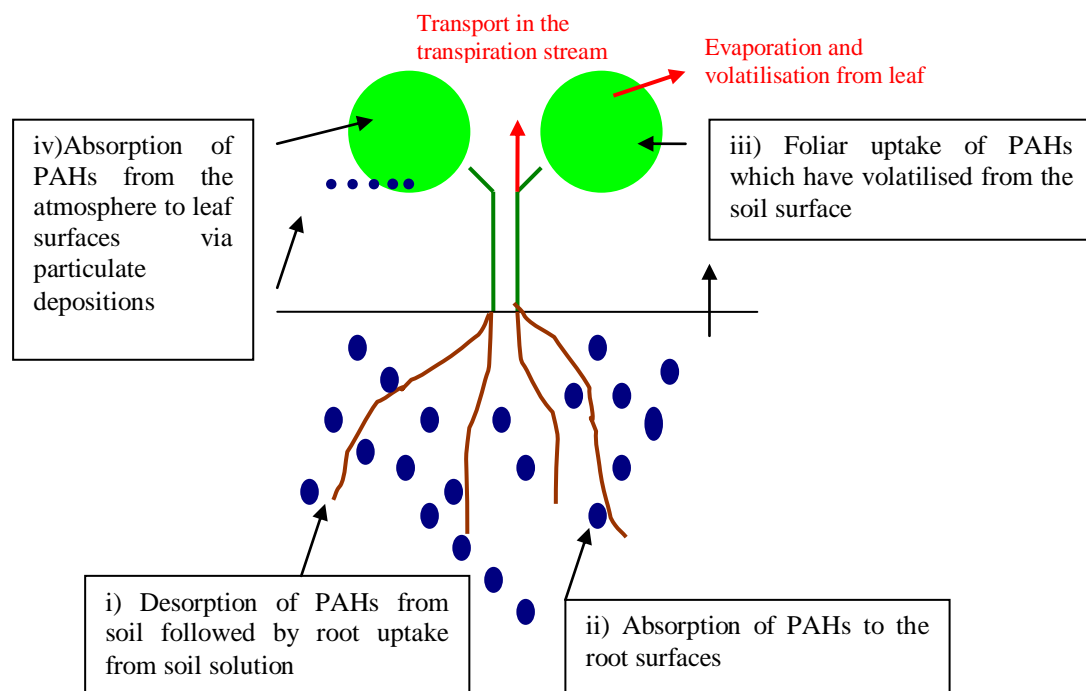


Fig.1.20: Principal pathways for plant uptake of PAHs (Adapted from Collins et al., 2006)

Many studies indicated if PAHs are taken up within plant tissues they are sequestered in either cell wall following conjugation with glucose and/ or other cell wall components or vacuoles. Little is known about the bioavailability of bound metabolites, but there may be a need to prevent the movement of PAHs into wildlife food chains (Harvey et al., 2001).

1.10 Impacts of petroleum hydrocarbon contamination on plants

For phytoremediation to be successful, plants have to establish themselves and grow in contaminated soils which present many stress factors for them such as water,

oxygen and nutrient deficiency and phytotoxicity (Merkl et al., 2005). Plants promote restoration of contaminated sites through plant-initiated biochemical processes, predominantly via stimulating the proliferation of PAH-degrading micro organisms within the rhizosphere (Wild et al., 2005 and references therein). So, a sufficient root growth is essential in phytoremediation applications, in order to support the growth of PAH-degrading micro organisms.

It has been reported that petroleum hydrocarbons inhibit plant growth, and root growth in particular (Merkl et al., 2005; Xu and Johnson, 1995; Currier and Peoples, 1954). Several studies carried out on the morphological differences in plants exposed to petroleum hydrocarbons showed that plant development including root and shoot biomass, root length and root elongation rate are reduced due to growth in contaminated soil, whereas the root diameter was found to have increased under these conditions (Merkl et al., 2005; Bengough, 2003; Bouma et al., 2000; Boot et al., 1990).

Whilst root biomass data express the input of the plant into root construction and maintenance (Bouma et al., 1996), a high specific root length is considered important in terms of water and nutrient acquisition per unit of carbon expenditure (Fitter, 1996; Yanai et al., 1995). Hence the reduction in root biomass and specific root length in plants grown in polluted soil suggest that the plants are at a disadvantage. Plant roots become coarse in crude-oil-contaminated soil, possibly as a stress response to the combination of mechanical impedance, drought conditions, temperature stress and nutrient deficiency which may be imposed on plant roots by crude oil contamination (Merkl et al., 2005). The thicker roots might also result from the increased lignification of cell walls which could be a stress response (Taiz and Zeiger, 1998; Boot and Mensink, 1990) induced by plant metabolism of petroleum hydrocarbons using reducing equivalents (NADH), and thus raising the redox status of the plant cell (Harvey et al., 2001 and references therein)

Also, when plants are exposed to stress, root growth rates decline (Enstone et al., 2003). Bengough (2003) found that mechanical impedance slows root elongation. As heavy crude oil consists of high asphaltenes content, contaminated soil has a higher

mechanical resistance to plant roots than uncontaminated soil (Merkl et al., 2005 a). The mechanical resistance together with other stress conditions could be accountable for the decline in root elongation rate, when plants are grown in hydrocarbon-contaminated soil. Moreover, Rentz et al. (2003) observed that poplar tree roots were unable to penetrate the petroleum smear zones, stained layers that form when petroleum hydrocarbons are sorbed in the unsaturated zone or when floating organic contaminants rise and fall with the water table (i.e. in Heath, Ohio) (Fig. 1.21). Together with relatively high total petroleum hydrocarbon concentrations, anaerobic conditions, which are possibly caused by micro organisms as they utilize the oxygen to metabolize the carbon sources (Lynch, 1990), often characterise the petroleum smear zones (Lee et al., 2001). Layer compaction may have inhibited poplar root growth at the Heath, Ohio, demonstration site, but the shortage of oxygen could also have played a significant role (Rentz et al., 2003).

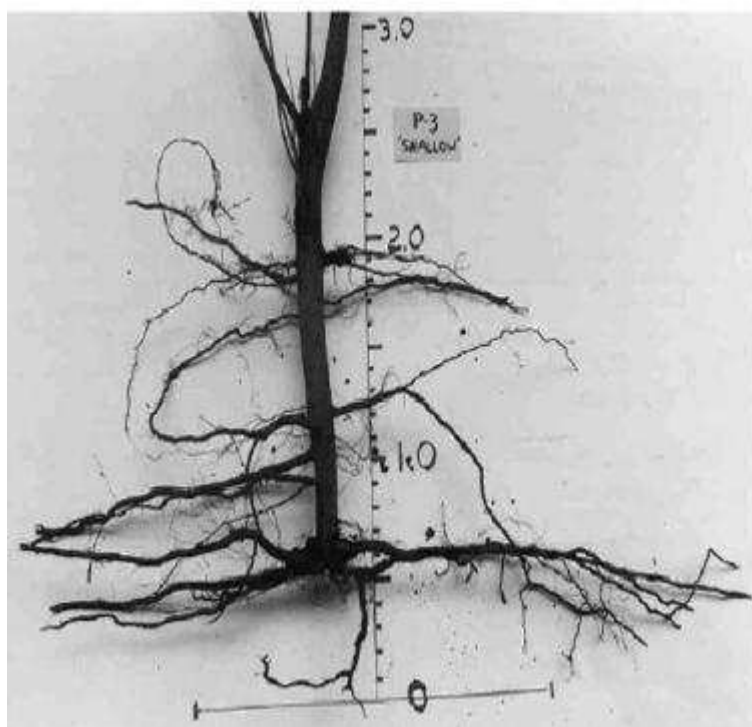


Fig.1.21: Two year old poplar root excavated from Heath, Ohio, phytoremediation site, showing 0.8m of root penetration, which stopped short of the smear zone (1.0m depth) (Presented directly as in Rentz et al., 2003).

Contrastingly, stimulation in plant growth has been documented following low-level crude oil contamination (McCann et al., 2000; Baker, 1973). McCann et al. (2000) conducted a laboratory study on the aquatic macrophyte, *Myriophyllum spicatum*

grown in test tubes, to determine the effect of creosote contamination (according to Mueller et al., 1989, typically, creosote is composed of approximately 85% PAHs, 10% phenolics, and 5% nitrogen-, sulphur-, and oxygen-containing heterocyclics) on the health of this species. Biphasic responses were observed for shoot length, node production and biomass, with shoot length showing statistically significant stimulation at a creosote concentration of 13.3mg L⁻¹ (McCann et al., 2000). Root number was significantly higher at a creosote concentration of 3.6mg L⁻¹ but this was the result of adventitious roots being produced along the length of the stem, as opposed to just at the base of the plant. Root length was found to be significantly reduced at 4.5mg L⁻¹ creosote concentration, even though this was within the concentration range that stimulated shoot growth. So, the increase in shoot growth observed in *Myriophyllum spicatum* here, at low-level creosote concentration (<13.3 mg L⁻¹) may not be a healthy plant response, as root length was simultaneously inhibited (McCann et al, 2000). The opposing effects observed may be because some components of creosote may have stimulatory effect on plant growth while others have an inhibitory effect, at the same nominal concentration (McCann et al., 2000). Additionally, an increase in pink pigmentation and changes in the location of root initiation were observed in the creosote concentration range that affected root length and numbers. This show the plants were stressed and were growing abnormally (McCann et al., 2000).

Moreover, in phenanthrene-treated 21 days' old *Arabidopsis* plants, the transcript levels of expansins (EXP8), genes which have known roles in cell wall loosening and cell enlargement, were found to be reduced in the reverse-transcription (RT) PCR experiments (Alkio et al., 2005). Phenanthrene-exposed plants also showed an increase in mRNA steady-state levels for PR1, a pathogenesis related protein which takes part in defence pathways (Alkio et al., 2005). Furthermore, a microcosm study carried out to determine the effect of oil sands effluent on cattail and clover showed an accumulation of novel dehydrins, stress proteins that protect plants against drought in the plants grown in the impacted site (Crowe et al., 2001). This may be however, the result of the osmotic nature of the effluent and not necessarily due to the hydrocarbon contamination (Crowe et al., 2001).

Additionally, a diversion in the normal metabolic pathway of plants under the influence of hydrocarbon-contamination has been reported. Significant decrease in the typical aromatic scent of vetiver (*Vetiveria zizanioides* L. Nash) roots was observed when the plants were grown in soil contaminated with crude oil (5% w/w), suggesting a change in plant metabolism (Brandt et al., 2006).

Most studies carried out on the effects of organic contaminants on plant growth used seedlings which were germinated in uncontaminated conditions. A few studies have reported the impacts of PAHs on germination. Smith et al. (2006), for example, carried out a germination and subsequent growth trial on 7 plants in soil spiked with a mixture of 7 PAHs (i.e. naphthalene, acenaphthene, fluorine, phenanthrene, anthracene, fluoranthene, pyrene) that matched the composition of the coal tar-contaminated soil sample at a total concentration of 1000mg kg^{-1} and soil from a former coking plant heavily contaminated with aged PAHs at a concentration of 5000mg kg^{-1} . The control and PAH-spiking treatments used a freely drained brown forest soil (pH 7) with a sand: silt: clay: organic matter ratio of 83: 10.3: 1.1: 5.6. The aged soil, containing 15 of the priority PAHs was obtained from a former coking plant (CPL, Chesterfield, UK). It was classed as a sandy loam soil with 58% sand and a 33% OM content (pH 6.5). The soil contained the following metals: Arsenic (18mg kg^{-1}), Cadmium (2mg kg^{-1}), Chromium (59mg kg^{-1}), Copper (36mg kg^{-1}), Mercury ($<0.5\text{mg kg}^{-1}$), Nickel (49mg kg^{-1}), Lead (174mg kg^{-1}), and Zinc (193mg kg^{-1}). The soil also contained sulphate (53mg kg^{-1}) (Source: Smith et al., 2006). The main findings of this study are summarised in table 1.5.

Table 1.5: Effect of PAH contamination on germination and subsequent growth

Common name	Botanical name	Type of plant	Soil type & PAH concentration	Treatment effect after 12 weeks growth
Cocks-foot	Dactylis glomerata	Grass	Coking plant soil 5000mg kg ⁻¹	less dry foliage weight (p<0.05) than the control
			Soil spiked with coal tar 1000mg kg ⁻¹	none
			PAH spiked soil 1000mg kg ⁻¹	none
Tall fescue	Festuca arundinacea	Grass	Coking plant soil 5000mg kg ⁻¹	less dry foliage weight (p<0.05) than the control
			soil spiked with coal tar 1000mg kg ⁻¹	less dry foliage weight (p<0.05) than the control
			PAH spiked soil 1000mg kg ⁻¹	none
Red fescue	Festuca rubra	Grass	Coking plant soil 5000mg kg ⁻¹	less dry foliage weight (p<0.05) than the control
			soil spiked with coal tar 1000mg kg ⁻¹	none
			PAH spiked soil 1000mg kg ⁻¹	less dry foliage weight (p<0.05) than the control
Perennial ryegrass	Lolium perenne	Grass	Coking plant soil 5000mg kg ⁻¹	none
			soil spiked with coal tar 1000mg kg ⁻¹	none
			PAH spiked soil 1000mg kg ⁻¹	none
Birdsfoot-trefoil	Lotus corniculatus	Legume	Coking plant soil 5000mg kg ⁻¹	less dry foliage weight (p<0.05) than the control
			soil spiked with coal tar 1000mg kg ⁻¹	less dry foliage weight (p<0.05) than the control
			PAH spiked soil 1000mg kg ⁻¹	less dry foliage weight (p<0.05) than the control
Red clover	Trifolium pratense	Legume	Coking plant soil 5000mg kg ⁻¹	less dry foliage weight (p<0.05) than the control
			soil spiked with coal tar 1000mg kg ⁻¹	less dry foliage weight (p<0.05) than the control
			PAH spiked soil 1000 mgkg ⁻¹	less dry foliage weight (p<0.05) than the control
White clover	Trifolium repens	Legume	Coking plant soil 5000mg kg ⁻¹	less dry foliage weight (p<0.05) than the control
			soil spiked with coal tar 1000mg kg ⁻¹	less dry foliage weight (p<0.05) than the control
			PAH spiked soil 1000mg kg ⁻¹	none

Source: Smith et al., (2006). No significant reduction in germination % was observed in any treatment, during the monitoring period of 2 weeks, following sowing (Smith et al., 2006).

Here the hydrocarbon-contamination did not affect the germination of the plant species tested, even though the subsequent growth was affected, apart from perennial ryegrass whose dry foliage weight was not affected by the contamination after the 12 weeks of growth. However, Adam and Duncan (1999) who conducted a study on the effect of diesel fuel on the growth of 22 plant species, including grasses, herbs, legumes and commercial crops, reported delayed seed emergence and reduced germination rates for a variety of plant species at relatively low diesel oil concentrations (25-50g kg⁻¹) (Fig. 1.22-1.24).

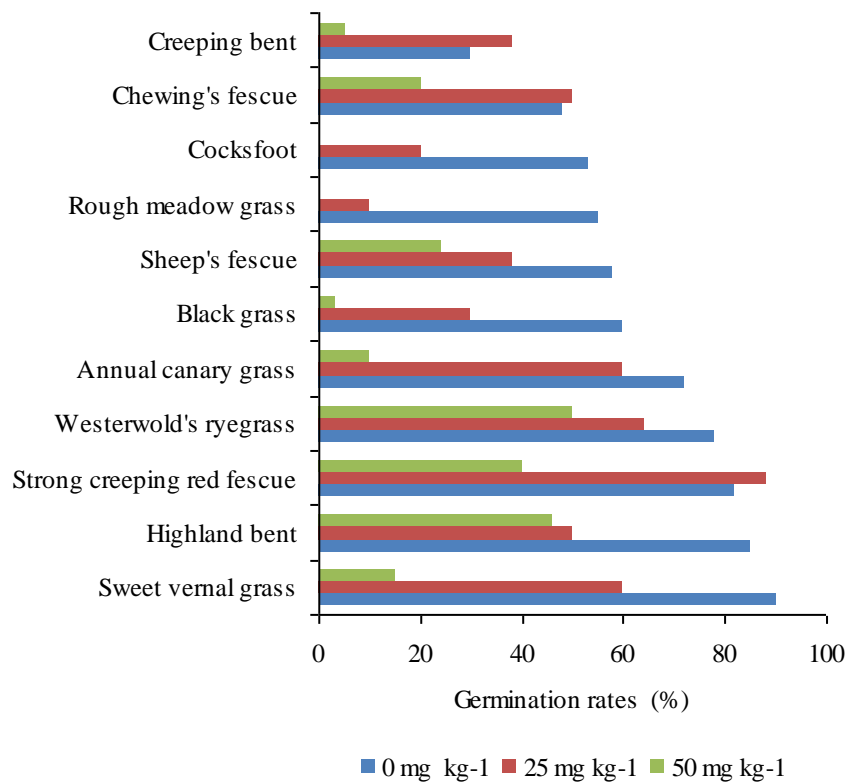


Fig.1.22: Germination rates (%) of different grasses exposed to varying concentrations of diesel oil, measured 14 days after planting at 20^oC (Adapted from: Adam and Duncan, 1999).

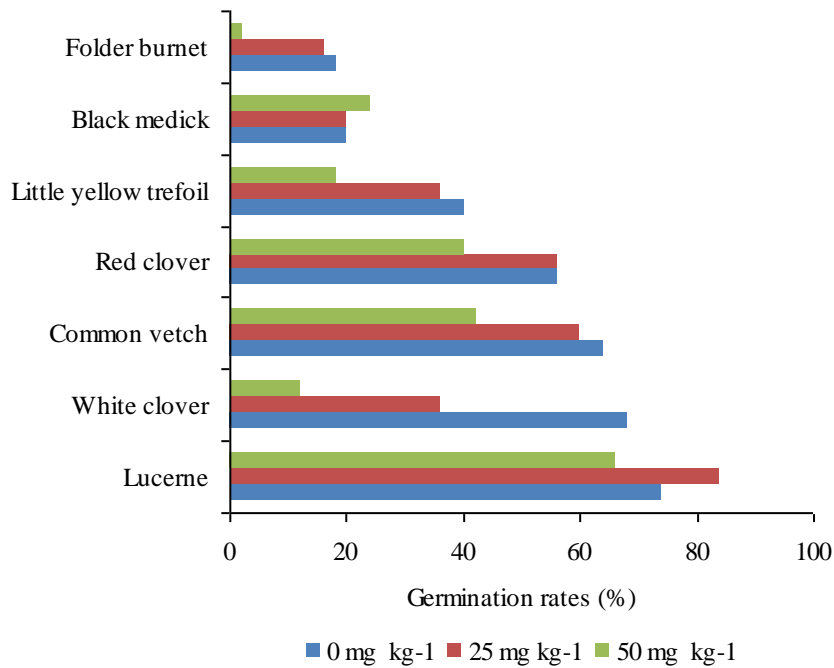


Fig.1.23: Germination rates (%) of different herbs and legumes exposed to varying concentrations of diesel oil, measured 14 days after planting at 20^oC (Adapted from: Adam and Duncan, 1999).

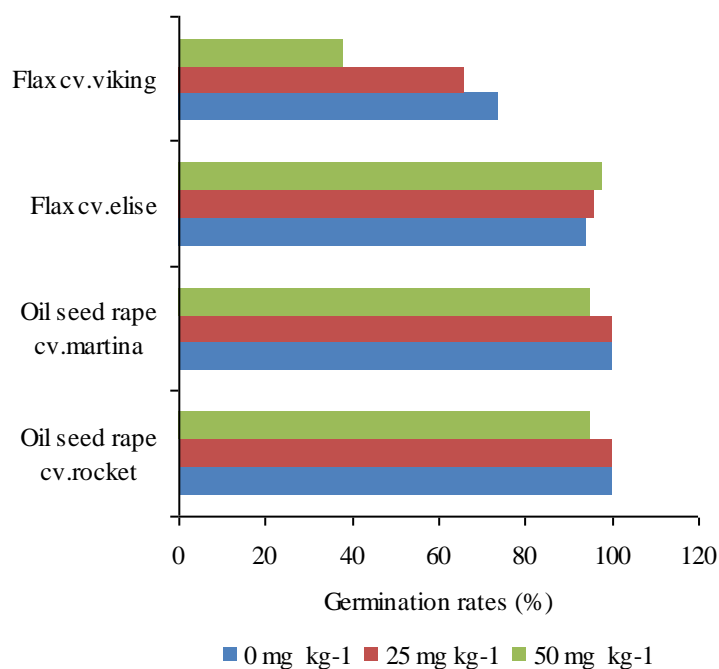


Fig.1.24: Germination rates (%) of different commercial crops exposed to varying concentrations of diesel oil, measured 14 days after planting at 20^oC (Adapted from: Adam and Duncan, 1999).

Adam and Duncan’s germination study showed differences between and within plant species with regard to their ability to germinate in diesel oil-contaminated soil. Here

the herbs, legumes and commercial crops tested appear to be unaffected by 25g kg⁻¹ diesel oil contamination, whereas rough meadow grass was found to be quite intolerant at this concentration. At 50g kg⁻¹ diesel oil contamination, half of the 22 plant species screened failed to reach a germination rate equal to 50% of the control rate. Two species of grass (cocksfoot and rough meadow grass) failed to germinate at all at this concentration (Adam and Duncan, 1999). This finding conflicts with the results of the study carried out by Smith et al. (2006), who found that the same two species were able to germinate successfully in spite of the contamination. Diesel oil is a complex mixture of hydrocarbons containing more potentially toxic, volatile, low molecular weight molecules, than the aged contaminated soils, whereas the aged soils contain a larger proportion of high molecular weight molecules that are less bio-available (Adam and Duncan, 1999), and this could explain the differences between the results of the studies conducted by Smith et al. (2006) and Adam and Duncan (1999).

Similar to the results of the study by Smith et al. (2006), subsequent growth was affected in plants grown in soil contaminated with diesel oil. The overall heights of plants grown in diesel oil-contaminated soil were stunted compared to control plants grown in uncontaminated soil. Specific effects of diesel contamination on particular plants are given in table 1.6. Since some plant species germinated as successfully as the controls, yet their development was impaired by the presence of diesel, delayed seed emergence as a cause for the growth differences was ruled out (Adam and Duncan, 1999).

Table 1.6: Effect of diesel contamination on the subsequent growth of specific plants

Name of the plant	Effect of diesel contamination on the subsequent growth of the plant
Oil seed rape (cv Martina)	Noticeable reduction in the production of shoot growth and root biomass
Canary grass	Production of adventitious roots on the stem
Flax	Lateral roots were increased.

Source: Adam and Duncan (1999)

In summary, the exposure of petroleum hydrocarbon contamination affects germination, affects plant growth and induces structural and physiological changes in plants. Plants also show defence responses to growth in hydrocarbon-contaminated mediums at molecular levels. Plant growth adaptations differ with the species of host plant, the type, amount and duration of contaminant exposure as well as the characteristics of the environment in which the plants are grown.

1.10 Summary

Petroleum hydrocarbon contamination is an environmental concern. Of the hydrocarbons, PAHs are the major worry because they cause many health problems including cancer and the inflammation of tissue in humans (Alkio et al., 2005). So, it is necessary to remediate contaminated sites. Sites with diffuse low to medium level pollution can be remediated with the use of biological techniques, such as phytoremediation (Schroder et al., 2002). Phytoremediation is an environmentally friendly, cost effective remediation method, in which plants are used to restore the polluted sites. The aim of planting hydrocarbon-contaminated sites is to break down and remove the hydrocarbon molecules. This is achieved by a combination of mechanisms of plant and soil interactions that improve the physical and chemical properties of contaminated soil, raising soil microbial activity, and increasing the contact between rhizosphere microbes and the toxic compounds in the contaminated soil (Smith et al., 2006; Aprill and Sims, 1990). Limited PAH uptake by plant roots also takes place (Wild et al., 2005; Gao et al., 2004; Harvey et al., 2001 and references therein). This is influenced by both the organic content of the soil in which the plants are grown and the plant root lipid contents (Collins et al., 2006; Gao et al., 2004).

Hydrocarbon contamination creates unfavourable soil conditions for plant growth, such as inhomogeneous spread of water, oxygen and nutrient deficiency, temperature stress, phytotoxicity and mechanical impedance to plant roots (Merkl et al., 2005 a). Phytoremediation as an in-situ clean up technology has the following challenges:

- a. Improve the poor germination of seeds in hydrocarbon-contaminated soil
- b. Increase the life span of the plants which are grown in contaminated soil

- c. Encourage the growth of plant roots which are essential for proliferating hydrocarbon-degrading micro organisms in the rhizosphere
- d. Avoid the danger of toxic molecules entering the food chain via root uptake

Different plant species show various stress responses and adaptations to survive the stress conditions caused by hydrocarbon-pollution. The responses of plants also vary with the type and amount of the contaminant as well as duration of exposure. Phytoremediation can be feasible if appropriate plant species are selected. They must have the seed structure to germinate in hydrocarbon-polluted soil, show sufficient morphological plasticity to survive stress situations induced by hydrocarbon-contamination, have an extended rhizosphere and appropriate root exudate patterns, positively influence the growth of hydrocarbon-degrading micro organisms in contaminated soil, and should also limit the uptake of toxic molecules through various adaptations to the root ultrastructure and cell wall components. Plants chosen should also be native to the area to be remediated so that they will be tolerant to the soil and environmental conditions. Additionally, plants that require little attention are preferable because cost is an important factor (Smith et al., 2006). Plants with deep, fibrous roots and fast growth, such as grasses, are generally considered useful in phytoremediation (Brandt et al., 2006).

1.11 Research questions

1. Hydrocarbon contamination affects germination and subsequent growth of different species of plants differently and this also depends on the type and amount of the contaminants (Smith et al., 2006; Adam and Duncan, 1999). What are the reasons for the failure/success of seed germination and subsequent growth of different plants due to exposure to hydrocarbon contamination (e.g. petroleum crude oil, PAHs)?
2. Petroleum hydrocarbon-contamination presents adverse conditions for the growth of plant roots (Merkl et al., 2005). How does growth in soil contaminated with petroleum hydrocarbons affect the growth direction of plant roots that possess different root architecture and how does this influence the establishment of plants in contaminated soils?
3. Root hairs: what is the effect of growth in petroleum hydrocarbon-contaminated soils on root hair abundance and length?

4. Environmental cues motivate modifications in structural and ultrastructural features of plants (Agarwal, 2006). What are the changes in root structural and ultrastructural features i.e. effect on root cortex, endodermis, size and number of xylem vessels, and stele that arise from growth in hydrocarbon-contaminated soils?
5. Can Nile red be used as a tool to probe the uptake of organic xenobiotics from soil into roots?
6. How do the root ultrastructural adaptations of a plant grown in soil contaminated with naphthalene, which is a bio available PAH that could impart toxic effects on plants, influence the pathway of an organic xenobiotic compound, modelled by the passage of Nile red across the root tissues?
7. Adaptation of an organism to changes in its growth environment is not possible without changes in metabolism. What are the differences in the metabolic profiles of a plant grown in soil contaminated with naphthalene?

1.8 Project lay-out

The mechanisms of interaction between petroleum hydrocarbon-contamination in soil and plants have not been clearly revealed yet. The aim of this research was to investigate the impacts that petroleum hydrocarbon-contamination in soil may have on plants, plant roots in particular. Scanning electron and epi-fluorescent microscopic techniques coupled with the chemical analysis of plant extracts using gas chromatography-mass spectrometry were used to investigate the structural, ultrastructural and metabolic modifications of plants arising from growth in petroleum hydrocarbon-contaminated soil as well as the presence of PAH in plant cells. The metabolic profiling of plant roots and shoots also renders an insight into the stress-related physiology of plants grown in hydrocarbon-contaminated soil. Here, sand was used instead of soil in order to avoid the complexity caused by the interaction of petroleum hydrocarbons with soil organic matter. The project work plan included the following activities in evaluating the morphological and physiological responses of plants to petroleum hydrocarbon-contamination:

- Growing different species of plants (tall fescue, brown top bent, carrot, beetroot and parsnip) in petroleum crude oil-contaminated sand as well as uncontaminated sand from seeds, using pots and rhizo-boxes. Visually

monitoring the differences in growth patterns of plants due to exposure to crude oil-contamination (see chapter 3).

- Scanning electron microscopic analysis of roots of plants (tall fescue and beetroot) grown in crude oil-contaminated sand and clean sand to identify the structural and ultrastructural differences between the roots from different treatments (see chapter 3).
- A preliminary study on the effect of different PAHs (naphthalene, anthracene, fluoranthene and benzo (a) pyrene) on the germination and subsequent growth of tall fescue (*Festuca arundinacea*). A detailed study on the effect of naphthalene-contamination on seed germination, growth patterns and root ultrastructural features of tall fescue as well as on the water balance parameters (e.g. matrix potential) of sand (see chapter 4).
- Examination of use of Nile red to probe the uptake of PAHs from soil into roots (see chapter 4).
- Investigating the passage of naphthalene across root tissues of tall fescue using Nile red, as a fluorescent molecular probe, using epi-fluorescent microscopic techniques (see chapter 4).
- Metabolic profiling of the root and shoot extracts of tall fescue plants grown in clean sand and naphthalene-contaminated sand, using gas chromatography-mass spectrometric techniques (see chapter 5).

The results of this investigation will be used to evaluate the viability of phytoremediation as a treatment tool for petroleum hydrocarbon-contaminated soil.

CHAPTER 2

Materials and Methods

2.1 Introduction

This chapter presents details of the materials and methods used during the study in evaluating the responses of plants to petroleum contamination in soil. An outline of the quality assurance and control (QA/QC) measures used in order to provide confidence in the results is given at the end of this chapter.

2.2 Soil water

2.2.1 Determination of soil water-holding capacity

When soil is saturated, all the pores of the soil are full of water, but after some time, the gravitational water drains out, leaving the soil at field capacity (soil water-holding capacity). Soil water-holding capacity was determined as detailed below:

Soil was autoclaved and allowed to air-dry in a laminar flow cabinet for 24 hours. The mass of a wet filter paper in a glass funnel was measured (A). The glass funnel and filter paper were dried at 105°C for an hour, and cooled in a desiccator. The mass of the dry filter paper and glass funnel was measured (B). Soil (about 20g) was added to the filter in the funnel and weighed (C). The funnel was plugged and the soil was submerged with distilled water (dH₂O) in the funnel for 1 hour. The plug was removed and the soil was allowed to drain for 1 hour covered with foil to avoid evaporation. The mass of the wet soil, filter paper and funnel were measured (D), then the set was dried at 105°C for 24 hours and cooled in a desiccator before measuring the dry mass (E). The soil water-holding capacity (WHC) was calculated on the basis of:

$$E-B = \text{Soil}_{\text{dry}}$$

$$D-A = \text{Soil}_{\text{wet}}$$

$$(\text{Soil}_{\text{wet}} - \text{Soil}_{\text{dry}}) / \text{Soil}_{\text{dry}} = \text{WHC (ml H}_2\text{O g}^{-1} \text{ soil dw)}$$

2.2.2 Determination of soil moisture content

Amount of moisture present in a unit of soil sample is termed soil water content or soil moisture content. The soil water content (WC) was calculated on the basis of:

$$C-B=Soil_{sample}$$

$$(Soil_{sample} - Soil_{dry}) / Soil_{dry} = WC \text{ (ml H}_2\text{O g}^{-1} \text{ soil dw)}$$

$$(Soil_{dry} / Soil_{sample}) * 100 = \% \text{ dry weight (w/w)}$$

The water content figures were used to calculate the amount of wet soil required to make up specific amount of soil in dry weight.

2.2.3 Determination of soil water potential

Soil water potential is the energy state of water in the soil and reflects how water will move in a soil as well as from the soil to the plant. Here, dielectric water potential sensors (Model: MPS-1; Manufacturer: Decagon Devices Inc.) were used to measure the water potential of naphthalene-treated and clean soil. The MPS-1 measures the dielectric permittivity of two engineered, porous ceramic disks sandwiched between stainless steel screens and the MPS-1 circuit board to measure their water content and then derive their water potential. The dielectric permittivity of water in the ceramic disks is 80 compared to a dielectric permittivity of 5 for the ceramic material and 1 for the air. The principle behind this technique is the second law of thermodynamics which states that connected systems with differing energy levels will move towards an equilibrium energy level. Here, a solid matrix equilibration technique is used. The ceramic material with a static matrix of pores is introduced into the soil and allowed to come into hydraulic equilibrium with the soil water. As the two are in equilibrium, measuring the water potential of the ceramic disks will give the water potential of the soil. Here water potential refers to matrix potential which is the most important component of water potential with regard to plant water relations (Decagon Devices Inc., 2007).

MPS-1 sensors were installed into soil at the bottom of the hole dug above 2cm from the base of the 10L plastic pots. The sandy soil was packed around the sensor with good contact to all ceramic surfaces, and the hole was back-filled with care. The

stereo plug of the MPS-1 sensors was plugged into one of the five ports on the EM50 datalogger. ECH₂O Utility was used to configure the ports for an MPS-1 and to set a measurement interval (60 minutes) for the logger. The soil water potential readings were read off from the screen of the datalogger.

2.3 Preparing treatment soil for contaminated treatment

2.3.1 Spiking soils with polycyclic aromatic hydrocarbons (PAHs)

Spiking soil with polycyclic aromatic hydrocarbons (PAHs) was carried out according to the methods described by Johnson et al. (2004). Glassware was washed with dichloromethane (DCM) to degrease. Soil was air-dried (after air-drying the soil contained 3-10% of water content as determined by gravimetric techniques) immediately prior to spiking and placed in the beaker for the addition of the PAH. The required amount of PAH was dissolved in 50ml of DCM. This dissolved PAH was added in aliquots to a quarter of the amount of soil needed to be spiked. The beaker was washed with 10ml DCM and the washings were added to the soil. The solvent was evaporated in the fume cupboard. During the solvent evaporation, the soil was stirred with a stainless steel spatula repeatedly to ensure homogeneity. Once all the PAH solution was added, the soil was left overnight in the fume cupboard prior to mixing with the remaining soil. Mixing the spiked and non-spiked (3/4 of the total amount of soil) soil was carried out in a sterile glass beaker in the fume cupboard, to give the required PAH concentration per kg soil.

The initial PAH concentration per kg soil was determined using GC-FID techniques. Two and a half grams (2.5g) of sand (ww) and 2.5g of anhydrous Na₂SO₄ were taken into a labelled extraction tube (volume: 10ml; make: Schott), 100µl toluene (20ppm) was added as the internal standard and the sand was extracted in 7800µl DCM and 1200µl dH₂O on a rotary extraction unit for 4 hours at 40 rpm. After the extraction, the tubes containing the extracts were stood still, allowing the extracts to settle for a few minutes. The extract was run through a column of anhydrous Na₂SO₄ taken in a clean 25ml glass column and the filtrate was collected into labelled, clean 10ml glass vials. The filtrates were transferred into labelled GC vials and analysed by GC-FID (Make: Agilent Technologies 6850 Network GC System; Software: ChemStation). GC conditions used were as follows:

Injection: 1 μ l; Temperature program: 50°C to 300°C at the rate of 6°C min⁻¹ and held at 300°C for 10 minutes. Helium was used as the carrier gas with the constant flow rate set at 1ml min⁻¹. Column: DB-5MS capillary column.

2.3.2 Mixing clean sand with petroleum crude oil-contaminated sand

The petroleum crude oil-contaminated sand was obtained from a major oil company (Shell). The following categories of hydrocarbons were present in the crude oil (HC)-contaminated sand (Table 2.1).

Table 2.1: The different categories of petroleum hydrocarbons of a soil that had soaked liquid petroleum leaked from a petroleum storage tank and their concentrations and percentages as a fraction of total dichloromethane (DCM)-extractable petroleum hydrocarbons (TEH) (soil supplier: Shell Company, UK; soil analysis was carried out by ALcontrol, UK).

Category	mg kg ⁻¹	Percentage as a fraction of total DCM-extractable petroleum hydrocarbons (%)
Aliphatic hydrocarbons	11, 900	18.25
Aromatic hydrocarbons	4, 200	6.44
Aromatic hydrocarbons (>C ₂₁ -C ₃₅)	3, 900	5.98
Total higher molecular weight petroleum hydrocarbons (>C ₉)	26, 900	41.26
Total dichloromethane (DCM)-extractable hydrocarbons (TEH)	65, 200	

The contaminated sand which had soaked liquid petroleum leaked from a petroleum storage tank was thoroughly mixed with clean sand to a final concentration of 35g kg⁻¹ total dichloromethane (DCM)-extractable hydrocarbons (TEH). Rhizo-box and pot experiments were conducted using this material. This material was mixed thoroughly with clean sand in appropriate ratios to get the desired TEH concentrations.

The initial TEH concentrations per kg sand used in experiments were determined using gravimetric technique. Soil extraction and filtration procedures were the same as in PAH extraction and filtration. Here, the filtrates were collected into pre-weighed 10ml glass vials. The solvent was left to evaporate in the fume hood overnight. The vials containing dry TEH were weighed the next day and the concentration of TEH per kg sand was calculated on this basis.

2.4 Setting up rhizo-boxes

Rhizo-boxes were constructed from 2 sheets of glass (12cm×12cm) separated by plastic spacers (2cm ×1cm) held together with clips (Fig. 2.1). The rhizo-boxes were cleaned with 70% (v/v) ethanol and dried in a laminar flow cabinet.

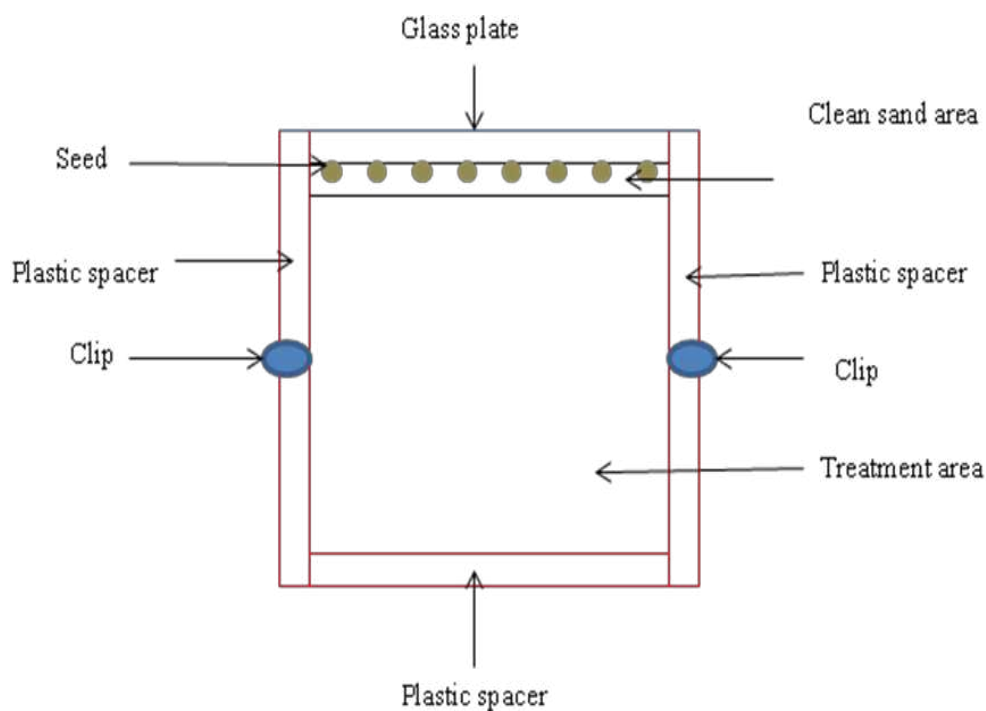


Fig. 2.1: Rhizo-box set up

The treatment soil was packed at a moisture content of 15% (w/w) (the moisture content % was determined by gravimetric techniques) in the rhizo-boxes (depth in profile 1-8cm). A top layer of clean sand (depth 2cm) was added as a seed bed. The walls of the rhizo-boxes were wrapped in aluminium foil to prevent the photo degradation of petroleum hydrocarbons and to avoid any adverse effect of light on root growth. The rhizo-boxes were placed indoors on a window sill and kept at an angle of 35° from vertical so that the roots growing downwards could be observed through the front glass covers (according to Kechavarzi et al., 2007) (Fig.2.2).

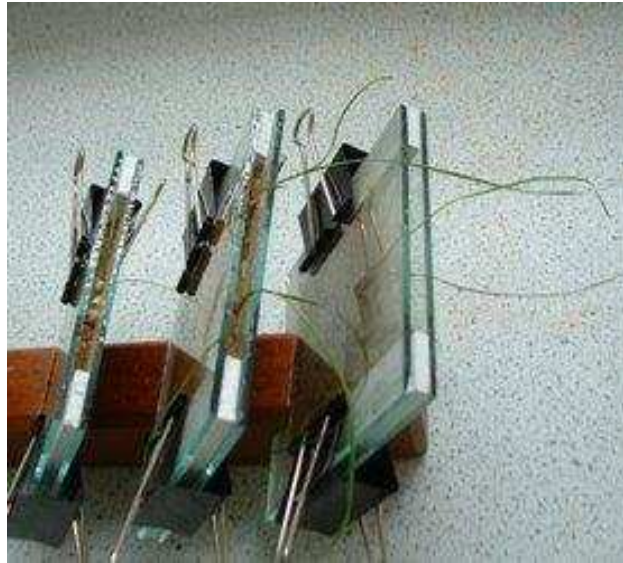


Fig.2.2: Rhizo-boxes kept at an angle of 35° from vertical

2.5 Seeding

Seeds were disinfected by soaking in 30% H₂O₂ for 20 minutes, washed 3 times in sterile dH₂O (according to Binet et al., 2001) and sown in the top clean sand layer (Fig.2.1). In some experiments, seeds were directly sown in contaminated sand, whereas in some others seeds were germinated on autoclave-sterilized (i.e. 126°C, 11 minutes, 15 psi) rock-wool cubes in a tray of water at 20°C.

2.6 Experimental designs, plant material and growth conditions

2.6.1 Experimental designs, plant material and growth conditions used in chapter 3

Plants were grown in sand contaminated with aged crude oil (10.8/ 16.5g TEH kg⁻¹ sand dw) in plastic pots/ rhizo-boxes at 20°C (Table 2.2). Plants in plastic pots were grown in the glasshouse whereas those in rhizo-boxes were grown on a window sill in the laboratory. In the experiment using a mixture of grasses, compost was added in some crude oil (HC)-treatments (Table 2.2). The seeds were germinated in a clean layer of agricultural sand to avoid germination failure. Some plants were also grown in clean sand for direct comparison. The sand used contained no organic matter. These experiments were therefore not subject to any contaminant-organic matter

interactions. For fertilization, a slow release plant food (osmocote) was mixed with sand to a concentration of 4.5g kg⁻¹ sand (dw). Watering was carried out on a daily basis, adjusting to 80% (w/w) of the soil's water holding capacity, to replace transpiration losses.

Table 2.2: Experimental design used in chapter 3

Plant species	Pots/ Rhizo- boxes	g TEH kg ⁻¹ sand (dw)	No. of rep.	No. of plants per rep.	Additional
Carrot (<i>Daucus carota</i>)	Pots (1L)	10.8	3	10	
Beetroot (<i>Beta vulgaris</i>)	Pots (1L)	10.8	3	10	
Parsnip (<i>Parsnica sativa</i>)	Pots (1L)	10.8	3	10	
A mixture of grasses [tall fescue (<i>Festuca arundinacea</i>), brown top bent (<i>Agrostis capillaries</i> L.) and perennial ryegrass (<i>Lolium perenne</i> L.)]	Pots (2L)	10.8	6	~50	In some HC-treatments, compost was added
Tall fescue (<i>Festuca arundinacea</i>)	Rhizo- boxes	16.5 & 10.8	3 rep for each	10	
Brown top bent (<i>Agrostis capillaries</i> L.)	Rhizo- boxes	16.5 & 10.8	3 rep for each	15	
Tall fescue (<i>Festuca arundinacea</i>)	Pots (1L)	10.8	10	~25	

Abbreviations used in table 2.2:

HC: crude oil; No.: Number; rep.: replicate; TEH: Total DCM (dichloromethane) extractable hydrocarbons.

2.6.2 Experimental designs, plant material and growth conditions used in chapter 4

a. Preliminary investigation (section 4.3a)

Table 2.3: Experimental design used in chapter 4, section 4.3a

	Plant species	mg PAH kg ⁻¹ sand (dw)	No. of rep.	No. of plants per rep.	Additional
a1.	Tall fescue (<i>Festuca arundinacea</i>)	0-1000 for B(a)P, Flt and Nap	3 rep for each	10	The concentrations of 0, 4, 40 and 1000mg PAH kg ⁻¹ sand (dw) were used in different layers in the gradient rhizo-fox experiment
a2.	Tall fescue (<i>Festuca arundinacea</i>)	1000 (Ant)	3 rep for each	10	Seeds were germinated in a 2cm thick layer of clean sand
a2.	Brown top bent (<i>Agrostis capillaries</i> L.)	1000 (Ant)	3 rep for each	10	Seeds were germinated in a 2cm thick layer of clean sand
a3.	Tall fescue (<i>Festuca arundinacea</i>)	800 (Nap)	3 rep for each	10	Seeds were germinated in rockwool cubes and 2 weeks old seedlings were transplanted into rhizo-boxes containing either clean or treated sand

Abbreviations used in table 2.3:

Ant: Anthracene; B(a)P: Benzo (a) pyrene; Flt: Fluoranthene; Nap: Naphthalene; No.: Number; rep: replicate

Some plants were also grown in clean sand for direct comparison. Plants were fed with a liquid fertiliser (lawn food; N: P: K=15:3:3) on a once weekly basis. Watering was carried out on a daily basis, adjusting to 80 % (w/w) of the soil's water holding capacity, to replace transpiration losses.

b. Main study using naphthalene as a model PAH (sections 4.3b-4.3e)

b1. 15ml of tall fescue seeds (origin: Kent; supplier: Emorsgate seeds, UK) were germinated directly either in clean sand or sand contaminated with naphthalene (0.8g kg⁻¹ dw) in 15cm diameter plastic pots. 6 replicates per treatment were established and each replicate contained ~90 plants after 1 month since seeds were sown.

b2. 100ml of tall fescue seeds (origin: Kent; supplier: Emorsgate seeds, UK) were germinated directly either in clean sand or sand contaminated with naphthalene (0.8g kg⁻¹ dw) in 10L plastic pots. The following set-ups were established:

Table 2.4: Experimental design showing number of replicates established for the water balance study described in chapter 4 (Chapter 4; Section 4.3 b-4.3d)

Treatment	Planted (to be water stressed and probes installed)	Planted (not to be water stressed)	Unplanted (to be water stressed and probes installed)
Control	2 replicates	7 replicates	2 replicates
Naphthalene	2 replicates	7 replicates	2 replicates

Each planted pot contained ~400 plants after 1 month since seeds were sown.

b3. Tall fescue seeds (origin: Kent; supplier: Emorsgate seeds, UK) were germinated on autoclave-sterilized (i.e. 126°C, 11 minutes, 15psi) rockwool cubes in a tray of water at 20°C. The seedlings were placed at a 45cm distance away from a 250W Grow Light (Model: Envirolite, 6400 K) on a 16 hour light and 8 hour dark cycle upon germination, but were moved to a 30cm distance after 1 week of growth. Six centimetre (6cm) - diameter plastic pots were filled with naphthalene-spiked sand (0.8g kg⁻¹ dw) or non-spiked (control) sand. A space was made in the pot centre to position the rockwool cube (containing the seedlings) with a bit of pressure applied. The rockwool cubes with plants were transferred to the pots once the roots reached the base of the rock- wool cubes. The pots were placed in individual trays. Eight (8) replicates were established and each replicate contained ~10 plants.

The pots were randomized and the plants were grown in a glasshouse at 20°C on a 16 hour light and 8 hour dark cycle upon germination, watered regularly unless exposed to water stress and fed with a liquid fertiliser (lawn food; N: P: K=15:3:3) on a once weekly basis.

2.6.3 Experimental designs, plant material and growth conditions used in chapter 5
Same as described in 2.6.2 b1.

2.7 Recording root shoot development and root hair analysis

Periodical recording of plant root development was carried out by tracing the roots on acetate transparencies and measuring root lengths with the aid of thread and measuring ruler. Shoot height was also measured and recorded periodically. Roots were systematically sampled, stained with the vital stain Evans blue for 15 minutes

and root hairs (transparent as well as those stained blue) were counted in 1cm root segments under a light microscope. Root segments (sectioned at 1/3 as a fraction of root length above the root tip) were also viewed through a scanning electron microscope (Cambridge model SEM90).

2.8 Root shoot biomass analysis

Plants were harvested after ~3-6 months of growth in treated and untreated sand. The amount of root and shoot biomass was measured on a fresh weight basis. For dry weight analysis, 3-6 replicates of weighed plant tissue were dried in an oven at 60°C for 24 hours. They were reweighed after drying and the water content was determined gravimetrically from the water losses and resulting change in mass associated with the drying. The dry weight percentage and water content percentage of plant tissues were calculated from the water content and fresh weight values.

2.9 Scanning Electron Microscopy (SEM)

2.9.1 Preparation of fixatives

Cacodylate buffer (pH 7.2)

Solution A: 0.2M solution of sodium cacodylate [42.8g of Na (CH₃)₂AsO₂·3H₂O in 1000 ml of dH₂O].

Solution B: 0.2 M hydrochloric acid solution (HCl)

A 4.2ml measure of solution B was added to 50ml of solution A, and made up with dH₂O to 200ml (according to Hayat, 1986).

Glutaraldehyde-Cacodylate fixative

An 8ml measure of 25% (w/v) glutaraldehyde was added to 50ml of 0.2 M cacodylate buffer, and made up with dH₂O to 100ml (according to Hayat, 1986). The concentration of prepared glutaraldehyde is 2% (w/v), and the molarity of the buffer is 0.1 M (Hayat, 1986).

Osmium tetroxide solution for post-fixation of plant tissues

Osmium tetroxide (OsO_4) was bought as glass ampoules containing 0.1g of osmium tetroxide. To prepare 10ml of 1% (w/v) osmium tetroxide solution:

A 10ml aliquot of dH_2O was measured into a stoppered bottle. The neck of the ampoule was scored, and broken with the ampoule tightly wrapped in tissue paper. The complete ampoule was added to the bottle, and the stopper replaced. The bottle was agitated using an ultrasonic bath to ensure the contents of the ampoule were completely dissolved in the distilled water. A 0.1g mass of osmium tetroxide was dissolved in 10ml of dH_2O in an ultrasonic bath to produce a 1% (w/v) solution. The whole procedure was carried out in the fume cabinet and the prepared osmium solution was used within 1 week.

2.9.2 Fixation steps

1. Root samples were washed thoroughly in dH_2O to remove loosely adhering materials without disturbing the specimen surfaces.
2. Roots were cut into approximately 1mm long segments in 0.1 M cacodylate buffer on a sheet of dental wax (Sigma Aldrich) using a sharp razor blade. Samples were placed in buffer solution (5ml) in 12ml volume exetainers fitted with rubber septa. The trapped air was evacuated with a vacuum pump to prevent cavitations in the xylem vessels.
3. Root segments were transferred to 2% (w/v) glutaraldehyde in glass vials and left for 1 hour at room temperature. This was followed by 2 buffer rinses of 20 minutes each.
4. Samples were fixed for 1 hour in 1% (w/v) OsO_4 solution followed by two 20 minute rinses with dH_2O .

2.9.3 Dehydration steps

1. Samples were dehydrated in ethanol (EtOH) in the following order of increasing concentrations:

Table 2.5: Concentrations of ethanol (EtOH) and duration of soaking plant tissues in EtOH during dehydration

Solution	% EtOH	% dH₂O	No. of washes	Duration of each wash (minutes)
Solution 1	30	70	2	30
Solution 2	50	50	2	30
Solution 3	70	30	2	30
Solution 4	80	20	2	30
Solution 5	90	10	2	30
Solution 6	95	5	2	30
Solution 7	100	0	1	30

100 % EtOH was dried with molecular sieves (Sigma Aldrich) to produce dry EtOH. Samples in 100 % EtOH were transferred to dry EtOH before critical point drying.

2. Critical point drying

Root samples were dried using an EMITECH K-850 critical point dryer (CPD) to avoid surface tension and prevent sample distortion during the desiccation process. Samples, desiccated in 100% ethanol, were placed in cellulose baskets in the CPD sample chamber and cooled to 5°C. The chamber was then flushed several times with CO₂, to replace 100% EtOH-intermediate solvent in the drying process, until no EtOH was present in the vented gas. The sample temperature was then raised to 35°C and 1350 psi (above the critical point of 31°C and 1072 psi) before allowing the CO₂ to purge very slowly (1000ml min⁻¹) from the sample chamber. The dried samples were stored in a desiccator before mounting on stubs for scanning electron microscopy.

2.9.4 Mounting and viewing root sections with a scanning electron microscope (SEM)

The critical point dried samples were mounted on aluminium stubs (Sigma Aldrich) using carbon tabs (Sigma Aldrich), coated with gold for 2 minutes with a sputter coater (model: Edwards S150B; pressure: 1mbar), and viewed with an S90 or S360 Cambridge model scanning electron microscope with a 20 kV electron beam at an 18mm working distance.

2.11 Epi-fluorescence Microscopy

2.10.1 Procedure for staining Casparian band structures for epi-fluorescence microscopy

Both naphthalene-treated and control roots were sectioned at one third as a fraction of the root length above the root tip. Thin cross sections were produced by drawing the corner of a sharp razor blade across the roots in a thin film of $1 \times$ PBS (Phosphate Buffered Saline) on parafilm on the surface of a dental wax sheet. Staining was carried out according to Brundrett et al. (1988). Freehand sections were transferred into a small watchglass and the sections were stained in 0.1% (w/v) berberine hemisulphate (Sigma; minimum 95%) which specifically stains Casparian bands, in dH_2O for 1 hour. The sections were rinsed through several changes of dH_2O and excess water was blotted off after each transfer. The root sections were transferred into 0.5% (w/v) aniline blue [water soluble (WS)] (Agar Scientific) in dH_2O for 30 minutes and then were rinsed in the same way. Here, counterstaining with aniline blue was carried out in order to quench unwanted fluorescence by substances other than Casparian bands. The sections were transferred into 0.1% (w/v) $FeCl_3$ (Fisher Scientific; assay > 97%) in 50% (v/v) glycerine (Aldrich Chemical Co.Ltd.; 98%) (prepared by adding glycerine to filtered aqueous $FeCl_3$), and after several minutes in this solution, transferred to slides and mounted in the same solution. The $FeCl_3$ mountant prevents decolourization.

2.10.2 Microscopic settings and obtaining images of roots stained with berberine hemisulphate

Sections were observed using Nikon 90i Eclipse epi-fluorescence microscope with UV illumination through a UV-2A filter block (excitation at 345nm; emission at 458nm). Photographs were taken within a few hours of staining.

2.10.3 Nile red stain preparation

A 2-3mg measure of the Nile red dye (Invitrogen) was transferred into a 1.5ml Eppendorf micro-centrifuge tube with 250 μ l of $1 \times$ PBS (Phosphate Buffered Saline) solution diluted with dH_2O from a $10 \times$ PBS solution (to make a litre of $10 \times$ PBS: dissolve 80g NaCl, 2g KCl, 14.4g $Na_2HPO_4 \cdot 2H_2O$ and 2.4g KH_2PO_4 into 800ml of dH_2O , before making it up to 1L with dH_2O . Adjust the pH to 6.8 with NaOH or HCl)

and 750 μ l of glycerol (the glycerol pipettes more easily if it is warmed up in the microwave for about 15 seconds). The Nile red dye was dissolved into the mixture through microwave heating, giving the solution a bright purple colour. The excess Nile red stain that was not dissolved was collected at the base of the tube through centrifugation at 6300 rpm for 30 seconds using a micro centrifuge. The supernatant was removed from the particulate residue and was used to stain the roots.

2.10.4 Procedure for staining vital roots with Nile red

Tall fescue plants grown in clean and naphthalene-contaminated sand were used for this purpose from the age of 2.5 months to 6 months. Roots that were still joined to living plants were exposed by using a soft brush to remove the sand. A small piece of rock-wool (pre-soaked in water) was placed into the cavity between the exposed roots and the sand. Nile red solution was applied to these roots as well as the piece of rock-wool backing, using a soft brush. The Nile red solution was also applied to another piece of rock-wool to form a protective stain-covered sleeve, before returning the root-ball to its pot. This was to mark the stained root. The plants were watered as usual and the stained roots were sampled after 48 hours.

2.10.5 Root preparation and fixing

The sampled roots were washed in 1 \times PBS solution and fixed in a 2% (w/v) paraformaldehyde (PFA) fixing solution for 1 hour. The PFA solution was prepared by diluting 5ml of 10 \times PBS with 30ml of dH₂O and was heated to 90°C in a microwave before adding 1g PFA (the PFA must be added in the fume hood after heating) and 500 μ l of 5 M NaOH (NaOH breaks the PFA ring allowing it to interact with the sample). The PFA solution should be made directly before its use. After fixing with PFA, the roots were washed in a buffer made from 3.8g of glycine dissolved in 1L of 1 \times PBS, to remove any un-reacted aldehyde groups. The samples were then washed in 1 \times PBS, and stored in fridge.

2.10.6 Sectioning the roots

Roots were immobilized in a few drops of 1 \times PBS within folded Parafilm on a dental wax surface, and then sectioned by drawing the corner of a sharp double-edged razor

blade across them repeatedly. The sections produced in this way were transferred to slides and mounted in Vectashield.

2.14.7 Microscopic settings and obtaining images of roots stained with Nile red

Sections were viewed using an epi-fluorescence microscope (Nikon eclipse 90i) fitted with a digital camera. Nile red fluorescence was viewed with a visual red excitation source through a Texas red HYQ filter block (excitation at 589nm; emission at 615nm) against a real light image backdrop. The images were formatted using the epi-fluorescence microscopic imaging software.

2.14.8 Overlaying images using microscopic imaging software

Nile red solution was applied gently to the living root with a soft brush. The stained roots were sampled after 48 hours, fixed in 2% (w/v) paraformaldehyde and stored in a refrigerator at 4°C to be used for berberine hemisulphate staining. The fixed roots were sectioned by hand in a few drops of PBS in parafilm on a dental wax surface. Berberine hemisulphate staining process was carried out according to Brundrett et al. 1988 (see section 2.10.1). The root sections were transferred to microscopic slides and mounted in FeCl₃ mountant. The distance travelled by Nile red was investigated using an epifluorescence microscope (Nikon Eclipse 90i) using Texas red HYQ filter (589nm peak excitation and 615nm peak emission). The root samples were also viewed with UV illumination (345nm peak excitation; 458nm peak emission). Photographs were taken within a few hours of berberine hemisulphate staining. The images showing the path of Nile red were overlaid with their berberine hemisulphate+ aniline blue stained counterparts using microscopic imaging software.

2.15 Gas chromatography-mass spectrometry (GC-MS)

2.11.1 Sampling

Roots and leaves were sampled from 6 months old living plants from both treatments on the same day at the same time period (early afternoon). Fresh fully expanded leaves and roots from similar depths in the pots were collected from each replicated

pot (3 rep) from each treatment. Sand was brushed off from the roots and roots were washed thoroughly with dH₂O.

2.11.2 Sample preparation

Samples were immediately frozen in liquid nitrogen and homogenised. Samples were freeze-dried using the following protocol:

- Freezing: at -45°C for 210 minutes at 200mTorr
- Primary drying: at -10°C for 600 minutes at 200mTorr; then at 0°C for 200 minutes at 100mTorr
- Secondary drying: at 22°C for 180 minutes at 100mTorr

Vials containing samples were capped tightly and stored at -80°C in the freezer until further analysis.

2.11.3 Extraction and derivatization

The extraction protocol was adapted from Du et al., (2011). Freeze-dried tissue powders (0.1g) were transferred into 10ml extraction tubes (Schott). Hundred micro litres (100µl) of ribitol (2mg L⁻¹) as internal standard and 4.2ml 80% HPLC grade aqueous methanol (v/v) were added and the tissue samples were extracted on a rotator extraction unit at 40 rpm for 120 minutes. The tubes containing extracts were subsequently incubated in a water bath at 70°C for 15 minutes and centrifuged at 2000g for 5 minutes. Seven hundred and fifty micro litres (750µl) of chloroform was added to the extracts in order to separate out the non polar phase. The mixture was vortexed thoroughly and centrifuged at 2000g for 2 minutes. Forty micro litres (40µl) of the polar phase was transferred into GC-vials and the solvents were evaporated in a centrifugal concentrator for 25 minutes under vacuum at room temperature. The dried polar phase was oximated with 40µl of methoxyamination reagent (methoxyamine hydrochloride dissolved in anhydrous pyridine at the concentration of 20mg ml⁻¹) at 37°C for 90 minutes. Here the carbonyl groups are the main targets for methoximation (see Fig. 2.3). Subsequent silylation was carried out with 70µl of MSTFA (N-Methyl-N-trimethylsilyl-trifluoroacetamide) at 37°C for 30 minutes. Here hydroxyl groups are the primary targets for silylation (see Fig. 2.4). The ratio of the volume of derivatising agent to sample was increased to ensure complete

derivatization. After derivatization procedure, the vials containing samples were briefly centrifuged for 5 seconds and the vials were left to cool in the fume hood for a few minutes, before analysis by GC-MS.

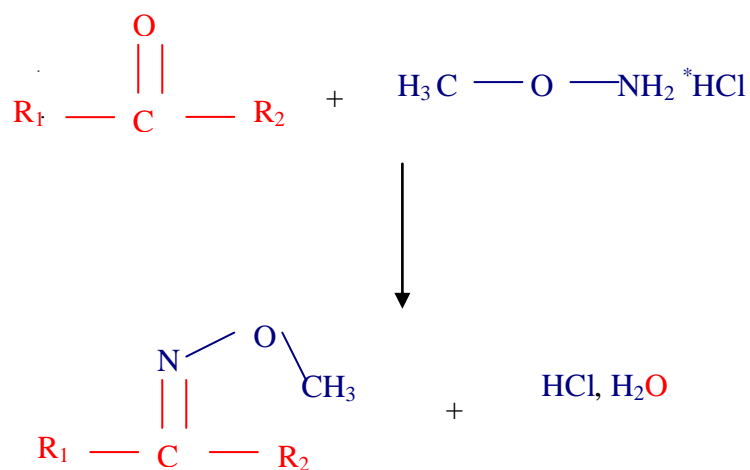


Fig. 2.3: An example of oximation (Adapted from Dettmer et al., 2007)

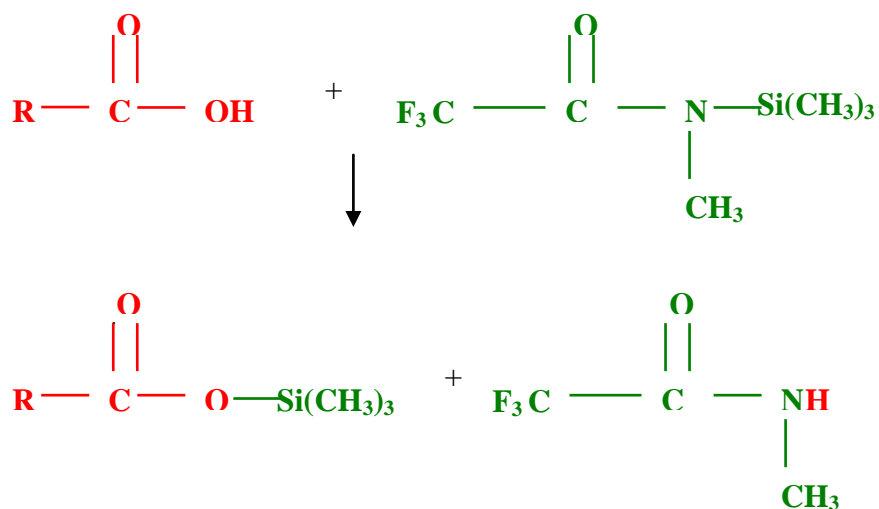


Fig. 2.4: An example of silylation (Adapted from Dettmer et al., 2007)

2.11.4 Gas chromatography- mass spectrometry (GC-MS) analysis

Samples were analysed with a PerkinElmer AutoSystem XL gas chromatograph coupled with a TurboMass mass spectrometer (PerkinElmer Inc., Waltham, MS). The published method (Du et al., 2011) was used with minor modifications. A 1 µl aliquot of the derivatised extract was injected into a Zebron ZB-17 5MS capillary column (30m × 0.25mm × 0.25 µm) (Phenomenex, Torrance, CA, US). The inlet temperature was set at 260°C. After a 5-minute solvent delay, initial GC oven temperature was set at 80°C. Two minutes after injection, the GC oven temperature was raised to 280°C (5° C min⁻¹), and finally held at 280°C for 13 minutes. The injection temperature was set to 280°C and the ion source temperature was adjusted to 200°C. Helium was used as the carrier gas with a constant flow rate set at 1 ml min⁻¹. The measurements were made with positive electron impact ionisation (70 eV) in the full scan mode (m/z 30-550). The metabolites were identified using MassLynx 4.0 software (PerkinElmer Inc.) coupled with a commercially available compound library: NIST Mass Spectral Database 2.0 (PerkinElmer Inc., Waltham, MS).

2.11.5 Data analysis

The individual spectra and chromatograms from GC-MS data files were deconvoluted with the aid of Automated Mass Spectral Deconvolution and Identification System (AMDIS) spectral deconvolution software package v2.69 (NIST, Gaithersburg), freely available at <http://chemdata.nist.gov/mass-spc/amdis/>, to carry out baseline corrections and purify spectrum from background noise. AMDIS deconvolution settings were as follow: adjacent peak subtraction was two, resolution was medium, sensitivity was low, shape requirement was high and component width was kept at 12. The ELU files generated by AMDIS were then fed to SpectConnect online services <<http://spectconnect.mit.edu/>> to align batches of ELU files from related chromatograms and to filter peaks. The integrated signals generated by SpectConnect were used for data normalisation and subsequent statistical analysis. Data normalisation was performed on Excel spreadsheet. Target compounds were identified by fragmentation patterns and matching spectra in a reference library (NIST Mass Spectral Database v. 2.0).

2.16 Quantification of naphthalene in root shoot tissues of tall fescue using gas chromatography-flame ionisation detection (GC-FID) technique

2.12.1 Sampling

Same as 2.11.1

2.12.2 Sample preparation

Same as 2.11.2

2.12.3 Extraction and analysis

Freeze-dried tissue powders (0.1g) were transferred into 10ml extraction tubes (Schott). The following sets of extraction tubes were prepared:

1. 0.1g sample, 100 μ l toluene (20 ppm) as internal standard and 2ml of cold dichloromethane (DCM): methanol: water (3:3:2 v/v) (3 reps)
2. 0.1g sample, 100 μ l toluene (20 ppm) as internal standard and 2ml of cold n-pentane: dimethyl formamide (DMF) (3:2 v/v) (3 reps)
3. 100 μ l toluene (20 ppm) as internal standard and 1350 μ l of DCM: chloroform: n-pentane (1:1: 1.6 v/v) (2 reps).

The samples were extracted on a rotator extraction unit at 40 rpm for 120 minutes. The tubes containing extracts were agitated using an ultrasonic bath at 20°C for 30 minutes and centrifuged at 2000g for 5 minutes. Seven hundred and fifty micro litres (750 μ l) of chloroform was added to the extracts extracted in DCM: methanol: water (No.1). The mixture was vortexed thoroughly and centrifuged at 2000g for 2 minutes. Non polar fractions were collected using glass capillary pipettes from the bottom layers from extraction 1 (extracting solvent: DCM: methanol: water + chloroform addition) and from the top layer from extraction 2 (extracting solvent: n-pentane: DMF) into labelled glass vials. The pooled non-polar phase was transferred into labelled GC vials and analysed by GC-FID (Make: Agilent Technologies 6850 Network GC System; Software: ChemStation). GC-conditions were the same as used in PAH determination (see section 2.3.1). The presence of naphthalene in tissue samples was confirmed by running naphthalene standard on GC in similar conditions and comparing the retention time of the standard with that of the peaks for the compounds eluted from tissue extracts.

2.17 Statistical analysis

Statistical significance was determined by a combined approach of Student's t-test in Microsoft Excel and a two-sample t-test in Genstat. Fisher's exact test was performed on the epi-fluorescent photomicrographs taken for each different treatment (chapter 4).

2.14 Quality assurance and control

2.14.1 Introduction

Systematic methods were used to achieve the required standards. A system (replications and direct comparisons) was used to deliver confidence in terms of the accuracy and reproducibility of the results, and in demonstrating an effect against untreated plants. The outputs were also related to similar findings reported in the literature.

2.14.2 Labelling systems

Rhizo-boxes, pots, vials, tubes, specimen stubs and all other relevant materials were clearly labelled with unique identifying references written either on adhesive labels or permanent ink, whichever was most suitable.

2.14.3 Calibration and controlling parameters

Equipment (balance) was always calibrated to ensure the drift did not fall outside the acceptable range. Root sample size for SEM preparation was controlled not to fall beyond the 1mm³ range to ensure adequate fixation. Pressure and temperature were controlled during critical point drying procedure (1072 psi and 31 °C) (Postek et al., 1980). The pressure and timing were controlled during sputter coating. Analytical reagent grade chemicals were used and glassware was always thoroughly cleaned. Controls were established in experiments for direct comparison.

2.14.4 Homogenization

During the preparation of replicates, a third of the mixed, spiked soil was transferred between the replicates and the sample prepared for storage (-20°C). The contents were

mixed again before transferring approximately half of what was left between the replicates and storage sample, and then mixed again before transferring the remainder. This ensured that the material was uniformly distributed between the different replicates, as soil particles that are either denser or smaller tend to accumulate at the base of the pile.

2.14.5 Replication

Replication was used to identify the level of variability in and between the different treatments, confirming the reproducibility of the results obtained, limiting the potential for systemic errors.

CHAPTER 3

Changes in root growth patterns and root ultra-structure arising from growth in sand contaminated with petroleum crude oil

3.1 Introduction

Phytoremediation is a green technique that aims to utilise plants to cleanse or amend polluted soils such as old gas work sites, to achieve complete mineralization of the contaminants to non toxic end products such as carbon dioxide and water, through plant-initiated biochemical processes. It has been demonstrated that enhanced degradation of petroleum hydrocarbons occurs in the rhizosphere due to plant-initiated changes in number and composition of microbial communities (Siciliano et al., 2003), stabilisation of pollutants by polymerisation reactions such as humification (Harvey et al., 2001; Walton et al., 1994) and a limited amount of plant uptake (Gao et al., 2004; Harvey et al., 2001). A healthy root growth and plant establishment in contaminated soils are essential for the plants to encourage remediation in the rhizosphere (Johnson et al., 2004). However, the presence of petroleum hydrocarbon contamination in soil may create an unfavourable environment for the successful development of plant roots (Brandt et al., 2006; Merkl et al., 2005). In addition to the complexity of plant physiology and biochemistry (Meagher, 2000), root architecture is of importance in the successful growth of plant roots in contaminated soils and the success of plant-initiated remediation of toxic organic compounds (Phillips et al., 2006; Siciliano et al., 2003). This study is aimed at addressing the question of how the root growth patterns are affected when different plant species that possess different root architecture are grown in crude oil-treated sand. Roots change physically and physiologically not only with age, but also due to changes in their environment (Enstone et al., 2003), and environmental stimuli can motivate chemical, biological and mechanical processes of a living system (Agarwal, 2006) which pave way to differences in gross ultrastructure. The root ultrastructural modifications in tall fescue (*Festuca arundinacea*) and beetroot (*Beta vulgaris*) due to growth in crude oil-treated sand (10.8g total extractable hydrocarbons kg⁻¹ sand dw) were studied with the aid of scanning electron microscopic techniques, to demonstrate an effect against untreated plants. The results of this investigation were used to choose the plant species that illustrated better establishment in crude oil- contaminated sand which

could also indicate better phytoremediation potential, among the plant species tested (parsnip, carrot, beetroot, brown top bent and tall fescue).

3.2 Results

a. Sensitivity of three different plant species that possess tap root system (parsnip, carrot and beetroot) to the exposure to crude oil contamination

Growth in sand contaminated with petroleum crude oil at the concentration of 10.8g total extractable hydrocarbons kg^{-1} sand (dw) (throughout this chapter crude oil is referred to as HC) stimulated different responses in three different plant species. To facilitate germination a layer of non-contaminated, clean agricultural sand was used as a seed bed. Still, the contamination totally prevented the germination of parsnip (*Parsnica sativa*).

Carrot (*Daucus carota*) germinated successfully with a score of 100%, but the plant growth was severely stunted in HC-treatment (Fig. 3.1& Fig.3.2). Also, from 3rd week of growth onwards, the carrot plants started to die in the HC-treatment. After 4 weeks, only 53.33 % of germinated plants were alive in HC treatment, whereas in control treatment none of the plants died during the trial that lasted for 3 months. Furthermore, at the age of 3 months, the carrot plants exposed to HC-contamination were ~6 times smaller in size ($p < 0.01$) (Fig. 3.2; Table 3.1) and weighed ~8 times less than the control plants.

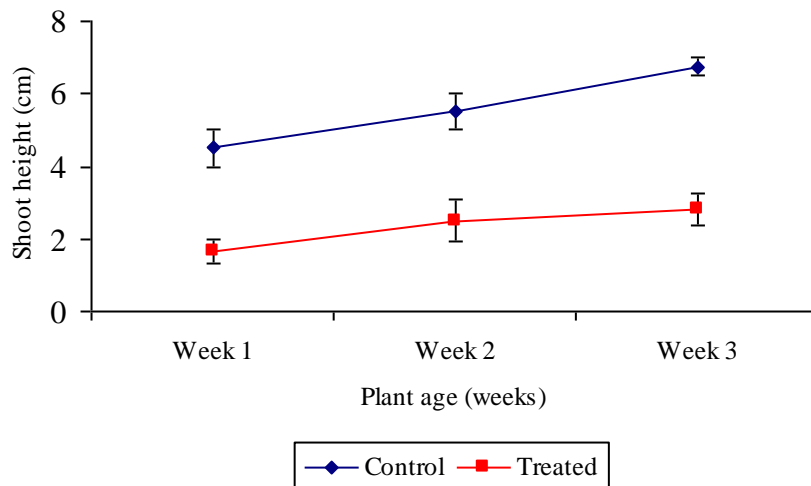


Fig.3.1: Shoot development of carrot during the first 3 weeks (N=3; $p < 0.05$ in the first two weeks; $p < 0.01$ in week 3; t-test). Error bar shows standard error of the mean. Shoot measurements were discontinued after 3 weeks of growth due to the death of the selected plants marked for shoot elongation study in HC-treatment.

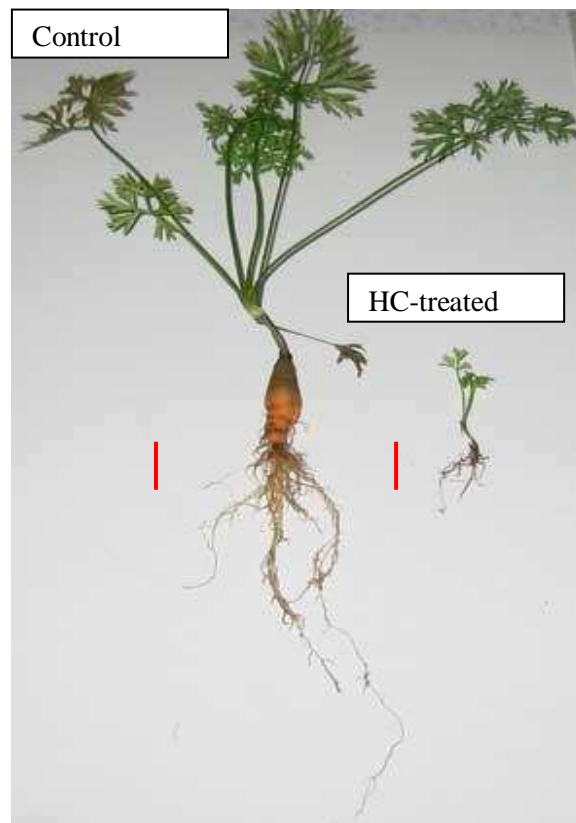


Fig.3.2: Carrot grown in clean sand (left) and HC-contaminated sand (right) for 3 months. Plant growth was significantly stunted in HC-treatment. The plant length was reduced by ~6 times in HC-treatment when compared to the controls ($p < 0.01$; N=3; t-test).

Table 3.1: Plant growth parameters of carrot grown in clean and HC-treated sand for 3 months. All t-tests are for differences between control and treated plants.

Plant growth parameters	Control Mean (\pm SE)	N	HC-contaminated Mean (\pm SE)	N	p value as determined by Student's t-test
Root length (cm)	11.67(\pm 1.20)	3	2.17(\pm 0.44)	3	p<0.01
Shoot height (cm)	16.67(\pm 2.03)	3	2.83(\pm 0.60)	3	p<0.01
Whole plant length (cm)	28.33(\pm 2.67)	3	5.00(\pm 1.00)	3	p<0.01
Plant weight (fw) (g)	2.33	Composite analysis	0.30	Composite analysis	-
Root: shoot (fw)	1.27	Composite analysis	0.42	Composite analysis	-

N=No. of samples; SE = standard error; p = probability

The germination percentage of beetroot (*Beta vulgaris*) was 60 (\pm 10) % in HC- treated sand, while the controls exhibited a 100% germination (p<0.05). As carrot, beetroot also showed a dwarfed growth in HC-treatment (Fig.3.3 - Fig.3.5). Similarly as carrot, from 3rd week of plant growth onwards, beetroot plants in HC-treatment started to die. After 4 weeks, only 55.55% of the germinated plants were alive in HC-treatment, whilst 90% plants were alive and healthy in control treatment (37% live HC-treated beetroot when compared to the controls). The beetroot plants in HC treatment had red/ purple tinted leaves in comparison to the bright green leaves of the control plants (Fig. 3.4). By the end of 3 months, the HC-treated beetroot plants were ~4.5 times smaller (p<0.001) (Fig. 3.5; Table 3.2) and 17.5 times lighter than the control plants.

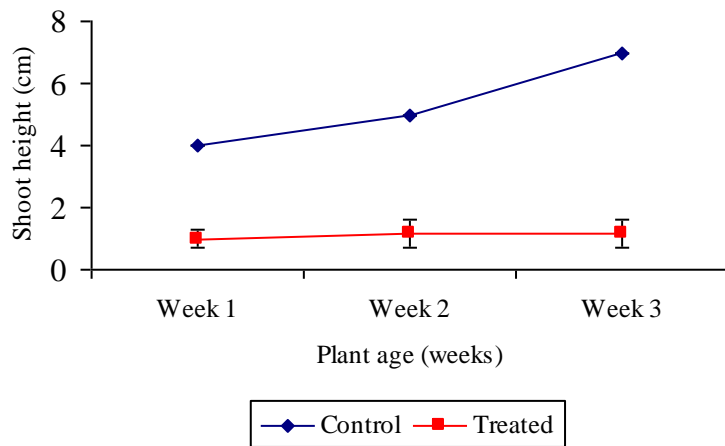


Fig.3.3: Shoot development of beetroot during the first 3 weeks (N=3; $p < 0.01$ in the first two weeks; $p < 0.001$ in week 3; t-test). Error bar shows standard error of the mean. Shoot measurements were discontinued after 3 weeks of growth due to the death of the selected plants marked for shoot elongation study in HC-treatment.



Fig. 3.4: Photograph of beetroot plants growing in HC-contaminated (left) and clean sand (right) for 2.5 months. Note the dark red or purple tinted leaves in plants exposed to HC-contamination, when compared to the bright green leaves in control plants of the same age.

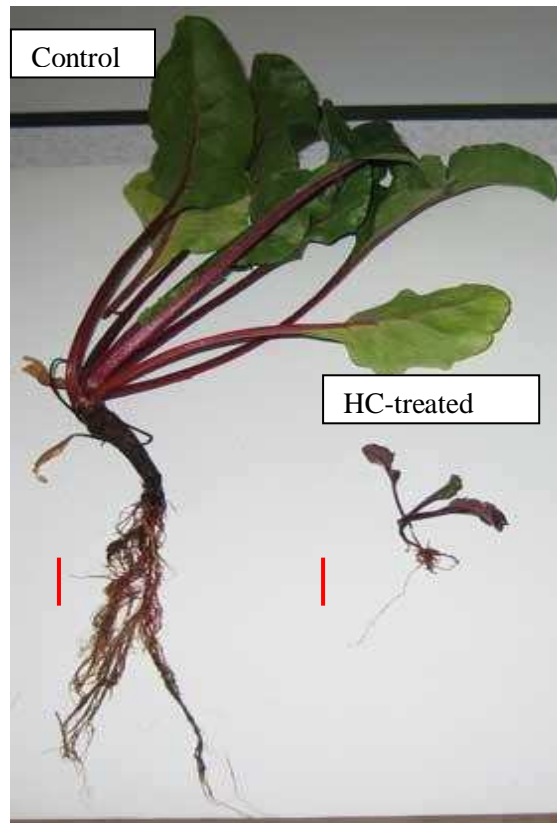


Fig.3.5: Beetroot grown in clean sand (left) and HC-contaminated sand (right) for 3 months. Plant growth was greatly stunted in HC-treatment. The plant length was reduced by ~4.5 times in HC-treatment when compared to the controls ($p < 0.001$; $N = 3$ (control) + 5 (treated); t-test).

Table 3.2: Plant growth parameters of beetroot grown in clean and HC-treated sand for 3 months. All t-tests are for differences between control and treated plants.

Plant growth parameters	Control Mean (\pm SE)	N	HC-contaminated Mean (\pm SE)	N	p value as determined by Student's t-test
Root length (cm)	17.33(\pm 2.85)	3	4.30(\pm 0.38)	5	$p < 0.01$
Shoot height (cm)	19.67(\pm 0.33)	3	3.90(\pm 0.60)	5	$p < 0.001$
Whole plant length (cm)	37.00(\pm 2.52)	3	8.20(\pm 0.81)	5	$p < 0.001$
Plant weight (fw) (g)	8.00	Composite analysis	0.46	Composite analysis	-
Root: shoot (fw)	0.24	Composite analysis	0.20	Composite analysis	-

N= No. of samples; SE = standard error; p = probability

b. Deviations in growth patterns of a grass mixture that possesses fibrous root system due to the exposure to crude oil contamination

A glasshouse pot experiment was established to study how the crude oil contamination [10.8g total extractable hydrocarbons kg⁻¹ sand (dw)] affect the growth patterns of a mixture of grasses containing tall fescue (*Festuca arundinacea*), brown top bent (*Agrostis capillaries* L.) and perennial ryegrass (*Lolium perenne* L.). In some HC-treatments, compost was added, in order to study the impact of compost addition on root growth in HC-treated sand. Seeds were germinated in a 2cm layer of non-contaminated, clean agricultural sand for all treatments. Plants were destructively sampled 3 months after germination and the plant growth patterns were visually examined.

At the age of three months, the control plants were densely populated and their roots had reached the bottom of the 2L plastic pots, producing a deep, dense root mass (Fig.3.6a). The HC-treated plants showed a lesser density ($p<0.01$) (Table 3.3), and possessed a differentially shaped root mass with a surface, dense root system, illustrating a preference of the plants to avoid contamination (Fig. 3.6b). In HC-treatments, in which compost was added, the plants grew in specific areas only, leaving patches of bare soil. The total density of plant population was much lower in HC-treatment that has compost addition, when compared to the controls ($p<0.001$) as well as treated with HC without compost ($p<0.01$), but the plants illustrated a deeply penetrated root system with longer roots ($p<0.01$) (Fig. 3.6c; Table 3.3). At 3 months of age, there were no significant differences in root length between control and HC-treatment without compost addition (Table 3.3). The shoots were shorter in HC-treatment, when compared to the controls ($p<0.05$), but the differences in shoot height between control and HC-treated with compost addition were not significant (Table 3.3).



Fig. 3.6: Root growth characteristics of a grass mixture (tall fescue, perennial ryegrass and brown top bent) grown in clean sand (a), HC-treated sand without compost addition (b) and HC-treated sand with compost addition (c) for 3 months. In control treatment (a), plants produced dense fibrous roots that extended into the sand to the depth of the pot. In HC treatment without compost addition (b), plant roots appeared to turn away from the contaminated soil matrix back into the top layer of the horticultural sand, producing a dense surface root mass. In HC-treatment that has compost addition (c), the roots penetrated deep into the pot, producing a deep root system, but the total plant population was lower when compared to the controls ($p < 0.001$) and the HC-treatment without compost addition ($p < 0.01$).

Table 3.3: Plant growth parameters of a grass mixture containing tall fescue, brown top bent and perennial ryegrass grown in clean sand and HC-treated sand that is either amended or not amended with compost, for 3 months

Plant growth parameters	a. Control Mean (\pm SE)	N	b. HC-contaminated Mean (\pm SE)	N	c. HC-contaminated with compost addition Mean (\pm SE)		p value as determined by Student's t-test
Population density (%)	92.33(\pm 3.93)	3 pots of plants	63.33(\pm 4.41)	3 pots of plants	35.00(\pm 2.89)	3 pots of plants	$p < 0.01$ between a & b and b & c; $p < 0.001$ between a & c
Root length (cm)	8.13 (\pm 0.95)	4	7.7 (\pm 0.41)	4	23.40(\pm 3.99)	4	$p < 0.01$ between a & c and b & c; NS between a & b
Shoot height (cm)	21.05 (\pm 1.34)	10	17.00(\pm 1.20)	10	20.10(\pm 0.89)	10	$p < 0.05$ between a & b; NS between a & c and b & c.

N=No. of samples; SE = standard error; p = probability; NS=not significant

b1. Differences in growth patterns of tall fescue (*Festuca arundinacea*) arising from growth in crude oil-treated sand

b1-1. Growth differences when exposed to a higher concentration of contaminants [16.5 g total extractable hydrocarbons kg^{-1} sand (dw)] and periodical monitoring of root shoot elongation

A rhizo-box experiment was established to study the impact of exposure to HC-contamination at a higher concentration [16.5g total extractable hydrocarbons kg^{-1} sand (dw)] on the growth of tall fescue (*Festuca arundinacea*) and to monitor the shoot and root development of the plants periodically. A 2cm layer of non-contaminated clean sand was used as a seed bed to facilitate germination. No differences were observed in germination between control and HC-treatment, but the shoot and root elongation of plants was reduced in HC-treatment until ~2.5 months of plant growth (Fig. 3.7, 3.8 & 3.9).

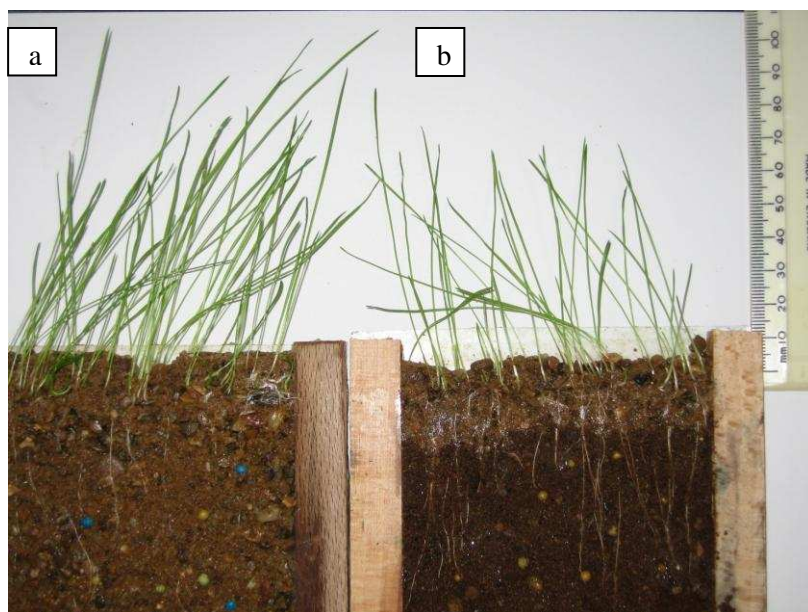


Fig. 3.7: Tall fescue grown in clean sand (a) and HC-treated sand [16.5g total extractable hydrocarbons kg^{-1} sand (dw)] (b) for ~2months.

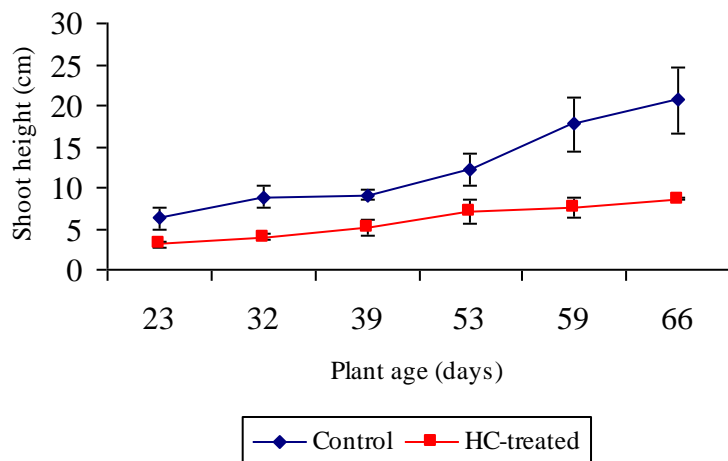


Fig. 3.8: Line graph showing the shoot elongation of 3 selected plants from each different treatment. Student's t-test was applied to each sampling period; $p < 0.05$ on day 32 and 39. Error bar shows standard error of the mean.

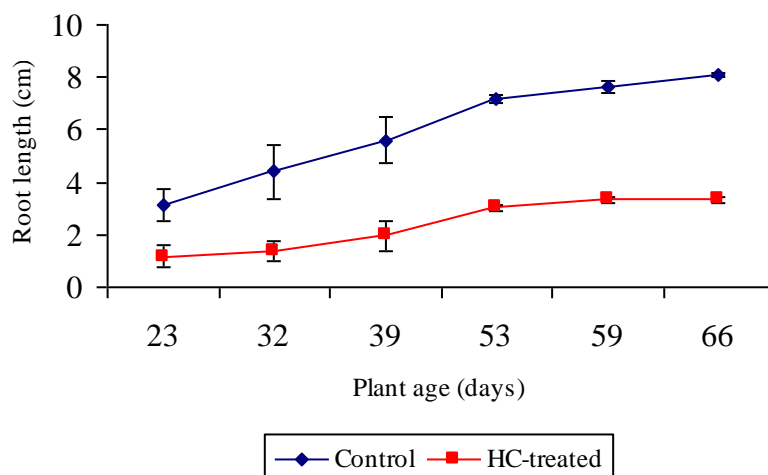


Fig.3.9: Line graph showing the root elongation of 3 selected plants from each different treatment. Student's t-test was applied to each sampling period; $p < 0.05$ on day 39 and $p < 0.001$ on day 53, 59 and 66. Error bar shows standard error of the mean.

Two months after germination, some plant roots were destructively sampled and stained with the vital stain Evans blue to study the impact of HC-contamination on the vitality of root hairs. The root sections viewed under a light microscope showed that higher percentage of root hairs stained blue in HC-treated roots (89% root hairs in HC-treated roots stained blue, whereas 47% root hairs stained blue in controls), illustrating the HC-contamination affects the vitality of root hairs negatively. The results also showed that the HC-treated roots had a lesser number of root hairs ($p < 0.001$) (Fig. 3.10). The scanning electron micrographs of plant root segments showed the HC-treated roots possessed fewer but also shorter root hairs (Fig. 3.11).

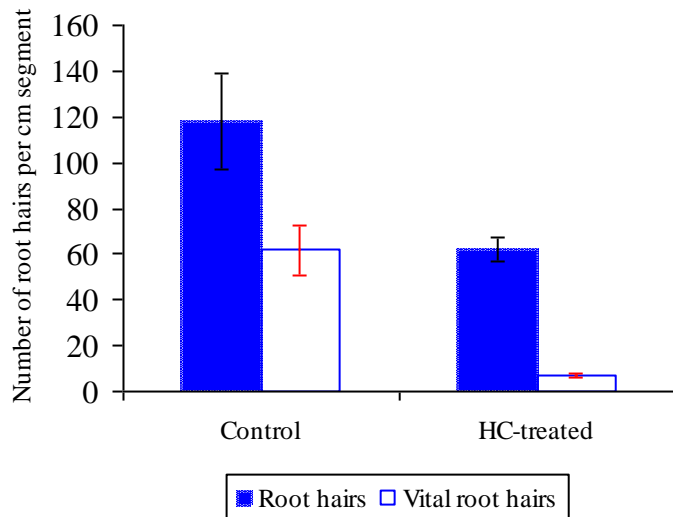


Fig. 3.10: Bar graph showing the difference in number of root hairs as well as the number of vital root hairs per cm segment of roots of 2 months old tall fescue demonstrated by a light microscopic study. Error bar shows standard deviation (N=3; $p < 0.001$; t-test).

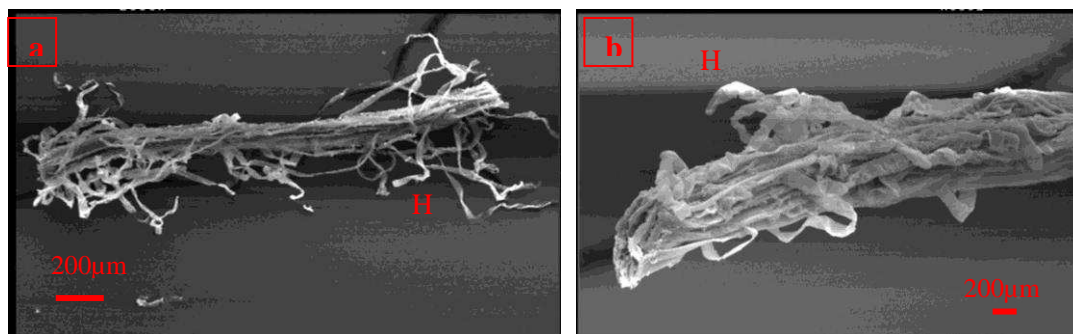


Fig. 3.11: Scanning electron micrographs of control (a) and HC-treated (b) tall fescue showing fragments of roots of 2 months old plants sectioned at one third as a fraction of root length above the root tip. H: root hair. Scale: 200µm.

b1-2. Growth differences when exposed to a lower concentration of contaminants [10.8 g total extractable hydrocarbons kg^{-1} sand (dw)]

A glasshouse pot experiment was established to study the impact of exposure to HC-contamination at a lower concentration [10.8g total extractable hydrocarbons kg^{-1} sand (dw)] on the growth of tall fescue (*F.arundinacea*). A 2cm layer of non-contaminated clean sand was used as a seed bed to facilitate germination. No differences were observed either in germination or in shoot development between control and HC-

treatment, but a clear-cut difference was observed in leaf pigmentation during the first month of plant growth. All HC-treated plants (10 replicates of pots; each pot contained ~25 plants) showed lack of dark pigmentation when compared to the controls. As shown in Fig. 3.6b, during the initial 3 months of plant growth, the HC-treated plants exhibited a deviation from normal root orientation responses to gravity, producing a dense, surface root mass. With time, however, tall fescue roots penetrated the contaminated soil matrix and grew successfully in it. It was also observed that the HC-treated roots had straightened at later stages, even though the curvatures were still partially expressed (Fig.3.12).



Fig.3.12: Root shape of tall fescue after growing in clean (a) and HC-treated (b) sand for 14 months

The scanning electron microscopic (SEM) images of roots revealed significant differences in the number and length of root hairs between control and treated tall fescue, 14 months after germination. The control plant roots were covered with many, long root hairs (Fig.3.13a), whilst the HC-treated roots possessed significantly less ($p < 0.001$) but also shorter root hairs ($p < 0.001$) (Fig. 3.13b). Root hairs in treated roots [$241.86 (\pm 34.69) \mu\text{m}$] were about one third the length of those of the control roots [$767.1 (\pm 94.58) \mu\text{m}$] ($p < 0.001$).

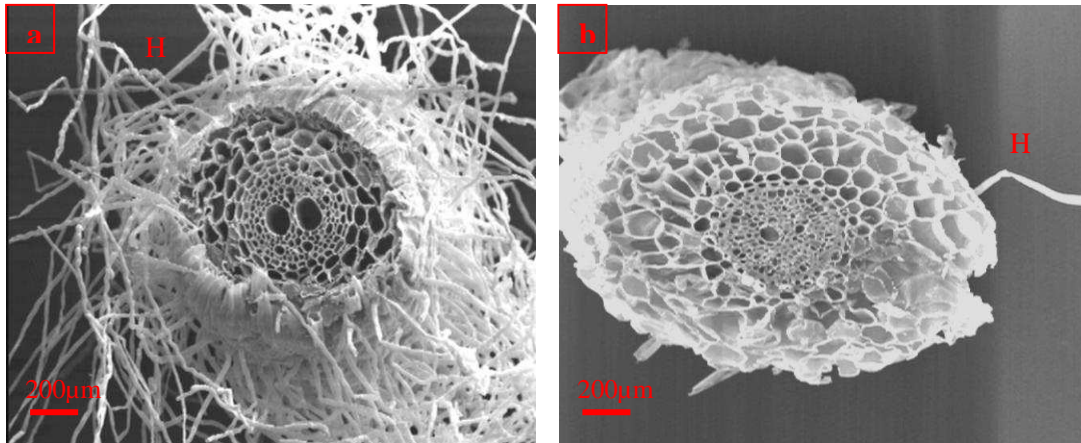


Fig.3.13: Scanning electron micrographs of control (a) and HC-treated (b) tall fescue showing cross sections of roots of 14 months old plants sectioned at one third as a fraction of root length above the root tip. H: root hair. Scale: 200µm.

b2. Differences in growth patterns of brown top bent (*Agrostis capillaries* L.) arising from growth in crude oil-treated sand

Similarly as described in section b1-1, a rhizo-box experiment was established using brown top bent (*A. capillaries* L.). In comparison to the germination rate of 95.56 (± 2.22) % in control treatment, only 15.56 (± 2.22) % seeds germinated in HC-treatment ($p < 0.001$) (Fig. 3.14; Table 3.4). Two months after germination, the shoot height of HC-treated brown top bent was ~3 times lower than that of the controls ($p < 0.001$) (Fig. 3.14; Table 3.4). The root length of the treated plants was 1.4 times shorter than that of the controls ($p < 0.001$) (Table 3.4). The treated roots possessed fewer root hairs among which only a lesser number was vital root hairs ($p < 0.001$) (Table 3.4). The HC-treated roots had 10% of vital root hairs, whereas the control roots possessed 56% of vital root hairs.

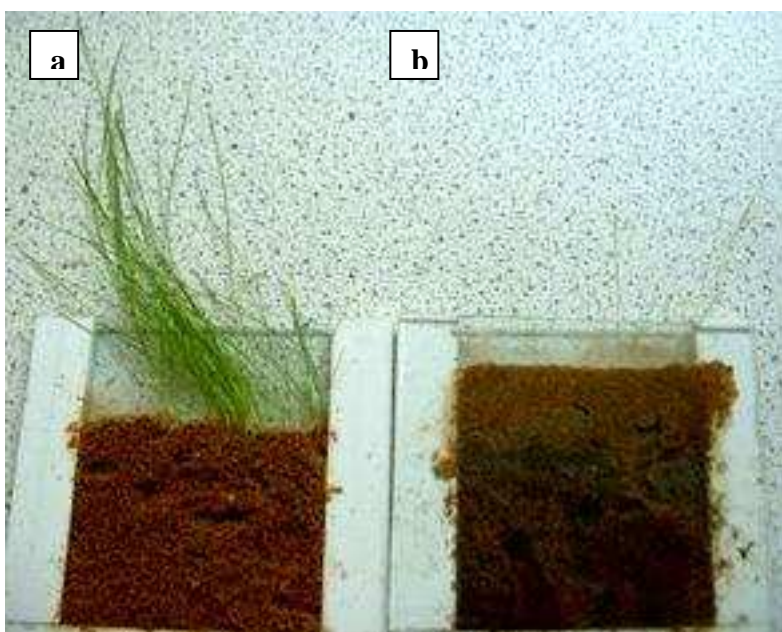


Fig.3.14: Brown top bent grown in clean sand (a) and HC-treated sand [16.5g total extractable hydrocarbons kg⁻¹ sand (dw)] (b) for ~2months. Similar results were obtained when the plants were grown in sand treated with a lower concentration of contaminants [10.8g total extractable hydrocarbons kg⁻¹ sand (dw)].

Table 3.4: Plant growth parameters of brown top bent grown in clean and HC-treated sand [16.5g total extractable hydrocarbons kg⁻¹ sand (dw)] for ~2 months. All t-tests are for differences between control and treated plants.

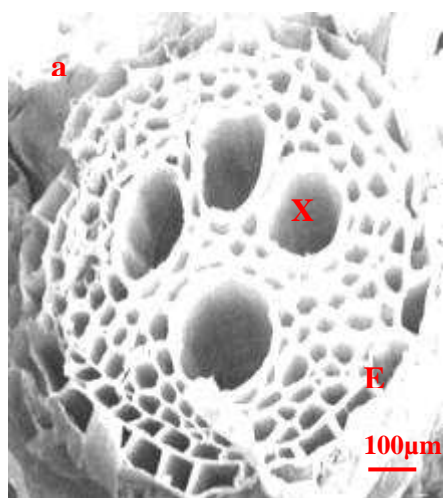
Plant growth parameters	Control Mean (\pm SE)	N	HC-contaminated Mean (\pm SE)	N	p value as determined by Student's t-test
Population density (%) (also reflects germination score)	95.56 (\pm 2.22)	3 rhizo-boxes of plants	15.56 (\pm 2.22)	3 rhizo-boxes of plants	p<0.001
Shoot height (cm)	10.80 (\pm 1.11)	3	3.67 (\pm 0.33)	3	p<0.001
Root length (cm)	5.20(\pm 0.44)	3	3.77 (\pm 0.14)	3	p<0.01
No. of root hairs per cm segment	120 (\pm 2)	3	21 (\pm 3)	3	p<0.001
No. of vital root hairs per cm segment	67 (\pm 2)	3	2 (\pm 1)	3	p<0.001

N=No. of samples; SE = standard error; p = probability

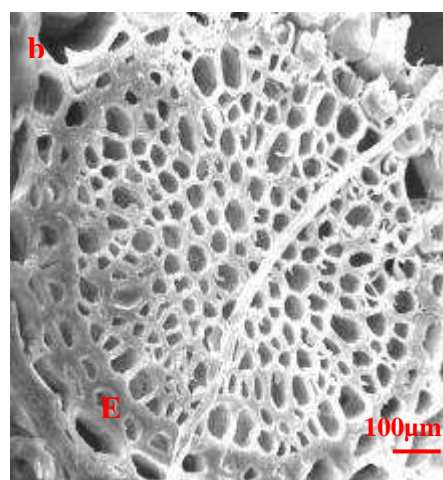
c. Root ultrastructural differences arising from growth in crude oil-treated sand (10.8g total extractable hydrocarbons kg⁻¹ sand dw)

A scanning electron microscopic study was carried out on tall fescue and beetroot plant roots after 3 months of growth in respective treatments. The root ultrastructural modifications of tall fescue were investigated through SEM techniques also after 6 months and 14 months of plant growth in HC-treated sand. An SEM study was not carried out on beetroot roots older than 3 months as the plants failed to survive the HC-contamination (10.8g total extractable hydrocarbons kg⁻¹ sand dw) longer than 3 months.

A preliminary scanning electron microscopic study revealed that the root hair zone begins more or less at the position of one third as a fraction of root length above the root tip in tall fescue (Fig.3.15). Hence, generally the roots were sectioned at one third as a fraction of root length throughout this investigation.



Sectioned at 1/3 as a fraction of root length above the root tip



Sectioned at 1/4 as a fraction of root length above the root tip

Fig.3.15: Scanning electron micrographs of roots of tall fescue (*Festuca arundinacea*) grown in clean (a) and HC-contaminated sand at the concentration of 10.8g TEH kg⁻¹ sand dw (b), showing transversal sections, taken at one third (a) and one fourth (b) as a fraction of root length above the root tip. Scale: 100 μ m. Key: E: endodermis; X: metaxylem vessel. Metaxylem vessels were not present in the contaminated root, presumably because the root was sectioned below the maturation/ root hair zone.

c1. Ultrastructural modifications illustrated by beetroot (*Beta vulgaris*) roots

HC-treated beetroot plants were ~4.5 times smaller than the control plants (Fig.3.5; Table 3.2) and therefore difficult to compare. Still, the scanning electron micrographs of treated beetroot roots exhibited enhanced thickening in the endodermis and smaller xylem vessels in comparison to their control counterparts (Fig.3.16).

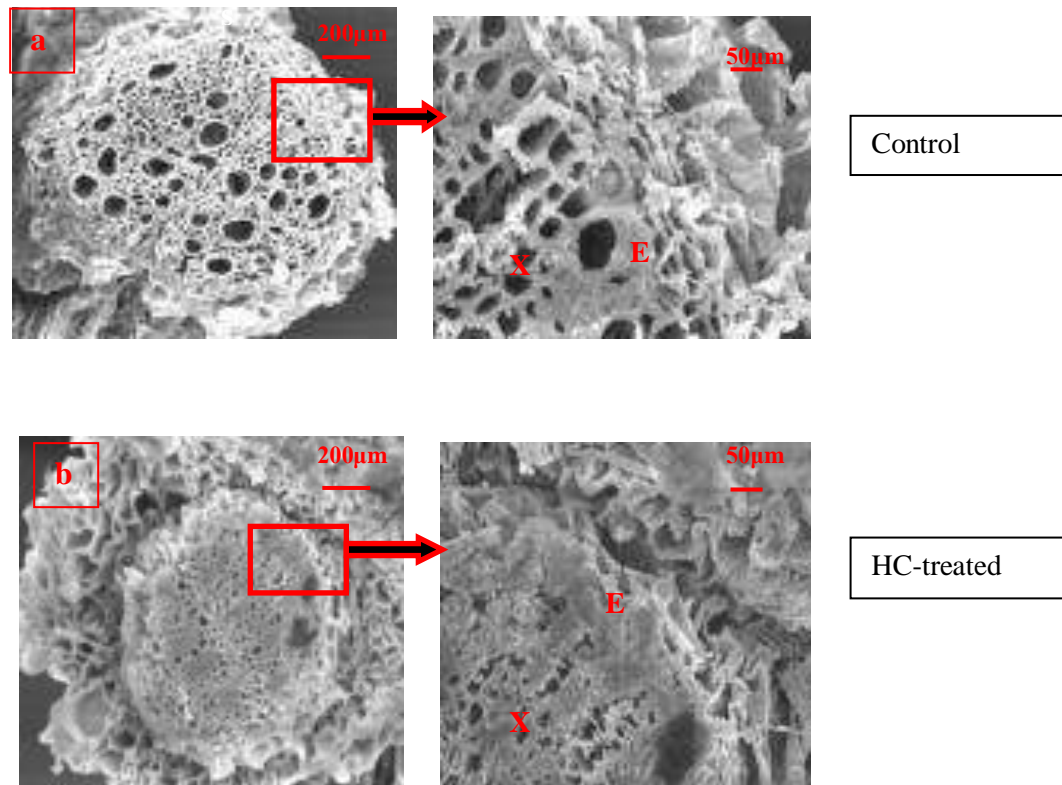


Fig.3.16: Scanning electron micrographs of 3 months old control (a) and HC-treated (b) beetroot showing transversal root sections at 1/3 as a fraction of root length above the root tip. Note the extensive thickening in the endodermis area (E) in b. Letters denote the following: E: endodermis; X: xylem vessel

c2. Ultrastructural modifications illustrated by tall fescue (*Festuca arundinacea*) roots

No distinct differences in the root ultrastructure of 3 months old tall fescue were observed between control and HC-treatment without compost addition (Fig. 3.17 a & Fig. 3.17 b), but the roots grown in HC-treated sand which was amended with the addition of compost possessed an enhanced cell wall thickening especially in their endodermis, and meta xylem vessels with a narrower bore (Fig. 3.17 c).

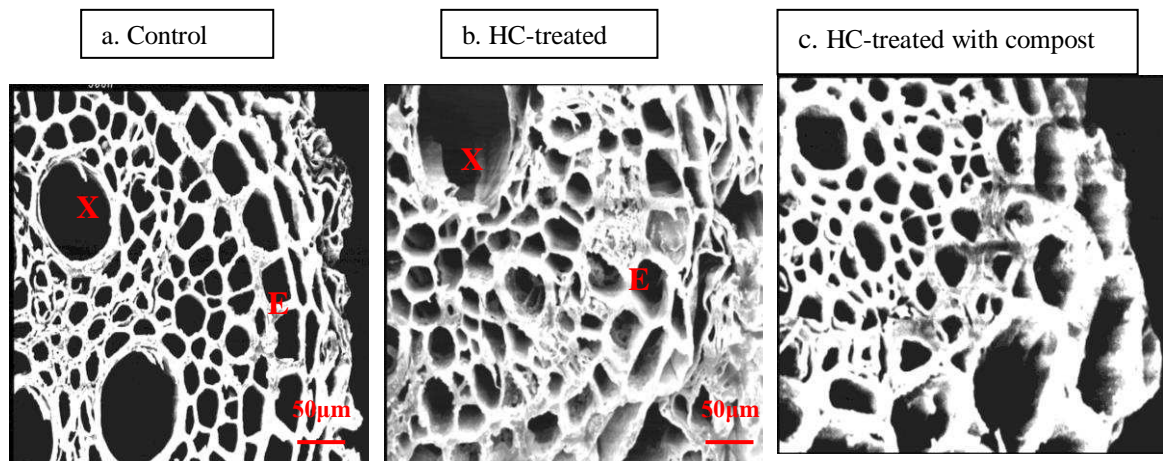


Fig.3.17: Scanning electron micrographs of tall fescue roots grown in clean sand (a), HC-treated sand (b) and HC-treated sand that had compost added to it (c), for 3 months, showing transversal root sections at the position of 1/3 as a fraction of root length above the root tip. Scale: 50µm. Letters denote the following: E: endodermis; X: metaxylem vessel. Note the differences in cell wall thickening especially in the endodermis and the reduced diameter of metaxylem vessel in plant root that was growing in HC-treated sand amended with compost (c).

The roots of tall fescue grown in HC-treated sand that was not amended with compost also showed an extensive thickening in the cell walls, especially in the endodermis, when compared to the controls, at the age of 6 months (>3 months of growth) (Fig.3.18).

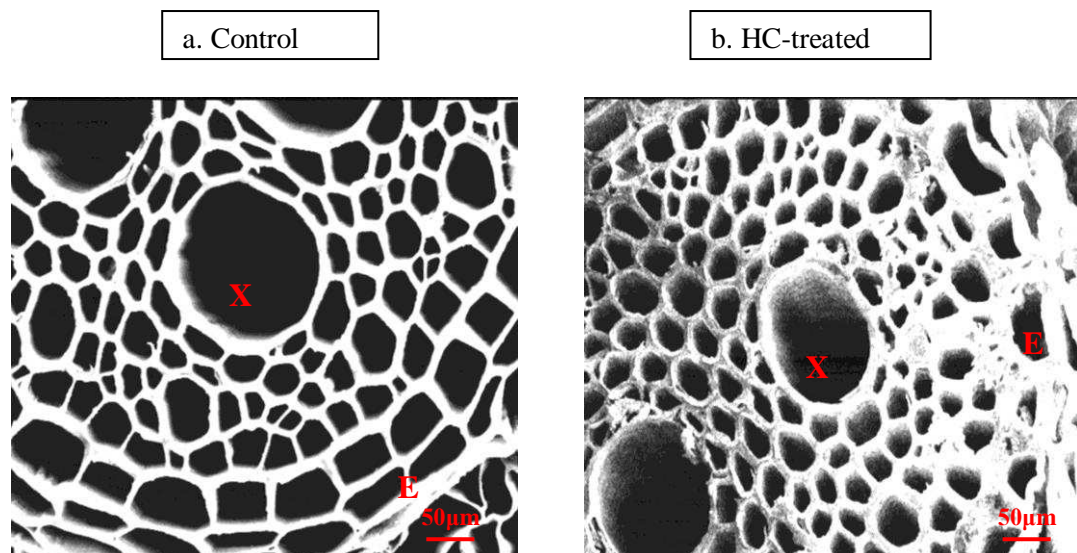


Fig. 3.18: Scanning electron micrographs of control (a) and HC-treated (b) tall fescue plants showing transversal root sections at 1/3 as a fraction of root length above the root tip. Age of plants: 6 months. Scale: 50µm. Letters denote the following: E: endodermis; X: metaxylem vessel. Note the differences in cell wall thickening especially in endodermis thickening in HC-treated plant root. At the time of sampling (6 months after germination), the roots were growing in HC-treated matrix.

Differences in root cortex between treatments could not be studied with the scanning electron micrographs obtained during the earlier plant growth period, as the root cortices were not preserved since critical point drying step was not included in the sample processing techniques employed earlier. Root samples were critical point dried before taking the SEM images of root sections of plants grown in clean and HC-treated sand for 14 months. Dramatically pronounced differences were observed in the root ultrastructure between control and HC-treated tall fescue after 14 months of growth in respective treatments (Fig.3.19). HC-treated tall fescue roots had bigger root diameters ($527.4\mu\text{m} \pm 29.11 \mu\text{m}$) than the controls ($457.8\mu\text{m} \pm 19.86 \mu\text{m}$) at the position of 1/3 as a fraction of root length above the root tip ($p < 0.05$) (Table 3.5). HC-treated plant roots had significantly enlarged cortex zone area compared to the control roots ($p < 0.001$) (Table 3.5), but showed no noticeable differences in the number of cortex cells (Fig. 3.19). In the HC-contaminated plant roots, the cortex cells were more of an isodiametric shape (Fig. 3.19 c, d) which contrasted with the more longitudinal cortical cell arrangement in control plant roots (Fig. 3.19 a, b). Also, partially collapsed cells were observed in the cortex area in treated roots (Fig.3.19 c). There were no significant differences in stele diameters between the two treatments (Table 3.5), but enhanced wall thickenings were observed in the cells around and inside stele and distinctively in the endodermis cells in the contaminated plant roots (Fig. 3.19 c, d) ($p < 0.001$) (Table 3.5), as observed in the earlier SEM study (Fig. 3.18b). Furthermore, the cells inside the stele of the HC-treated roots were noticeably smaller (Fig. 3.19 d). The SEM images of cross root sections showed a decrease in the size of the vessel elements in the HC-treated roots (Fig. 3.19 c, d) ($p < 0.001$) (Table 3.5). Furthermore, there was an increase in wall thickening of xylem elements in HC-contaminated plant roots when compared to their control counterparts (Fig. 3.19 d) ($p < 0.001$) (Table 3.5).

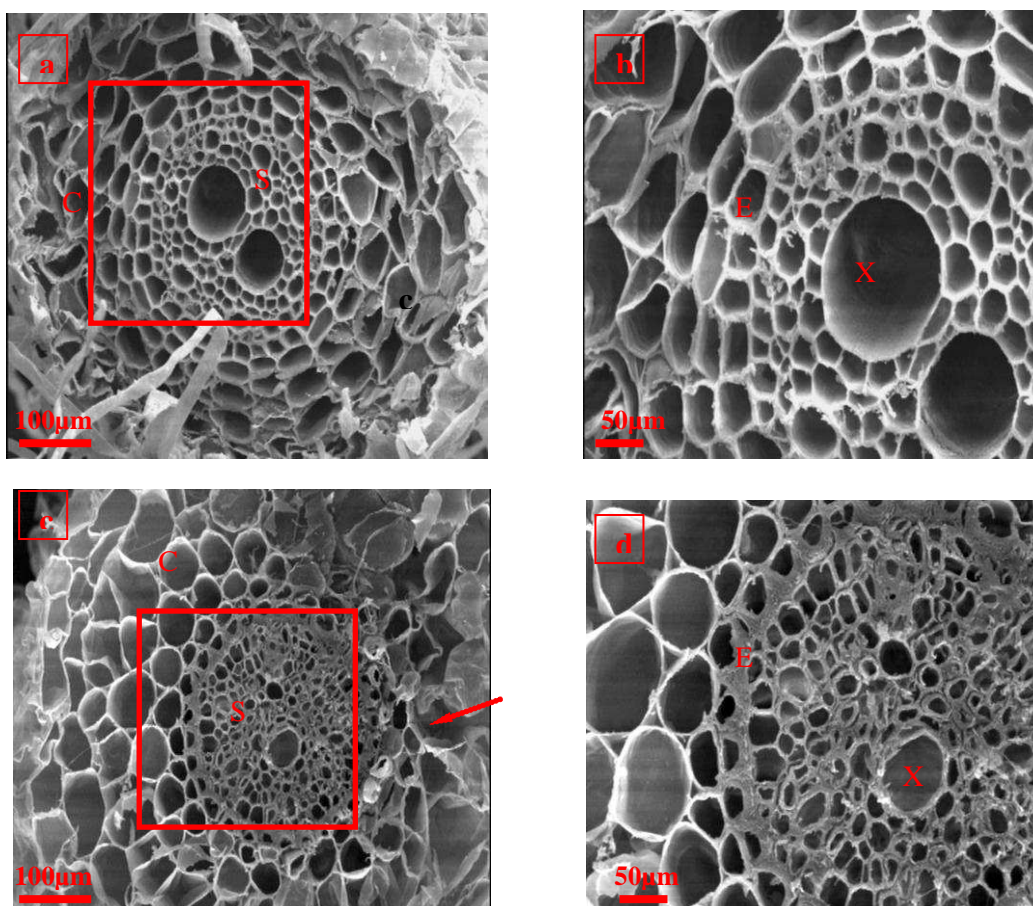


Fig. 3.19: Scanning electron micrographs of 14 months old control (a, b) and HC-treated (c, d) tall fescue showing cross sections of roots sectioned at one third as a fraction of root length above the root tip. Scale: a, c: 100µm; b, d: 50µm. Letters denote the following: C: cortex; E: endodermis; S: stele; X: metaxylem vessel. Arrow in c indicates partially collapsed cortex cells/ distortions in cortical area.

Table 3.5: Descriptive statistics for root ultrastructural parameters of 14 months old tall fescue roots at the position of 1/3 as a fraction of root length above the root tip. All t-tests are for differences between control and treated plants.

Root ultrastructural parameters	Control Mean (\pm SE)	N	HC-contaminated Mean (\pm SE)	N	p value as determined by Student's t-test
Root diameter (μ m)	457.78 (\pm 19.86)	8	527.46 (\pm 29.11)	6	p<0.05
Stele diameter(μ m)	196.78 (\pm 10.77)	8	193.77(\pm 9.59)	6	NS
Stele diameter:Root diameter ratio	0.43 (\pm 0.01)	8	0.37(\pm 0.02)	6	p<0.01
Cortex zone area(mm ²)	0.12 (\pm 0.004)	8	0.22 (\pm 0.02)	6	p<0.001
Total metaxylem area (μ m ²)	4339.00(\pm 386.08)	8	683.07 (\pm 96.42)	6	p<0.001
Metaxylem wall thickness (μ m)	0.63 (\pm 0.09)	8	2.14 (\pm 0.12)	6	p<0.001
Endodermis wall thickness (μ m)	2.21(\pm 0.20)	8	5.99 (\pm 0.07)	6	p<0.001

N=No. of samples; SE = standard error; p = probability; NS= not significant

Figure 3.20 summarises the relationship between xylem wall thickness and metaxylem area in the roots of tall fescue grown in clean sand and HC-treated sand for 14 months.

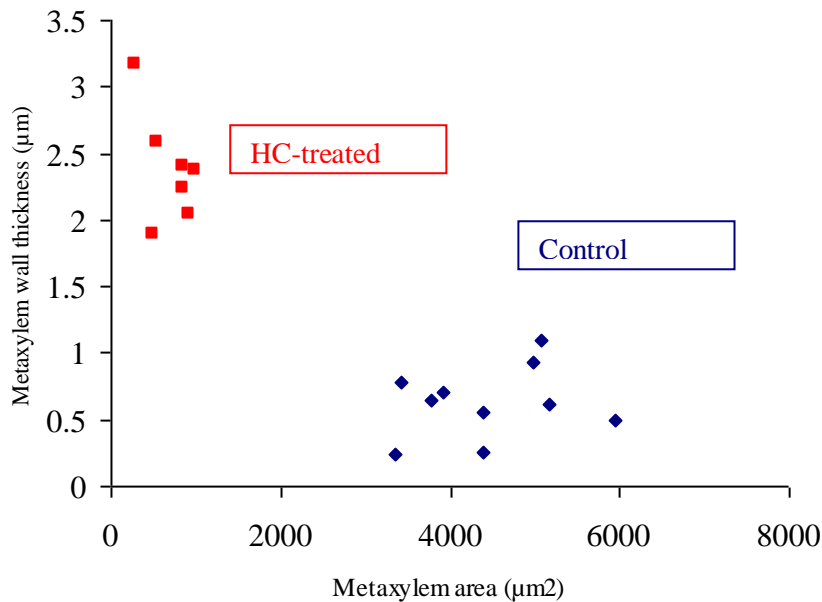


Fig.3.20: The relationship between metaxylem wall thickness and total metaxylem area in control (indicated by blue diamonds; $r=0.25$) and HC-treated (indicated by red squares; $r=-0.53$), 14 months old tall fescue plant roots at the position of one third as a fraction of root length above the root tip.

d. A biphasic dose response illustrated by crude oil-treated tall fescue (*Festuca arundinacea*) to enhanced drought conditions

Fourteen months old tall fescue plants were left without watering for a period of 2 weeks. Unexpectedly, the plants (10 replicates of pots each containing ~25 plants) grown in HC-treated sand (10.8g total extractable hydrocarbons kg^{-1} sand dw) remained visually unaltered, whereas the control plants showed signs of wilting and started to die off. The differences in visual drought resilience between treatments were significant ($p<0.001$).

3.3 Discussion

Roots of land plants are in direct contact with their soil environment in which they perform their functions of anchorage, absorption, conduction, and storage of water, nutrients, and foods. When the soil is contaminated with HC, the soil characteristics

change. Due to the hydrophobicity of the HC molecules which wrap around the soil particles, water spreads inhomogeneously in HC-treated soil. A difference in the water drainage pattern between HC-treated soil matrix and clean sand was observed consistently. Water appeared to stay on top of the contaminated soil matrix (Fig.3.21) and then quickly ran through the holes at the bottom of the pots and through the very small gaps in rhizo-boxes which contained HC-treated sand. Baker (1973) had reported that water drains rapidly in oil-impregnated soil, after an initial water logging. This may lead to deficiency of available water for plant root absorption, subsequently reducing mineral and oxygen intake.



Fig.3.21: Photograph showing water staying on top of the HC-contaminated soil matrix, before quickly running through the holes at the bottom of the pot

This anomaly in water drainage patterns may contribute to leaching of nitrogen (N), a major element which is required in relatively large quantities in connection with all growth processes in plants including the synthesis of chlorophyll. The HC-contamination may also affect the soil pH which strongly influences nitrification (Leggo and Ledesert, 2010); therefore this may also have an adverse effect on N available for absorption by plant roots, especially in sand that has a very low buffering capacity. Additionally, Newman and Reynolds (2004) reported that the presence of HC-molecules increases the C: N ratio in the soil, decreasing the availability of N for plant root absorption. So the changes in leaf colour and stunted

growth of carrot, beetroot and tall fescue (only during the initial growth period of up to 2.5 months) plants growing in HC-contaminated conditions may suggest that the treated plants were suffering from N deficiency. Stunted growth and lack of dark pigmentation can be produced by the deficiency of elements other than N, such as phosphorous (P) magnesium (Mg), sulphur (S), manganese (Mn) and iron (Fe). So generally plant nutrition may be poor in HC-contaminated soil matrix due to leaching, inhomogeneous spreading of water and higher levels of C content. The competitions between proliferated micro organisms in the rhizosphere of HC-treated plants (Siciliano et al., 2003) and plant roots for nutrients may also contribute to the scarcity in the supply of nutrients available for plants (Merkl et al., 2005).

Furthermore, the components of HC could be phytotoxic. The HC-treated beetroot plant leaves exhibited dark red/ purple discolouration. Vazquez et al. (1989) reported reddish-brown discolouration at the base of the leaf blades of cadmium (Cd)-treated bean plants (*Phaseolus vulgaris*), and attributed it to Cd-toxicity. The discolouration of HC-treated beetroot leaves and the plants' premature death may also suggest that HC contamination imposes toxic effects on plants. Still, the dark red/ purple leaf colouration of HC-treated beetroot could be due to P deficiency as reported by (Wallace, 1943), which could have been caused by water deficiency. Moreover, the HC-treated tall fescue and brown top bent possessed a lesser number of vital root hairs per cm segment of roots ($p < 0.001$), suggesting toxic as well as water stress effects of HC on plant roots.

Whilst the control roots were woolly with many, long root hairs, the HC-treated tall fescue roots possessed significantly less ($p < 0.001$), but also shorter root hairs ($p < 0.001$). These results were consistent for both younger (Fig. 3.11) and older roots (Fig. 3.13). Ample moisture and a good oxygen supply are necessary to promote abundant development of root hairs (Taiz and Zeiger, 1998; Weaver, 1926). Hence, the inhibited development of root hairs in HC-treated tall fescue as well as in HC-treated brown top bent could be due to lack of moisture and oxygen supplies. Since root hairs are significant in increasing the surface area for the absorption of soil ions and to a lesser extent soil pore water (Taiz and Zeiger, 1998), the reduction of root

hairs observed in HC-treated plant roots would reduce the mineral ion absorption by plant roots, consequently affecting the nutrient status of the plants.

During the first 3 months of growth, the HC-treated grass roots showed deviations from normal root orientation responses to gravity (Fig. 3.6b). In nature, gravity is the main stimulus in directing the downward growth of the root system. However, roots also respond to other stimuli in their environment ((Pages et al., 2000), such as differences in the amount of moisture and oxygen supplies, the roots being attracted towards moist soil areas and favourable oxygen supplies (Weaver, 1926). Under such influences, the root tip pursues a general downward course through the soil, its slight movement from side to side aiding it in penetrating the zone beneath, which presents unfavourable conditions (Weaver, 1926). The turning of the roots back into the clean layer of sand, the curvatures and the change in shape of the root mass of the treated plants (Fig. 3.6b) may be due to the limited supplies of oxygen and moisture in the HC-contaminated zones. On the other hand, plants grown in HC-treated sand which was amended with compost were growing straight into the contaminated matrix (Fig.3.6c), producing much longer roots than the controls and HC-treated plants without compost addition, of the same age ($p < 0.01$). This suggests that the compost either absorbed the HC components, reducing their concentrations in the sand or alternatively produced a preferential pathway for the roots to follow. However, the plant population density in HC-treated sand amended with compost was lower when compared to the controls ($p < 0.001$) and HC-treatment without compost addition ($p < 0.01$), perhaps because the compost used was immature.

The HC-treated tall fescue and beetroot roots exhibited an extensive thickening in their root cell walls, especially in their endodermis, as well as smaller xylem vessels. The 3 months old HC-treated tall fescue roots, which showed a tendency to coil back into the top layer of clean, agricultural sand, however, did not have an extensive thickening or smaller xylem vessels (Fig. 3.17b). The roots of the plants of the same age, grown in HC-treated sand amended with compost, that did not show deviations from normal root growth orientation, exhibited a clearly discernible enhanced cell wall thickening, particularly in the endodermis, and xylem vessels with narrower bore (Fig. 3.17c). Environmental stresses are known to induce increased lignifications in cell walls and enhanced development of the endodermis (Soukup et al., 2004; Enstone

et al., 2003). The clearly observed enhanced thickenings, particularly in the endodermis of plant roots growing in the HC-treated matrix may suggest that the endodermis acts as a barrier to HC contaminants, preventing them from being taken up into xylem vessels via apoplastic fluxes. Barcelo et al. (1988) reported a decrease in vessel size in Cd-treated bush bean stems. A substantial decrease in the size and number of xylem elements were also observed in seminal wheat roots exposed to higher temperatures (40°C) by Huang et al. (1991). So, the decrease of xylem vessel size in plant roots growing in HC-treated sand in our study, also suggests that unfavourable conditions are imposed on plant roots by the HC contaminants. Decrease of metaxylem vessels, presumably due to enhanced wall thickening, and the endodermis thickenings were more prominently observed in tall fescue roots growing in HC-treated sand for a longer period of time (14 months) (Fig. 3.19). In addition to the characteristics of the species, place and time of origin, the root structure is influenced by the environmental conditions. The more the root elongates from the base; the higher can get the environmental influence (Sobotik and Haas, 2009). The dramatically pronounced differences in root anatomy between tall fescue roots grown in clean sand and HC-treated sand for 14 months, were perhaps, due to higher environmental influence, as the roots at this time point had elongated further from the base and were deep inside the HC-treated matrix.

The curvatures of HC-treated tall fescue roots were observed to be straightened at later stages (after the acclimatisation period of 3 months), suggesting that the deviations from normal root orientations towards gravity were only temporary. The results suggest that the roots had retained a commitment to their prestimulus vertical orientation, and reverted to it, perhaps, following changes in the biomechanical properties of cell walls responsible for wall elasticity in the zone of curvature (Stankovic et al., 1998). Stankovic et al. (1998) conducted a study on autonomic straightening of gravitropic curvature of cress roots. Their study showed that curved roots returned closer to the prestimulus vertical, indicating the existence of an inherent, autonomic or default tendency for disorientated organs to revert to a previous equilibrium orientation. Their study also showed that the curvatures were not completely reversed in cress roots. Even though the root mass of the older tall fescue plants was not restricted to clean zone and not very curvy, some curvatures continued to be expressed in HC-treated roots in our study (Fig. 3.12b), possibly due

to the existing environmental vectors such as limited moisture and oxygen supplies in the contaminated zone.

Partially collapsed cortex cells were observed in the cortex area in HC-contaminated tall fescue roots (Fig. 3.19 c). Enstone et al. (2003) demonstrated partial collapse of the cortex in seminal roots of wheat seedlings exposed to water stress conditions. So, the partially collapsed cells in the cortical zone of tall fescue roots exposed to HC contamination suggests that water is a key limiting resource in HC-contaminated soil resulting in plants suffering from water stress. The narrower bore of metaxylem vessels in roots growing in HC-treated sand may suggest that the water economy of the plants can be affected. The decrease in size of xylem vessels exhibited by HC-treated tall fescue is possibly an insurance strategy of the plants to limit the water loss due to transpiration by reducing the bore of the xylem vessels to supply leaves with water and nutrients, when lower amounts of water are available.

Increased cortex zone due to isodiametric shaped cortex cells were observed in HC-treated tall fescue roots. Similarly, Barcelo et al. (1988) reported an increased cortex zone in Cd-treated bush bean stems due to isodiametrically-shaped cortex cells. So, the arrangement of more or less isodiametric shaped cortex cells observed in HC-treated tall fescue roots (Fig.3.19 c) may indicate a response of plant roots to phytotoxicity imposed by the presence of HC contaminants in the soil environment. By increasing cortical zone area, the plants could increase the distance the toxic substances in the cellular pathway have to travel in order to reach the xylem vessels, restricting the toxicants in the soil pore water from entering the stele via symplastic stream. Most importantly, the extensively thickened endodermis in HC-treated roots could restrict the entry of HC contaminants into the inner core of the roots via apoplastic fluxes.

The modifications in root ultrastructural features of HC-treated tall fescue suggest both symptoms akin to water stress and structural defences against the penetration of HC-contaminants into the inner core of the roots. A rather unexpected result was obtained when the older tall fescue plants (14 months of age) were subjected to water stress, by not watering the plants for two weeks. The control plants began to show

wilting appearance and started to die off, whereas the HC-treated tall fescue proved to be resilient. These pave way to the hypothesis that the presence of HC contaminants in soil creates scarcity of plant available water, stimulating drought adaptive responses in tall fescue roots and motivating the formation of a barrier to water loss, which consequently restricts the entry of the xenobiotic hydrocarbons into the inner core of the roots. This hypothesis was tested and the results are discussed in chapter 4.

The severely stunted growth of beetroot plants grown in HC-treated sand made it difficult to compare the root anatomy between control and treated plants of the same age. Still, the HC-treated beetroot roots illustrated an extensive thickening in the endodermis and smaller xylem vessels as the HC-treated tall fescue roots. However, beetroot failed to establish in the HC-contaminated sand, whereas tall fescue was well-adapted to survive the stress conditions caused by HC-contamination, particularly after an acclimatisation period of 3 months. The morphological plasticity illustrated by tall fescue roots in delaying the contact with the contaminants by turning back into the non-contaminated seed bed could have contributed towards the plants' successful establishment in HC-treated sand. Still, brown top bent, which also possesses similar root architecture as tall fescue showed a remarkably reduced germination ($p < 0.001$) and much inhibited growth ($p < 0.001$) due to the exposure to HC-contaminants. Hence, the structural and ultrastructural characteristics of plant roots are not the only features accountable for the successful establishment of a plant species in HC-treated sand. Metabolically induced changes responsible for the adaptability of tall fescue to growth in sand treated with naphthalene (a readily bio available PAH which is also a component of HC) were studied and the results are discussed in chapter 5.

CHAPTER 4

Responses of tall fescue (*Festuca arundinacea*) to growth in naphthalene-contaminated sand: xenobiotic stress versus water stress

4.1 Introduction

Plants respond to environmental constraints by modifying their structural and ultrastructural features (Agarwal, 2006), in order to adapt to the changes in their growth environment. Results in chapter 3 showed that growth in sand contaminated with petroleum crude oil (HC), caused extensive endodermal cell wall thickening, increased cortical zone and partial collapse of the cortex in the roots of tall fescue (*Festuca arundinacea*). Enstone et al. (2003) demonstrated partial collapse of cortex in seminal wheat roots as a symptom of water stress, whilst an accelerated maturation of endodermis has been documented under stress conditions (Soukup et al., 2004; Enstone et al., 2003). An increased cortical zone has been suggested as a phenomenon to restrict entry of toxic compounds into the inner core of the roots and shoots (Collins et al., 2006 and references therein; Barcel'o et al., 1988). So, the modifications in root features observed in HC-treated tall fescue roots in our study (Chapter 3), suggests that interplay of drought stress responses and xenobiotic stress responses occurs in tall fescue roots when grown in HC-treated soils.

The water status of plant tissues is determined by the pattern of water exchange between the plant and the environment (Slatyer, 1967). Modifications in root ultrastructure bear direct relevance to the changes in functional properties of the roots. Casparian Strip has the dual functions of preventing the cortex cells from drying out in water deficit conditions (Jupp and Newman, 1987) as well as keeping out foreign bodies that may be harmful to the plants, from being delivered into the inner core of the roots (Enstone et al., 2003). Hence it was of importance to investigate the differences between control and contamination-treated plant roots in terms of Casparian strip, together with other root ultrastructural features (e.g. root cortex). Berberine hemisulphate is known to stain Casparian strip specifically and has been used by Brundrett et al. (1988) in their study of plant tissues. A similar approach was used here to study the difference in the abundance of Casparian band structures between control and treated roots.

Crude oil (HC) is a highly heterogeneous material containing aliphatic and aromatic hydrocarbons including polycyclic aromatic hydrocarbons (PAHs). PAHs are considered as particularly harmful environmental pollutants because of their carcinogenic and/ or mutagenic potential, ubiquity and persistence (Janska et al., 2006). PAHs can be of either high molecular weight (HMW) or low molecular weight (LMW), and differ in their water solubility and volatility. Here, a preliminary study was carried out to test the effect of exposure to different PAHs on seed germination and subsequent plant development. The PAHs selected were naphthalene, fluoranthene, anthracene and benzo (a) pyrene (up to a concentration of 1000mg kg⁻¹ sand dw) that show differences in their physico chemical characteristics such as molecular weight, solubility in water and volatility (see table below).

Table 4.1: Physico-chemical parameters of naphthalene, fluoranthene, anthracene and benzo (a) pyrene [B(a)P]

PAH	Vapour pressure (Pa)	Henry's law constant (H) (Pa.m ³ mol ⁻¹) at 25° C	Solubility in water (mg L ⁻¹)	Molecular weight (g mol ⁻¹)
Naphthalene	1.04×10 ¹	57.4	31	128.2
Fluoranthene	7.00×10 ⁻³	1.1	0.26	202.3
Anthracene	1.00×10 ⁻³	3.28	0.045	178.2
Benzo (a) pyrene [B(a)P]	7.00×10 ⁻⁷	0.01	0.004	252.3

Source of vapour pressure and H for naphthalene, anthracene and B(a)P: Mackay et al. (2000); Source of vapour pressure for fluoranthene: Váňová, 2009; Source of H for fluoranthene: De Maagd et al. (1998). Henry's law constant (H) (Pa.m³mol⁻¹) is the ratio of partial pressure in air (Pa) to the concentration in water (mol m⁻³) and it expresses the relative air-water partitioning tendency (Mackay et al., 2006). Source of solubility in water: Farrell-Jones (2003).

Based on the results of the initial study, naphthalene was chosen as the model toxic PAH which is present in crude oil (exact concentration unknown) to further the investigation, probing into the responses of plants to water stress and xenobiotic stress. Simultaneously, the water balance aspects of naphthalene-treated sand as opposed to the non-contaminated, clean sand were investigated.

Water is held in soil in various ways:

- a. Chemical water: This is an integral part of the molecular structure of soil minerals, held tightly by the electrostatic forces to the surfaces of clay crystals and other minerals.
- b. Gravitational water: This is held in large soil pores and drains out rapidly under the action of gravity (Fig. 4.1A).
- c. Capillary water: This is held in pores that are small enough to hold water against gravity, whilst allowing roots to absorb it. This water occurs as a film around soil particles and in the pores between them, and is the main source of plant moisture (Fig. 4.1B). As this water is withdrawn, the larger pores drain first followed by the smaller pores. The finer pores present resistance to the removal of water. As water is withdrawn, the film becomes thinner and harder to detach from the soil particles. The particles and pores of the soil act like a wick and the capillary action can move upwards through soil up to 3 metres, in response to suction.

When soil is saturated, all the pores are full of water, but after some time (usually a day), all gravitational water drains out, leaving the soil at field capacity (soil water-holding capacity) (Fig.4.1B). At soil water-holding capacity, plants draw water out of the capillary pores readily. When no more water can be withdrawn, and the only water left is in the micro-pores, the soil is said to be at wilting point (Fig.4.1C) (Better soils, www.soilwater.com.au).

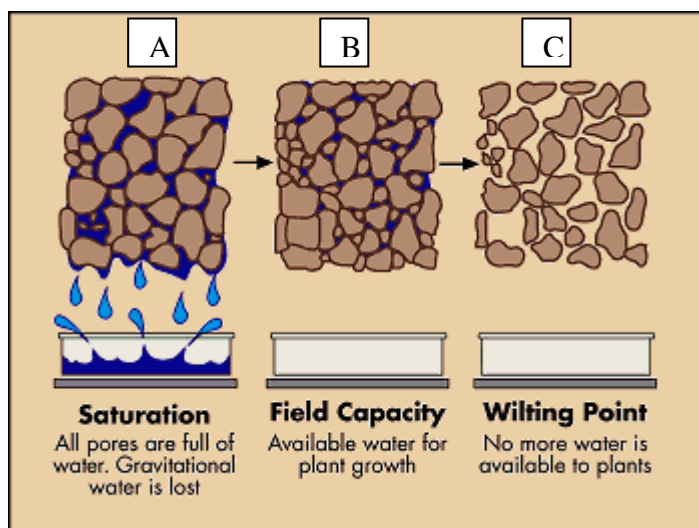


Fig.4.1: Illustration of saturation, field capacity and wilting point (Apart from labelling A, B and C, the figure is directly presented as in Dept of Agriculture Bulletin, 462, 1960)

Soil factors have major impacts on soil water status and water supply to plant roots (Slatyer, 1967). In soil-water relations, water content and water potential of soil are of principal importance. Water content can be perceived as an integral component of the hydrological cycle (Orfánus and Eitzinger, 2010) and is useful when it comes to describe the water balance of a soil, such as how much water is moving in, out, or being stored in a soil (Slatyer, 1967). The water potential of soil relates to the energy status of the soil pore water and can show how water will move in a soil as well as from the soil to the plant. Additionally, water potential can be used to determine plant availability of water and soil stress. Many different factors contribute to the total water potential (Ψ_t) of soil:

$$\Psi_t = \Psi_o + \Psi_p + \Psi_g + \Psi_m$$

Here, Ψ_p , Ψ_g , Ψ_o and Ψ_m are pressure, gravitational, osmotic, and matrix components respectively. Among these different components, matrix potential is crucial for plant water relations. When water is in contact with hydrophilic solid particles such as sand particles, adhesive intermolecular forces form between the water and the solid. The forces between the water molecules and the sand particles in combination with attraction among water molecules give rise to surface tension and the formation of menisci within the sand matrix. To break these menisci, force/pressure has to be applied. The magnitude of matrix potential depends on the width of the menisci and the chemical composition of the solid matrix. Strong (very negative) matrix potentials bind water to soil particles within very dry soils. Plants then have to create even more negative matrix potentials within tiny pores in the cell walls of their leaves and establish a water deficit gradient to extract water from the soil and allow physiological activity to continue through dry periods (Taiz and Zeiger, 1998 and references therein). Here MPS-1 sensors that function according to the equilibrium law (2nd law of thermodynamics) were introduced into the soil for direct measurements of soil water potential, and gravimetric techniques were employed for soil water content measurements.

The changes in root growth patterns and root ultrastructure of tall fescue due to growth in naphthalene-treated sand under both well-watered and drought conditions were studied and directly compared with those of the plants grown in clean sand. Nile

red, a vital fluorescent lipid stain was used to stain the root ultrastructures that possess a hydrophobic character and to probe the uptake of naphthalene which is hydrophobic in nature, across the root tissues. As the octanol water partition coefficient of Nile red is in similar range as naphthalene (Greenspan et al., 1985), this proved a powerful technique to visualize the path of naphthalene into the living roots of tall fescue.

A generalised root can be divided into different zones such as root cap, divisional zone, elongation zone, root hair zone and branching zone. The elongation zone represents a region of intense growth, through continual root exploration into previously unoccupied soils (Wild et al., 2005), whereas the root hair zone represents a region of tissue involved in intense absorption of soil minerals (Taiz and Zeiger, 1998), and perhaps soil-bound organic chemicals as well. The cells are in continual transition, but essentially remains the same age for each growth zone (Wild et al., 2005). A preliminary scanning electron microscopic study revealed that the root hair zone begins more or less at the position of one third as a fraction of root length above the root tip in tall fescue (Fig. 3.15A, B). Hence, generally the root ultrastructural adaptations and the entry of Nile red across the root tissues were studied predominantly at one third as a fraction of root length throughout this investigation, as in the previous chapter (chapters 3).

The results as regards the impacts of naphthalene contamination in soil on seed germination, changes in root growth patterns and root structural and ultrastructural features are discussed in the light of soil water stress and xenobiotic stress.

4.2 Materials and Methods

4.2.1 Spiking sand with polycyclic aromatic hydrocarbons (PAHs)

Spiking sand with PAHs was carried out according to the methods described by Johnson et al. (2004) (Further details are given in section 2.3.1).

4.2.2 An initial gradient rhizo-box experiment to examine the effect of naphthalene, fluoranthene, and benzo (a) pyrene [B(a)P] on seed germination and plant development:

In order to study the effects of different PAHs that show differences in their physico chemical characteristics, on plants, at various concentrations, a preliminary, gradient rhizo-box experiment was conducted, in which different concentrations of fluoranthene, naphthalene, and benzo (a) pyrene [B(a)P] were used in different layers (Fig. 4.2; Table 4.2). Here the 3 above mentioned PAHs were selected on the basis of:

Naphthalene: The most volatile (Henry’s law constant (H): 57.4 Pa.m³mol⁻¹ at 25°C; Source: Mackay et al., 2000) and water-soluble (31 mg L⁻¹; Source: Farrell-Jones, 2003) LMW PAH among the EPA PAHs

Fluoranthene: The most abundant EPA PAH in rural, urban as well as forest soils (Wild and Jones, 1995).

Benzo (a) Pyrene: A HMW PAH with carcinogenic properties (Farrell-Jones, 2003)

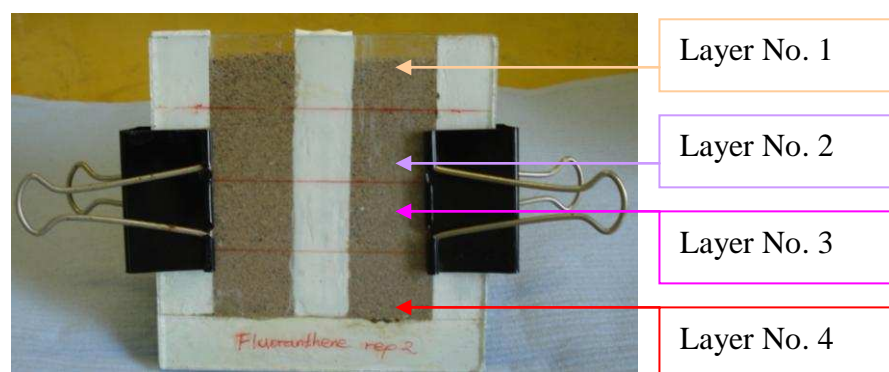


Fig.4.2: Rhizo-box set up showing the different layers consisting of different concentrations of PAH (e.g. fluoranthene).

Table 4.2: PAH concentrations used in the different layers in the gradient rhizo-box experiment

Layer No.	Experimentally added PAH concentration (mg kg ⁻¹)
1	0
2	4 (urban soil concentration) (Wild and Jones, 1995)
3	40 (minimum target level) (Wild and Jones, 1995)
4	1000 (most experimented level) (Smith et al., 2006; Binet et al., 2001)

Tall fescue seeds (5 seeds) were sown in the top layer (layer No. 1) and seed germination and plant growth were monitored. Control treatments were established using non-contaminated sand in all 4 layers. Three replicates were established for each treatment.

4.2.3 Experimental protocol to test the effect of exposure to anthracene at the concentration of 1000mg kg⁻¹ sand dw on seed germination and plant development

A 2cm thick layer of clean, agricultural sand was used as a seed bed to facilitate seed germination and growth of tall fescue (5 seeds were sown in each rhizo-box) and brown top bent (*Agrostis capillaries* L.) (15 seeds were sown in each rhizo-box) in anthracene-treated (1000mg PAH kg⁻¹ sand dw) sand in separate rhizo-boxes. Control treatments were established using non-contaminated sand. Three replicates were established for each treatment.

4.2.4 Experimental protocol to test the effect of exposure to naphthalene at the concentration of 800mg kg⁻¹ sand dw on tall fescue: Seed germination in rockwool cubes

Tall fescue seeds (10) (origin: Kent; supplier: Emorsgate seeds, UK) were germinated on autoclave-sterilized (126°C, 11 minutes, 15psi) rockwool cubes in a tray of water at 20°C. The seedlings were placed at a 45cm distance away from a 250W Grow Light (Model: Envirolite, 6400 K) on a 16 hour light and 8 hour dark cycle upon germination, but were moved to a 30cm distance after 1 week of growth. Six cm diameter plastic pots and 12cm×12cm×2cm rhizo-boxes were filled with naphthalene-spiked sand (800mg kg⁻¹ dw) or non-spiked (control) sand. A space was made in the pot centre to position the rockwool cube (containing the seedlings) with a bit of pressure applied. The rockwool cubes with plants were transferred to the pots and rhizo-boxes once the roots reached the base of the rockwool cubes (at 2 weeks since sowing). The pots were placed in individual trays. 8 replicates (4 replicates for rhizo-box set up and 4 for pot set up) were established.

4.2.5 Experimental protocol to test the impacts of naphthalene contamination on seed germination and plant growth patterns: Direct sowing in sand medium

Fifteen ml of tall fescue seeds (origin: Kent, Amenity; supplier: Emorsgate seeds, UK) were germinated directly either in clean sand or sand contaminated with

naphthalene (800mg kg^{-1} dw) in 15cm diameter plastic pots. Six replicates per treatment (3 replicates for Kent origin, 3 for Amenity origin) were established and each replicate contained ~90 plants after 1 month since seeds were sown. Additionally, 100ml tall fescue seeds (origin: Kent; supplier: Emorsgate seeds, UK) were sown in either clean sand or sand contaminated with naphthalene (800mg kg^{-1} dw) in 10L plastic pots. Three replicates per treatment were established using 10L pots and each replicate contained ~400 plants after 1 month since seeds were sown. Furthermore, 2 replicates of unplanted treatments containing either clean sand or naphthalene-treated sand were established using 10L pots. MPS-1 sensors were installed in the 10L pots. The pots were randomized and the plants were grown in a glasshouse at 20°C on a 16 hour light and 8 hour dark cycle upon germination.

4.2.6 Watering and nutrition

Plants were watered regularly to 80% of water holding capacity (water holding capacity of the clean sand was used for the determination of watering regime) and fed with a liquid fertiliser (lawn food; N: P: K=15:3:3; 6.7ml liquid fertilizer per L of water) on a once weekly basis, unless exposed to water stress.

4.2.7 Determination of water potential of naphthalene-treated and clean sand

Dielectric water potential sensors (Model: MPS-1; Manufacturer: Decagon Devices Inc.) were used to measure the water potential of naphthalene-treated and clean sand. The MPS-1 measures the dielectric permittivity of two engineered, porous ceramic disks sandwiched between stainless steel screens and the MPS-1 circuit board to measure their water content and then derive their water potential. The dielectric permittivity of water in the ceramic disks is 80 compared to a dielectric permittivity of 5 for the ceramic material and 1 for the air. The principle behind this technique is the second law of thermodynamics which states that connected systems with differing energy levels will move towards an equilibrium energy level. Here, a solid matrix equilibration technique is used. The ceramic material with a static matrix of pores is introduced into the sand and allowed to come into hydraulic equilibrium with the soil pore water. As the two are in equilibrium, measuring the water potential of the ceramic disks will give the water potential of the sand. Here water potential refers to

matrix potential which is the most important component of water potential with regard to plant water relations (Decagon Devices Inc., 2007).

MPS-1 sensors were installed into sand at the bottom of the hole dug above 2cm from the base of the 10L plastic pots. The sandy soil was packed around the sensor with good contact to all ceramic surfaces, and the hole was back-filled with care. The stereo plug of the MPS-1 sensors was plugged into one of the five ports on the EM50 datalogger. ECH₂O Utility was used to configure the ports for an MPS-1 and to set a measurement interval (60 minutes) for the logger. The soil water potential readings were read off from the screen of the datalogger.

4.2.8 Determination of soil moisture content of naphthalene-treated and clean sand

Weighed mass of soil (at field capacity and plant wilt point state) was dried in oven at 105°C for an hour, and cooled in a desiccator. Water content of naphthalene-treated and control sand was determined according to associated change in mass after drying. For unplanted treatments, soil was taken out with a core borer and the soil moisture content was determined at 3 different depths of the potted sand (top 3cm layer, mid 3cm layer and bottom 3cm layer).

4.2.9 Determination of dry weight and moisture content percentage of plant root shoot tissues

Plants were harvested after 78 days (non-water stressed plants) and 94 days (water stressed plants) of growth in naphthalene-treated and clean sand. The amount of root and shoot biomass was measured on a dry weight basis. Three replicates of weighed plant tissue were dried in an oven at 60°C for 24 hours. They were reweighed after drying and the water content was determined gravimetrically from the water losses and resulting change in mass associated with the drying. The dry weight percentage and water content percentage of plant tissues were calculated from the water content and fresh weight values.

4.2.10 Scanning Electron Microscopy (SEM)

Roots were cut into approximately 1mm long segments in 0.1M cacodylate buffer on a sheet of dental wax (Sigma Aldrich) using a sharp razor blade. Samples were placed in buffer solution (5ml) in 12ml volume exetainers fitted with rubber septa. The trapped air was evacuated with a vacuum pump to prevent cavitations in the xylem vessels. The samples were fixed in 2.5% Glutaraldehyde (v/v) in 0.1M cacodylate buffer (pH 7.2), post fixed in 1% osmium tetroxide (OSO_4) (w/v) in distilled water (dH_2O), dehydrated in an ethanol series (30, 50, 70, 80, 90, 95, 100 %), and critical point dried through carbon dioxide (Model of critical point dryer: EMITECH K-850). The samples were then mounted on aluminium stubs (Sigma Aldrich) using carbon tabs (Sigma Aldrich) and coated with gold for 2 minutes using a sputter coater (model: Edwards S150B; pressure: 1mbar). All material was observed with an S360 Cambridge model scanning electron microscope with a 20kV electron beam at an 18mm working distance.

4.2.11 Epi-fluorescent microscopy

4.2.11a. Staining Casparian band structures

Berberine hemisulphate staining process was carried out according to Brundrett et al. (1988). Freehand sections were transferred into a small watchglass and the sections were stained in 0.1% (w/v) berberine hemisulphate (Sigma; minimum 95%) which specifically stains Casparian bands, in dH_2O for 1 hour. The sections were rinsed through several changes of dH_2O and excess water was blotted off after each transfer. The root sections were transferred into 0.5% (w/v) aniline blue [water soluble (WS)] (Agar Scientific) in dH_2O for 30 minutes and then were rinsed in the same way. Here, counterstaining with aniline blue was carried out in order to quench unwanted fluorescence by substances other than Casparian bands. The sections were transferred into 0.1% (w/v) FeCl_3 (Fisher Scientific; assay>97%) in 50% (v/v) glycerine (Aldrich Chemical Co.Ltd.; 98%) (prepared by adding glycerine to filtered aqueous FeCl_3), and after several minutes in this solution, transferred to slides and mounted in the same solution. The FeCl_3 mountant prevents decolourization. The root samples (12 roots and 4 replicates were used: 3 roots from each replicated pot) were viewed with UV

illumination (345nm peak excitation; 458nm peak emission). Photographs were taken within a few hours of berberine hemisulphate staining.

4.2.11b. Nile red as a tool to probe the uptake of hydrophobic xenobiotics from soil into roots

Nile red stain preparation

A 2-3mg measure of the Nile red dye (Invitrogen) was transferred into a 1.5ml Eppendorf micro-centrifuge tube with 250µl of 1 × phosphate buffered saline solution (PBS) diluted with dH₂O from a 10 × PBS solution (to make a litre of 10 × PBS: dissolve 80g NaCl, 2g KCl, 14.4g Na₂HPO₄ .2H₂O and 2.4g KH₂PO₄ into 800ml of dH₂O, before making it up to 1L with dH₂O. Adjust the pH to 6.8 with NaOH or HCl) and 750µl of glycerol (the glycerol pipettes more easily if it is warmed up in the microwave for about 15 seconds). The Nile red dye was dissolved into the mixture through microwave heating, giving the solution a bright purple colour. The excess Nile red stain that was not dissolved was collected at the base of the tube through centrifugation at 6300 rpm for 30 seconds using a micro centrifuge. The supernatant was removed from the particulate residue and was used to stain the roots.

Procedure for staining vital roots with Nile red

Tall fescue plants germinated in rockwool cubes and grown in clean and naphthalene-contaminated sand were mainly used for this purpose at the plant age of 3 months. Tall fescue sown directly in clean and treated sand and grown in 15ml diameter pots were used for further study at the plant age of 6 months. Both the control and treatment plants were kept at optimum growth conditions, i.e., regular watering, regular nutrition addition, sufficient light and favourable temperature and the only difference between treatments was maintained as the presence or absence of naphthalene in growth medium. Roots that were still joined to living plants were exposed by using a soft brush to remove the sand. A small piece of rockwool (pre-soaked in water) was placed into the cavity between the exposed roots and the sand. Nile red solution was applied to these roots as well as the piece of rockwool backing, using a soft brush. The Nile red solution was also applied to another piece of rockwool to form a protective stain-covered sleeve, before returning the root-ball to

its pot. This was to mark the stained root. The plants were watered as usual and the stained roots were sampled after 48 hours.

Root preparation and fixing

The sampled roots were washed in $1 \times$ PBS solution and fixed in a 2% (w/v) paraformaldehyde (PFA) fixing solution for 1 hour. The PFA solution was prepared by diluting 5ml of $10 \times$ PBS with 30ml of dH₂O and was heated to 90°C in a microwave before adding 1g PFA (the PFA must be added in the fume hood after heating) and 500µl of 5M NaOH (NaOH breaks the PFA ring allowing it to interact with the sample). The PFA solution should be made directly before its use. After fixing with PFA, the roots were washed in a buffer made from 3.8g of glycine dissolved in 1L of $1 \times$ PBS, to remove any un-reacted aldehyde groups. The samples were then washed in $1 \times$ PBS, and stored in fridge.

Sectioning the roots

Roots were immobilized in a few drops of $1 \times$ PBS within folded Parafilm on a dental wax surface, and then sectioned by drawing the corner of a sharp double-edged razor blade across them repeatedly. The sections produced in this way were transferred to slides and mounted in Vectashield.

Microscopic settings and obtaining images of roots stained with Nile red: A preliminary work

In order to understand how Nile red is taken up by plant roots and stain its tissues, a preliminary work was carried out in which living tall fescue roots were stained with Nile red. The root section stained by Nile red was viewed through UV-2A filter cube (also called DAPI; excitation at 345nm; emission at 458nm), FITC filter cube (excitation at 494nm; emission at 518nm) and Texas red HYQ filter cube (excitation at 589nm; emission at 615nm) and a multi-colour fluorescence time-lapse imaging was obtained through the microscopic imaging software using Nikon 90i Eclipse epi-fluorescence microscope.

Microscopic settings and obtaining images of roots stained with Nile red to probe the uptake of hydrophobic xenobiotics across the root tissues

Sections of roots painted with Nile red in their vital state were viewed using an epi-fluorescence microscope (Nikon eclipse 90i) fitted with a digital camera. Nile red fluorescence was viewed with a visual red excitation source through a Texas red HYQ filter block (excitation at 589nm; emission at 615nm) against a real light image backdrop. The images were formatted using the epi-fluorescent microscopic imaging software.

4.2.11c. Further staining with berberine hemisulphate and overlaying images using microscopic imaging software

Nile red solution was applied gently to the living root with a soft brush. The stained roots were sampled after 48 hours, fixed in 2% (w/v) PFA and stored in a refrigerator at 4°C to be used for berberine hemisulphate staining. The fixed roots were sectioned by hand in a few drops of PBS in parafilm on a dental wax surface. Berberine hemisulphate staining process was carried out according to Brundrett et al. (1988) (further details are given in section 4.2.11a). The distance travelled by Nile red was investigated using an epi-fluorescence microscope (Nikon Eclipse 90i) using Texas red HYQ filter (589nm peak excitation and 615nm peak emission). The root samples were also viewed with UV illumination (345nm peak excitation; 458nm peak emission). Photographs were taken within a few hours of berberine hemisulphate staining. The images showing the path of Nile red were overlaid with their berberine hemisulphate+ aniline blue stained counterparts using microscopic imaging software.

4.2.12 Statistical analysis

Statistical significance was determined by a combined approach of Student's t-test in Microsoft Excel and a two-sample t-test in Genstat. Fisher's exact test was performed on the epi-fluorescent photomicrographs taken for each different treatment.

4.3 Results

a. Impacts of exposure to polycyclic aromatic hydrocarbons (PAHs) on plants: A preliminary investigation

a1. The effect of naphthalene, fluoranthene, and benzo (a) pyrene [B(a)P] on seed germination and plant development of tall fescue: An initial gradient rhizo-box experiment

Germination was poor in fluoranthene and naphthalene-treatments, as recorded 2 weeks after sowing. Plant development was markedly inhibited in fluoranthene and naphthalene treatments, but the effect was more drastic in the fluoranthene-treatment. Contrastingly, root shoot growth enhancements were observed in plants grown in B(a)P treatment. In naphthalene and fluoranthene treatments, the plant roots had not reached the bottom layer (layer No. 4) that contained 1000mg PAH kg⁻¹sand (dw), whereas they had not only grown into the bottom layer (Layer No. 4) in B(a)P treatment, but the roots were longer than those grown in clean sand, as observed after 2.5 months of growth in respective treatments. The shoot height of plants grown in B(a)P-treated sand was also higher, when compared to the controls.

a2. Effect of exposure to anthracene at the concentration of 1000mg kg⁻¹ sand dw on seed germination and plant development

a2-1. Effect of exposure to anthracene on tall fescue

Tall fescue seeds failed to germinate in one replicate of anthracene treatment. In the other two replicates, in which the seeds germinated, germination was reduced, but no significant differences were observed in shoot height, root length and number of root hairs per cm segment of roots of plants between treatments (Fig.4.3 -4.5).

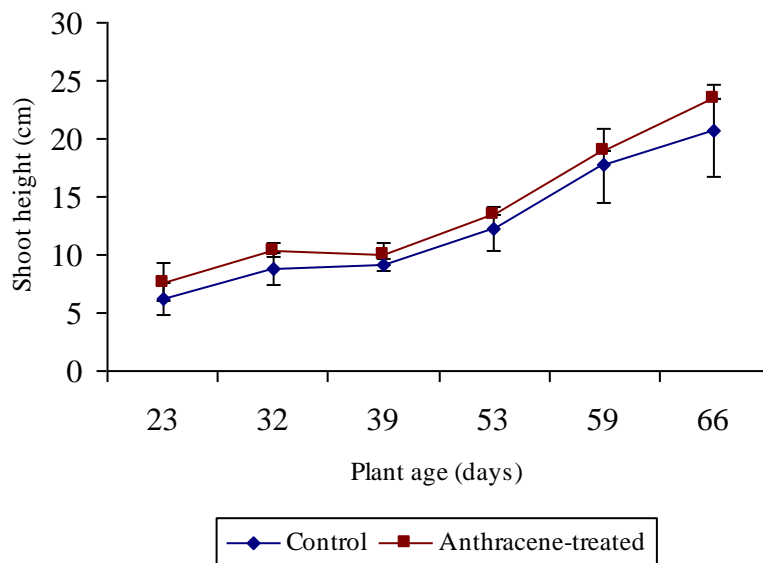


Fig.4.3: Line graph showing the shoot elongation of tall fescue plants from control (blue) and anthracene (brown) (1000mg kg^{-1} sand dw)-treatment for a period of 66-days (N=3 for controls; N=2 for anthracene treatment; from day 53 onwards N=1 for anthracene treatment as the plants were sampled for root hair analysis). Error bar shows standard error of the mean. Student's t-test was applied to each sampling period. In no case were the differences between control and treated plants significant.

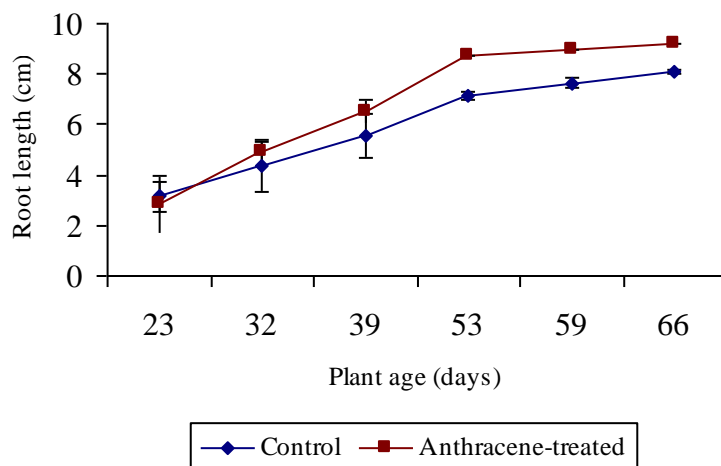


Fig.4.4: Line graph showing the root elongation of tall fescue plants from control (blue) and anthracene (brown) (1000mg kg^{-1} sand dw)-treatment for a period of 66 days (N=3 for controls; N=2 for anthracene treatment; from day 53 onwards N=1 for anthracene treatment as the plants were sampled for root hair analysis; day 53, 59 and 66 were not possible to compare as N=1 for anthracene treatment). Repeat measurement ANOVA indicated no significant difference between treatments. Error bar shows standard error of the mean. Here the variance decreased from day 53 onwards as the roots approached the bottom of the rhizo-box containing the root growth medium, i.e, sand. The sand profile was 10cm deep for anthracene treatment and 8cm deep for control treatment.

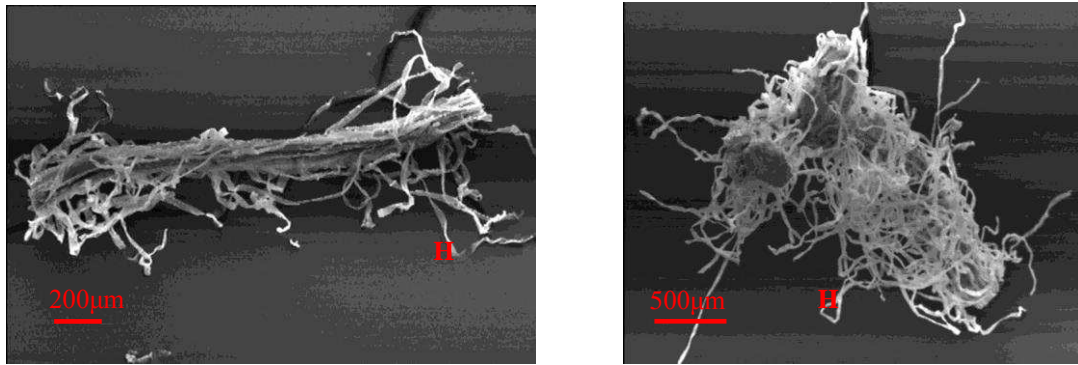


Fig.4.5: Scanning electron micrographs of tall fescue root fragments grown in clean sand (left) (scale: 200µm) and in anthracene-treated (1000mg kg⁻¹ sand dw) sand (right) (scale: 500µm) for ~2 months. Differences in number of root hairs per cm segment and in root hair length were not significant between treatments (Student's t-test). H: Root hair

Furthermore, the roots of tall fescue grown in anthracene-treated (1000mg kg⁻¹ sand dw) sand for ~2 months did not exhibit an enhanced thickening in their endodermis when compared to their control counterparts, as shown by the scanning electron micrograph below (Fig. 4.6). The thickness of endodermis cell walls was in a similar range in anthracene-treated roots when compared to their control counterparts (1-2µm) (N=3), at one third as a fraction of root length above the root tip.

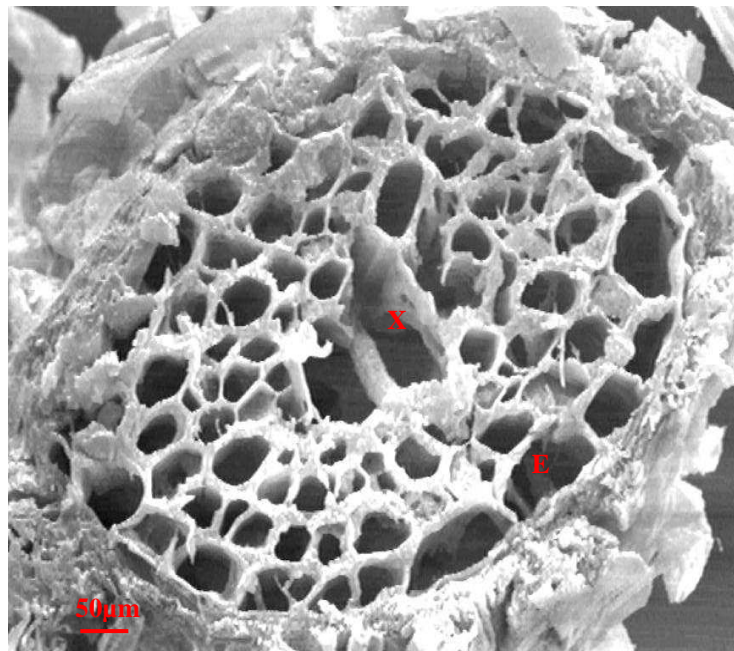


Fig.4.6: Scanning electron micrograph of tall fescue grown in anthracene-treated (1000mg kg⁻¹ sand dw) sand for 66 days, showing transversal root section at 1/3 as a fraction of root length above the root tip. Scale: 50 µm. Letters denote the following: E: Endodermis; X: Metaxylem vessel.

a2-2. Effect of exposure to anthracene on brown top bent (*Agrostis capillaries* L.)

Exposure of brown top bent (*Agrostis capillaries* L.) to anthracene (1000mg kg^{-1} sand dw) dramatically inhibited its germination ($p < 0.001$) and shoot development ($p < 0.01$) (Fig.4.7; Table 4.3). However, there were no significant differences in root length and number of root hairs per cm segment of root between treatments (Table 4.3).

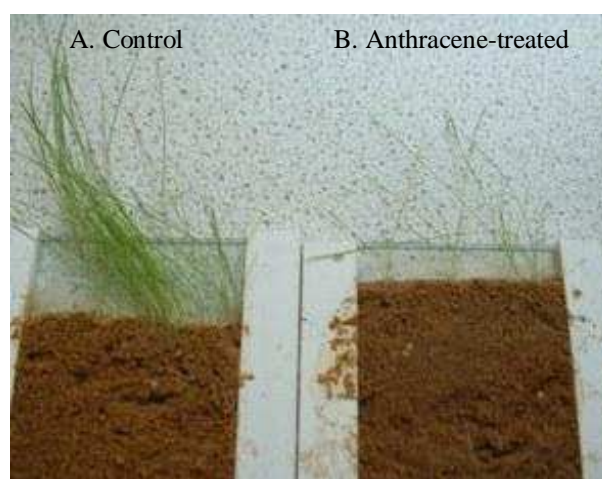


Fig.4.7: Brown top bent grown in clean sand (A) and anthracene-treated [1000mg kg^{-1} sand (dw)] sand (B) for ~2months.

Table 4.3: Descriptive statistics for plant parameters of 66 day old brown top bent from control and anthracene (1000mg kg^{-1} sand dw) –treatment. All t-tests are for differences between control and treated plants.

Plant growth parameters	Control Mean (\pm SE)	N	Anthracene-treated Mean (\pm SE)	N	p value as determined by Student's t-test
Population density (%) (also reflects germination score)	97.80 (\pm 2.22)	3	28.90 (\pm 2.22)	3	$p < 0.001$
Shoot height (cm)	12.33 (\pm 1.45)	3	5.17 (\pm 0.44)	3	$p < 0.01$
Root length (cm)	6.17 (\pm 0.44)	3	6.97 (\pm 0.25)	3	NS
No. of root hairs per cm segment	133 (\pm 9)	3	145 (\pm 6)	3	NS

N= No. of samples; SE = standard error; p = probability; NS= not significant

a3. Effect of exposure to naphthalene at the concentration of 800mg kg^{-1} sand dw on tall fescue: Seed germination in rockwool cubes

Growth in naphthalene-treated sand temporarily inhibited the growth of tall fescue initially, whilst also affecting the dark pigmentation in plant leaves (Fig. 4.8A), but after 2.5 months of growth, the naphthalene-treated tall fescue showed enhanced

growth compared to the control plants (Fig.4.8B). Also, the naphthalene-treated roots possessed significantly less ($p<0.001$), but also shorter root hairs ($p<0.001$) (Table 4.4). Additionally, the naphthalene-treated roots had smaller vessel area ($p<0.05$) and enhanced endodermis thickening ($p<0.001$) when compared to their control counterparts (Table 4.4).

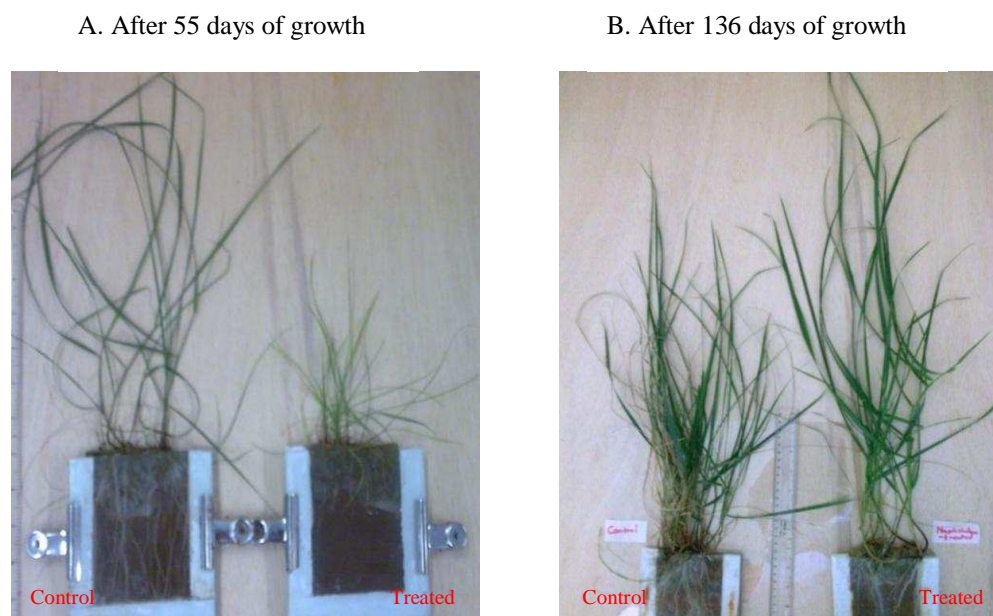


Fig.4.8: Tall fescue showing resistance to growth in sand contaminated with naphthalene at the concentration of 800mg kg^{-1} sand (dw). Tall fescue plants from control (left) and naphthalene (right) - treatment, after 55 days (A) and 136 days (B) of growth.

Table 4.4: Descriptive statistics for structural and ultrastructural parameters (root hair, xylem vessel and endodermis wall thickness) of tall fescue roots grown in clean sand and naphthalene-treated (800mg kg^{-1} sand dw) sand for 2.5 months, at the position of 1/3 as a fraction of root length above the root tip. All t-tests are for differences between control and treated plants.

Root structural/ ultrastructural parameter	Control Mean (\pm SE)	N	Naphthalene- treated Mean (\pm SE)	N	p value as determined by Student's t-test
No. of root hairs per mm segment of root	28 (\pm 3)	4	5 (\pm 1)	4	$p<0.001$
Root hair length (μm)	820.50 (\pm 10.11)	4	520.77 (\pm 11.70)	4	$p<0.001$
No. of xylem vessels	5 (\pm 2)	4	3 (\pm 1)	4	NS
Total metaxylem area (μm^2)	4024.50 (\pm 446.41)	4	2683.09 (\pm 127.09)	4	$p<0.05$
Endodermis wall thickness (μm)	2.16 (\pm 0.11)	4	3.20 (\pm 0.10)	4	$p<0.001$

N =No. of samples; SE = standard error of the mean; p = probability; NS= not significant

Here seeds were germinated in rockwool cubes and 2 weeks old seedlings were transplanted into plastic pots containing either naphthalene-treated (800mg kg^{-1} sand dw) sand or clean sand.

b. Impacts of naphthalene contamination on seed germination, plant growth patterns and the abundance of Casparian strip

b1.Effect of naphthalene contamination on the germination of tall fescue seeds

In treatments where tall fescue seeds were sown directly in naphthalene-treated sand, initially, there was a reduction in germination score when compared to the controls. With time, more seeds germinated in both treatments, but the germination percentage was lower in naphthalene treatments until 2 weeks from sowing (Fig.4.9).

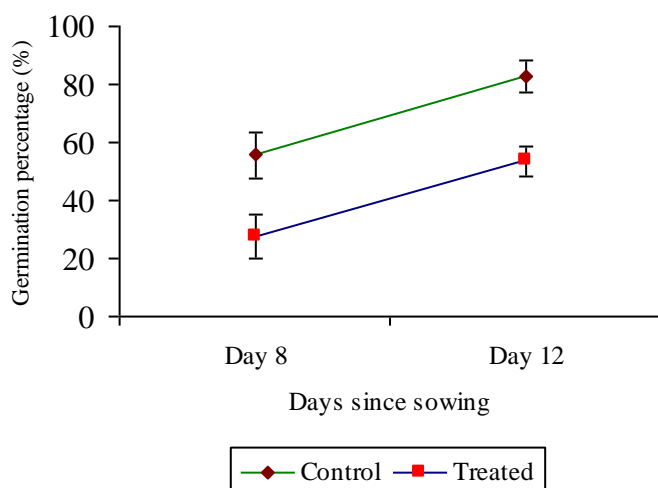


Fig.4.9: Line graph showing the differences in the percentage of germination of tall fescue seeds between control and naphthalene-treatments on day 8 and 12 since sowing. Error bar shows standard error of the mean (N=3; NS on day 8; $p<0.05$ on day 12 as determined by Student's t-test). The graph relates to the experimental design using 15cm diameter plastic pots. The results were similar when a larger number of seeds were sown in larger pots (10 L) (N=3; $p<0.01$ on 8th day since sowing; Student's t-test).

b2. Effect of naphthalene contamination on the initial root growth of tall fescue

The plants grown in sand contaminated with naphthalene exhibited a temporary inhibition in root development with 8-fold reduction in root length ($p<0.001$), whilst not showing any significant differences in shoot height, when compared to the controls (Fig. 4.10).

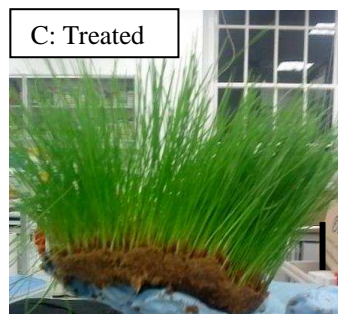
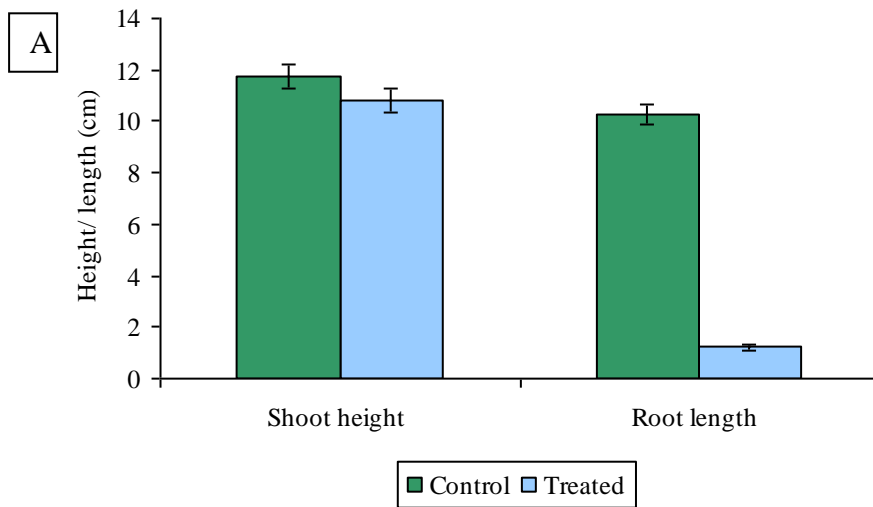


Fig.4.10: (A) Bar graph showing differences in initial shoot and root development between tall fescue grown in clean sand and sand contaminated with naphthalene. The age of the plants: 3 weeks. There were no significant differences in shoot height between the two treatments, but the root length was greatly reduced in plants grown in naphthalene-treated sand [N=12 (control) +18 (treated); $p < 0.001$ for root length as determined by Student's t-test). Error bar shows standard error of the mean. Photographs of 3 weeks old tall fescue grown in (B) clean sand and (C) sand contaminated with naphthalene. (B): Plant roots reached the bottom of the pot and had a well-established root system that held the potted sand together (C): Roots had not passed beyond the top 3cm sand in the pot. The rest of the potted sand separated upon taking the plants out of the pot in the absence of a well-established root ball.

b3. Differences in root growth patterns during the acclimatisation period due to exposure to naphthalene contamination

An acclimatisation period was established by keeping the plants at constant temperature (20° C) in the greenhouse, watering them regularly and feeding them with liquid fertilizer once a week for a period of up to 3 months.

After 78 days of growth in clean and naphthalene-treated sand, the plants were taken out of the pots and root growth was visually examined. Consistently with the previous results (chapter 3), the contaminated plants exhibited visually thicker roots, whilst also showing a deviation from the normal root orientation responses to gravity. At 78 days of plant growth, the roots in contaminated treatment had not passed beyond the upper two thirds of the plant-pots, whereas in control treatments, the plants produced a fine, dense root system that reached the bottom of the pots. However, there was no significant difference in root length between the two treatments at this time point (Fig.4.11). The roots from both treatments were sampled and a scanning electron microscopic study was carried out. The scanning electron micrographs (SEM) revealed 1.6-fold increase in root diameter ($p < 0.01$) and 1.8 -fold increase in distance from root epidermis to root stele ($p < 0.001$) in naphthalene-treated plants when compared to the controls (Fig.4.12). At 78 days of plant growth, no significant differences were observed with regard to the root endodermis thickening between the two treatments.

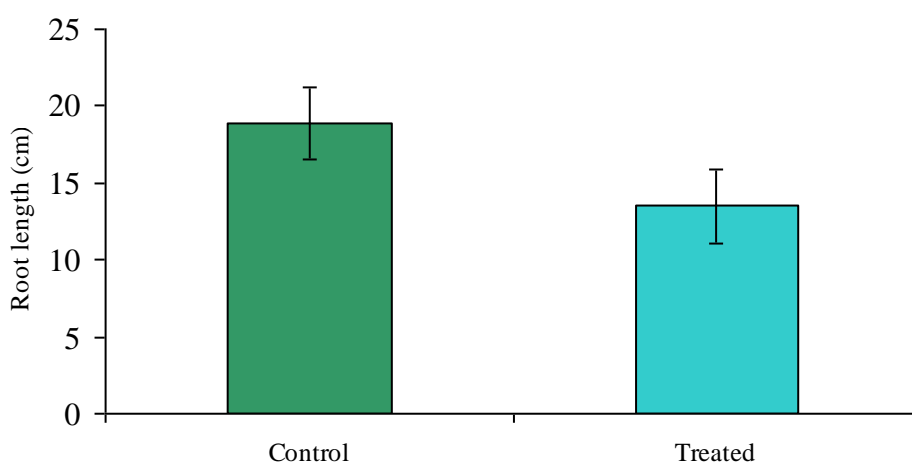


Fig. 4.11: Bar graph showing the root lengths of tall fescue grown in clean sand and sand treated with naphthalene [N=7(control) +5 (treated); NS; Student's t-test]. Error bar indicates standard error of the mean. Age of the plants: 78 days.

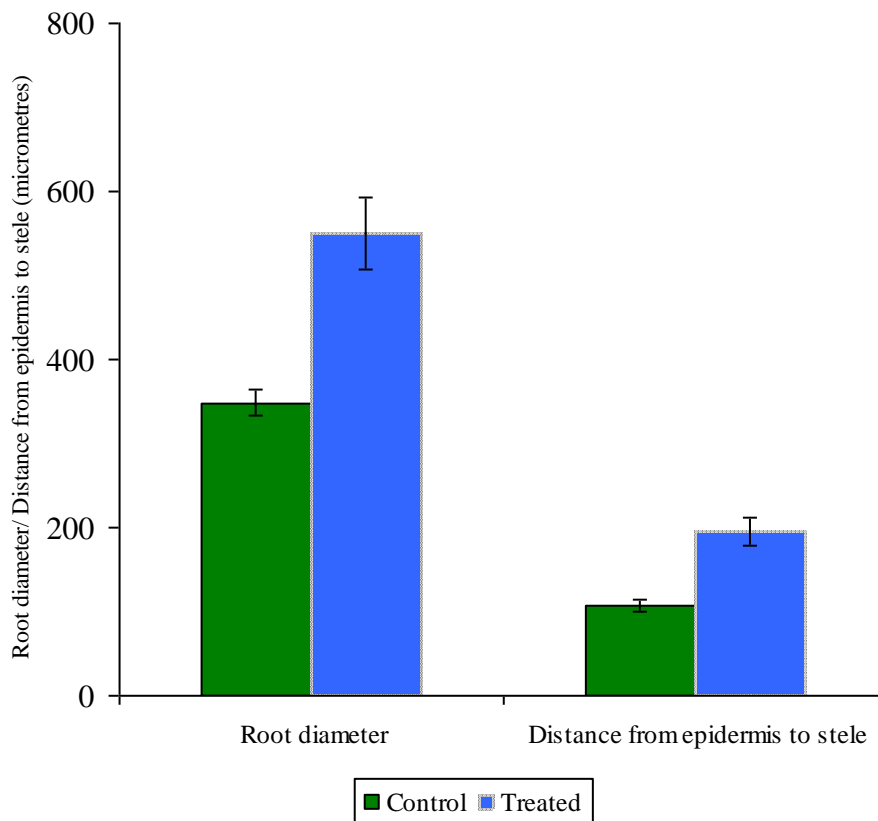


Fig.4.12: Bar graph showing the differences in root diameter ($p < 0.01$ as determined by Student's t-test) and distance from root epidermis to root stele ($p < 0.001$ as determined by Student's t-test) between tall fescue grown in clean sand and sand treated with naphthalene. [N=6 (control) +5(treated)]. Error bar indicates standard error of the mean. Age of the plants: 78 days.

b4. Effect of growth in naphthalene-contaminated sand on biomass and moisture content of plant tissues during the acclimatisation period

After 78 days of growth, the root mass of contaminated plants was 1.84 times lower on a fresh weight basis (Table 4.5), and 1.48 times lower on a dry weight basis (Fig. 4.13). The shoot fresh weight and dry weight of control plants and plants grown in treated sand were in a similar range (Fig. 4.13; Table 4.5). The dry weight percentage was higher in treated plant tissues (Fig.4.14), revealing lesser water in their tissues. On average, the moisture content was 6.33 % less in the shoots and 8.65 % less in the roots of treated tall fescue, in comparison to their control counterparts (Table 4.5).

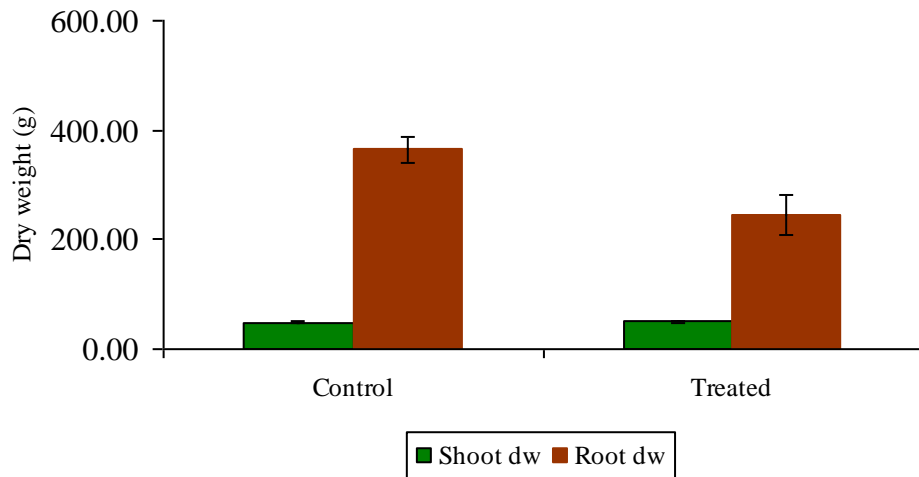


Fig.4.13: Differences in shoot and root dry weight between control and naphthalene-treated tall fescue after growth of 78 days in respective treatments (N=3; NS for both shoot dw and root dw; Student's t-test). Error bar shows standard error of the mean.

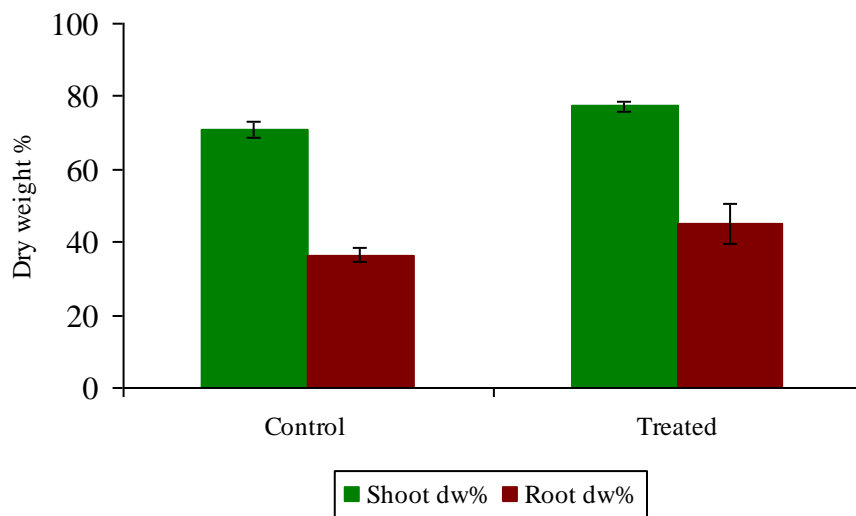


Fig.4.14: Bar graph showing the dry weight percentage of root and shoot tissues of tall fescue grown in clean sand and naphthalene-treated sand for 78 days (N=3; NS for both shoot dw% and root dw%; Student's t-test). Error bar indicates standard error of the mean.

Table 4.5: Differences in fresh weight and moisture content % of plant tissues between treatments during plant acclimatisation period. All t-tests are for differences between control and treated plants.

Bio mass parameters	Control Mean (\pm SE)	N	Treated Mean (\pm SE)	N	p value as determined by Student's t-test
Shoot biomass (fw) (g)	68.60	Composite analysis	64.70	Composite analysis	-
Root biomass (fw) (g)	1003.40	Composite analysis	546.20	Composite analysis	-
Shoot M.C%	29.08 (\pm 2.67)	3	22.75 (\pm 1.76)	3	NS
Root M.C%	63.62 (\pm 2.40)	3	54.98 (\pm 6.61)	3	NS

M.C=moisture content; SE = standard error of the mean; p = probability; NS= not significant; N=number of samples

The measurements were taken after plants were grown in clean and naphthalene-treated sand for 78 days.

b5. Root growth patterns and root ultrastructural modifications of naphthalene-treated tall fescue beyond the acclimatisation period of 3 months: Major emphasis on Casparian strip

Once past the initial acclimatisation period of 3 months, no visual differences were observed between control and naphthalene-treated tall fescue either in root growth or shoot growth patterns (Fig.4.15).



Fig. 4.15: Tall fescue grown in clean sand (A) and naphthalene-treated sand (B) for 14 weeks. The photograph relates to the experiment in which seeds were germinated in rockwool cubes and plants were transferred to 6cm diameter plastic pots filled with either clean sand or sand contaminated with naphthalene (800mg kg^{-1} sand dw) at seedling stage. The results were similar when the plants were grown directly in naphthalene-treated sand (800mg kg^{-1} sand dw).

Still, differences in root ultrastructural features were observed between control and treated roots beyond the acclimatisation period. Particularly, the epi-fluorescent microscopic images of naphthalene-treated roots stained with berberine hemisulphate (0.1% w/v), counterstained with aniline blue (0.5% w/v) and viewed under UV illumination (excitation at 345 nm; emission at 458 nm) revealed Casparian strips spanning across their hypodermis, i.e. in the layer beneath the epidermis (Fig.4.16 B1, B2), whereas exodermal Casparian bands were absent in the control roots (Fig.4.16 A1, A2), at the same position behind the root tip ($p < 0.01$) (see Table 4.6). Furthermore, some cells in the endodermis of the control roots, particularly those opposite to the protoxylem vessels did not possess Casparian strip or suberin lamella, revealing the presence of passage cells (Fig. 4.16 A1, A2). The treated roots, on the other hand, possessed a well-developed endodermis, illustrating well-formed Casparian strip and suberin lamellae and lacked passage cells (Fig. 4.16 B1, B2). The plant roots exposed to naphthalene contamination possessed an extensively thickened endodermis and distortions in cortical zone, when compared to their control counterparts (Fig. 4.16).

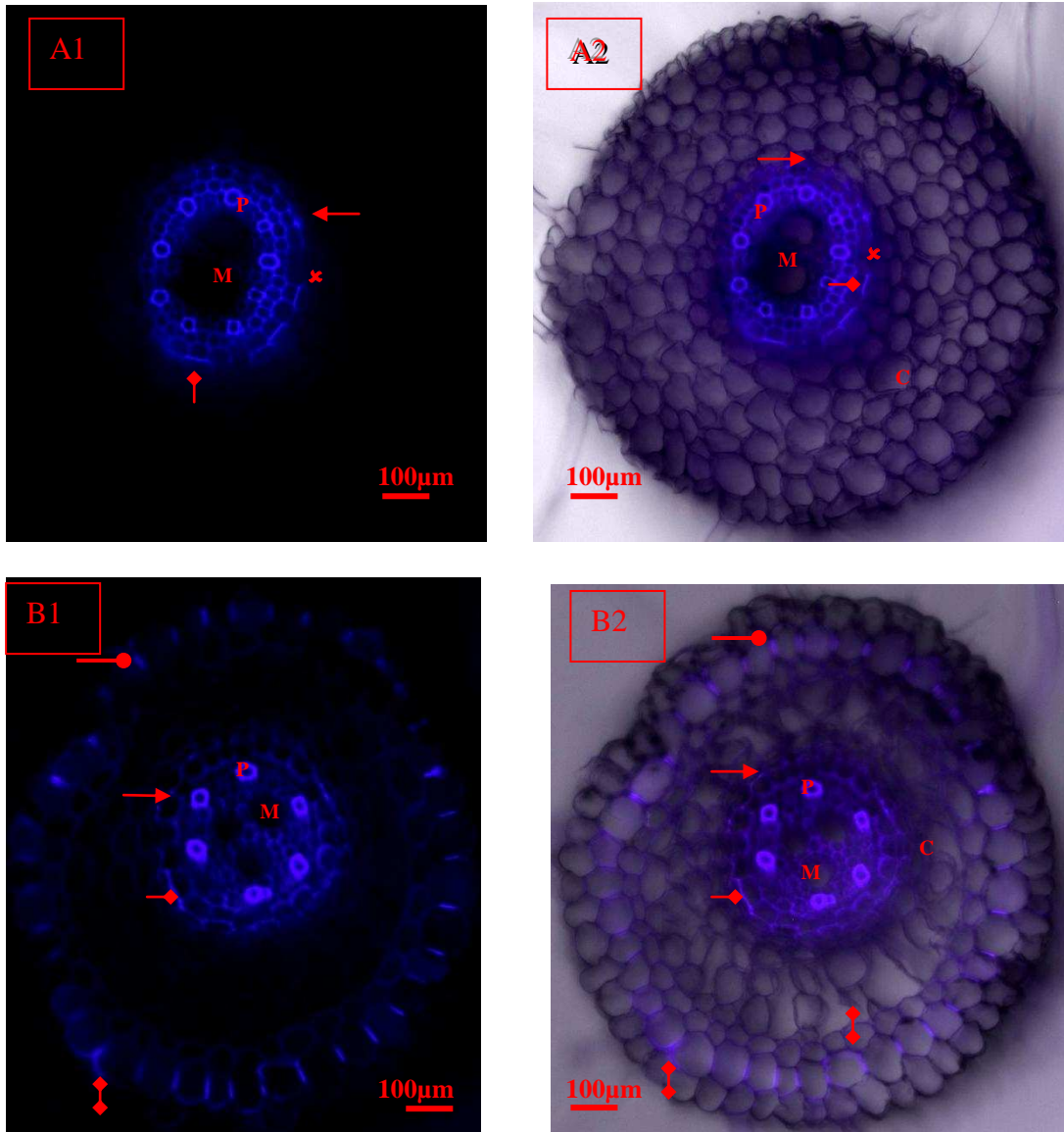


Fig.4.16: Fluorescent (A1, B1) and superimposed (A2, B2) images of control (A1, A2) and naphthalene-treated (B1, B2) 6 months old tall fescue roots stained with berberine hemisulphate, counterstained with aniline blue and viewed with UV illumination (excitation at 345nm; emission at 458nm), showing cross sections at the position of one third as a fraction of root length above the root tip. Scale: 100µm (N=12; $p < 0.01$ as determined by Fisher's exact test). Here the radial fluorescing bands are Casparian bands and the lateral fluorescing bands are suberin lamellae. The results relate to the experiment in which seeds were germinated in rockwool cubes and plants at seedling stage were transferred to 6cm diameter plastic pots filled with either clean sand or sand contaminated with naphthalene (800mg kg^{-1} sand dw).

Key:

→	Casparian strip (endodermis)	✕	Passage cell (endodermis)
—●	Casparian strip (exodermis)	P	Protoxylem
C	Cortex	↔	Suberin lamellae (endodermis)
M	Metaxylem	◊◊	Suberin lamellae (exodermis)

Table 4.6: Contingency table showing the difference in the abundance of exodermal Casparian bands at one third as a fraction of root length of tall fescue grown in clean (Control) and naphthalene-treated (Treated) sand

Treatments	Exodermis was present (N)	Exodermis was absent (N)	P value as determined by Fisher's exact test
Control	2	10	
Treated	10	2	p<0.01

N=number of samples; p = probability

c. Effect of growth in naphthalene- contaminated sand on plants' resilience to drought

c1. Differences in the onset of wilting

When exposed to drought, plants grown in clean sand showed wilting appearance first, in comparison to the treated plants. A well-pronounced, clear-cut visual drought resilience effect was observed in treated plants, when tall fescue germinated in rockwool cubes and grown in clean and treated sand for 3 months, were left without watering for a consecutive 4 days. The plants grown in naphthalene-treated sand remained visually unaltered, whereas the control plant leaves showed signs of wilting (Fig.4.17).



Fig.4.17: Tall fescue grown in clean sand (A) and naphthalene-treated sand (B) for 3 months, after left without watering for 4 days. (A): Leaves of the plants showed signs of wilting. (B): Plants remained visually unaltered (N=4 replicates; each replicate contained ~10 plants; the difference between treatments with regard to wilting was clear cut). The photographic result relates to the experiment in

which seeds were germinated in rockwool cubes and plants were transferred to 6cm diameter plastic pots filled with either clean sand or sand contaminated with naphthalene (800mg kg^{-1} sand dw) at seedling stage.

c2. Examination of root ultrastructural features of tall fescue exposed to water stress for 4 days: A short exposure to drought

The scanning electron micrographs of transversal sections of roots of plants grown in clean and naphthalene-treated sand for 3 months, and exposed to water stress for 4 days, are shown in Fig. 4.18. The images revealed an extensively thickened endodermis, differential organisation of cortex cell files as well as partial collapse/distortions in the cortical zone in naphthalene-treated roots (Fig. 4.18B). Partial collapse of cortex cells and a concomitant increase in cortical zone were observed in control roots too (Fig. 4.18A), as the plants were exposed to water stress before sampling the roots for SEM study. Still, the control root endodermis had relatively thin cell walls ($1\text{-}2\mu\text{m}$ in thickness) in comparison to the treated root endodermis ($2\text{-}4\mu\text{m}$ in thickness), at the same position behind the root tip, and the images of the control roots were visually distinguishable from those of the treated roots (Fig. 4.18).

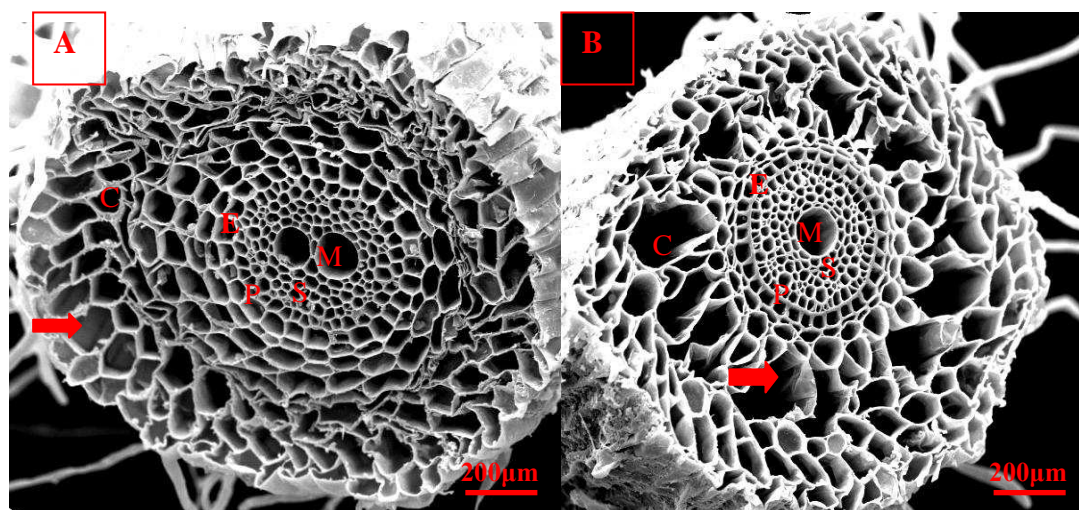


Fig.4.18: Scanning electron micrographs of transversal sections of roots of tall fescue grown in clean sand (A) and naphthalene-treated sand (B) for 3 months and exposed to water stress for 4 days, sectioned at one third as a fraction of root length above the root tip. Scale: $200\mu\text{m}$. Key: C: Cortex; E: Endodermis; S: Stele; M: Meta xylem vessel; P: Protoxylem vessel. Arrow indicates partial collapse of the cortex cells. The images relate to the experiment in which seeds were germinated in rockwool cubes and plants were transferred to 6cm diameter plastic pots filled with either clean sand or sand contaminated with naphthalene (800mg kg^{-1} sand dw) at seedling stage.

c3. Examination of root shoot growth parameters of tall fescue exposed to severe water stress

Plants grown from seeds directly sown in either clean or naphthalene-treated sand were subjected to water stress twice for a period of 1-2 weeks. At 94 days of age, after having undergone 2 water stress spells, the plants exposed to naphthalene contamination had 1.85 times greater root mass on a fresh weight basis (Table 4.7) and 2.72 times greater root mass on a dry weight basis ($p < 0.01$) than the control plants (Fig. 4.19). The root dry weight % was also higher in plants grown in treated sand ($p < 0.05$) (Fig.4.20), whereas their root moisture content % was lower when compared to their control counterparts ($p < 0.05$) (Table 4.7). No significant differences were observed in shoot dry weight, shoot dry weight % and shoot moisture content % between treatments.

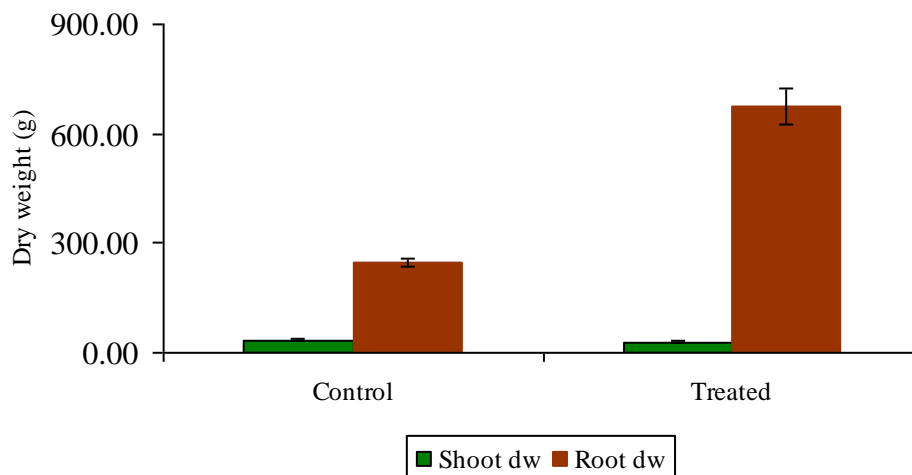


Fig.4.19: Differences in shoot and root dry weight between control and naphthalene-treated tall fescue at the age of 94 days, after exposed to severe water stress. Error bar shows standard error of the mean. Differences in root dry weight between treatments were significant ($N=3$; $p < 0.01$ as determined by Student's t-test). Error bar is obscured in shoot dry weight due to smaller variance between samples.

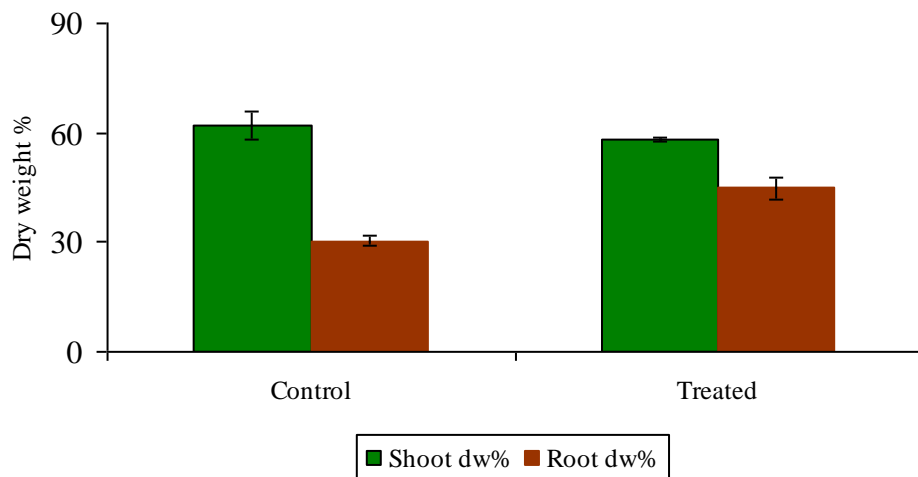


Fig.4.20: Bar graph showing the dry weight percentage of root and shoot tissues of tall fescue grown in clean sand and naphthalene-treated sand for 94 days, after exposed to severe water stress. Error bar shows standard error of the mean. Differences in root dry weight % between treatments were significant ($p < 0.05$ as determined by Student's t-test; $N=3$).

Table 4.7: Differences in fresh weight and moisture content % of plant tissues between treatments, after exposed to severe water stress. All t-tests are for differences between control and treated plants.

Root, shoot growth parameters of plants	Control Mean (\pm SE)	N	Treated Mean (\pm SE)	N	p value as determined by Student's t-test
Shoot biomass (fw) (g)	55.60	Composite analysis	51.70	Composite analysis	-
Root biomass (fw) (g)	817.10	Composite analysis	1507.60	Composite analysis	-
Shoot M.C%	38.15(\pm 3.83)	3	41.86(\pm 0.43)	3	NS
Root M.C%	69.69(\pm 1.39)	3	55.26(\pm 3.18)	3	$p < 0.05$

M.C=moisture content; SE = standard error; p = probability; NS= not significant; N=number of samples

c4. Examination of root ultrastructural features of tall fescue exposed to severe water stress: A long exposure to drought

The scanning electron micrographs of 94 day old plant roots at plant wilt point state revealed the cortex cells partially collapsed in control roots as well as in treated roots (Fig. 4.21). The statistical analysis on the SEM images of control and treated roots showed no significant differences in root diameter as well as in the distance from root epidermis to root stele (Fig. 4.22). Still, the endodermis of plant roots grown in treated sand exhibited more thickening in their cell walls [$3.99 (\pm 0.26) \mu\text{m}$], in comparison to the controls [$1.54 (\pm 0.21) \mu\text{m}$], and the difference between treatments

with regard to endodermis thickening was significant ($p < 0.0000001$) (Fig. 4.23).

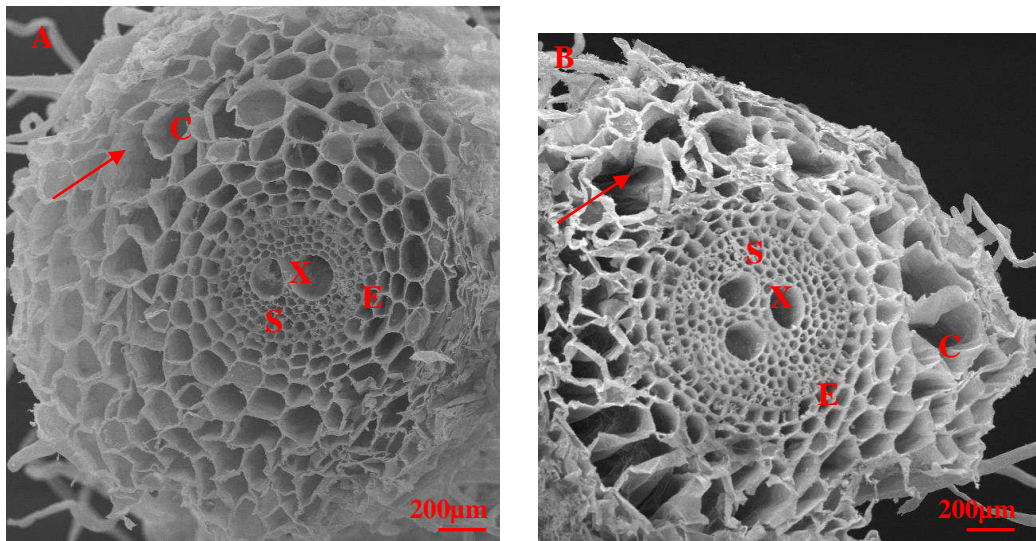


Fig.4.21: Scanning electron micrographs of control (A) and naphthalene-treated (B) tall fescue showing cross sections of roots of 94 days old plants at plant wilt point state, sectioned at one third as a fraction of root length above the root tip. Scale: 200µm. Letters denote the following: C-cortex; E-endodermis; S-stele; X-metaxylem vessel. Arrow shows partial collapse in the cortical zone of plant roots.

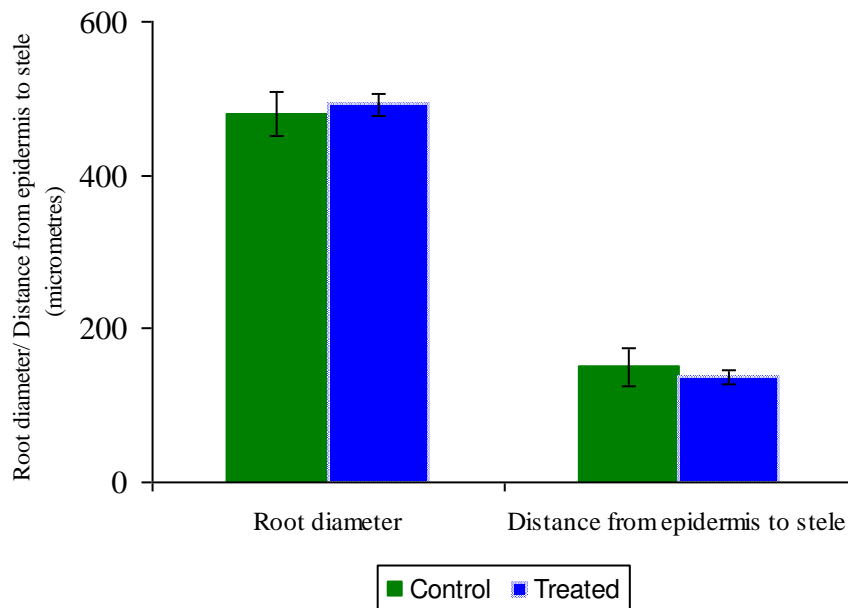


Fig. 4.22: Bar graph showing the values for distance between root epidermis and root stele and root diameter of 94 days old control and naphthalene-treated tall fescue, exposed to severe water stress. Error bar shows standard error of the mean (N=6; NS for both root diameter and distance from epidermis to stele; Student's t-test).

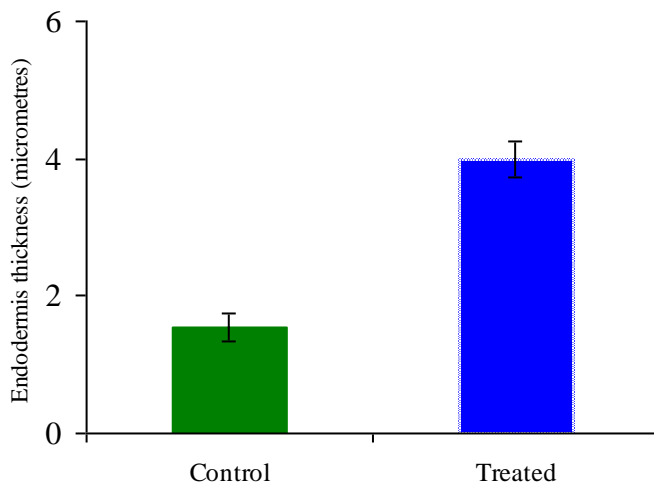


Fig. 4.23: Bar graph showing the values for endodermis thickness of 94 days old control and naphthalene-treated tall fescue, exposed to severe water stress. Error bar shows standard error of the mean (N=14; $p < 0.0000001$ as determined by Student's t-test).

d. Soil-water relations

d1. The effect of naphthalene on the water status of the treated sand

At field capacity (saturated conditions), the difference in moisture content % between naphthalene-treated sand [83.33 (± 0.17) %] and clean sand [82.70 (± 0.25) %] was not significant (Fig. 4.24A). At field capacity, the soil matrix potential was significantly ($p < 0.001$) more negative in naphthalene-treated sand [-14.00 (± 0.71) kPa] than in clean sand [-10.00 (± 0.00) kPa] (Fig. 4.24B). At field capacity, the moisture content and matrix potential were similar in planted and unplanted soils. So the moisture content % and matrix potential data from both planted and unplanted soils were pooled together for analysis of variance between naphthalene and control treatment.

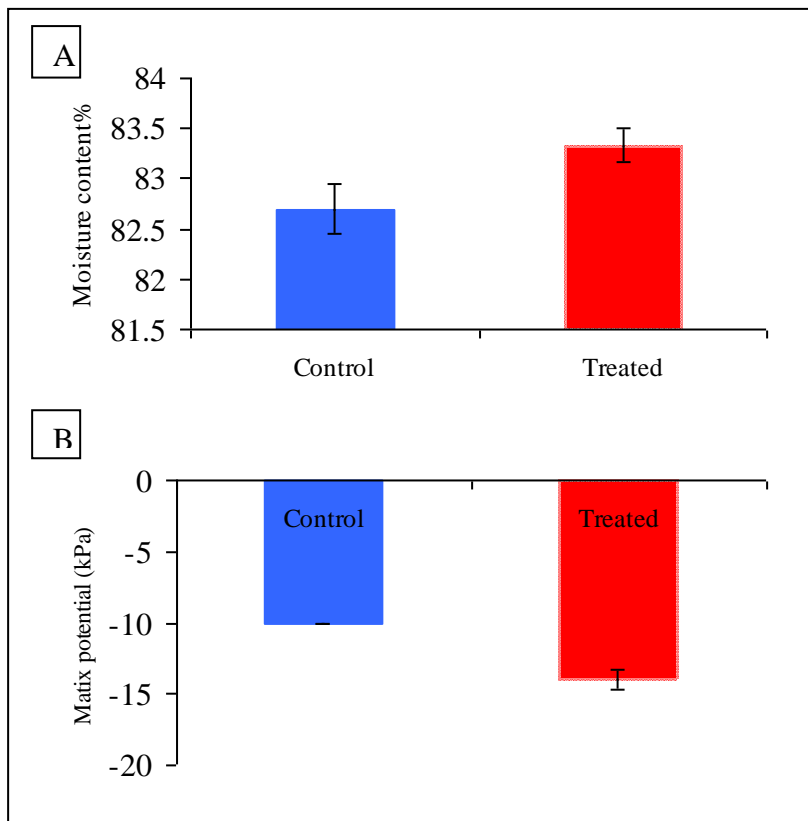


Fig.4.24: Bar graph showing the difference in (A) moisture content % (N=15; NS; Student's t-test) and (B) matrix potential (N=4; $p < 0.001$; two-sample t-test in GenStat) between clean and naphthalene-contaminated sand at field capacity (saturated conditions). Error bar shows standard error of the mean. The sand had been treated with naphthalene at the concentration of 800 mg kg^{-1} sand (dw) for 94 days at the time of measurement.

The unplanted soils were left to dry out for a period of 16 days, after being subjected to regular addition of a constant amount of water [100ml of water per day; initially each pot contained 7kg of sand (dw)]. After being subjected to water stress, the moisture content % was less in the top 3cm layer in naphthalene treatment [2.6 (± 0.34)], when compared to the controls [3.43 (± 0.25)]. The mid and bottom portions (each portion was of 3cm in depth) of the potted sand in naphthalene treatment exhibited higher moisture content % [4.93 (± 0.15) and 5.22 (± 0.51) respectively] than the control [3.92 (± 0.26) and 4.18 (± 0.09) respectively] (Fig. 4.25A). The MPS-1 sensors were installed in the bottom 3cm layer of the potted sand. At unsaturated, water-deficit conditions, the treated sand exhibited stronger (more negative) matrix potential [-17.50 (± 1.50) kPa] in unplanted treatments, when compared to their control counterparts [-12.00 (± 1.00) kPa] (Fig. 4.25B).

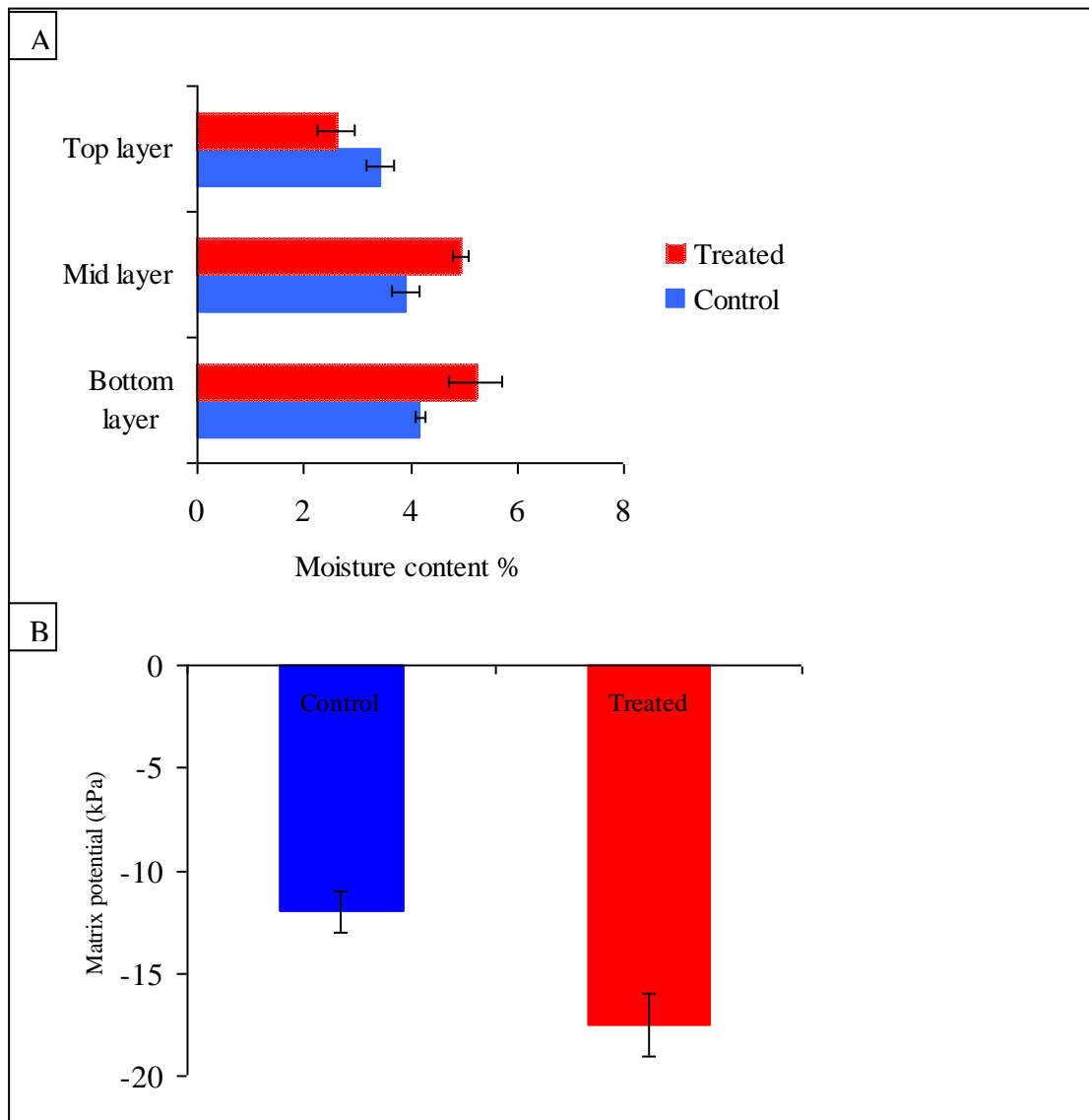


Fig.4.25: Bar graph showing the differences in (A) moisture content % in top, mid and bottom portions of the potted sand [N=5 (control)+ 8 (treated) ; $p < 0.01$ for mid layer as determined by Student's t-test) and (B) matrix potential (N=2; NS; Student's t-test) between unplanted treatments at unsaturated, water-deficit conditions. Error bar shows standard error of the mean. The sand had been treated with naphthalene at the concentration of 800 mg kg^{-1} sand (dw) for 78 days at the time of measurement.

The weight measurements of planted pots taken for a consecutive 10 days during the period of 66-75 days of plant growth showed there were differences in net weight gain after watering between treatments. Net weight gain occurred to a lesser extent in naphthalene-treatment up to day 71, when compared to the controls, after adding the same amount of water to both treatments (data not shown). Net water loss, as recorded prior to watering, also occurred to a lesser extent in naphthalene treatment during the same period of plant growth, when compared to the controls (data not shown).

The cumulative water loss and loss in pot weight over time were smaller in naphthalene treatment among the unplanted pots of sand too, but the differences were not significant.

The matrix potential in naphthalene-treated sand containing plants became less negative over time under a regular watering regime, when compared to the initial state, but the differences in matrix potential between control and naphthalene treatment remained significant (Fig. 4.26).

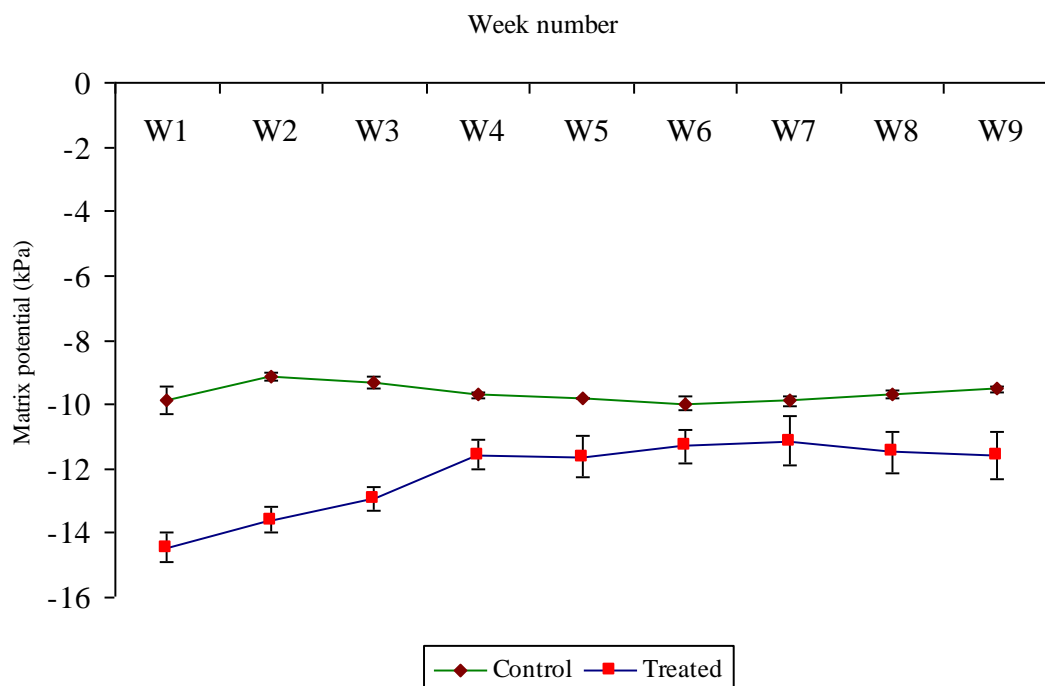


Fig. 4.26: Line graph showing the matrix potential readings over time under regular watering regime in representative planted pots. Error bar shows standard deviation from mean hourly readings per week.

Furthermore, when the plants were subjected to water stress for a consecutive 8 days, during plant age of 62-70 days (Week 10), the matrix potential change occurred to a

lesser extent in naphthalene treatment when compared to the controls. The matrix potential readings taken at 18.00 pm on day 70, after the treatments were subjected to water stress for a period of 8 days, showed the differences in matrix potential were significant between treatments (Table 4.8).

Table 4.8: Differences in matrix potential at 18.00 pm on day 70, after the plants were subjected to water stress during 62-70 days of plant growth in clean and naphthalene-treated sand. The t-test is for differences in matrix potential between control and treated sand.

Soil water balance parameter	Control Mean (\pm SE)	N	Treated Mean (\pm SE)	N	p value as determined by two-sample t-test in GenStat
Matrix potential (kPa)	-739.00(\pm 45.26)	2	-81.00 (\pm 14.14)	2	p<0.01

SE = standard error; p = probability; N=number of replicates

When the same plants were subjected to water stress again from 81 days of plant age onwards, by not watering them for 14 days consecutively, the matrix potential in both treatments reached plant wilt point. The plant wilt point was -626 (\pm 14.18) kPa in control treatment, whereas it was -676 (\pm 53.90) kPa in naphthalene treatment (Fig. 4.27B). However, the accuracy of the readings of the MPS-1 sensors was limited to > -500 kPa (Decagon Devices Inc., 2007). At plant wilt point stage, the control sand contained 1.22 (\pm 0.26) moisture content %, whereas the naphthalene-treated sand possessed 0.67 (\pm 0.06) moisture content % (Fig. 4.27A).

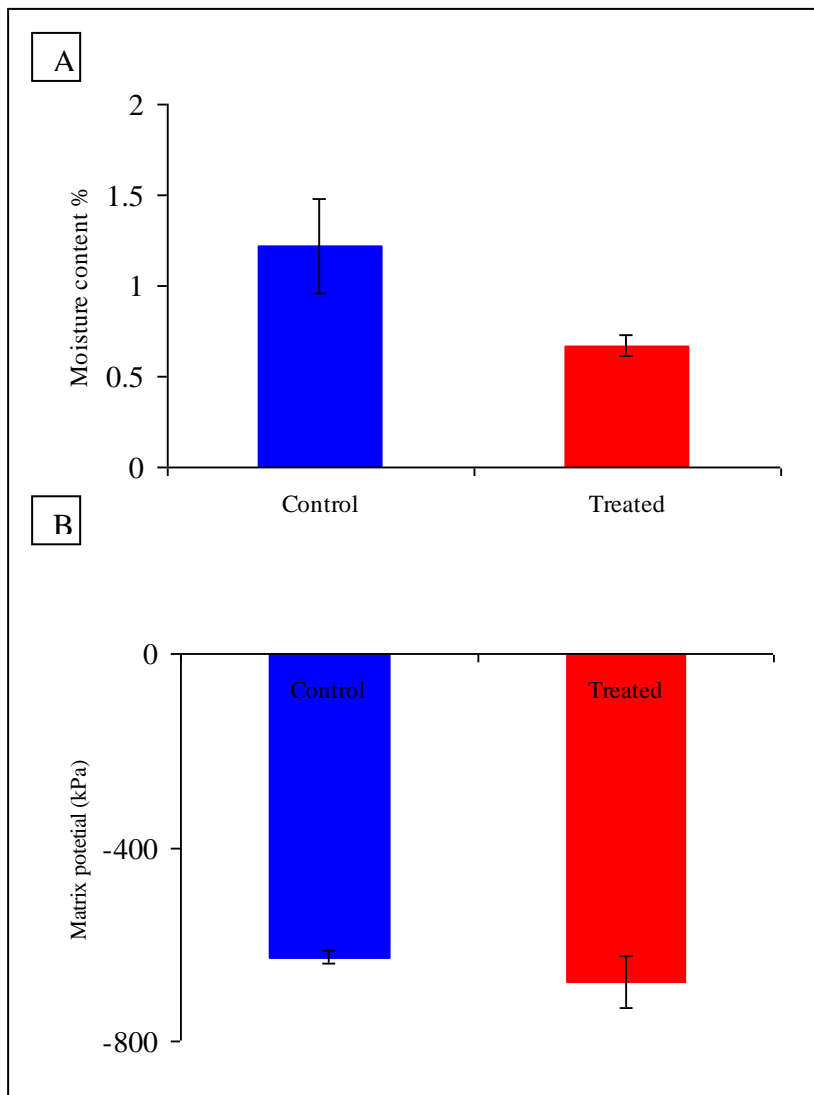


Fig.4.27: Bar graph showing the difference in (A) moisture content % (N=6; NS; Student's t-test) and (B) matrix potential (N=2; NS; Student's t-test) between control and naphthalene treatment at plant wilt point. Error bar shows standard error of the mean. The sand had been treated with naphthalene at the concentration of 800mg kg⁻¹ sand (dw) for 94 days at the time of measurement.

e. Resistances to the uptake of hydrophobic xenobiotic solutes across the root tissues of tall fescue grown in naphthalene-treated sand: Nile red as a hydrophobic molecular probe

e1. Nile red as a tool to probe the uptake of hydrophobic organic xenobiotics from soil into roots: Result of the preliminary investigation

The preliminary investigation showed Nile red can be used to stain root ultrastructures that possess hydrophobic character as well as to probe the uptake of hydrophobic xenobiotics across the root tissues. The multicolour time-lapse image revealed highly intense fluorescence in the exodermis and endodermis which looked red (Fig.4.28A).

Protoxylem vessels also fluoresced with high intensity, but looked yellow (Fig. 4.28A), perhaps due to the presence of glycine-rich proteins in these vessels as documented by Riser and Keller (1992). Epidermis also fluoresced intensely with a red to reddish yellow emission. Generally, red/yellow emission ratio varied from epidermis to proto xylem vessels, suggesting variations in the hydrophobicity of lipid-like components across the root. Some yellow emissions were observed in the intercellular air spaces between the cortex cells (Fig. 4.28A), presumably due to the presence of protein components secreted into the intercellular air spaces (VandenBosch et al., 1989). The observations suggested that, the pathway of Nile red across root tissues is predominantly apoplastic as the plasma membranes containing phospholipids were not stained, and that the dye is concentrated in the exodermis and endodermis during its passage, presumably due to the hydrophobic nature of suberin and lignin in these ultrastructures and enters the stele via the passage cells present in the endodermis and is taken up by the protoxylem vessels, where it is absorbed.

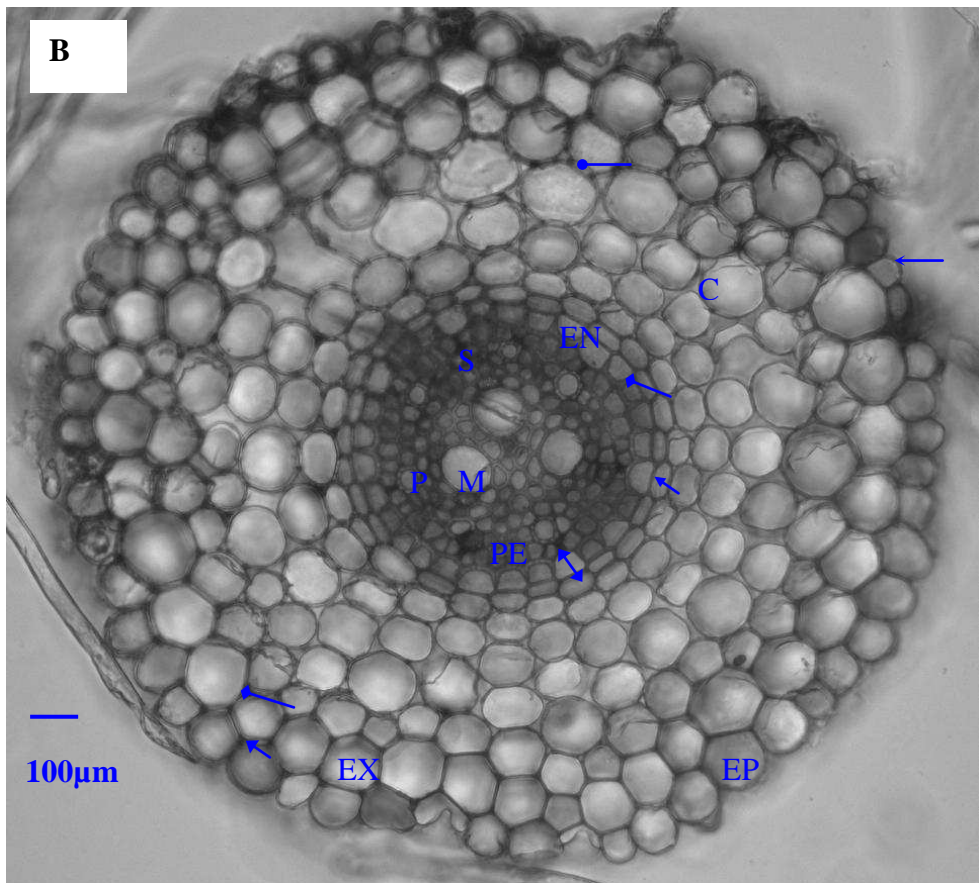
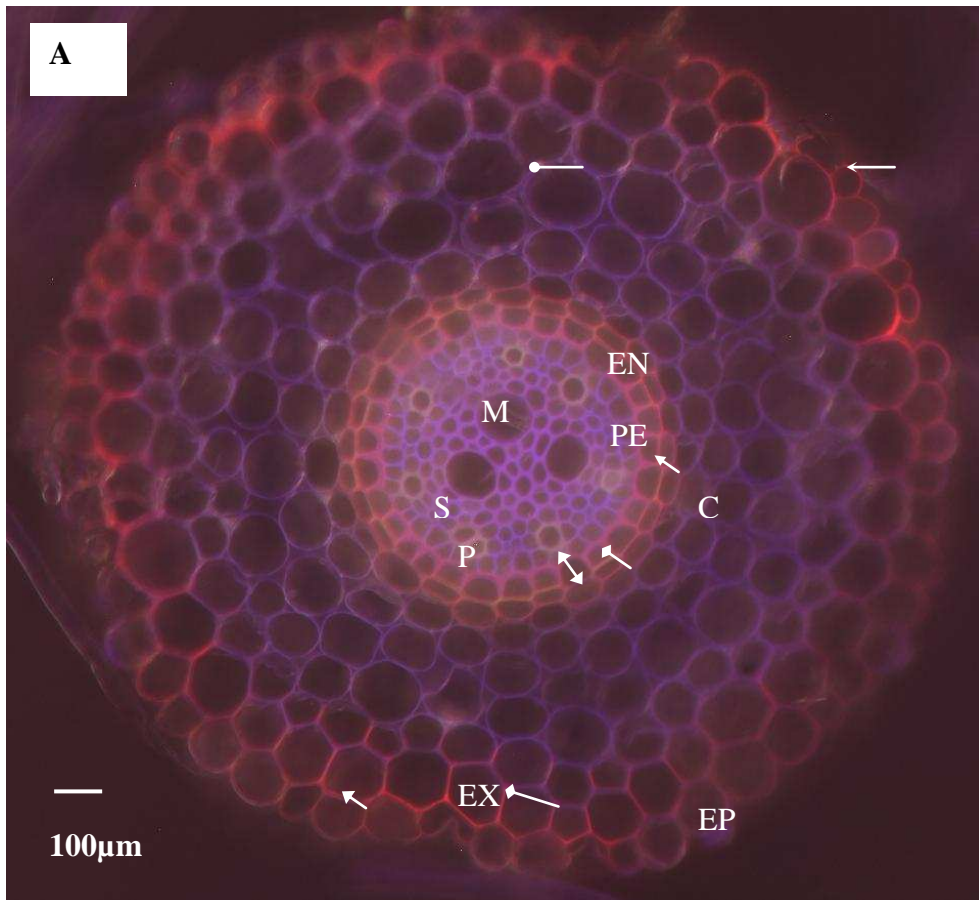


Fig.4.28: A: Epi fluorescent micrograph of a cross section of a tall fescue root painted with Nile red in its vital state, sectioned at two third as a fraction of root length above the root tip and viewed through UV-2A filter (excitation at 345nm; emission at 458nm), FITC filter block (excitation at 494nm; emission at 518nm) and Texas red HYQ filter cube (excitation at 589nm; emission at 615nm). The multicolour image was produced by overlaying images using microscopic imaging software. B shows the bright field counterpart of the image. Scale: 100µm.

Letters denote the following:

C: cortex; EN: endodermis; EP: epidermis; EX: exodermis; M: metaxylem vessel; P: protoxylem vessel; PE: pericycle; S: stele

Arrow indicates suberin lamellae; Double arrow indicates passage cell in the endodermis that does not have suberin lamellae deposition; Diamond arrow indicates Casparian strip. Open arrow indicates cuticular epidermis. Oval arrow indicates yellow fluorescence in the intercellular spaces between cortex cells. Autofluorescence of root cell components was negligible when viewing root sections painted with Nile red.

e2. Uptake of xenobiotic solutes into protoxylem vessels exemplified by the path of Nile red

The fluorescent hydrophobic probe ‘Nile red’ was applied to the epidermis of the living roots of 3 months old tall fescue plants which were watered regularly, to mimic and visualise the uptake of naphthalene into the roots through the transpiration stream. The epi-fluorescent micrographs taken with the use of Texas red HYQ filter (excitation at 589nm; emission at 615nm) revealed that Nile red applied to the living roots grown in naphthalene-contaminated sand was unable to penetrate the root tissues beyond the endodermis (Fig.4.29B1, B2; Table 4.9), whereas those grown in clean sand showed evidence of Nile red uptake into the protoxylem vessels beyond the endodermis (Fig.4.29A1,A2; Table 4.9).

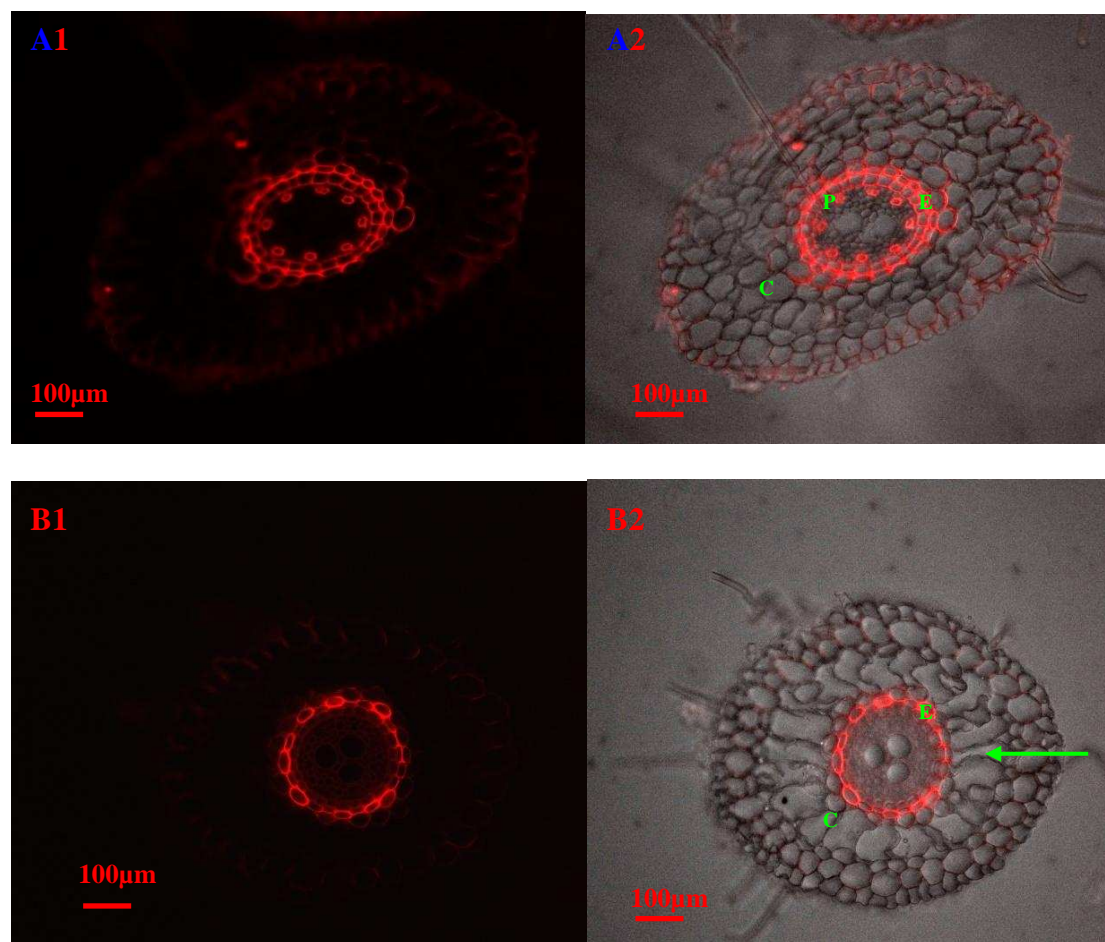


Fig.4.29: Fluorescent (A1, B1) and superimposed (A2, B2) images of control (A1, A2) and naphthalene-treated (B1, B2) 3 months old tall fescue roots painted with Nile red in their vital state and viewed through Texas red HYQ filter (excitation at 589nm; emission at 615nm), showing cross sections at one third as a fraction of root length above the root tip. Scale: 100µm (N=10; $p < 0.0001$ as determined by Fisher's exact test). Letters denote the following: C: Cortex; E: Endodermis; P: Protoxylem vessel. Arrow indicates partially collapsed cortex area. The results relate to the experiment in which seeds were germinated in rockwool cubes and plants at seedling stage were transferred to 6cm diameter plastic pots filled with either clean sand or sand contaminated with naphthalene (800mg kg^{-1} sand dw).

Table 4.9: Contingency table showing the difference in the uptake of Nile red into protoxylem vessels, at one third as a fraction of root length of tall fescue grown in clean (Control) and naphthalene-treated (Treated) sand

Treatments	Nile red uptake into protoxylem vessels was observed (N)	Nile red uptake into protoxylem vessels was not observed (N)	P value as determined by Fisher's exact test
Control	10	0	
Treated	0	10	$p < 0.0001$

N=number of samples; p = probability

The overlaid images obtained through the use of Texas red HYQ filter and UV illumination of roots that were painted with Nile red in their vital state and consequently stained with berberine hemisulphate (0.1% w/v), further illustrated the

connections between root ultrastructural parameters and the passage of hydrophobic xenobiotic solutes, exemplified by the path of Nile red. The control root images showed well-defined Casparian strip in the endodermis and Nile red uptake into the protoxylem vessels through the relatively thin cell-walls of the endodermis containing passage cells (Fig.4.30A1-A3, Fig.4.31A1, A2). Neither Casparian strip nor passage cells were observed in the endodermis due to enhanced cell wall thickening (Fig. 4.30B1-B3, Fig.4.31B1,B2), but well-formed exodermal Casparian strips were present in the roots that were previously exposed to naphthalene contamination (Fig. 4.30B1-B3). The overlaid images of naphthalene-treated roots showed that the passage of Nile red was prevented from being delivered into the stele due to well-matured endodermis lacking passage cells (Fig. 4.30B1-B3, Fig.4.31B1, B2).

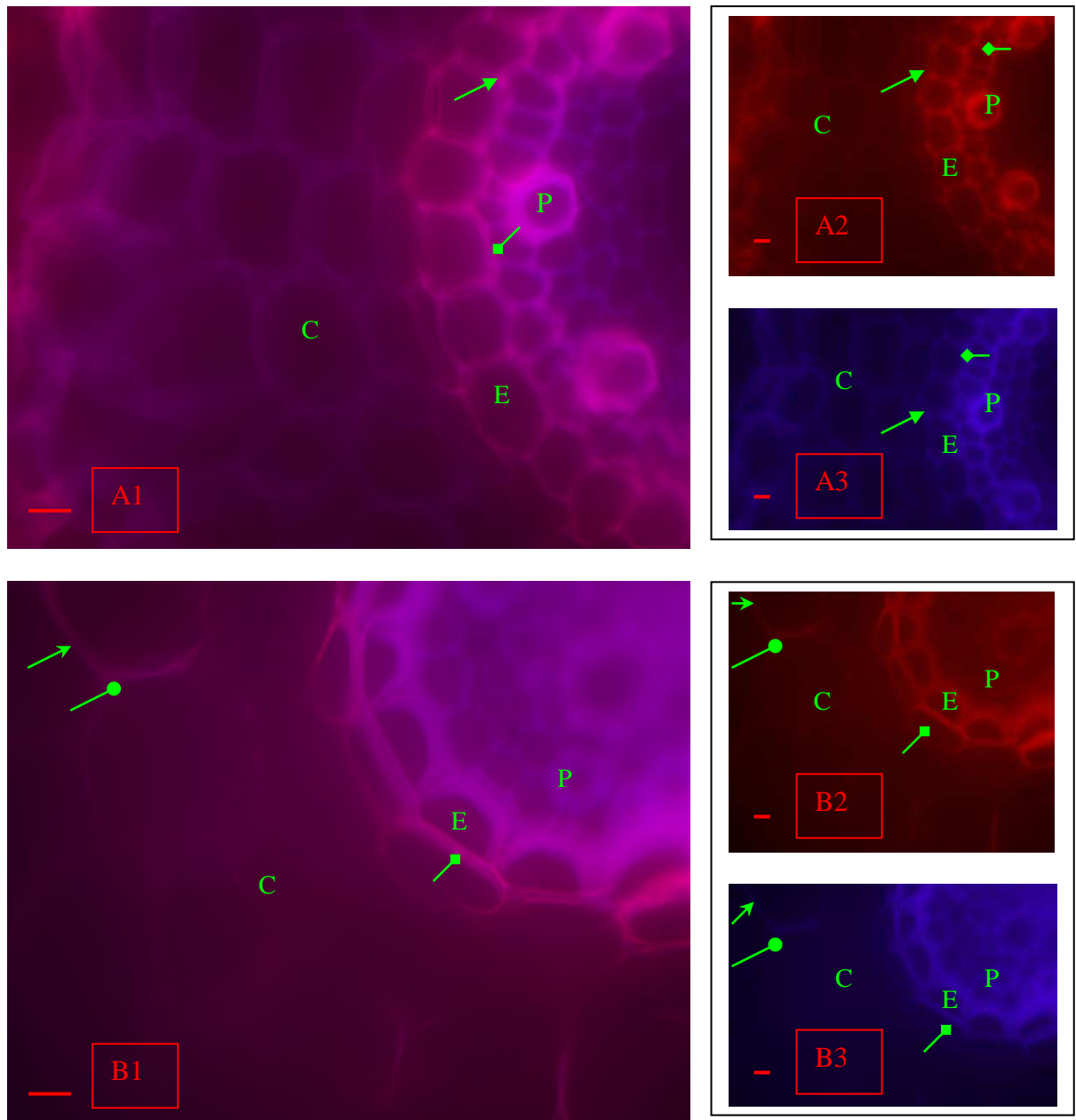


Fig.4.30: Epi-fluorescent micrographs of control (A1-A3) and naphthalene-treated (B1-B3) 6 months old tall fescue, showing parts of transversal root sections at one third as a fraction of root length above the root tip, viewed through Texas red HYQ filter (excitation at 589nm; emission at 615nm) (A2, B2) and UV illumination (excitation at 345nm; emission at 458nm) (A3, B3). The images on the left hand side (A1, B1) had been produced by overlaying images obtained through Texas red HYQ filter and UV illumination and were zoomed in. Scale: 600 μ m. Control roots (A1-A3) show well-defined Casparian strips in the endodermis and uptake of Nile red into protoxylem vessels through the relatively thin cell walls of their endodermis. Treated roots (B1- B3) show lack of uptake of Nile red into protoxylem vessels due to an extensively thickened endodermis and a well-formed exodermis. Here the radial fluorescing bands are Casparian bands and the lateral fluorescing bands are suberin lamellae. The results relate to the experiment in which tall fescue seeds (origin: Kent) were directly sown and grown in naphthalene-treated sand.

Key:

→	Casparian strip (endodermis)	E	Endodermis
—●	Casparian strip (exodermis)	P	Protoxylem vessel
C	Cortex	→◆	Suberin lamellae (endodermis)
		→	Suberin lamellae (exodermis)

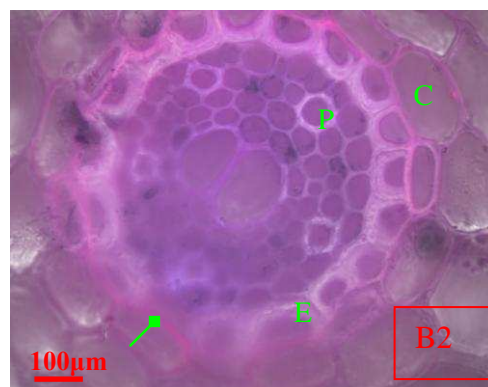
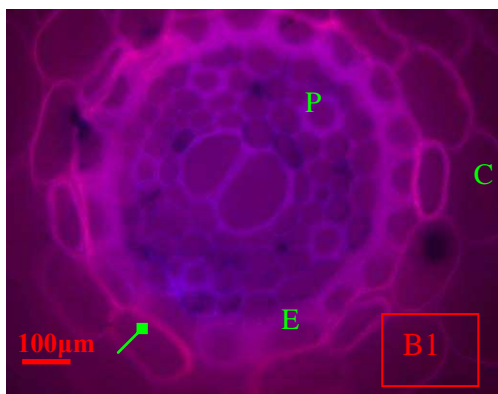
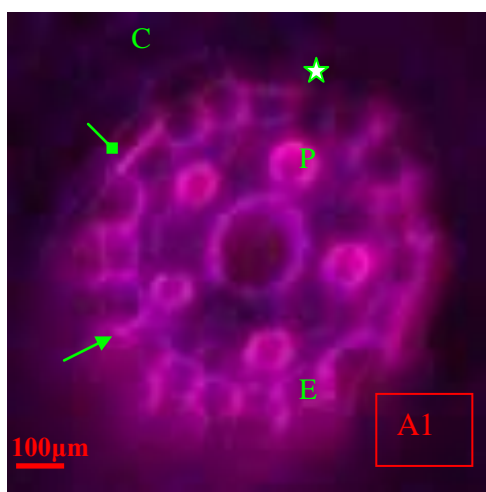


Fig.4.31: Fluorescent (A1, B1) and superimposed (A2, B2) images of control (A1, A2) and naphthalene-treated (B1, B2) 6 months old tall fescue, showing transversal root sections at one third as a fraction of root length above the root tip. The images were produced by overlaying images obtained through Texas red HYQ filter (excitation at 589nm; emission at 615nm) and UV illumination (excitation at 345nm; emission at 458nm). Scale: 100µm. Note the uptake of Nile red into protoxylem vessels via the passage cells (indicated by star symbol) present in the endodermis of control roots (A1,A2) and lack of uptake in treated roots (B1, B2) which show absence of passage cells in their endodermis. Here the radial fluorescing bands are Casparian bands and the lateral fluorescing bands are suberin lamellae. The results relate to the experiment in which tall fescue seeds (origin: Amenity) were directly sown and grown in naphthalene-treated sand.

Key:

→	Casparian strip (endodermis)	☆	Passage cell
C	Cortex	P	Protoxylem vessel
E	Endodermis	→◆	Suberin lamellae (endodermis)

4.4 Discussion

The results of the preliminary investigation indicated that exposure to naphthalene, anthracene and fluoranthene had a negative impact on seed germination, presumably due to the toxicity and volatile nature of these PAHs. On the other hand, exposure to B(a)P did not affect seed germination. These preliminary results are in accordance with the study carried out by Adam and Duncan (1999) that showed reduction in germination score of several plant species exposed to diesel oil contamination, particularly at a higher concentration (50g kg^{-1} soil). Adam and Duncan (1999) suggested that diesel oil contains more potentially toxic, volatile, LMW PAHs, thereby affecting the seed germination of plants negatively. Contrastingly, Smith et al. (2006) demonstrated that the soils heavily contaminated with aged PAHs did not affect seed germination of a mixture of grasses and legumes. The aged soils contain a larger proportion of high molecular weight molecules that are less bio available as well as less volatile (Adam and Duncan, 1999), and this may be the reason for the successful germination of plants in contaminated soils in the study of Smith et al. (2006) as well as in our study using B(a)P.

Growth in naphthalene and fluoranthene-treated sand produced a negative effect on plant growth, especially on root growth. The effect was more drastic in fluoranthene treatment. This may be because, fluoranthene has a greater tendency to change into various by products after photo modification by UV light than naphthalene, and many of these photoproducts are unstable in the presence of visible light (Kmentová, 2003), perhaps rendering the molecule much more toxic toward plants.

Interestingly, growth enhancements were observed in anthracene and B(a)P

treatments. The presence of PAHs in soil could produce a barrier effect on the acquisition of water and oxygen, which could hinder plant development, but the enhanced development of plants grown in anthracene and B(a)P-treated sand seemingly rule out the physical impacts of hydrophobic PAHs on plant growth. On the other hand, the inhibition on shoot development shown by brown top bent due to growth in anthracene-treated sand indicates variation in responses of different plant species to exposure to anthracene contamination.

The impacts of PAH-contamination on soil-water balance aspects were investigated using naphthalene as a model PAH at the concentration of 800mg kg^{-1} sand dw. At field capacity, the treated sand exhibited more or less the same moisture content % as the clean sand. As the moisture content % of both treated and clean sand was in a similar range, the naphthalene contamination did not affect the water balance of the soil. On the other hand, the matrix potential of naphthalene-treated sand was more negative [$-14.00 (\pm 0.71)$ kPa] than that of the clean sand [$-10.00(\pm 0.00)$ kPa], at saturated conditions (field capacity) ($p < 0.001$). Soil matrix potential is influenced by the width of the menisci of soil pore water and chemical composition of the soil. As the width of the meniscus of soil pore water becomes smaller, the soil matrix potential will become more negative (Slatyer, 1967). When the solid matrix contains hydrophobic substances, it may affect the permeability of water and therefore will make the matrix potential more negative too. The treated sand exhibited stronger (more negative) matrix potential, presumably because naphthalene molecules which were added to the sand wrapped around the sand particles, reducing the width of menisci within the capillary pores of the sand as well as reducing the permeability of water due to their hydrophobic nature (Fig.4.32).

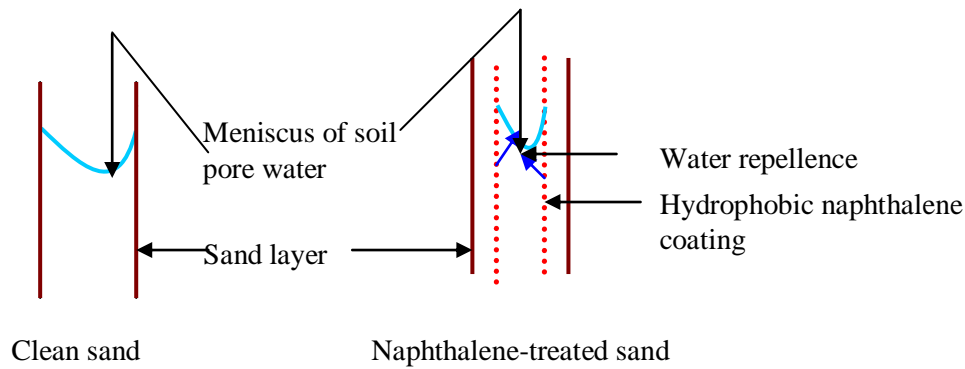


Fig.4.32: A hypothetical schematic diagram showing the reduced width of meniscus of soil pore water and water repellence in naphthalene-treated sand in comparison to the clean sand.

Also, when the unplanted treatments were left to dry out after a similar watering regime, the moisture content percentage was higher in the mid ($p < 0.01$) and bottom layers of the treated sand when compared to the controls. Perhaps, the smaller width of menisci of soil pore water in treated sand could have reduced the evaporation rate from the middle and basal portions of the potted sand. Still, the matrix potential was more negative in unplanted treated sand at water deficit conditions. The stronger matrix potential of naphthalene-treated sand than that of the clean sand at similar/higher moisture content % implies naphthalene-treated sand possesses more or the same amount of water, under same watering regime, but less plant available water, exhibiting soil stress. So, growth in naphthalene-treated sand exposes the plants to drought conditions.

A lesser number of seeds germinated in the naphthalene treated sand as recorded for two weeks since the time of sowing. Seeds need to absorb sufficient moisture to break seed dormancy as well as require preferable temperature and oxygen supplies to germinate successfully. The reduced and delayed germination of tall fescue seeds in treated sand could be due to a lesser amount of available water, but other factors such as a lesser amount of oxygen supply, toxicity and the volatility of naphthalene could have been responsible for this effect too.

The root length of plants grown in naphthalene-treated sand was 8-fold less than that of control plants ($p < 0.001$), during the initial three weeks of growth, but the differences in shoot height were not significant between the two treatments. The much inhibited root growth of treated plants at this stage may suggest that the plants were exposed to chemical stress due to naphthalene contamination. Huang et al.

(2004) have shown that plants produce ethylene, a plant hormone, which inhibits root growth in response to chemical stress, and similar may be true here. The plants showed delays in root elongation, perhaps to restrict the transport of toxic chemicals from root to shoots (Huang et al., 2004). However, other factors such as lack of available water in naphthalene-treated sand could also be responsible for this initial root growth inhibition.

An accelerated lateral growth and deviations from normal root orientation responses to gravity were exhibited by the roots growing in naphthalene-treated sand, during the acclimatisation period of 2.5-3.0 months, indicating root stress responses to unfavourable factors. The accelerated lateral growth influenced by an increase in the cortical zone may be a plant root adaptation to restrict the entry of harmful molecules into root xylems which represent the predominant route by which contaminants move from the root system to the shoots through translocation (Collins et al., 2006 and references therein). When plants were subjected to water stress during 62-70 days of plant growth, the matrix potential dropped to a lesser extent in naphthalene-treatment. This may be because, at this time point, the treated plant roots had not reached the bottom of the pots to extract water from the basal region of the pots where the sensors were installed.

The weight measurements of planted pots showed that the net gain of water after watering and net loss of water as recorded prior to watering were smaller in naphthalene treatment when compared to the controls, during the 66-76 days of plant growth. The cumulative water loss and loss in pot weight over time were smaller in naphthalene treatment among the unplanted pots of sand too, but the differences were not significant. These results suggest that the spread and drainage of water in naphthalene-treated sand as well as its loss to the atmosphere via evaporation were reduced by the sand matrix differences due to the hydrophobic nature of the naphthalene molecules that wrapped around the sand particles, but the physiological differences between the control and treated plants account for the major difference in water loss/ uptake between treatments, i.e. the contamination-treated plants absorb and transpire less amount of water. At the age of 78 days, the contaminated plant roots and shoots had lower fresh weight than their control counterparts, but had increased dry weight percentage. This indicates the treated plants had less water in

their tissues, partly because water was only scarcely available in naphthalene-treated sand for plant uptake and partly due to differences in the biochemical composition of the plant tissues leading way to uptake and storage of less water.

When subjected to prolonged water stress the cortex zone increased in roots grown in clean sand, as in naphthalene-treated roots due to partial collapse/distortions of the cortex cells. Furthermore, the differences in root diameter and distance from epidermis to root stele were not significant between water-stressed control and water-stressed contamination-treated roots. Hence the root ultrastructural modifications observed in contamination-treated roots (eg. increased root diameter, distortions in cortical zone, enhanced endodermis thickness) are not unique to PAH toxicity, but are associated with drought stress as well. However, the drought stress effect on the root ultrastructure of plants grown in clean sand was not as extreme as the effect of naphthalene contamination on root ultrastructural features, especially on root endodermis. These results suggest that the presence of naphthalene in sand causes a xenobiotic stress which is combined with drought stress, and that tall fescue develops an accelerated lateral growth and extensive thickening in the endodermis, at least in part, as a response to drought. It has been reported that stress conditions such as drought stimulates the onset of suberization and an accelerated maturation of endodermis and exodermis (Soukup et al., 2004; Enstone et al., 2003). The epifluorescent micrographs of the roots stained with berberine hemisulphate showed a clear banding of Casparian strip spanning across the hypodermis in the treated roots, whereas a suberised exodermis was absent in the control roots at the same position behind the root tip.

The root growth patterns and root anatomical features of treated tall fescue expressed symptoms akin to drought such as partial collapse of the cortex. Interestingly, when subjected to water stress, the treated plants demonstrated resilience. This superior performance of treated tall fescue than the controls could be explained by the theory of 'Hormesis'. It has been reported that when organisms are exposed to toxins or other stressors below a certain threshold level, they become more resistant to tougher challenges by producing a squadron of defence molecules (Mattson and Calabrese, 2008). Growth in naphthalene-treated sand exposes the plants to drought conditions, as demonstrated by the stronger matrix potential of the treated sand. The treated

plants could have become resistant to this drought stress, perhaps, by producing drought stress proteins in their tissues. Crowe et al. (2001) have reported an accumulation of novel dehydrins, stress proteins that protect plants against drought in cattail and clover exposed to drought conditions, and this may account for the drought resilience of treated tall fescue in our study too. Still, the root ultrastructural adaptations could have also been responsible for the drought resilience effect observed in tall fescue grown in treated sand. The suberised hypodermis, in particular, could have played a significant role in the drought resilience exhibited by treated tall fescue, presumably by impeding the radial efflux of water from the root when the soil solution becomes hypertonic. After being exposed to severe water stress, naphthalene-treated sand in which tall fescue plants were grown possessed a lower moisture content percent when compared directly to its control counterpart, even though the differences between treatments were not significant, suggesting that the suberised exodermis in treated plants could have prevented the water efflux. Jupp and Newman (1987) reported that a well developed exodermis, if in place in grass roots, prevents cortex cells from drying out from water deficit conditions. Additionally, the increased suberisation in treated tall fescue roots could have caused reduced water uptake, increasing the efficiency of water usage by the plants. The less amount of water in the treated plant tissues is, perhaps, due to the increase in suberisation as well as due to collapse of some cortex cells.

The drought resilience effect was particularly well-expressed after the acclimatisation period and in experimental designs in which seeds were germinated in rockwool cubes and plants at seedling stage were transferred to the contaminated environment. These results indicate the positive influences of a favourable environment for the initial growth and an acclimatisation period on the enhanced performance of plants under more stressful conditions. Nonetheless, irrespective of whether the seeds were germinated in rockwool cubes or sown directly in treated sand, drought resilience trend was observed in tall fescue grown in naphthalene-treated sand.

There were no visual differences in root growth patterns and root lengths between treatments after the acclimatisation period of 3 months, indicating the roots were able to grow in the contaminated sand later on, without restrictions. The high vapour pressure and Henry's law constant of naphthalene promote the PAH's tendency to be

discharged to the air easily. Heitkamp et al. (1987) reported that 12-15% of naphthalene was lost by volatilisation during the first two weeks of incubation in their sediment-water microcosm study. They also reported that naphthalene was readily degraded to CO₂ by the natural micro biota in the sediment-water microcosms tested, with no apparent lag phase, but that the rate of mineralization differed according to the source of the environmental sample. The authors showed that the ecosystem which was known to be chronically exposed to petrogenic chemicals had 2.4 weeks, the ecosystem that was chronically exposed to agricultural chemicals had 3.2 weeks, and a pristine ecosystem had 4.4 weeks, as half-life for naphthalene mineralization. They found cis-1,2-dihydroxy-1,2-dihydronaphthalene, 1-naphthol, salicylic acid, and catechol were metabolites of naphthalene, through high pressure liquid chromatography, thin layer chromatography and gas chromatography-mass spectrometric techniques. Through the use of isotope labelling, they demonstrated that 5-8% of naphthalene residues remained in the sediment after 8 weeks of exposure to naphthalene, suggesting a portion of naphthalene was probably adsorbed onto sediments and thus biologically unavailable.

The tendency of naphthalene to volatilise and biodegrade generally makes its half life too short to build up in the environment over time. However, naphthalene has a tendency to adsorb to aquifer material (Ehrlich et al., 1982) and solid organic materials, which reduces its bioavailability for micro organisms and thus its biodegradability (Heitzer et al., 1992; Weissenfels et al., 1992). In contaminated subsurface soils naphthalene is present as a dense nonaqueous-phase liquid, a form of trapped pools of organic liquid or as immobilized macroporous ganglia (U.S.Department of Health and Human Services, 2005). Slow dissolution of naphthalene and other PAHs from this dense nonaqueous-phase liquid into the aqueous phase causes them to be unavailable to the micro organisms, thus resulting in the dissolution of the PAHs being the rate-limiting step in their biodegradation (Thomas et al. 1986). There is considerable variability in reported naphthalene soil half-lives. The estimated half-life of naphthalene reported for a solid waste site was 3.6 months (Howard 1989).

The naphthalene-treated sand possessed stronger (more negative) matrix potential after 94 days since the sand had been treated with naphthalene, and after 94 days of

plant growth in the treated sand, indicating that the presence of naphthalene and or its metabolites and the physical barrier effect the hydrophobic contaminants produce on water acquisition could still be there. Adsorption of naphthalene to root exudates, aquifer materials and lipid-rich root surfaces such as rudimentary cutin could have caused the persistence of naphthalene and or naphthalene by-products in the sand medium after 94 days of plant growth. This shows that in addition to the contaminant-dilution effect due to volatilisation and biodegradation, plant root adaptations are also of major importance in the unrestricted growth of tall fescue roots in naphthalene-treated sand, after the acclimation period of 3 months.

Proliferation of naphthalene-degrading micro organisms within the rhizosphere of plant roots grown in PAH-contaminated soils has been reported by Siciliano et al. (2003). Perhaps, the plant roots could have been able to overcome the challenges in their root growth environment caused by naphthalene contamination, by stimulating the proliferation of naphthalene-biodegrading micro organisms within the dynamic region of the rhizosphere. It has been reported that micro organisms present in the contaminated subsurface soils appeared to be acclimated to the presence of PAHs and were found to mineralize naphthalene (8–55%) in sediment-water microcosms under aerobic conditions (U.S.Department of Health and Human Services, 2005). At the end of 14 weeks of growth in treated sand, tall fescue plants had a well-spread, deep, dense root system as well as an increased root biomass (dw) than the controls ($p < 0.01$), suggesting a potential of this species for PAH remediation.

Naphthalene and its methylated derivatives are considered some of the most acutely toxic compounds in the water-soluble fraction of petroleum (Anderson et al., 1974). The preliminary result showing the root growth patterns were more or less the same in anthracene and B(a)P treatments as in control treatment from the beginning suggests that the changes in initial root growth patterns and root structural and ultrastructural features shown by tall fescue to growth in naphthalene-treated sand were predominantly motivated by xenobiotic stress. Tall fescue roots grown in naphthalene-treated sand possessed root ultrastructural modifications beyond the acclimatisation period of 3 months. From 3 months of growth in treated sand onwards, tall fescue possessed a well-suberised apoplastic barrier system that could have enabled the plants to prohibit the efflux of water from the root cortex cells under

water deficit conditions as well as the influx of hydrophobic xenobiotics toward the inner core of the roots. Roots grown in sand treated with anthracene, which is practically insoluble in water was not structurally modified in terms of the endodermis thickness as well as in root hair development. Hence, a stronger apoplastic barrier system and root hair inhibition may have been induced in plant roots grown in naphthalene-treated sand, predominantly as a response to chemical stress, in order to prevent the inflow of the toxic molecules toward the inner core of the roots. The effect of these stronger apoplastic barriers in roots, especially the abundance of Casparian strip, on the passage of xenobiotic compounds across root tissues was investigated using Nile red as a hydrophobic molecular probe.

Generally solutes enter the plant roots via apoplastic pathway which is a non-selective transport pathway, providing a ready path for the movement of some materials parallel to the cell surface, by combining with the walls of the neighbouring cells as well as the intercellular air spaces (Brett and Waldron, 1996, 1990). In the cellular, symplastic pathway, which includes cell cytoplasm, vacuoles and plasmodesmata, the general characteristics of the cell wall, such as rigidity, the make up of cross-linked macromolecules and possession of a net negative charge influence the plant cell's choice of cell-signalling molecules: most of them are small and either neutral or negatively charged (Brett and Waldron, 1996, 1990) and will therefore prevent the entry of bigger or positively charged molecules through symplastic stream. Molecules in the symplastic stream are shunted from the symplastic path into the apoplastic flow at the endodermis by the Casparian strip (Wild et al., 2005; Enstone et al., 2003). The Casparian strip is composed of suberin and lignin and prevents the unimpeded movement of apoplastic substances into the stele as well as the backflow of ions from the stele. Berlow (2005) drew an analogy between Casparian strip in plant roots and the 'customs' in a 'port', because of the role of the Casparian strip in retaining the substances that may be harmful to the plants from being delivered into the root stele. However, not all endodermal cells develop Casparian strip in their radial walls. These cells without Casparian strip in their radial walls or suberin lamellae in their tangential walls, called passage cells, are generally situated opposite to the protoxylem poles and facilitate solute uptake (Fig.4.33). When casparian band structures are formed in the hypodermis, i.e. in the layer beneath the epidermis, it is called exodermis. The exodermis may also develop suberin lamella and prevents the

apoplastic inflow of ions near the root surface (Fig.4.33), but does not affect the backflow of ions from the stele (Enstone et al., 2003).

Nile red is a fluorescent hydrophobic probe, which fluoresces intensely in the confines of a lipid hydrophobic environment (Greenspan et al., 1985). Nile red applied to the epidermis of living roots was not able to pass beyond the endodermis of the treated roots, as the dye was prevented by the Casparian strip and suberin lamellae from advancing further, through its retention by these lipophilic ultrastructures. The lack of passage cells in the endodermis of the treated roots could have prohibited the dye from being delivered into the root stele. On the other hand, Nile red uptake into protoxylem vessels occurred via the passage cells in the endodermis of the control roots. Hence, the well-formed exodermis and extensively thickened endodermis lacking passage cells could be functioning as an efficient apoplastic barrier system that withholds the delivery of hydrophobic xenobiotic compounds across the root tissues via apoplastic fluxes into the inner core of the roots (see Fig. 4.33), if previously exposed to the contaminants. The increased cortical zone as well as cortical cell distortions observed in treated roots could have contributed towards the restrictions on the entry of Nile red into protoxylem poles too, as the stain had to travel further to reach the endodermis.

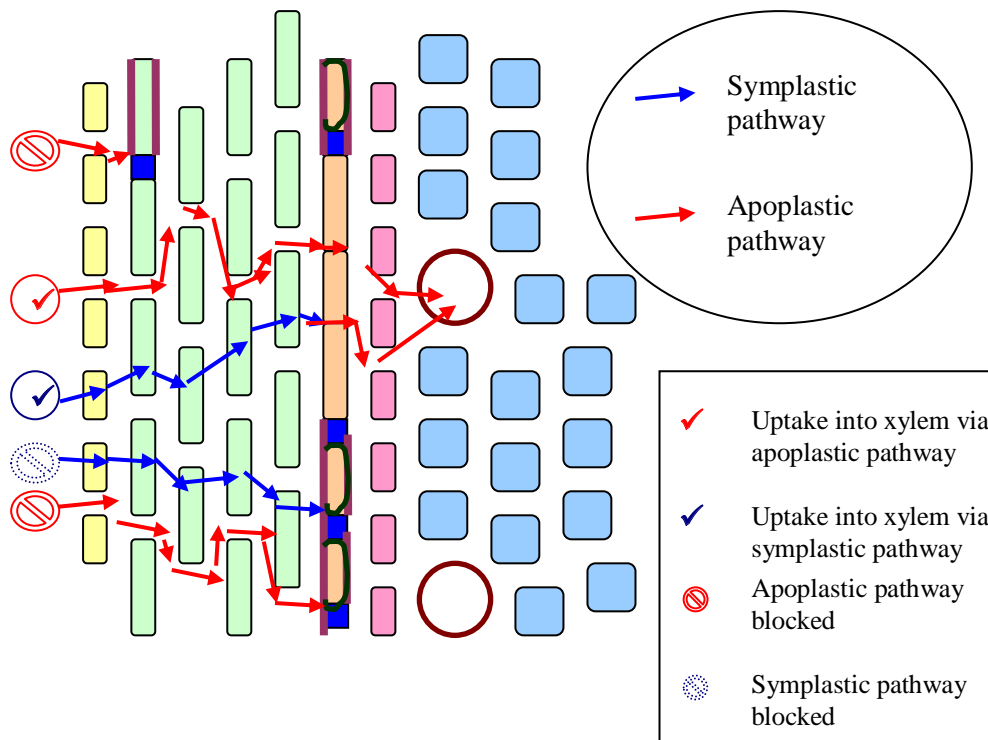
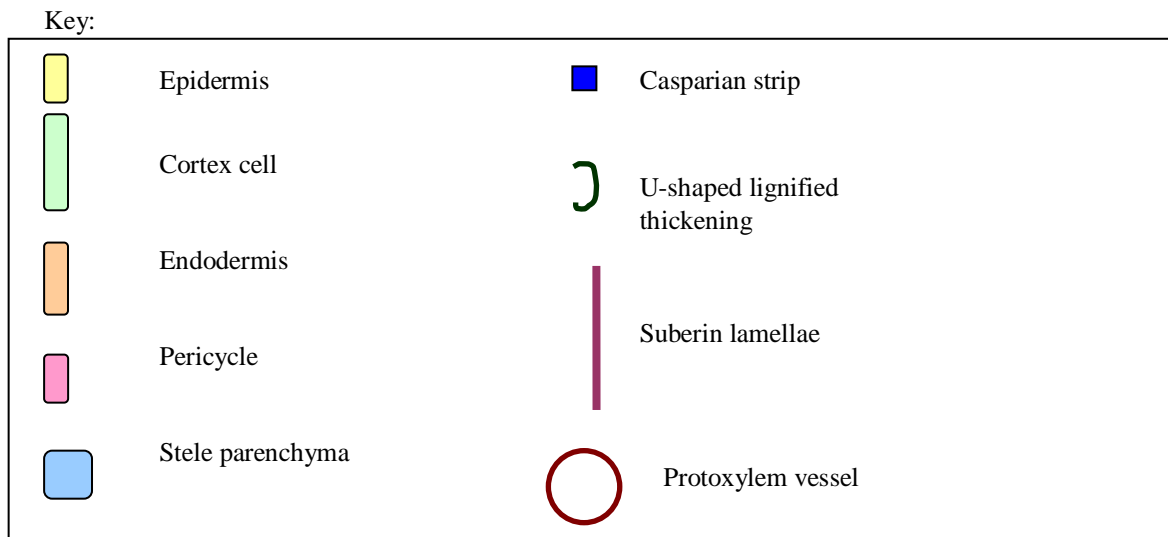


Fig.4.33: Schematic diagram of the water and solute transportation pathways across root tissues



Similarly, Wild et al., (2005) showed that the radial movement of anthracene and phenanthrene did not extend beyond the cortex cells to reach the vascular tissues of maize and wheat from a contaminated sand medium over a 56-day period, in their study. The results documented by Wild et al. (2005) using two-photon excitation

microscopy (TPEM) are in accordance with our results on Nile red uptake. It would be interesting to investigate further the pathway of naphthalene/ naphthalene metabolites within tall fescue root using stable isotope labelled naphthalene, in order to understand the fate of these compounds within the root-soil system. Still, the results obtained so far lead to a positive conclusion that tall fescue adapted to growth in PAH-contaminated sand withstands the uptake of potentially harmful, hydrophobic xenobiotic molecules into the xylem poles that represent the predominant translocation pathway toward shoots.

Molecular modifications which enable the plants to adapt structurally as well as metabolically to naphthalene stress coupled with drought stress could have been stimulated in tall fescue grown in treated sand. The plant roots and shoots were metabolically profiled in order to understand the plant adaptations at molecular level. The results of the investigation carried out at the angle of plant metabolomics are presented and discussed in chapter 5.

4.5 Conclusions

Exposure to the relatively water soluble, volatile, LMW PAH, naphthalene, delayed the seed germination of tall fescue. Tall fescue plants initially responded to naphthalene contamination by showing a temporary root growth inhibition, followed by accelerated lateral growth and deviation from normal root orientation responses to gravity. There were no visual differences in root growth patterns and root lengths between treatments after the acclimatisation period of 3 months, but differences were observed in root ultrastructural features. Naphthalene-treated sand possessed stronger matrix potential than the clean sand at soil-water holding capacity, exhibiting lack of plant available water. Consistent to this, the roots of tall fescue grown in naphthalene-treated sand showed partial collapse of the cortex cells as well as higher dry weight %, suggesting water stress/ scarcity of available water. The treated roots also possessed a well-formed exodermis and greater abundance of Casparian strip and suberin lamellae. Tall fescue grown in naphthalene-treated sand withstood drought stress better than the control plants, perhaps enhanced by these root ultrastructural adaptations. The penetration of hydrophobic xenobiotics into root xylems, exemplified by the path of Nile red was limited in tall fescue roots previously exposed to naphthalene contamination due to the existence of a stronger apoplastic barrier

system lacking passage cells as well as an increased cortical zone. The results showed that interplay of drought stress and xenobiotic stress occurs in sand contaminated with relatively water-soluble, LMW PAHs such as naphthalene and that the plants adapt to these key stress conditions through changes in initial root growth patterns as well as root structural and ultrastructural modifications.

References

Adam, G. and Duncan, H., 1999. The effect of diesel fuel on growth of selected plant species. *Environmental Geochemistry and Health*, 21, pp. 353-357.

Agarwal, U.P., 2006. Raman imaging to investigate ultrastructure and composition of plant cell walls: distribution of lignin and cellulose in black spruce wood (*Picea mariana*) *Planta*, 224, pp. 1141-1153.

Anderson, J.W., Neff, J.M., Cox, B.A., et al., 1974. Characteristics of dispersions and water soluble extracts of crude and refined oils and their toxicity to estuarine crustaceans and fish. *Marine Biology*, 27, pp. 75-88.

Barcel'ó, J., V'azquez, M.D. and Poschenrieder, Ch., 1988. Cadmium-Induced structural and ultrastructural changes in the vascular system of bush bean stems. *Botanica Acta*, 101, pp. 254-261.

Berlow, S., 2005. Roots exposed! [online] Maximum Yield-Indoor Gardening. Available at :< [http://www. Maximum Yield. Com.](http://www.MaximumYield.Com)> [Accessed 20 November 2011].

Better Soils. [online] Available at: <<http://www.soilwater.com.au>> [Accessed 10 October 2011].

Binet, P., Portal, J.M. and Leyval, C., 2001. Application of GC-MS to the study of anthracene disappearance in the rhizosphere of ryegrass. *Organic Geochemistry*, 32(2), pp.217-222.

Brett, T.C. and Waldron, W.K., 1990, 1996. The cell wall and intercellular transport. In: M.Black and B.Charlwood, eds. 1996. *Physiology and Biochemistry of Plant Cell Walls*. London: Chapman & Hall, pp.151-172.

Brundrett, M.C., Enstone, D.E. and Peterson, C.A., 1988. A berberine-aniline blue fluorescent staining procedure for suberin, lignin, and callose in plant tissue. *Protoplasma*, 146, pp.133-142.

Collins, C., Martin, I. and Fryer, M., 2006. Evaluation of models for predicting plant uptake of chemicals from soil. (Science Report- SC050021/SR) Bristol: Environment Agency.

Crowe, A.U., Han, B., Kermode, A.R., et al., 2001. Effects of oil sands effluent on cattail and clover: photosynthesis and the level of stress proteins. *Environmental Pollution*, 113(3), pp. 311-322.

Decagon Devices Inc., 2007. Manual, Water potential probe.

De Maagd, P.G.-J., ten Hulscher, T.E.M., Van den Heuvel, H., et al., 1998. Physicochemical properties of polycyclic aromatic hydrocarbons: aqueous solubilities, n-octanol/water partition coefficients, and Henry's law constants. *Environmental Toxicology and Chemistry*, 17, pp. 252-257.

Department of Agriculture Bulletin, 462, 1960.

Ehrlich, G.G., Goerlitz, D.F., Godsy, E.M., et al., 1982. Degradation of phenolic contaminants in ground water by anaerobic bacteria: St. Louis Park, Minnesota. *Ground Water*, 20(6), pp. 703-710.

Enstone, D.E., Peterson, C.A. and Ma, F., 2003. Root endodermis and exodermis: structure, function, and responses to the environment. *Journal of plant growth regulation*, 21, pp.335-351.

Farrell-Jones, J., 2003. Petroleum hydrocarbons and polyaromatic hydrocarbons. In: C.K. Thompson and P.C. Nathanail, eds. 2003. *Chemical analysis of contaminated land*. Oxford: Blackwell Publishing Ltd.

Greenspan, P., Mayer, E.P. and Fowler, S.D., 1985. Nile red: a selective fluorescent stain for intracellular lipid droplets. *The Journal of Cell Biology*, 100, pp. 965-973.

Heitkamp, M.A., Freeman, J.P. and Cerniglia, C.E., 1987. Naphthalene Biodegradation in Environmental Microcosms: Estimates of Degradation Rates and Characterization of Metabolites. *Applied and Environmental Microbiology*, 53 (1), pp.129-136.

Heitzer, A., Webb, O.F., Thonnard, J.E., et al., 1992. Specific and quantitative assessment of naphthalene and salicylate bioavailability by using a bioluminescent catabolic reporter bacterium. *Applied and Environmental Microbiology*, 58, pp.1839-1846.

Howard, P.H., 1989. *Handbook of environmental fate and exposure data for organic chemicals*. Vol. 1. Lewis Publishers, pp. 408-421.

Huang, X-D., El-Alawi, Y., Penrose, D.M., et al., 2004. Response of three grass species to creosote during phytoremediation. *Environmental Pollution*, 130, pp. 453-463.

Janska. M., Hajslova, J., Tomaniova, M., et al., 2006. Polycyclic aromatic hydrocarbons in fruits and vegetables grown in the Czech Republic. *Bulletin of Environmental Contamination and Toxicology*, 77(4), pp.492-499.

- Johnson, D.L., Maguire, K.L., Anderson, D.R., et al., 2004. Enhanced dissipation of chrysene in planted soil: the impact of a rhizobial inoculum. *Soil biology and biochemistry*, 36(1), pp. 33-38.
- Jupp, A.P. and Newman, E.I., 1987. Morphological and anatomical effects of severe drought on the roots of *Lolium-perenne* L. *New Phytologist*, 105(3), pp. 393-402.
- Kmentova', E., 2003. Response of plant to fluoranthene in environment. Ph.D. Masaryk University.
- Mackay, D., Shiu, W. and Ma, K., 2000. Physical-chemical and environmental fate handbook. CRC Press LLC.
- Mackay, D., Shiu, W. and Ma, K., 2000. Physical-chemical and environmental fate handbook. CRC Press LLC.
- Mattson, M. and Calabrese, E., 2008. When a little poison is good for you, *NewScientist*, [online] Available at: <<http://www.NewScientist.com>> [Accessed 06 August 2008].
- Orfánus, T. and Eitzinger, J., 2010. Factors influencing the occurrence of water stress at field scale. *Ecohydrology*, 3(4), pp. 478-486.
- Ryser, U. and Keller, B., 1992. Ultrastructural localisation of a bean glycine-rich protein in un lignified primary walls of protoxylem cells. *The Plant Cell*, 4, pp.773-783.
- Siciliano, S.D., Germida, J.J., Banks, K., et al., 2003.Changes in microbial composition and function during a polyaromatic hydrocarbon phytoremediation field trial. *Applied and Environmental Microbiology*, 69, pp. 483-489.
- Slatyer, R.O., 1967. Plant-water relationships. London: Academic Press Inc.
- Smith, M.J., Flowers, T.H., Duncan, H.J. et al., 2006. Effects of polycyclic aromatic hydrocarbons on germination and subsequent growth of grasses and legumes in freshly contaminated soil and soil with aged PAHs residues. *Environmental pollution*, 141(3), pp. 519-525.
- Soukup, A., Mala, J., Hrubcova, M., et al., 2004. Differences in anatomical structure and lignin content of roots of pedunculate oak and wild cherry-tree plantlets during acclimation. *Biologia Plantarum*, 48 (4), pp. 481-489.
- Taiz, L. and Zeiger, E., 1998. *Plant Physiology*. 2nd ed. Massachusetts: Sinauer Associates.
- Thomas, J.M., Yordy, J.R., Amador, J.A., et al., 1986. Rates of dissolution and biodegradation of water-insoluble organic compounds. *Applied and Environmental Microbiology*, 52(2), pp. 290-296.

U.S.Department of Health and Human Services, 2005. Toxicological profile for naphthalene, 1-methylnaphthalene, and 2-methylnaphthalene. [pdf] Georgia: Agency for Toxic Substances and Disease Registry. Available at: <<http://www.atsdr.cdc.gov/toxprofiles/tp67.pdf>> [Accessed 16 April 2012].

VandenBosch, K.A., Bradley, D.J.I., Knox, J.P. et al., 1989. Common components of the infection thread matrix and the intercellular space identified by immunocytochemical analysis of pea nodules and uninfected roots. *The EMBO Journal*, 8(2), pp.335 – 342.

Váňová, L., 2009. The use of in vitro cultures for effect assessment of persistent organic pollutants on plants. Ph.D. Masaryk University.

Weissenfels, W.D., Klewer, H.J. and Langhoff, J., 1992. Adsorption of polycyclic aromatic hydrocarbons (PAHs) by soil particles: influence on biodegradability and biotoxicity. *Applied Microbiology and Biotechnology*, 36, pp.689-696.

Wild, E., Dent, J., Thomas, G.O. and Jones, K.C., 2005. Direct observation of organic contaminant uptake, storage and metabolism within plant roots. *Environmental Science and Technology*, 39(10), pp. 3695-3702.

Wild, S.R. and Jones, K.C., 1995. Polynuclear aromatic hydrocarbons in the United Kingdom environment. A preliminary source inventory and budget. *Environmental Pollution*, 88 (1), pp.91-108.

CHAPTER 5

Differences in hydrophilic metabolome of tall fescue (*Festuca arundinacea*), grown in naphthalene-treated sand reflects plant adaptive responses to stress: a gas chromatography-mass spectrometric study

5.1 Introduction

The metabolome of a living system such as plant roots and shoots is comprised of a complex molecular mixture, including all the metabolites in that system at a certain time. It represents the molecular phenotype of the system, in a given set of physiological conditions. Metabolic profiles express the physiological picture of a plant system encoded at the molecular level. These could also identify biochemical responses of a living organ to external factors such as exposure to xenobiotics (Gromova and Roby, 2010). Mass spectrometry coupled with a separation technique such as gas chromatography as an analytical tool, makes decoding a plant metabolome at molecular resolution, with confidence, possible. The aim of this investigation was to understand the underlying physiology related to stress-adaptive responses of tall fescue (*Festuca arundinacea*) grown in naphthalene-treated sand. Here, the focus was on the hydrophilic portion of the plant metabolome. Naphthalene metabolism within plant tissues, as with naphthalene microbial degradation, requires introduction of oxygen into the rings, which would increase the PAH solubility and chemical reactivity (Meulenberg et al., 1997; Wilson and Jones, 1993; Sutherland, 1992) as well as making the PAH relatively polar. It was of principal interest to gain knowledge with regard to the fluxes of naphthalene metabolites in vivo. Moreover, previous results of our study indicated an increased root mass of plants grown in naphthalene-treated sand (see chapter 4). Hence it was of importance to confirm whether a major shift in translocation of photosynthetic sugars occurs in treated plants, through qualitative and quantitative analysis of sugar metabolites. Furthermore, sugars are of particular interest, as they play important roles as both nutrients and regulatory molecules, contributing to stress tolerance (Bolouri-Moghaddam et al., 2010).

5.2 Materials and Methods

5.2.1 Plant materials and growth conditions

Tall fescue (*Festuca arundinacea*) (origin: Kent; supplier: Emorsgate seeds, UK) were seeded and grown in clean sand and sand treated with naphthalene [800mg PAH kg⁻¹ sand (dw)], in 15cm diameter plastic pots in a glass house on a 16 hour light and 8 hour dark cycle upon germination. Plants were watered regularly and fed with liquid fertilizer (lawn food: N: P: K=15: 3: 3) on a once weekly basis.

5.2.2 Sampling

Roots and leaves were sampled from 6 months old living plants from both treatments on the same day at the same time period (early afternoon). Fresh fully expanded leaves and roots from similar depths in the pots were collected from each replicate pot (3 replicates) from each treatment. Sand was brushed off from roots and roots were washed thoroughly with distilled water.

5.2.3 Sample preparation

Samples were immediately frozen in liquid nitrogen and homogenised. Samples were freeze dried using the following protocol:

- Freezing: at -45° C for 210 minutes at 200mTorr
- Primary drying: at -10° C for 600 minutes at 200mTorr; then at 0° C for 200 minutes at 100mTorr
- Secondary drying: at 22° C for 180 minutes at 100mTorr

Vials containing samples were capped tightly and stored at -80° C in the freezer until further analysis.

5.2.4 Extraction and derivatization

The extraction protocol was adapted from Du et al. (2011). Freeze dried tissue powders (0.1g) were transferred into 10ml extraction tubes (Schott). Hundred micro litres (100µl) of ribitol (2mg L⁻¹) as internal standard and 4.2ml 80% HPLC grade aqueous methanol (v/v) were added and the tissue samples were extracted on a rotator extraction unit at 40 rpm for 120 minutes. The tubes containing extracts were subsequently incubated in a water bath at 70° C for 15 minutes and centrifuged at

2000g for 5 minutes. Seven hundred and fifty micro litres (750 μ l) of chloroform was added to the extracts in order to separate out the non polar phase. The mixture was vortexed thoroughly and centrifuged at 2000g for 2 minutes. Forty micro litres (40 μ l) of the polar phase was transferred into GC-vials and the solvents were evaporated in a centrifugal concentrator for 25 minutes under vacuum at room temperature. The dried polar phase was oximated with 40 μ l of methoxyamination reagent (methoxyamine hydrochloride dissolved in anhydrous pyridine at the concentration of 20mg ml⁻¹) at 37° C for 90 minutes. Here the carbonyl groups are the main targets for methoximation. Subsequent silylation was carried out with 70 μ l of MSTFA (N-Methyl-N-trimethylsilyl-trifluoroacetamide) at 37° C for 30 minutes. Here hydroxyl groups are the primary targets for silylation. The ratio of the volume of derivatising agent to sample was increased to ensure complete derivatization. After derivatization procedure, the vials containing samples were briefly centrifuged for 5 seconds and the vials were left to cool in the fume hood for a few minutes, before analysis by GC-MS.

5.2.5 Gas chromatography- mass spectrometry (GC-MS) analysis

Samples were analysed with a PerkinElmer AutoSystem XL gas chromatograph coupled with a TurboMass mass spectrometer (PerkinElmer Inc., Waltham, MS). The published method (Du et al., 2011) was used with minor modifications. A 1- μ l aliquot of the derivatised extract was injected into a Zebron ZB-17 5MS capillary column (30m \times 0.25mm \times 0.25 μ m) (Phenomenex, Torrance, CA, US). The inlet temperature was set at 260° C. After a 5-minute solvent delay, initial GC oven temperature was set at 80° C. Two minutes after injection, the GC oven temperature was raised to 280° C (5° C min⁻¹), and finally held at 280° C for 13 minutes [For the analysis of the authentic sample of 1- Naphthol (Sigma Aldrich; ReagentPlus), the GC oven temperature was raised to 280° C from the initial temperature of 80° C, at the rate of 10° C min⁻¹ and finally held at 280° C for 6.50 minutes]. The injection temperature was set to 280° C and the ion source temperature was adjusted to 200° C. Helium was used as the carrier gas with a constant flow rate set at 1ml min⁻¹. The measurements were made with positive electron impact ionisation (70 eV) in the full scan mode (m/z 30-550). The metabolites were identified using MassLynx 4.0 software (PerkinElmer Inc.) coupled with a commercially available compound library: NIST Mass Spectral Database 2.0 (PerkinElmer Inc., Waltham, MS) as well as the fragmentation patterns

of the analytes.

The authentic sample of 3-indole acetic acid (Sigma Aldrich) was analysed with Agilent 6890 GC coupled with Agilent 5973 MSD. The GC-MS conditions for the reference 3-indole acetic acid were as follows:

Column: Agilent DB5 (30m × 0.25mm × 0.25µm)

Oven temperature: 60° C for 2 minutes; then the temperature was raised to 250° C (5° C min⁻¹), and finally held at 250° C for 5 minutes

Carrier gas: Helium at 1ml min⁻¹

Data system: Agilent Chemstation

Injector: Split/ splitless at 220° C

Injection volume: 0.1 µl

Detector: Transfer line temperature at 250° C; Source temperature at 230° C; Quad temperature at 150° C

5.2.6 Selection criteria for the identification of compounds

The EI positive total ion chromatograms for polar compounds extracted from root and shoot tissues of the plants grown in clean and treated sand showed about 200 different components. Having appreciated that each and every one of these components possesses their own unique functions, only 14 compounds from plant tissues were identified with the aid of NIST Mass Spectral Database (v.2.0) and the retention time indices. Intensity of response as well as non-interference by signals from reagent blanks were chosen as the major criteria for compound identification, but the internal standard ribitol, naphthol and fructans were exceptions for the intensity of response criterion. Patterns of fragmentation processes and fragment ions during electron ionisation documented by de Hoffmann and Stroobant (2002) were used as guides for the interpretation of EI mass spectra.

5.2.7 Data analysis

The individual spectra and chromatograms from GC-MS data files were deconvoluted with the aid of Automated Mass Spectral Deconvolution and Identification System (AMDIS) spectral deconvolution software package v2.69 (NIST, Gaithersburg), freely available at <http://chemdata.nist.gov/mass-spc/amdis/>, to carry out baseline

corrections and purify spectrum from background noise. AMDIS deconvolution settings were as follows: adjacent peak subtraction was two, resolution was medium, sensitivity was low, shape requirement was high and component width was kept at 12. The ELU files generated by AMDIS were then fed to SpectConnect online services <<http://spectconnect.mit.edu/>> to align batches of ELU files from related chromatograms and to filter peaks. The integrated signals generated by SpectConnect were used for data normalisation and subsequent statistical analysis. Data normalisation was performed on Excel spreadsheet. Target compounds were identified by fragmentation patterns and matching spectra in a reference library (NIST Mass Spectral Database v. 2.0).

5.2.8 Statistical analysis

Statistical significance was determined by t-test assuming unequal variances using the built-in toolkit in Microsoft Excel.

5.3 Results

5.3.1 Identification of compounds

Visual inspection of the EI positive total ion chromatograms for polar compounds extracted from root and shoot tissues of the plants grown in clean and treated sand revealed a complex profile with about 200 different components (see Fig. 5.1 and 5.2 respectively). In both chromatograms, 12 compounds were notably more intense than the remainder. One of these (RT 35.85 min) corresponded to an ion peak associated with the reagent blank (see Fig 5.3). The remaining more intense peaks corresponded to compounds that were tentatively identified from analysis of their mass spectral features and reference to the NIST Mass Spectral Database (see Table 5.2). Derivatization was performed to silylate OH/NH groups and oximate aldo and keto groups with the aim of detecting all polar compounds with these functional groups. Steric hindrance in the molecules may nevertheless have prevented complete derivatization, whilst silylation of the OH function in carboxylic groups will be limited.

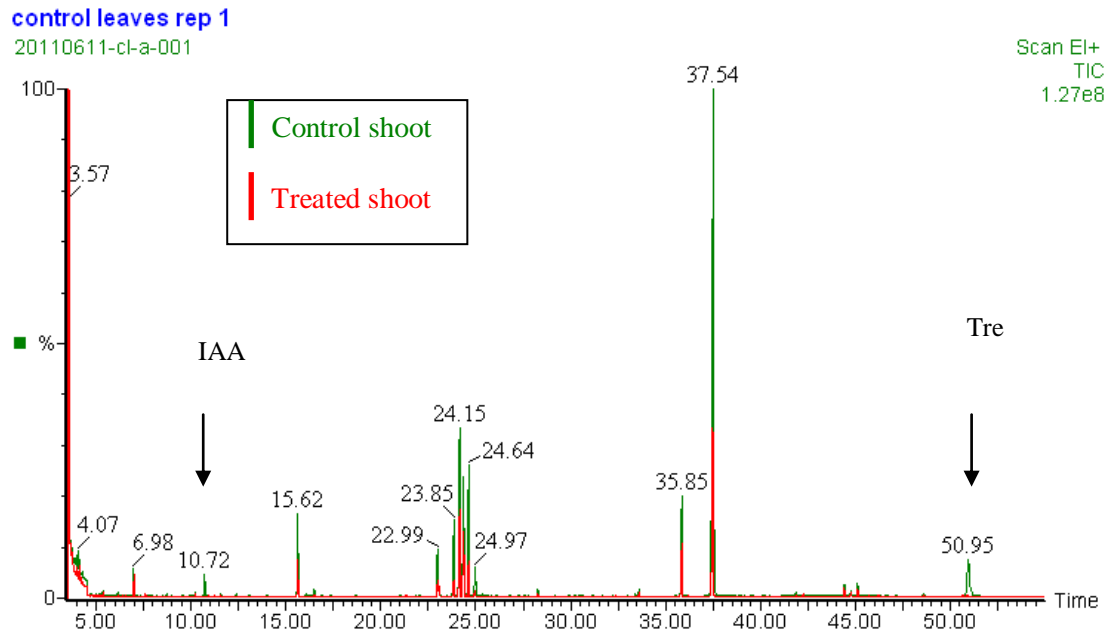


Fig.5.1: Overlaid EI positive total ion chromatograms for polar compounds extracted from leaf tissues of tall fescue grown in clean sand (green) and sand contaminated with naphthalene (red). IAA: Indole Acetic Acid; Tre: Trehalose. Note the greatly subdued expression or absence of signal in treated leaves for the putative IAA and Tre.

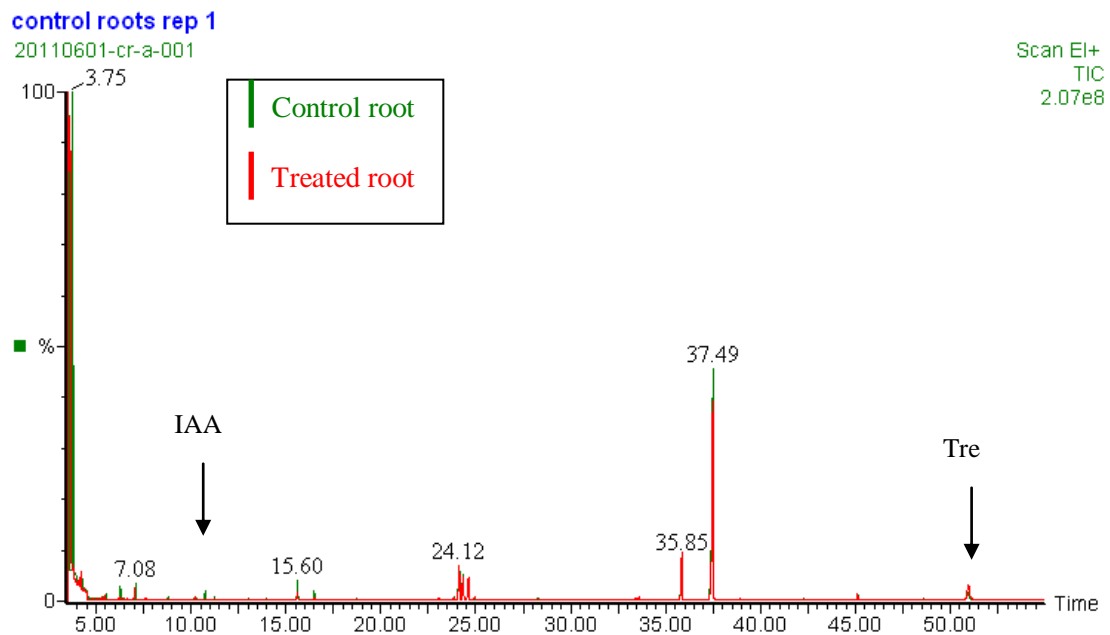


Fig.5.2: Overlaid EI positive total ion chromatograms for polar compounds extracted from root tissues of tall fescue grown in clean sand (green) and sand contaminated with naphthalene (red). IAA: Indole Acetic Acid; Tre: Trehalose. Note the subdued expression or absence of signal for the putative IAA and a well-pronounced signal for 'Tre' in treated roots.

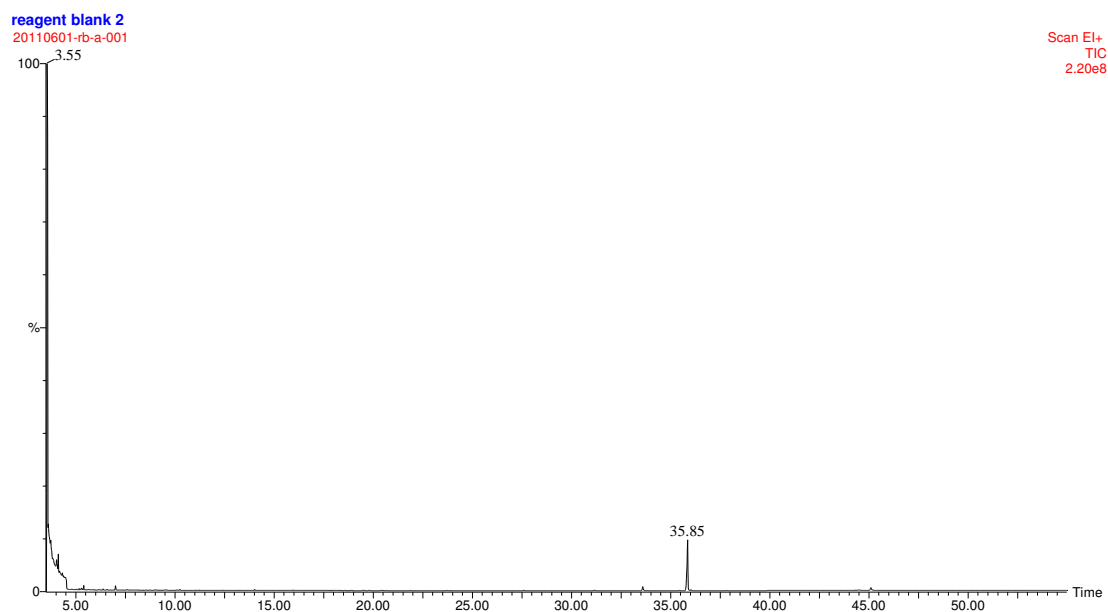


Fig.5.3: Representative EI positive total ion chromatogram for reagents used in the extraction and derivatization of plant tissues

Amongst the major peaks, none corresponded to compounds that resembled polar derivatives of naphthalene, such as naphthol or glycolsylated/ malonylated derivatives. Naphthalene epoxide was also ruled out because of its sparing solubility in the tissue extraction medium, methanol.

However a minor ion peak (RT 10.71-10.73) in treated roots which was of interest as it was subdued in expression when compared to the untreated, was considered from mass spectral information as either naphthol, naphthalene or derivatives of these two compounds, or, on the other hand, indole acetic acid or its derivatives.

The mass spectra for the compounds in treated (Fig 5.4) and untreated (Fig. 5.5) roots were compared with each other and with that for naphthol (see Fig. 5.6 and 5.7). Neither spectrum resembled the spectrum obtained for authentic naphthol (see Fig. 5.6 and 5.7) nor were they similar to one another i.e. the compounds in treated and untreated roots were different.

In treated roots (Fig. 5.4) the spectrum showed the presence of a major ion peak at m/z 142 and two minor peaks at m/z 70 and 216 as well as higher molecular weight ions at $>m/z$ 360. Based on the limited level of fragmentation observed and the absence of any TMS derivative which would otherwise indicate the presence of an

OH group, these spectral features suggested a compound with a high degree of aromaticity that was resistant to fragmentation. Taken together with the presence of high molecular weight ions, the profile might correspond to a naphthol derivative e.g. glycosylated or malonylated naphthol (Taguchi et al., 2010) (see appendix 1).

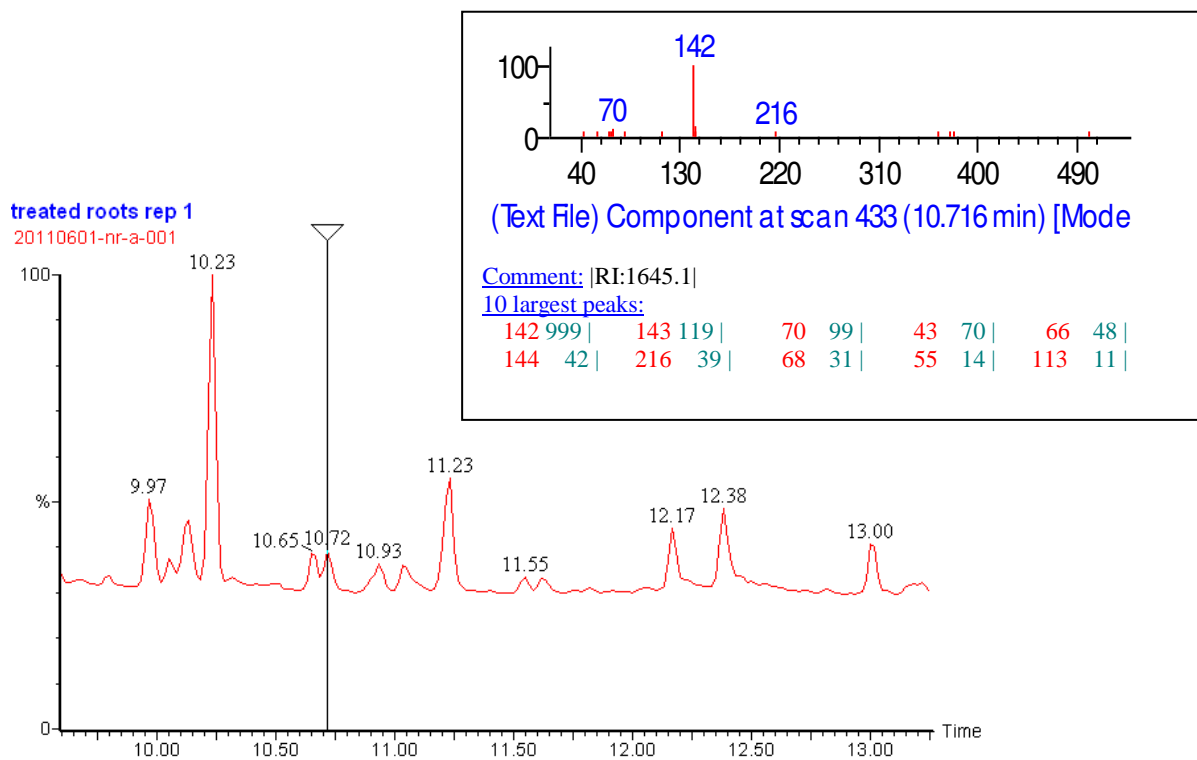


Fig.5.4: Zoomed part of EI positive total ion chromatogram for the compounds extracted from root tissues of tall fescue grown in naphthalene-contaminated sand. Inset: The extracted mass spectrum for the compound eluting at 10.72 minutes. RI: Retention Index.

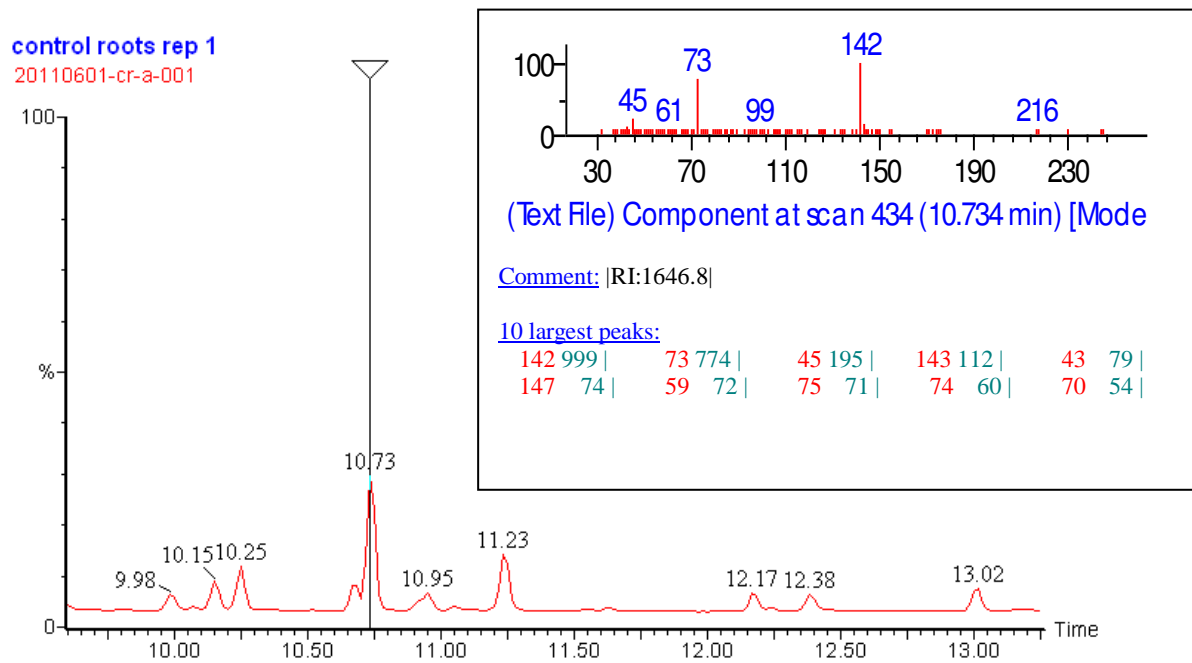


Fig.5.5: Zoomed part of EI positive total ion chromatogram for the compounds extracted from root tissues of tall fescue grown in clean sand. Inset: The extracted mass spectrum for the compound eluting at 10.73 minutes. RI: Retention Index

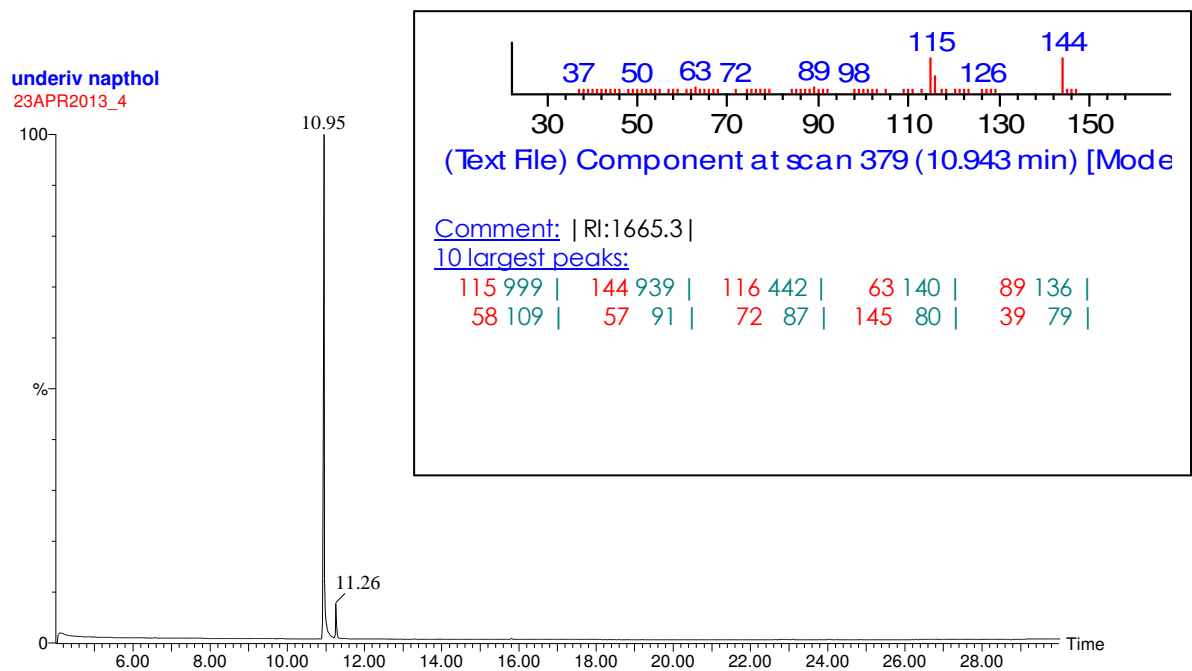


Fig.5.6: EI positive total ion chromatogram for 1-Naphthol dissolved in chloroform (GC-grade). Inset: The extracted mass spectrum for 1-Naphthol. RI: Retention Index

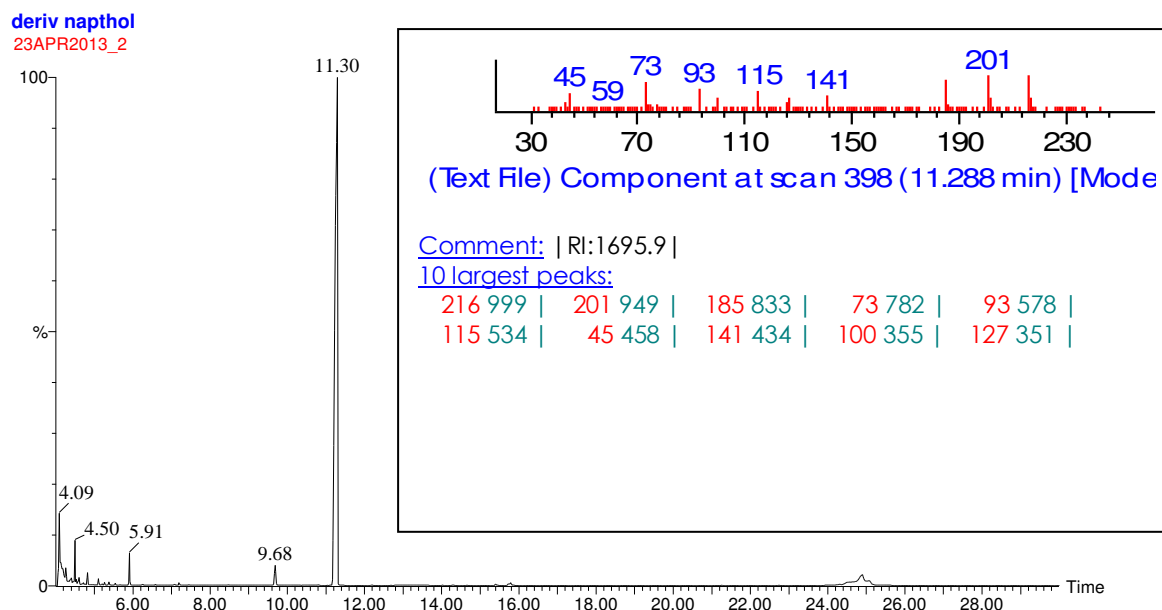


Fig.5.7: EI positive total ion chromatogram for silylated 1-naphthol. Inset: The extracted mass spectrum for silylated 1-naphthol. RI: Retention Index.

In the untreated roots, the spectrum for the compound RT 10.73 showed a similar major ion peak at $m/z/142$ and minor peak at m/z 216 but additionally a TMS-peak at m/z 73 and ion at m/z 147, which suggested a compound with two OH groups or an OH and NH group, as well as ions at m/z 230 and 245. The major ion peak at m/z 142 is interesting because the mass spectrum for indole acetic acid has a characteristic peak at m/z 142 (see table 5.1). In these experiments, silylation of the carboxyl function on indole acetic acid is extremely unlikely; nevertheless, silylation could be via the NH function on the indole ring. These features together suggest the presence of IAA in untreated roots. The spectrum was compared with that for authentic indole acetic acid silylated using the same technique (see Fig. 5.8 and Table 5.1).

Table 5.1: Comparison of spectra of a peak at RT 10.73 min in plant samples with silylated authentic indole acetic acid. Similar ion abundance in spectra is indicated by ^a

RT 10.73 spectrum - silylated untreated root extract	2 TMS indole acetic acid	1 TMS indole acetic acid
ND	m/z 319	ND
m/z 245 ^a	m/z 245 ^a	m/z 245
m/z 230 ^a	m/z 230 ^a	m/z 230
ND	m/z 202 BP	m/z 202
m/z 175 ^a	m/z 175 ^a	m/z 175
m/z 173 ^a	m/z 173 ^a	m/z 173
m/z 216 ^a	m/z 216 ^a	m/z 216
m/z 147 ^a	m/z 147 ^a	147
m/z 142 BP	m/z 142 ^a	m/z 142 ^a
m/z 131 ^a	m/z 130 ^a	m/z 130 BP
m/z 77 ^a	m/z 77 ^a	m/z 77
m/z 75 ^a	m/z 75 ^a	m/z 75 ^a
m/z 73 ^a	m/z 73 ^a	m/z 73 ^a
m/z 45 ^a	m/z 45 ^a	m/z 45 ^a

The spectrum for the RT 10.73 compound had a base peak (m/z 142) which was different to that for either 1 TMS indole acetic acid (m/z 130) or 2 TMS indole acetic acid (m/z 202), but shared an identical fragmentation pattern to that of 2 TMS indole acetic acid: a major peak at m/z 73, medium-intensity peaks at m/z 45 and 147 and minor peaks at m/z 216, 230 and 245. Some of these peaks were also present in similar abundance in the spectrum for 1 TMS indole acetic acid (see Table 5.1).

Acids in the plant samples were likely to have been methylated as a result of the use of methanol, anhydrous hydrochloric acid and heat treatment (>60⁰ C), therefore there is a likelihood that the RT 10.73 compound could be a methyl ester of indole acetic acid which has been subsequently silylated via the NH function. Since the authentic sample of 3-indole acetic acid was not methylated but only silylated, information on the fragmentation patterns of methylated, 1 TMS indole acetic acid could not be obtained from the GC-MS analysis of reference 3-indole acetic acid here.

In summary, the RT 10.73 compound in plant samples was not identified, but the spectral features shown by this compound could be consistent with the presence of methylated, 1 TMS indole acetic acid (see appendix 1).

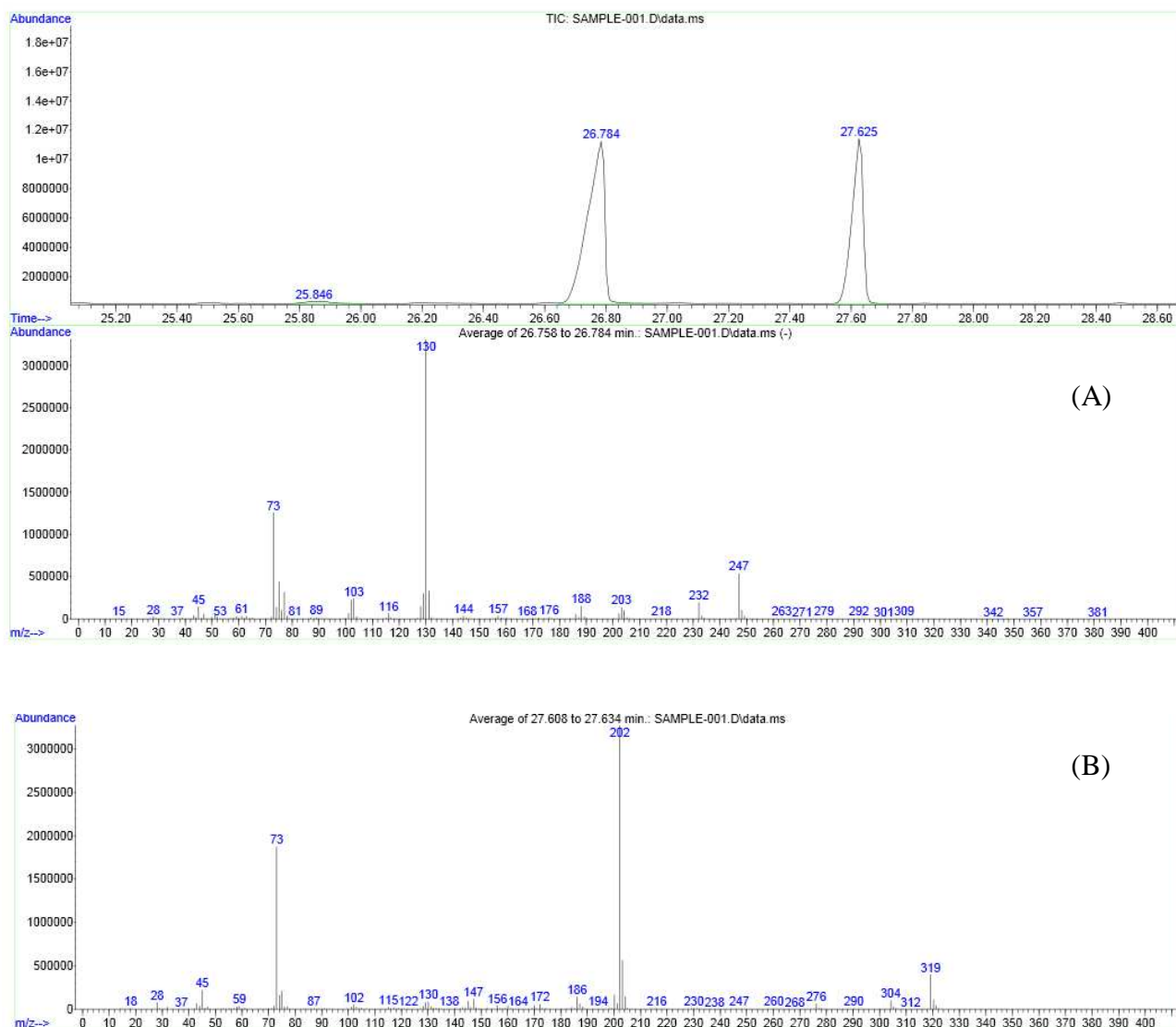
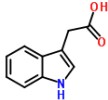
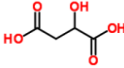
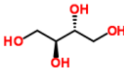
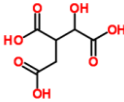
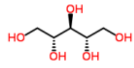
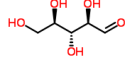
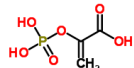
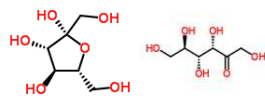
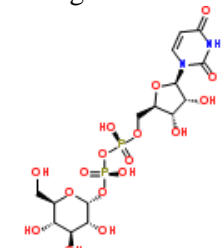
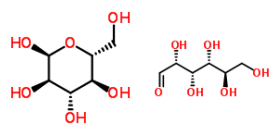
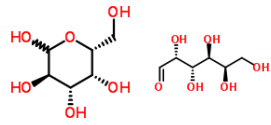
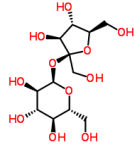
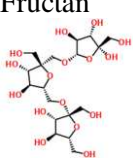


Fig.5.8: EI positive total ion chromatogram for the trimethylsilylated 3-Indole acetic acid and mass spectra for compounds RT 26.78 min (A) and RT 27.63 min (B) corresponding to 1 TMS Indole acetic acid and 2 TMS Indole acetic acid respectively from reference to the mass spectral database library

Apart from erythritol, malic acid, isocitric acid and pyruvic acid, the remaining compounds were all identified as sugars. Glucose was distinguished from galactose, and sucrose from trehalose, from the higher intensity of response and differences in their retention time. Sucrose was the most abundant sugar based on intensity of the ion peak.

Table 5.2: List of 14 metabolites tentatively identified from mass spectra analysis and database inspection in the shoots and roots of tall fescue grown in clean sand and sand contaminated with naphthalene for 6 months plus the internal standard (differentiated by the italic font). ^a detected only in treated roots. ^b detected only in treated leaves. The principal diagnostic features used in the identification of compounds along with their mass spectra are given in appendix 1.

No.	Retention time (RT) (min)	Compound	Abbreviation	Derivative
1	10.71	<p>There is a major ion peak at m/z 142 and a minor ion peak at m/z 216. A high molecular weight ion peak at m/z ~500 is present. The spectrum shows less intense fragmentation when compared to the spectrum obtained for the peak with similar RT (RT 10.73 min) in shoots and untreated roots. Naphthol was suggested from database inspection but ruled out after comparison with authentic naphthol^a</p>		TMS
2	10.73	<p>Indole acetic acid</p> 	IAA	TMS
3	15.63	<p>Malic acid</p> 	MA	TMS
4	16.09	<p>Erythritol</p> 	Ery	4 TMS
5	16.51	<p>Isocitric acid</p> 	ICA	TMS

6	21.04	Ribitol 		5 TMS
7	23.00	Ribose 	Rib	Methyloxime-, 4 TMS
8	23.86	Phosphoenol pyruvic acid 	PEP	TMS
9	24.17	Fructose 	Fru	Methyloxime-, 5 TMS
10	24.36	UDP-glucose 	UDP-Glc	Methyloxime-, 6 TMS
11	24.64	Glucose 	Glc	Methyloxime-, 5 TMS
12	24.97	Galactose 	Gal	Methyloxime-, 5 TMS
13	37.54	Sucrose 	Suc	8 TMS
14	50.67	Fructan ^b 	Fructan	Poly TMS

15	50.96	Trehalose 	Tre	8 TMS
----	-------	--	-----	-------

5.3.2 Differential abundances of polar compounds in the leaves and roots of tall fescue grown in naphthalene-contaminated sand in comparison to the controls

The EI total ion chromatograms for polar compounds extracted from shoot (leaf) and root tissues of tall fescue are shown in Fig. 5.1 and 5.2, and the zoomed in spectra for the sugars RT=22.00-26.00 min in Fig 5.9 and 5.10. The recovery of ribitol, the internal standard extracted together with the plant tissues was lesser in root compared to leaf extracts indicating a lesser extraction efficiency, which was attributed to the different chemistries and cell architectures of roots and leaves, roots being more heavily lignified with phenolic derivatives than leaves. Therefore the integrated signals of peak areas for the polar compounds were normalised with regard to the recovery of ribitol, and these are shown in table 5.3 and Fig 5.11.

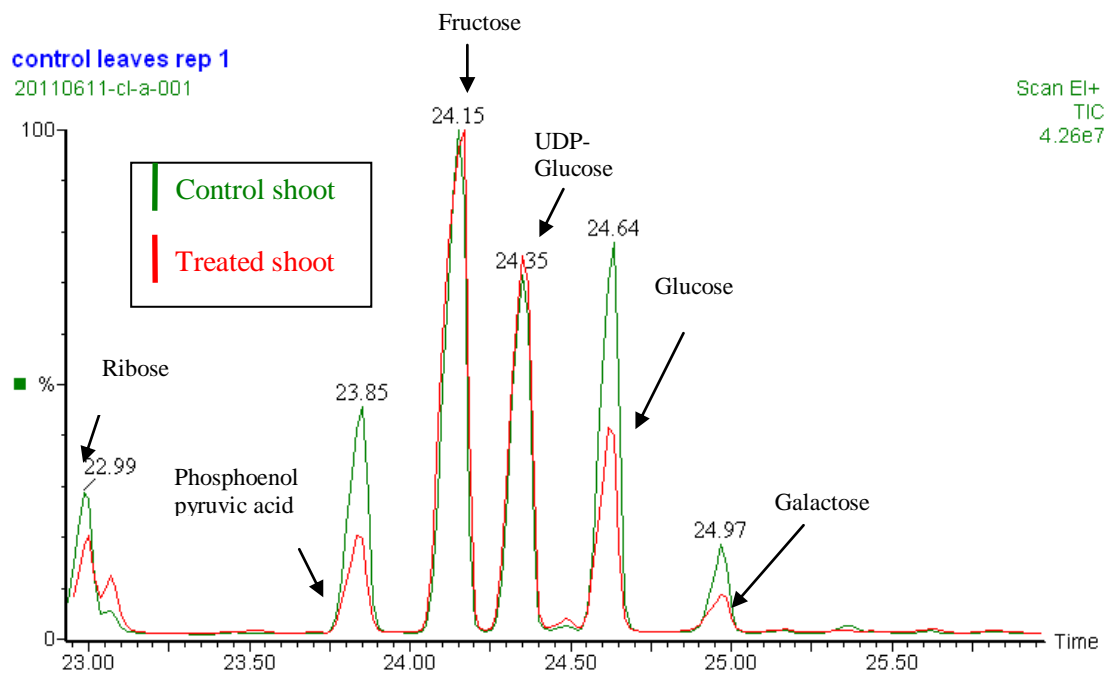


Fig.5.9: Overlaid EI positive total ion chromatograms for polar compounds extracted from shoot tissues of tall fescue grown in clean sand (green) and sand contaminated with naphthalene (red), showing the retention time region between 22.00-26.00 minutes.

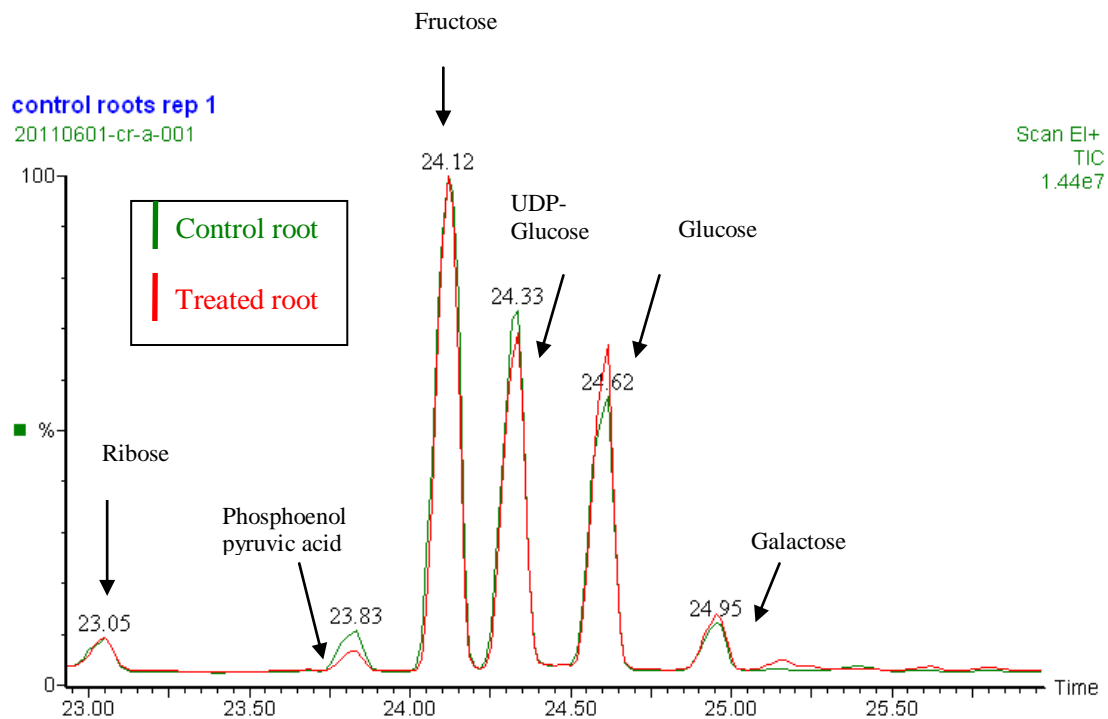


Fig.5.10: Overlaid EI positive total ion chromatograms for polar compounds extracted from root tissues of tall fescue grown in clean sand (green) and sand contaminated with naphthalene (red), showing the retention time region between 22.00-26.00 minutes.

Table 5.3: Descriptive statistics for normalised integrated signals of peak areas for the polar compounds extracted from the shoots and roots of tall fescue grown in clean sand and sand contaminated with naphthalene (0.08% w/w) for 6 months. All t-tests are for differences between control and treated plants.

Name of the molecule	Shoots		p value as determined by two-tail t-test assuming unequal variances	Roots		p value as determined by two-tail t-test assuming unequal variances
	Control Mean(\pm SE) (E+07)	Treated Mean (\pm SE) (E+07)		Control Mean(\pm SE) (E+07)	Treated Mean (\pm SE) (E+07)	
RT 10.71	ND	ND	–	ND	0.21(\pm 0.09)	–
Indole acetic acid	2.69(\pm 0.19)	0.13(\pm 0.01)	<0.001	11.73(\pm 2.60)	0.40(\pm 0.36)	<0.05
Malic acid	9.93(\pm 1.88)	3.06(\pm 0.32)	<0.05	44.20(\pm 11.7)	79.17(\pm 14.8)	NS
Erythritol	0.50(\pm 0.04)	0.03(\pm 0.002)	<0.001	ND	ND	–
Isocitric acid	1.34(\pm 0.12)	0.18(\pm 0.01)	<0.001	20.59(\pm 6.64)	13.85(\pm 2.14)	NS
Ribose	6.81(\pm 1.61)	3.03(\pm 0.28)	NS	6.48(\pm 2.24)	27.81(\pm 4.46)	<0.01
Phosphoenol pyruvic acid	1.33(\pm 0.13)	0.90(\pm 0.19)	NS	9.93(\pm 2.28)	17.17(\pm 2.52)	NS
Fructose	20.67(\pm 4.80)	14.41(\pm 1.51)	NS	121.05(\pm 18.11)	351.46(\pm 60.89)	<0.05
UDP-Glucose	9.31(\pm 3.51)	6.75(\pm 1.47)	NS	113.13(\pm 26.44)	388.87(\pm 37.48)	<0.01
Glucose	16.71(\pm 4.14)	4.93(\pm 0.85)	<0.05	71.11(\pm 21.94)	324.55(\pm 35.35)	<0.01
Galactose	6.09(\pm 0.86)	1.52(\pm 0.13)	<0.01	12.12(\pm 3.39)	50.83(\pm 5.90)	<0.01
Sucrose	63.20(\pm 7.85)	18.83(\pm 2.50)	<0.01	277.52(\pm 122.61)	1326.55(\pm 244.22)	<0.05
Fructans	ND	0.43(\pm 0.07)	–	ND	ND	–
Trehalose	12.05 (\pm 2.05)	0.33 (\pm 0.08)	<0.01	46.33(\pm 15.84)	392.23 (\pm 30.03)	<0.001

N (No. of samples) =4 (GC runs 1-2); ND=not detected; NS= not significant; p = probability; SE = standard error of the mean.

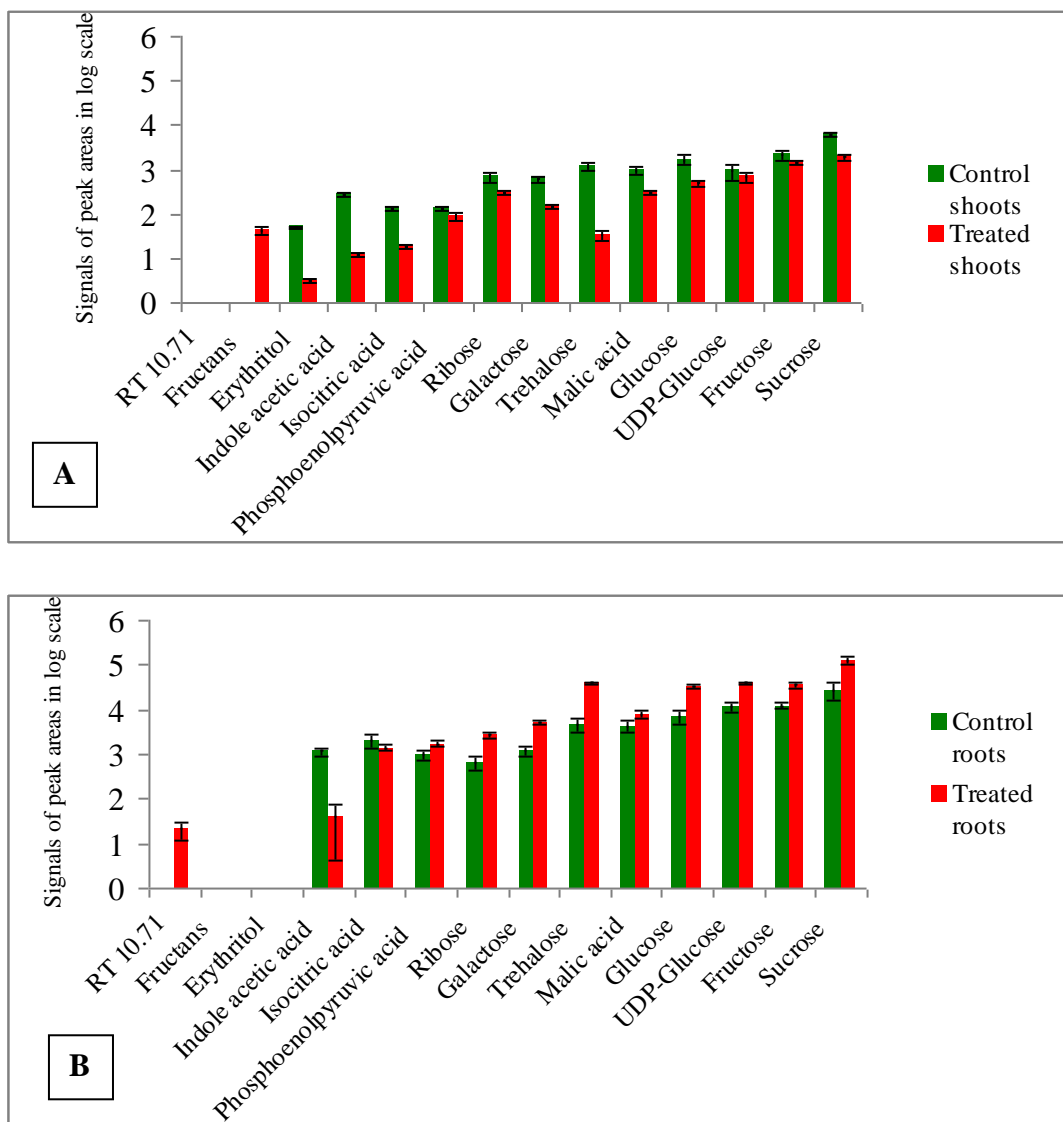


Fig. 5.11: Bar graph showing the differences in the abundance of polar compounds in shoots (A) and roots (B) of tall fescue between control (green) and naphthalene-contaminated (red) treatments. Error bars show standard error of the mean [N=4 (GC runs 1-2)].

Apart from the putative IAA, shoots from naphthalene treatments generally had a lesser amount of polar compounds compared to untreated shoots, but in treated roots, polar compounds were more abundant than in untreated roots. The patterns obtained for ribose, glucose, UDP-glucose, fructose and galactose are depicted in the XY scatter graph that shows the mean values of the normalised integrated signals of peak areas for simple sugars in the shoots and roots of tall fescue from control and contaminated treatments (Fig.5.12).

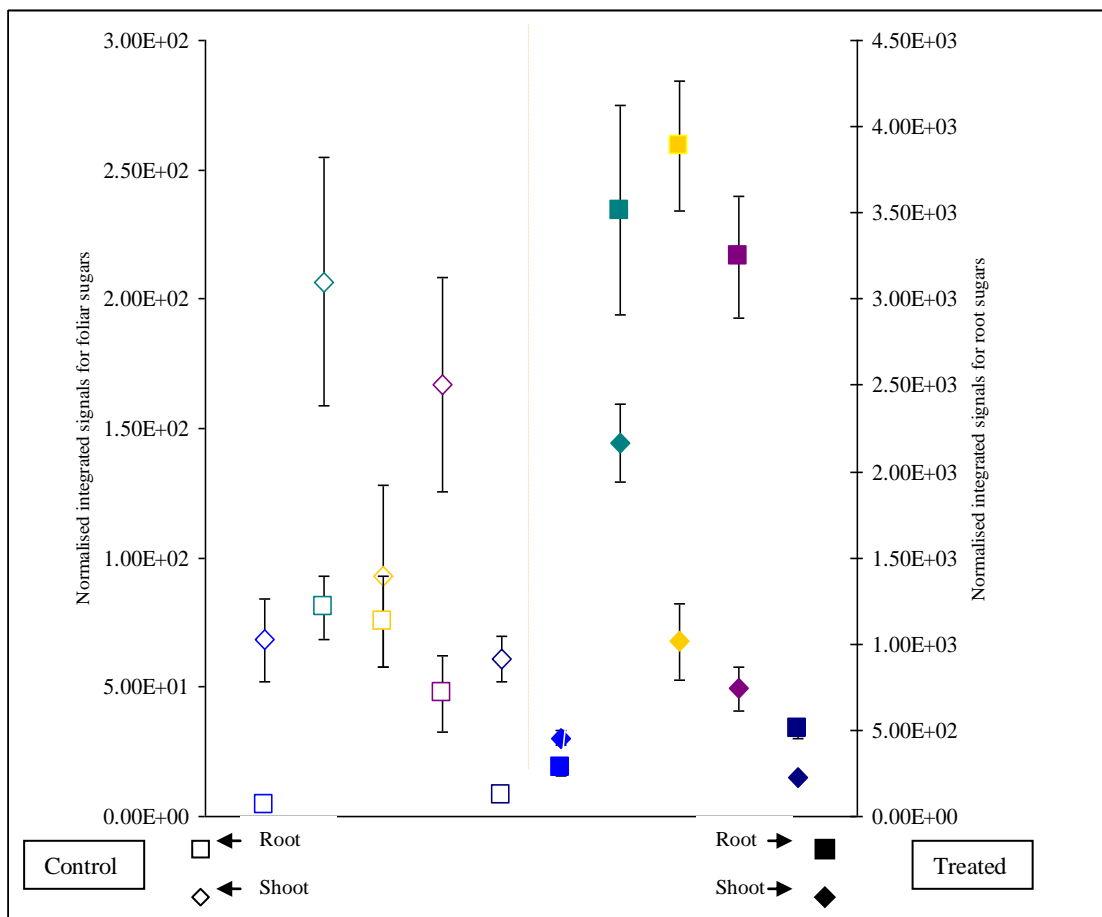


Fig.5.12: XY scatter graph showing the mean values for the abundances of simple sugars and the nucleotide sugar UDP-Glucose in the root (indicated by squares) and shoot (indicated by diamonds) tissues of tall fescue grown in clean sand (left) and sand contaminated with naphthalene (right; differentiated by filled shapes). Error bars indicate standard error of the mean. Some error bars are obscured by the symbols due to the small integrated signals of peak areas for some compounds. N=4 (GC runs 1-2). The scale on left hand side is for the abundance of foliar (shoot) sugars; the scale on the right hand side is for the abundance of root sugars.

The compounds are colour coded.

Key: **Pale Blue: Ribose; Green: Fructose; Gold: UDP-Glucose; Purple: Glucose; Dark Blue: Galactose.**

The results for the putative compound IAA are notable:

- 1 IAA was prominently less in the treated roots (Fig.5.14) compared to shoots.
- 2 In treated shoots, IAA was particularly subdued compared to untreated shoots (Fig 5.13) consistent with IAA degradation in treated plant tissues.

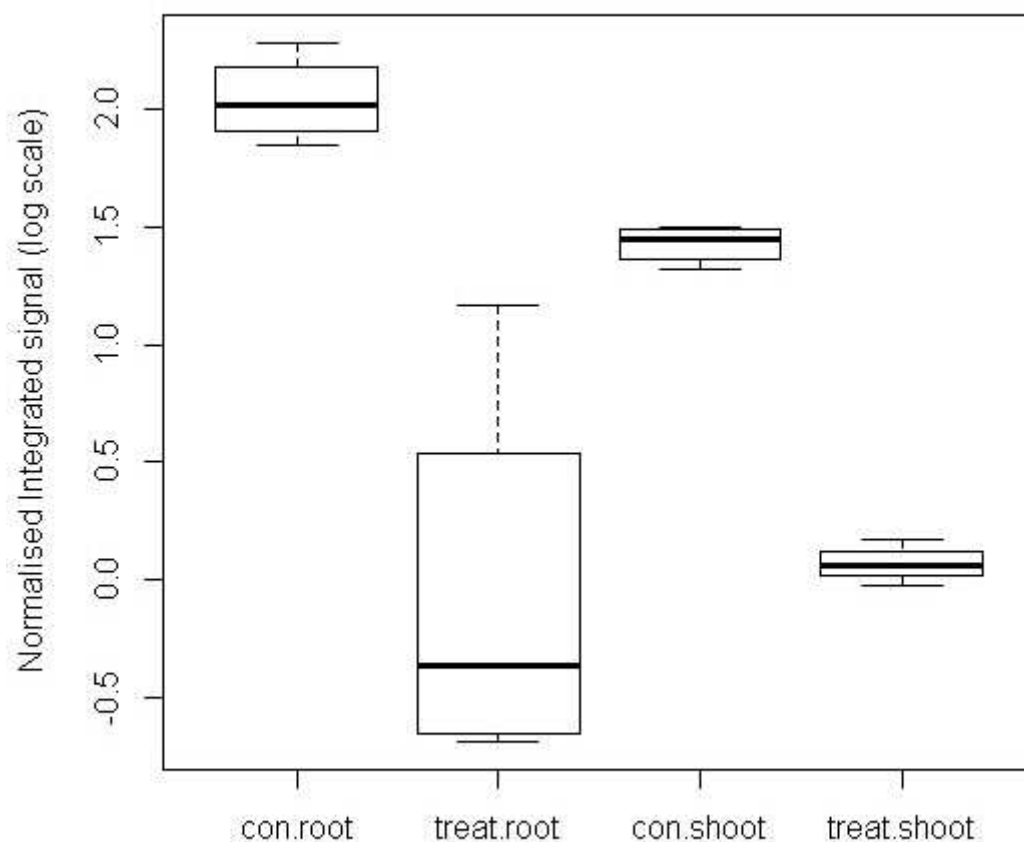


Fig. 5.13: Box and whisker plot showing the differences in the abundance of the putative IAA in the root ($p < 0.05$; $N=4$, t-test) and shoot tissues ($p < 0.001$; t-test; $N=4$) of tall fescue grown in clean sand (abbreviated as con.) and sand contaminated with naphthalene (abbreviated as treat.).

Generally pools of sugars or sugar like compounds were found in greatly pronounced abundances in roots than in leaves in treated plants when compared to the controls (Table 5.4). The ratio of both sucrose and trehalose abundance between roots and shoots for example, was many times higher in treated plants ($p < 0.01$) compared to untreated. In the case of sucrose, for untreated control plants the ratio was 3.82 (± 1.68), but 65.27 (± 5.90) in treated plants. For trehalose it was 4.02 (± 1.47) ($p < 0.01$) in control plants but 1284.07 (± 173.75) in treated. No statistically significant differences were observed between control and treated plants with regard to phosphoenolpyruvic acid. However, the root: shoot ratio of phosphoenolpyruvic acid was >3 times higher than that of control plants ($p < 0.01$): in control plants it was 7.03 (± 1.40), but 23.70 (± 3.51) in treated plants (Fig. 5.14). The same trend was observed for isocitric acid and malic acid (Table 5.3).

The sugar alcohol, erythritol showed a different trend: a lower abundance of erythritol ($p < 0.001$) was observed in the shoots of tall fescue grown in treated sand (Table 5.3) compared to control, but erythritol was not detected in either treated or control roots.

The fructans also behaved differently: they were not detected in control shoots, but were found in the treated shoots giving a signal adjacent to the signal for trehalose (Fig.5.15). Fructans were not detected in the roots of plants from either treatment.

Table 5.4: Descriptive statistics for the ratios between root and foliar (shoot) pools of sugars extracted from tall fescue grown in clean sand and sand contaminated with naphthalene for 6 months. All t-tests are for differences between control and treated plants.

Compound name	Control Mean(\pm SE)	Naphthalene-contaminated Mean(\pm SE)	p value as determined by two- tail t-test assuming unequal variances
Ribose	0.91(\pm 0.39)	9.72(\pm 1.09)	<0.01
Fructose	5.78(\pm 1.65)	22.80(\pm 2.08)	<0.001
UDP-Glucose	21.67(\pm 4.38)	51.08(\pm 4.13)	<0.01
Glucose	5.24(\pm 1.27)	56.79(\pm 4.28)	<0.001
Galactose	1.79(\pm 0.54)	32.35(\pm 4.21)	<0.01
Sucrose	3.82(\pm 1.68)	65.27(\pm 5.90)	<0.01
Trehalose	4.02(\pm 1.47)	1284.07(\pm 173.75)	<0.01

N (No. of samples) =4 (GC runs 1-2); p = probability; SE = standard error of the mean

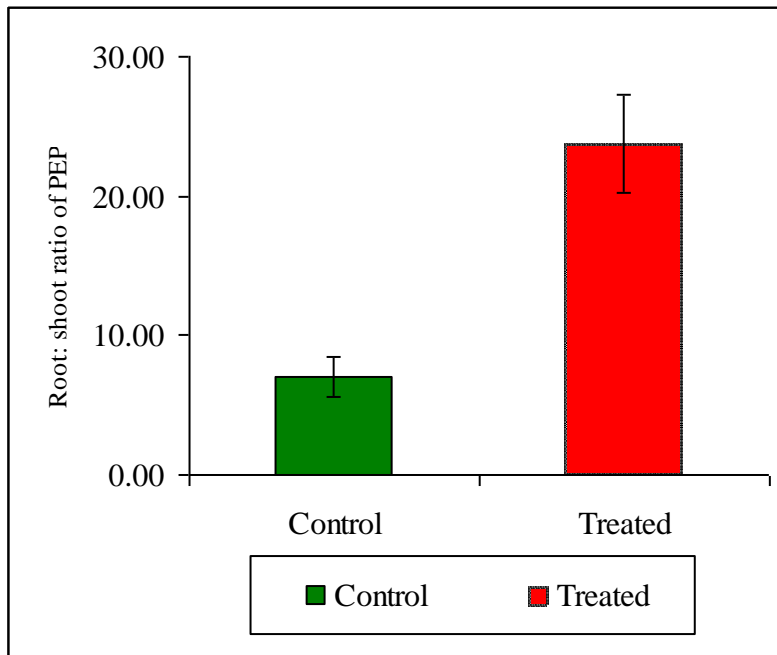


Fig. 5.14: Bar graph showing the difference in the ratio between root and foliar (shoot) pools of phosphoenol pyruvic acid/ phosphoenolpyruvate (PEP) between treatments ($p < 0.01$; t-test; $N = 4$). Error bars show standard error of the mean.

control leaves rep 1

20110611-cl-a-001

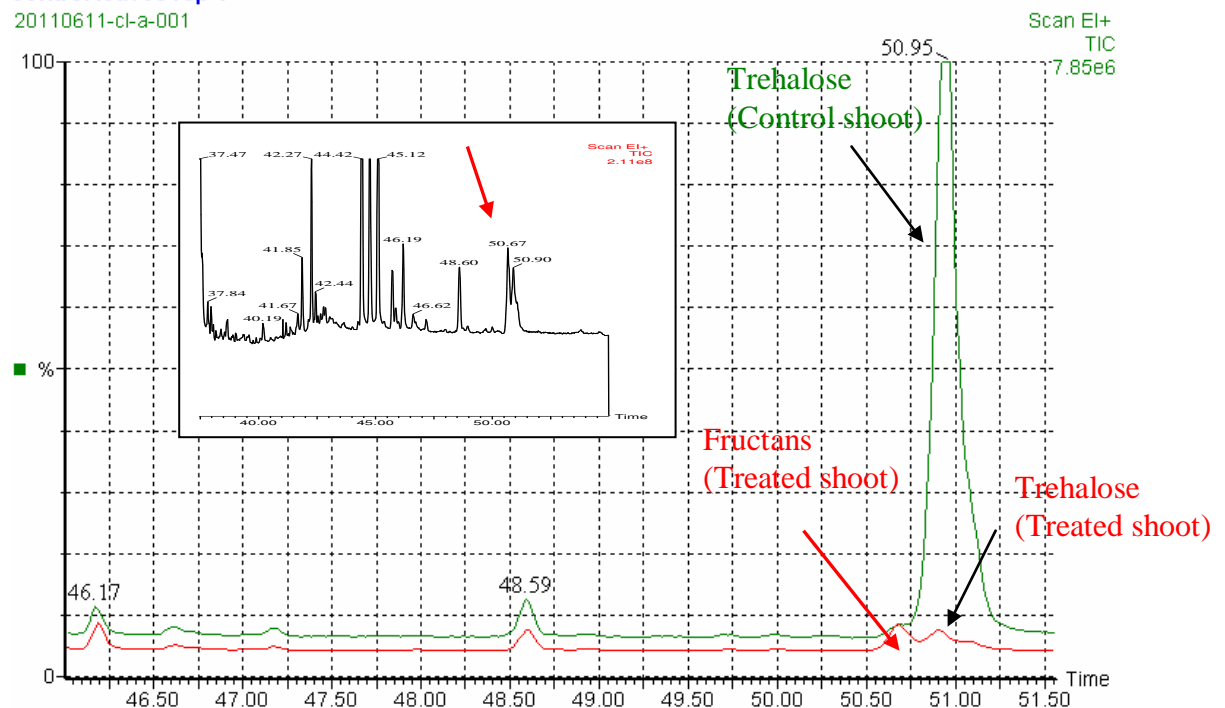


Fig. 5.15: Overlaid EI positive total ion chromatograms for polar compounds extracted from shoot tissues of tall fescue grown in clean sand (green) and sand contaminated with naphthalene (red), showing the retention time region between 46.00-51.50 minutes. Inset: Magnified ($\times 124$) part of the chromatogram for compounds extracted from treated shoots showing the presence of signal for fructans (retention time 50.67 minutes) (indicated by red arrow).

5.4 Discussion

Naphthalene is a hydrophobic volatile compound, which would normally be expected to be degraded by bacteria to CO₂ and H₂O within the rhizosphere of plants (see for example, Liste and Alexander (2000)). However, Wild et al. (2005) using two photon excitation microscopy showed that the three ring structures, phenanthrene and anthracene, could be transported via the apoplastic streams within roots of maize or wheat and degraded in mature cortical cells. It is therefore likely that naphthalene, two ring structure, was transported into the roots of naphthalene-treated plants.

Once within the plant, naphthalene is usually detoxified and stored. Harms (1992) for example, found that by far the greater quantity of labelled 4-chloroaniline was deposited as non-extractable residue in the roots of wheat hydroponic cultures.

One well-documented pathway of detoxification and storage has been suggested to involve initial oxidation to naphthol using cytochrome P-450 and NADPH followed by glycosylation with UDP-dependent glycosyltransferases, then transportation and storage into plant cell vacuoles. It has alternatively been postulated that naphthol might be oxidised further by the peroxidase catalysed hydro peroxidation externally to the plant cell, and deposited within the lignin architecture of plant cell walls (Harvey et al., 2001). In this work however, no evidence was found for naphthol, although the presence of conjugated naphthalene derivatives cannot be ruled out. Further work using a stable isotope labelled naphthalene is required in order to obtain direct evidence for the incorporation of naphthalene into the plant or plant-initiated microbial metabolism.

On the other hand, analysis of the mass spectral features of RT 10.73 compound in plant samples suggested the presence of indole acetic acid (IAA) in plant roots and shoots with much lesser amounts in naphthalene- treated compared to untreated plants. Its identity needs to be proven unambiguously by for example methylation of acidic protons or use of HPLC techniques, nevertheless, if present, the differences in amount between treated and untreated plants is of great interest because IAA is a plant hormone which induces cell elongation and cell division in the cells where it is present and its effects are typically regulated by changes in its cellular concentration, either via non-decarboxylative or decarboxylative oxidation. Decarboxylative IAA oxidation is proposed to be triggered by the activity of basic isoperoxidases (Gaspar et

al., 1991 and references therein) generating a peroxide, which drives a further chain of coupled oxidation reactions involving phenols (Grambow, 1986). The consequence of coupled IAA oxidation with phenols is thought to result in cell wall thickening by for example, formation of isodityrosyl or diferulate cross-links links between protein or pectins respectively (Fry, 1986), as well as lignification and suberisation - and IAA degradation. The plasmalemma-cell wall free space of the apoplast is speculated to be the preferential site for the interaction between the basic isoperoxidases and IAA, but membrane-associated peroxidases might also be operating (Gaspar et al., 1991 and references therein). Either way, the fact that naphthalene-treated root tissues contained thickened cell wall structures that appeared heavily lignified (well-formed exodermal casparian bands, enhanced lignified thickenings of the endodermis lacking passage cells (chapter 4)) is consistent with peroxidase activity in these tissues coupled to IAA degradation. These changes in root ultrastructure in treated plants could relate to restricting the entry of the xenobiotic naphthalene into the inner core of the roots as well as oxidising naphthol as extracellular cell wall bound conjugates. This would also be consistent with a detoxificant role that has been ascribed to IAA oxidation (Machackova et al., 1988); hence the degradation of the putative IAA in treated roots may suggest a strategy of the plant to detoxify the xenobiotic naphthalene/ naphthalene metabolites which might be present in its system. In turn, by regulating the concentration of free IAA, a strategy of plants to execute a control over an otherwise uninhibited root growth in an unfavourable situation is suggested.

Peroxidase-catalysed oxidation of IAA localized between cell wall and plasma membrane are associated with redox activities involving NADH or NADPH and the formation of H₂O₂, also indicating a stress response. As noted above, the peroxidase-catalysed oxidative coupling of phenols has the potential to cross-link the polysaccharide and glycoprotein molecules to which they are bound, promoting a 'tight' structure which is devoid of hydrolytic enzymes. Whilst this could be of general significance in building up and strengthening the structure of the growing cell, it could also be an important variable, changing the physical properties of the cell walls in response to environmental stimuli (Gaspar et al., 1991 and references therein).

These stress-induced redox reactions in cells could either directly or indirectly cause a drain on reducing equivalents such as NADPH and NADH, reducing the cellular capacity to reduce dioxygen to water, causing the concentration of intracellular O₂ and consequently reactive oxygen species (ROS) such as the hydroxyl radical $\cdot\text{OH}$, the superoxide radical O₂^{•-} and hydrogen peroxide H₂O₂ to rise and an unstable hyperoxidant state to develop. In an attempt to reduce the concentration of ROS and to compensate the hyperoxidant state, lignifications and depositions in the cell wall can be induced in cells (Harvey et al., 2001). The higher concentrations of ROS: reducing equivalents in fungal cells had been shown to cause gross disorganisation of cellular ultrastructure (Zacchi et al., 2000). The enhanced thickening in the root endodermis, perhaps due to increased lignification and the quantity of 'bound' residues, and disorganisation in root cortex zone of tall fescue grown in naphthalene-treated sand in our study (chapter 4) could also be due to the increased concentrations of ROS under stress conditions.

Oxidative stress which is a deleterious process caused by the overproduction of ROS could lead to cell damage leading to various disease states, senescence and ageing in both plants and animals (Sohal and Weindruch, 1996). In order to survive the oxidative stress, the organisms need to evolve antioxidant defence processes (Halliwell, 2006). Glucose and the activity of organellar hexokinase take central positions in the antioxidant network of plant cells, as they emerge as important regulators of cytosolic ROS. Glucose has been reported to boost the glycosylation of phenolic compounds, the synthesis of ascorbic acid and contribute to hormone homeostasis (Bolouri-Moghaddam et al., 2010 and references therein). Glucose was calculated to be 4.6 times more in abundance in treated roots when compared to the controls (Table 5.3; p.181). The synergistic interaction of glucose and phenolic compounds may create an integrated redox system, reducing ROS and increasing stress tolerance, mainly due to signalling effects and triggering the production of specific ROS scavengers (Bolouri-Moghaddam et al., 2010 and references therein). Recently, it was proposed that when present at higher concentration, soluble sugars such as glucose, might act as ROS scavengers themselves (Van and Valluru, 2009). The increased root: shoot concentrations of glucose in contaminated plants in our study, demonstrates that tall fescue resists the oxidative stress due to the

overproduction of ROS caused by PAH contamination, by allocating more glucose to its root tissues ($p < 0.01$) and controlling the damages via glucose signalling and ROS scavenging.

Whilst glucose signalling has been specifically associated with active cell division, respiration, cell wall biosynthesis and sugar-mediated feedback regulation of photosynthesis, sucrose signalling appears to be associated with anthocyanin production and with the regulation of storage- and differentiation-related processes (Ritsema et al., 2009; Solfanelli et al., 2006; Weber et al., 2005). In higher plants, it is also the major transport compound bringing carbon skeletons from photosynthetically active leaves to sink tissues such as roots. The root: shoot concentration of sucrose was 17 times higher in treated plants than untreated ($p < 0.01$) (Table 5.4; p.185) and this could explain the higher root mass observed in treated plants previously (chapter 4). Furthermore, together with glucose, sucrose has been recognised as an integrating regulatory molecule controlling gene expression related to plant metabolism, stress resistance, growth and development (Ramon et al., 2008; Rolland et al., 2006; Pego et al., 2000); hence the increased levels of sucrose in treated roots could contribute to the stress tolerance effectively.

Moreover, trehalose which has protective functions against drought stress (Higashiyama, 2002) was expressed in treated roots 8 times as much as in control roots ($p < 0.001$) (Table 5.3; p.181). Trehalose is a natural α -linked disaccharide formed by an α , α -1, 1-glucoside bond between two α -glucose units and has high water retention properties. This sugar is postulated to form a gel phase as cells dehydrate, preventing any damage to the internal organelles, whilst allowing normal cellular activities to be resumed upon rehydration without any major lethal damage to the organs. The resurrection plant *Selaginella*, which grows in desert and mountainous areas, is able to revive upon rehydration, after undergoing severe dehydrations, due to the function of trehalose. This non-reducing disaccharide possesses the advantage of being an antioxidant too (Higashiyama, 2002). Hence, the strikingly higher abundance of trehalose found in treated tall fescue roots compared to the control roots, could explain the adaptability of tall fescue plants to growth in sand treated with hydrophobic PAHs which create a drought environment for them. The higher levels of trehalose in treated root tissues could also demonstrate the ability of

the treated plants to withstand water stress to a greater degree than the control plants at later stages (chapter 4).

Furthermore, other sugars or sugar like compounds were also found in greater abundance in treated roots, suggesting sugar accumulation as well as a strategy of the plants to produce higher levels of defence-promoting compounds.

Galactose forms part of glycolipids and glycoproteins and its polymer galactan is a component of hemicellulose (Nassau et al., 1996). Hence, the higher abundance of galactose in treated roots may suggest a stronger system of cell walls and cell membranes. Rapid conversion from galactose to glucose is favoured in many species via the production of UDP-glucose, which is a sugar nucleotide (Peter et al., 1995). UDP-glucose can also be produced together with fructose from the degradation of sucrose by the enzyme sucrose synthase, which is located in the cytosol of most plant tissues (Taiz and Zeiger, 1998). UDP-glucose participates in glycosyltransferase reactions. It is involved in the production of lipopolysaccharides and glycosphingolipids, a class of cell membrane lipids. Glycosphingolipids and glycoproteins found on the surface of oligosaccharide could provide cells with distinguishing surface markers that can serve in cellular recognition and cell-to-cell communication, including lipid signalling (Rademacher et al., 1988). Therefore, the higher levels of UDP-glucose in treated roots may have important applications with regard to restricting xenobiotic uptake and the survival of the organ under stress conditions.

Additionally, ribose has been found in higher levels in treated roots. Ribose comprises the backbone of RNA, the essential biopolymer responsible for genetic transcription (Merck, 1989). So, the increased levels of ribose in treated roots may suggest a rise in genetic transcription leading to an increase in the concentrations or types of, perhaps, stress-related proteins synthesised. Ribose, once phosphorylated, could become a subunit of ATP, NADH and other important components critical for cellular metabolism (Merck, 1989). So, the higher abundance of ribose in treated roots suggests increased levels of root metabolism. The increased concentration of ribose in treated roots may also suggest a plant strategy to replace used-up reducing equivalents such as NADH coupled with a reduction in ROS levels.

In respiratory metabolism, reduced C sources, glucose and fructose in particular, are oxidized by a multi-step process. The reactions can be subdivided into glycolysis, the tricarboxylic acid cycle (TCA) and the electron transport chain. Fructose which is the other sugar substrate besides glucose in the initial series of glycolytic reactions, and glucose were found in higher abundance in treated roots. So this could suggest an increase in C fluxes to enter the glycolytic pathway in treated roots. In the last series of glycolytic reactions, phosphoenolpyruvate (PEP), which is an excellent phosphate donor for ATP formation, is formed. The differences in phosphoenolpyruvic acid, which could directly relate to PEP, in plant tissues, were not significant between treatments, suggesting the glycolytic pathway is not affected in treated plants either in shoots or roots. The ratio of the expression of this glycolytic intermediate, PEP, between roots and shoots, however, was higher in treated plants ($p < 0.01$). As PEP is irreversibly catalyzed by the enzyme pyruvate kinase to yield ATP and pyruvate, this result suggests more metabolic activities in the root organs than in the shoots of the treated plants.

Once inside the mitochondrial matrix, pyruvate is oxidatively decarboxylated and conjugated to CoA and enters the TCA cycle. Isocitrate and malate are intermediate compounds in the TCA cycle. Isocitric acid and malic acid were identified among the polar compounds extracted from plant tissues in our study. The root: shoot ratio of isocitric acid ($p < 0.01$) and malic acid ($p < 0.001$) were higher in treated tall fescue, emphasising the possibility of higher metabolic activities in treated roots.

Malic acid was found in higher abundance in treated roots than the control roots. This together with the general increase in the abundance of sugar pools in treated roots may suggest a possible increase in root exudations. Nearly 5% to 21% of all photosynthetically fixed C is transferred to the rhizosphere through root exudates, representing a significant C cost to the plant (Walker et al., 2003). Root exudates act as chemical messengers to communicate and initiate biological and physical interactions between roots and soil organisms, and participate in regulating the soil microbial community in the rhizosphere (Siciliano et al., 2003; Walker et al., 2003). The increase in reduced C resources in treated roots in comparison to the controls may suggest a change in root exudation patterns of the treated plants.

The higher amount of sugar molecular pools in treated roots also indicates an

accumulation of reduced C sources in the roots of plants grown in naphthalene-treated sand. The highly lignified cells and distorted cortex zone of treated tall fescue roots evidenced by our SEM study (chapter 4) indicate a reduced capacity of the treated root cells to store sugars as starch or other storage compounds. Hence these sugar or sugar-like compounds in combination with phenolic compounds may be predominantly used in creating an integrated redox system in treated root tissues via recycling and production of sugar and phenolic compound radicals.

On the other hand, the polar compounds extracted from the shoots of treated tall fescue were found in lower abundances than their control counterparts. In treated plant shoots, the abundances of the principal sugars such as glucose ($p < 0.05$) and sucrose ($p < 0.01$) were lower, when compared to their control counterparts. The same was observed with galactose ($p < 0.01$) and trehalose ($p < 0.01$). This is presumably due to the sugar-mediated feedback regulation from the plant roots with a reduced sink-strength under stress conditions. This suggests sugars observed in treated roots in higher abundances could not have been burnt or stored but accumulated within the root cells, cell walls in particular. Apart from the feedback regulation effect, a major shift in translocation of these photosynthetic sugars to the root organs of the treated plants could have caused the concentration of foliar sugars in treated shoots to decrease. The lower levels of chlorophyll illustrated by lack of dark pigmentation in treated plant leaves (chapters 3 and 4) could have been also responsible for the lesser amounts of foliar sugars. The lesser amounts of sugar alcohols and organic acids such as erythritol ($p < 0.001$), isocitric acid ($p < 0.001$) and malic acid ($p < 0.05$) observed in treated shoots could be due to lesser amounts of foliar sugars to synthesise these components.

The abundance of the compound speculated to be IAA was remarkably reduced in treated shoots ($p < 0.001$); hence foliar IAA could have also been degraded in treated plants. Presumably, this could have been conducted through non-decarboxylative oxidation of IAA, which is not considered to be catalysed by peroxidases (Grambow, 1986). Bandurski et al. (1988) associate non-decarboxylative IAA oxidation with the peroxidation of unsaturated fatty acids at the membrane level. Foliar IAA degradation in treated plants could also suggest ROS accumulation in treated shoots, presumably due to the root to shoot communication via stress-mediated sugar

signalling pathways.

Sugar starvation can lead to ROS accumulation (Couee, et al., 2006). So, the increased allocation of sugars to root tissues or reduced photosynthetic activity as a result of feedback regulation, could have caused sugar depletion and accompanied ROS accumulation in treated shoots. Moreover, fructans, which were not detected in the control shoots, were found in the shoots of treated plants. Vacuolar fructans has the function of stabilising cell membranes under stress conditions (Bolouri-Moghaddam et al., 2010). So, the plants could have been able to prevent the damage caused by foliar ROS accumulation, by generating fructans in their shoot tissues to stabilise the leaf cell membrane against oxidative stress.

Roots were in direct contact with the xenobiotic naphthalene, and therefore exposed to PAH phytotoxicity, whereas shoots were not. However, volatilisation from soil followed by gaseous deposition of volatile PAHs such as naphthalene onto the plant leaves via the waxy cuticle and stomata or suspension of soil particles by wind and rain followed by dry and wet deposition of particles on aboveground tissues or desorption from soil followed by root uptake from soil solution leading to transport in the transpiration stream within the xylem could provide a path or paths for the accumulation of organic chemicals in the aerial parts of the plants (Collins et al., 2006). The study of Gao et al. (2004) is suggestive of translocation from root to shoot in transpiration stream as the major pathway of xenobiotics accumulation in shoots. There were subtle indications of the presence of glycosylated/ malonylated derivatives of polar naphthalene metabolites in the roots, but not in the shoot tissues of treated plants, suggesting the xenobiotic chemical had not been translocated to the shoots via transpiration stream. This result in combination with the results of the investigation using Nile red as a molecular probe (chapter 4) suggest the effective apoplastic barrier system in treated roots may have prevented the entry of the PAH metabolites into the inner core of the roots that contains the xylem vessels.

It has been reported that when organisms are exposed to toxins or other stressors under a certain threshold level, a squadron of defence molecules are generated and transported to all the tissues in the organism including the organs not exposed to the threat. These defence molecules not only protect the organ which is under threat, but

enhances its function too, whilst strengthening the defence pathways within the organism to resist tougher challenges (Mattson and Calabrese, 2008; Baker, 1973). The results of this study indicate the shoot tissues of treated plants are protected from PAH toxicity, whilst echoing some of the oxidative stress responses of their roots. The gene expression controlling metabolism could have been altered in treated tall fescue in order to adapt to the growth conditions modified by PAH contamination effectively. An investigation into the stress-related proteins and alterations of the gene expressions in treated tall fescue could provide further understanding towards the adaptability of tall fescue to growth in naphthalene-contaminated sand.

5.5 Conclusions

There were subtle indications of the presence of further oxidised/ glycosylated/ malonylated polar naphthalene metabolites in the root tissues of tall fescue grown in naphthalene-treated sand. A compound speculated to be IAA was either degraded or down regulated in treated plants. Tall fescue grown in naphthalene-treated sand possessed an increased root: shoot ratio of the concentration of sugars, including the principal sugars glucose and sucrose as well as trehalose, which possesses water retention properties. This demonstrated that tall fescue plants were able to resist the oxidative stress due to the overproduction of ROS, caused by the xenobiotic stress coupled with drought stress in the toxic as well as hydrophobic root growth environment, by allocating more sugars, more glucose, sucrose and trehalose, in particular, to its roots tissues. The results indicated synergistic interactions between sugars or sugar-like compounds and phenolic compounds may assist to create an integrated redox system and contribute to stress tolerance in tall fescue adapted to growth in naphthalene-treated sand. The intimate connection of diverse sugar responses with molecular level adaptations to environmental stress was evident throughout this study.

References

- Baker, J.M., 1973. Growth stimulation following oil pollution. In: E.B. Cowell, ed. 1973. The ecological effects of oil pollution on Littoral Communities. Essex: Applied Science Publishers, pp. 72-77.
- Bandurski, R.S., Schulze, A., Leznicki, A., et al., 1988. Regulation of the amount of IAA in seedling plants. In: M. Kutacek, R.S. Bandurski, J. Krekule, eds. 1988. Physiology and biochemistry of auxins in plants. Acad Praha, pp. 21-32.

- Bolouri-Moghaddam, M.R., Roy, K.L., Xiang, L., et al., 2010. Sugar signalling and antioxidant network connections in plant cells. Review Article. *FEBS Journal*, 277, pp. 2022-2037.
- Collins, C., Martin, I. and Fryer, M., 2006. Evaluation of models for predicting plant uptake of chemicals from soil. (Science Report- SC050021/SR) Bristol: Environment Agency.
- Couee, I., Sulmon, C., Gouesbet, G., et al., 2006. An involvement of soluble sugars in reactive oxygen species balance and responses to oxidative stress in plants. *Journal of Experimental Botany*, 57, pp. 449-459.
- de Hoffmann, E. and Stroobant, V., 2002. *Mass Spectrometry: Principles and Applications*. 2nd ed. Ontario: John Wiley & Sons, Ltd.
- Downard, K., 2004. *Mass Spectrometry. A Foundation Course*. Cambridge: The Royal Society of Chemistry.
- Du, H., Wang, Z., Yu, W., et al., 2011. Differential metabolic responses of perennial grass *Cynodon transvaalensis* × *Cynodon dactylon* (C₄) and *Poa Pratensis* (C₃) to heat stress. *Physiologia Plantarum*, 141, pp. 251-264.
- Fry, S.C., 1986. Cross-linking of matrix polymers in the growing cell walls of angiosperms. *Annual Review of Plant Physiology*, 37, pp.165-186.
- Gao, Y. and Zhu, L., 2004. Plant uptake, accumulation and translocation of phenanthrene and pyrene in soils. *Chemosphere*, 55, pp. 1169-1178.
- Gaspar, Th., Penel, C., Hagege, D., et al., 1991. Peroxidases in plant growth, differentiation and development processes. In: J. Lobarzewski, H. Greppin, C. Penel, and Th. Gaspar, eds. 1991. *Biochemical, molecular and physiological aspects of plant peroxidases*. University of Geneva, Switzerland, pp. 249-280.
- Grambow, H.J., 1986. Pathway and mechanism of the peroxidase catalyzed degradation of indole-3-acetic acid. In: H. Greppin, C. Penel, Th. Gaspar, eds. 1986. *Molecular and physiological aspects of plant peroxidases*. University of Geneva, Switzerland, pp. 31-41.
- Gromova, M. and Roby, C., 2010. Toward *Arabidopsis thaliana* hydrophilic metabolome: assessment of extraction methods and quantitative ¹H NMR. *Technical Focus. Physiologia Plantarum*, 140, pp. 111-127.
- Halliwell, B., 2006. Reactive species and antioxidants. Redox biology is a fundamental theme of aerobic life. *Plant Physiology*, 141, pp. 312-322.
- Harms, H.H., 1992. In-vitro systems for studying phytotoxicity and metabolic fate of pesticides and xenobiotics in plants. *Pesticide Science*, 35 (3), pp. 277-281.
- Harvey, P.J., Campanella, B.F., Castro, P.M.L., et al., 2001. Phytoremediation of Polyaromatic hydrocarbons, Anilines and Phenols. Review Articles:

- Phytoremediation. *ESPR-Environmental Science and Pollution Research*, pp. 1-19.
- Higashiyama, T., 2002. Novel functions and applications of trehalose. *Pure and Applied Chemistry*, 74 (7), pp. 1263–1269.
- Liste, H.H. and Alexander, M., 2000. Plant promoted pyrene degradation in soil. *Chemosphere*, 40, pp. 7-10.
- Machackova, I., Ullmann, J., Krekule, J. and Opatrny, Z., 1988. Comparison of in vivo IAA decarboxylation rate with in vitro peroxidase, IAA oxidase activities. In: R. Kutacek, R.S. Bandurski, J. Krekule, eds. 1988. *Physiology and biochemistry of auxins in plants*. Acad Praha, pp. 87-91.
- Mattson, M. and Calabrese, E., 2008. When a little poison is good for you, *NewScientist*, [online] Available at: <<http://www.NewScientist.com>> [Accessed 06 August 2008].
- Merck, 1989. *The Merck Index: An Encyclopedia of Chemicals, Drugs, and Biologicals*. New Jersey: Merck & CO., Inc.
- Meulenberg, R., Rijnaarts, H.H.H.M., Doddema, H.J., et al., 1997. Partially oxidised polycyclic aromatic hydrocarbons show an increased bioavailability and biodegradability. *FEMS Microbiology Letters*, 152, pp. 45-49.
- Nassau, P.M., Martin, S.L., Brown, R.E., et al., 1996. Galactofuranose Biosynthesis in *Escherichia coli* K-12: Identification and Cloning of UDP-Galactopyranose Mutase. *Journal of Bacteriology*, 178 (4), pp. 1047-1052.
- Pego, J.V., Kortstee, A.J., Huijser, C., et al., 2000. Photosynthesis, sugars and the regulation of gene expression. *Journal of Experimental Botany*, 51, pp. 407-416.
- Peter, H. R. and George, B.J., 1995. Carol J. Mills, ed. 1995. *Understanding Biology*. 3rd edition. W.M.C. Brown. p. 203.
- Preis, M., 2010. Analysis of the peroxidase-catalysed oxidation of hydroxamic acids. Ph.D. University of Greenwich.
- Rademacher, T.W., Parekh, R.B. and Dwek, R.A., 1988. Glycobiology. *Annual Review of Biochemistry*, 57, pp. 785-838.
- Ramon, M., Rolland, F. and Sheen, J., 2008. Sugar sensing and signalling. *The Arabidopsis Book*. American Society of Plant Biologists. doi: 10.1199/tab.0117.
- Ritsema, T., Brodmann, D., Diks, S.H., et al., 2009. Are small GTPases signal hubs in sugar –mediated induction of fructan biosynthesis? *PLoS ONE*, 4(8), e6605, doi:10.1371/journal.pone.0006605.
- Rolland, F., Winderickx, J. and Thevelein, J.M., 2001. Glucose sensing mechanisms in eukaryotic cells. *Trends in Biochemical Sciences*, 26, pp. 310-317.
- Siciliano, S.D., Germida, J.J., Banks, K., et al., 2003. Changes in microbial

composition and function during a Polyaromatic Hydrocarbon Phytoremediation Field Trial. *Applied and Environmental Microbiology*, 69, pp. 483-489.

Sohal, R.S. and Weindruch, R., 1996. Oxidative stress, caloric restriction, and aging. *Science*, 273, pp.59-63.

Solfanelli, C., Poggi, A., Loreti, E., et al., 2006. Sucrose-specific induction of the anthocyanin biosynthetic pathway in *Arabidopsis*. *Plant Physiology*, 140, pp. 637-646.

Sutherland, J.B., 1992. Detoxification of polycyclic aromatic hydrocarbons by fungi. *Journal of Industrial Microbiology*, 9, pp.53-62.

Taguchi, G., Ubukata, T., Nozue, H. et al., 2010. Malonylation is a key reaction in the metabolism of xenobiotic phenolic glucosides in *Arabidopsis* and tobacco. *Plant Journal*, 63 (6), pp. 1031-1041.

Taiz, L. and Zeiger, E., 1998. *Plant Physiology*. 2nd ed. Massachusetts: Sinauer Associates.

Taylor, V.F., March, R.E., Longerich, H.P., et al., 2005. A mass spectrometric study of glucose, sucrose, and fructose using an inductively coupled plasma and electrospray ionisation. *International Journal of Mass Spectrometry*, 243, pp. 71-84.

Van den Ende, W. and Valluru, R., 2009. Sucrose, sucrosyl oligosaccharides, and oxidative stress: scavenging and salvaging? *Journal of Experimental Botany*, 60, pp. 9-18.

Walker, T.S., Bais, H.P., Halligan, K. M., et al., 2003. Metabolic profiling of root exudates of *Arabidopsis thaliana*. *Journal of Agricultural and Food Chemistry*, 51(9), pp. 2548-2554.

Weber, A.P., Schwacke, R. and Flugge, U.I., 2005. Solute transporters of the plastid envelope membrane. *Annual Review of Plant Biology*, 56, pp. 133-164.

Wild, E., Dent, J., Thomas, G.O., et al., 2005. Direct observation of organic contaminant uptake, storage and metabolism within plant roots. *Environmental Science and Technology*, 39(10), pp. 3695-3702.

Wilson, S. and Jones, K., 1993. Bioremediation of soil contaminated with polynuclear aromatic hydrocarbons (PAHs): a review. *Environmental Pollution*, 81, pp. 229-249.

Zacchi, L., Morris, I. and Harvey, P.J., 2000. Disordered ultrastructure in lignin-peroxidase-secreting hyphae of the white-rot fungus *Phanerochaete chrysosporium*. *Micobiology*, 146, pp. 759-765.

CHAPTER 6

Discussion

Phytoremediation is a green technique used to restore polluted sites through plant-initiated biochemical processes. Its effectiveness, however, depends on the successful establishment of plants in the polluted sites. Plant responses to growth in soils contaminated with petroleum hydrocarbons need to be taken into account, if plants are to be used to clean up petroleum hydrocarbon contamination. The research described in this thesis was aimed at investigating the changes in seed germination, root growth patterns, root structure, uptake of hydrophobic xenobiotics across the root tissues and hydrophilic metabolome arising from growth in sand contaminated with petroleum hydrocarbons, and with the low molecular weight, bio available polycyclic aromatic hydrocarbon (PAH), naphthalene, in particular.

To date, sand has rarely been used in phytoremediation studies and most studies have used nutrient medium or soil/ sediments contaminated with PAHs/ diesel oil/ crude oil to investigate the xenobiotic uptake or stress responses of plants. We have used sand as plant growth medium, as sand provides plant roots a strong real-life physical substrate to attach to and grow into, whilst also facilitating root uptake of the organic contaminants as it does not contain soil organic matter (SOM) that the PAHs preferentially bind to. The sand was autoclaved before use, but plant growth in either clean or treated sand for a period of time could allow the flux of micro organisms into the growth medium.

Most of the higher plants' life begins as a seed. A seed contains an embryo, a seed coat and usually food reserves to see it through germination. Seeds germinate under optimum environmental conditions. They require sufficient supply of water and oxygen as well as favourable temperature in order to germinate. When sown directly in sand treated with petroleum crude oil (HC) ($10.8 \text{ g TEH kg}^{-1} \text{ sand dw}$), plant seeds (tall fescue, brown top bent, carrot, beetroot, brown top bent and parsnip) either failed to germinate or germination was remarkably poor. The presence of hydrophobic petroleum hydrocarbons may act as a water-impermeable barrier in soil and interfere with the movement of water in soil pores, and this consequently will affect the supply of water and oxygen in contaminated soil matrix, thereby affecting seed germination

negatively. When a layer of clean sand was used as a seed bed to facilitate germination, tall fescue (*Festuca arundinacea*) and carrot (*Daucus carota*) germinated successfully, whereas beetroot (*Beta vulgaris*) ($p < 0.05$) and brown top bent (*Agrostis capillaries* L.) ($p < 0.001$) showed reduced germination, whilst parsnip (*Parsnica sativa*) totally failed to germinate. This shows that together with scarcity in water and oxygen supplies, HC-contamination also exposes plants to other unfavourable factors, perhaps higher temperature due to the darker solar radiation absorbing properties of the crude oil as well as toxicity (Merkl et al., 2005) and that variations in sensitivity to the exposure to HC-contamination exist among seeds of different plant species.

Crude oil (HC) is composed of a complex mixture of hydrocarbons including polycyclic aromatic hydrocarbons (PAHs). Since PAHs are considered as particularly toxic, an initial investigation was carried out on the effects of anthracene, fluoranthene, naphthalene (LMW PAHs) and benzo (a) pyrene [B(a)P] (a HMW PAH) on seed germination, using tall fescue as the model plant. A layer of clean sand was used as a seed bed to facilitate germination; still, seed germination was inhibited due to the exposure to the LMW PAHs anthracene, fluoranthene and naphthalene. On the other hand, exposure to B(a)P did not affect seed germination. These preliminary results are in accordance with the study carried out by Adam and Duncan (1999) that showed reduction in germination score of several plant species exposed to diesel oil contamination, particularly at a higher concentration (50 g kg^{-1} soil). Adam and Duncan (1999) suggested that diesel oil contains more potentially toxic, volatile, LMW PAHs, thereby affecting the seed germination of plants negatively. Contrastingly, Smith et al. (2006) demonstrated that the soils heavily contaminated with aged PAHs did not affect seed germination of a mixture of grasses and legumes. The aged soils contain a larger proportion of high molecular weight molecules that are less bio available as well as less volatile (Adam and Duncan, 1999), and this may be the reason for the successful germination of plants in contaminated soils in the study of Smith et al. (2006) as well as in our study using B(a)P.

When sown directly in naphthalene-treated sand (0.8 g kg^{-1} sand dw), initially, there was a reduction in germination score ($p < 0.01$) of tall fescue seeds, but more seeds germinated with time. After one month since sowing, no significant differences were

observed in plant population density between control and naphthalene-contaminated treatments, perhaps due to dilution of the concentration of naphthalene which may have occurred through volatilisation.

Among the plant species tested (carrot, beetroot, tall fescue, brown top bent and parsnip), only tall fescue established well in HC-treated sand. Compared to the seeds of brown top bent, carrot, beetroot and parsnip, tall fescue seeds were larger and would presumably have had sufficient food reserves to produce stronger seedlings to withstand the unfavourable conditions present in HC-treated sand. The larger seeds with sufficient food reserves could have been a reason for the increase in germination with time, when tall fescue seeds were sown directly in naphthalene-treated sand.

The subsequent growth of carrot and beetroot in HC-treated sand showed extremely stunted growth. The roots of carrot and beetroot are storage organs and once they have elongated to a point where they can gain sufficient moisture, the roots expand laterally. However, the roots were not able to grow deep into the soil and could not access sufficient water, due to the presence of crude oil in the contaminated matrix affecting water and oxygen supplies. When grown in HC-treated sand, the roots of carrot and beetroot that possess tap root architecture followed the normal root orientation responses to gravity. The root growth of carrot and beetroot was stunted as the roots grew into the contaminated matrix from the clean sand matrix, and the plants started to die. Rentz et al. (2003) demonstrated that poplar tree roots were unable to penetrate the petroleum smear zones at the Heath, Ohio, demonstration site, presumably due to layer compaction, but shortage of oxygen could have been also a reason why the plant roots stopped short of the smear zone (Rentz et al., 2003). Bengough (2003) reported that mechanical impedance slows root elongation. Stress factors present in HC-treated sand such as water deficiency, shortage of oxygen, toxicity and mechanical impedance (Merkl et al., 2005) could have been accountable for the failure of carrot and beetroot to establish well in HC-treated sand.

Contrastingly, the subsequent growth of a mixture of grasses composed of tall fescue, brown top bent and perennial ryegrass (*Lolium perenne* L.) in HC-treated sand showed deviations from normal root orientation responses to gravity. During the initial 3 months of growth in HC-treated sand, the grass roots possessing fibrous root

system, exhibited a tendency to turn back into the uncontaminated, clean sand. Auxin-promoted differential growth in roots is responsible for the responses to directional stimuli (i.e. gravity) called gravitropism. According to the Cholodny-Went model, auxin is transported to the lower side of the roots during gravitropism. Statoliths (starch-filled amyloplasts) in the statocytes are involved in the normal perception of gravity, but they are not absolutely required. Phytotropins such as naphthylphthalamic acid interfere with gravitropism (Taiz and Zeiger, 1998). Unfavourable factors such as the limited supplies of oxygen and moisture in growth zones may also promote deviations from normal root orientation responses to gravity (Pages et al., 2000; Weaver, 1926). Hence, the grass roots showed morphological plasticity to avoid the stress conditions in the contaminated zones by growing sideways initially.

Adam and Duncan (1999) studied the pattern of root development of selected plant species using a model soil system contaminated with diesel oil. Their initial observations indicated that plant roots avoided diesel oil contaminated areas completely when they had uncontaminated soil to grow into. When there was no available uncontaminated soil, roots grew through contaminated regions until they found an area of uncontaminated soil (Adam and Duncan, 1999). Similar results with regard to the spatial distribution of roots of ryegrass were found in a study carried out by Kechavarzi et al. (2007). It is important to note that diesel oil generally contaminates the top few metres of the soil (surface soil) and contamination is not uniform throughout the site (Adam and Duncan, 1999).

The establishment of the mixture of grasses possessing fibrous root systems in HC-contaminated sand was much better when compared to that of carrot and beetroot, perhaps due to the plasticity exhibited by grass roots in changing root growth directions, initially. Yet, when grown separately, brown top bent failed to establish well in HC-treated sand, due to the remarkably poor germination as well as growth inhibitions. Plant initiated remediation of organic contaminants within the rhizosphere may be an important requirement for plants to establish well in petroleum hydrocarbon-contaminated soils. The reason why, unlike tall fescue which showed a successful establishment, brown top bent failed to establish well in HC -treated sand, is perhaps due to its small root surface area, being in itself not large enough to

promote the proliferation of hydrocarbon-degrading micro organisms. Merkl et al. (2005 a) documented that no significant remediation occurred in crude oil (5% w/w)-treated soil in which Indian Goose Grass (*Eleusine indica*) was grown, due to the plant's small root surface area. On the other hand, once past the initial acclimatisation period of ~ 3 months, the treated tall fescue possessed a higher root mass (dw) ($p < 0.01$) than their control counterparts, as well as a well spread out, deep root system, illustrating a potential of this species for phytoremediation. The differences in plant establishment observed between tall fescue and brown top bent could also be attributed to many other factors such as differences in root exudate patterns, cell wall components and cellular signalling pathways.

Tall fescue grown in HC-treated sand, produced a well-developed shoot system which was not different from their control counterpart, either in terms of biomass or height, whilst exhibiting initial root growth inhibitions. Growth of tall fescue in naphthalene and fluoranthene-treated sand produced growth inhibitions, but interestingly in anthracene and B(a)P-contaminated sand, tall fescue exhibited an enhanced root shoot development, when compared to the control plants. Anthracene and B(a)P are practically insoluble in water, therefore less toxic to plants. Still, water scarcity and accompanied oxygen deficiency may exist in anthracene and B(a)P-contaminated soils. Growth in anthracene-treated sand reduced the shoot height of brown top bent, demonstrating differences in responses between plant species to the exposure to anthracene contamination at the concentration of 1 g kg^{-1} sand dw. The reduction in shoot height in anthracene-treated brown top bent may be due to the dust like seed structure of the plant species, not having sufficient food resources to produce a robust seedling, when the growth conditions are not optimal. The reason for the growth stimulation exhibited by tall fescue due to exposure to anthracene and B(a)P contamination is not clear.

Similar root growth patterns as observed when grown in HC-treated sand were observed in tall fescue grown in naphthalene-treated sand. Additionally, differences in shoot growth patterns were observed between plants that were exposed to contamination since seeding and those which were provided with a clean environment for seed germination. The plants grown directly in naphthalene-treated sand exhibited an initial multi-fold reduction in root length ($p < 0.001$), perhaps due to the production

of ethylene due to chemical stress as shown by Huang et al. (2004), but showed no significant differences in shoot height, when compared to the controls. The plants germinated in rockwool cubes and transplanted into contaminated sand at seedling stage showed a temporary inhibition in both root and shoot development.

During the acclimatisation period of 2.5-3.0 months, tall fescue plant roots from HC/naphthalene-treatment showed an accelerated lateral growth ($p < 0.01$), whilst also exhibiting deviations from normal root orientation responses to gravity. During the acclimatisation period, the treated tall fescue possessed 1.83-times less root mass than their control counterpart on fresh weight basis (1.45-times less on dw basis), whilst having similar shoot biomass as the controls. At ~3months of age, the treated tall fescue had 1.72-fold higher root biomass than their control counterpart on fresh weight basis (1.94-times higher on dw basis) ($p < 0.01$), whilst maintaining similar shoot biomass as the control plants. These results imply that tall fescue was able to adapt to the contaminated conditions well, perhaps owing to the complex interactions between contaminants, soil, plant roots and micro organisms in the rhizosphere. Siciliano et al. (2003) have documented an increase in naphthalene-degrading micro organisms and naphthalene mineralisation in soil planted with tall fescue, whilst Liste and Alexander (2000 b) reported degradation of phenanthrene and pyrene in the soil planted with tall fescue. These results demonstrate that tall fescue promote phytostimulation within the rhizosphere and can be used to remediate PAH-contaminated soils, depending on the type and amount of the contaminants, soil organic matter and environmental parameters (e.g. temperature and rainfall). The successful establishment of a vegetative cover of tall fescue in contaminated sites is of importance also in the interest of reducing pollutant leaching to groundwater and preventing the dispersal of polluted dusts through wind and water erosion (Vangronsveld et al., 1995 a, b, 1996). Plant-based in situ stabilization, termed 'phytostabilization', stabilises potentially toxic contaminants, preventing contaminant migration (Vangronsveld and Cunningham, 1998). Soil amendments could also decrease the plant availability of the pollutants and thus limit eventual toxicity.

With time, grass roots, tall fescue roots in particular, elongated further from the base and grew deep into the HC/naphthalene-contaminated matrix. The results suggest that the roots had retained a commitment to their prestimulus vertical orientation, and

reverted to it, perhaps, following changes in the biomechanical properties of cell walls responsible for wall elasticity in the zone of curvature as suggested by Stankovic et al. (1998), regarding their study on autonomic straightening of gravitropic curvature of cress roots. The fact that tall fescue was able to revert to normal root orientation responses to gravity with time, could also be translated as an alleviation of toxicity. Degradation of HC components/ naphthalene may have taken place within the dynamic region of the rhizosphere, presumably because of 'phytostimulation'. This could also relate to having evolved an effective barrier within the root, to protect the tissues against the diffusion of potentially toxic, xenobiotic solutes from soil solution into the root.

Data about the adverse effects of organic contaminants on plant roots are mostly limited to root biomass, root elongation, root diameter and root surface area. It was of interest, therefore, to study the changes to root structure including root ultrastructural features arising from growth in sand contaminated with petroleum hydrocarbons. For this, scanning electron microscopy (SEM) along with fluorescent microscopy proved invaluable.

The scanning electron micrographs revealed that, whilst roots of tall fescue grown in clean sand were woolly with many long root hairs, roots grown in HC-treated sand possessed significantly less ($p < 0.001$) but also shorter root hairs ($p < 0.001$). The root sections stained with Evans blue and viewed under a light microscope showed that higher percentage of root hairs stained blue in HC-treated roots ($p < 0.001$), indicating that the HC-contamination affects the vitality of root hairs negatively. The effect on root hairs were similar in HC-treated brown top bent ($p < 0.001$). On the other hand, no significant differences were observed in the abundance and length of root hairs between control and anthracene-treated tall fescue and brown top bent, suggesting toxicity may be the key factor that inhibits root hair development. Similar to the results observed by Alkio et al. (2005) on the effect of phenanthrene on root hairs, the exposure to naphthalene had a negative influence on root hair development in tall fescue, significantly reducing their number and length ($p < 0.001$), strengthening the concept that relatively water-soluble, more bio available petroleum hydrocarbons influence root hair development negatively. Whilst restricting the uptake of toxic compounds across the root in transpiration stream, the inhibition of the development

of root hairs which are essential for soil ions absorption (Neergaard et al., 2000; Taiz and Zeiger, 1998) may affect the nutrient uptake of plant roots growing in contaminated soil, at least partially. The lack of dark pigmentation observed in HC/naphthalene-treated tall fescue during the acclimatisation period of 2.5-3 months may be due to retarded uptake of nutrients (chapters 3 & 4).

Scanning electron micrographs showed that the HC /naphthalene-treated tall fescue roots possessed an enhanced thickening in the root endodermal cell walls ($p < 0.001$) when compared to their control counterparts. No significant differences in the endodermis thickening was observed between treatments, during the acclimatisation period of < 3 months, i.e., during the time when tall fescue roots showed a deviation from normal root orientation responses to gravity. The plant roots growing in HC-treated sand amended with compost, on the other hand, grew straight into the contaminated matrix, perhaps because the compost absorbed the oil and provided the plant roots a preferential pathway to follow, and possessed a thickened endodermis at an earlier age than the plants grown in HC-treated sand which was not amended with compost, i.e., < 3 months of age. The results indicate thickening in the endodermis is induced in plant roots upon prolonged contact with contaminated matrix. Beetroot roots grown in HC-treated sand also possessed a thickened endodermis. Interestingly, roots of tall fescue grown in anthracene-treated sand did not possess an enhanced thickening in their root endodermis, when compared to the controls, suggesting maturation of endodermis is induced as a response to toxicity. The well-formed, mature endodermis in HC/ naphthalene-treated roots could indicate defence responses of plants to restrict the entry of potentially toxic substances into xylem vessels beyond this apoplastic barrier.

Plant peroxidases are centrally important in the construction of the plant cell wall as a barrier against xenobiotics in the environment. The cellular respiratory metabolite and reducing agent NADH regulates plant peroxidase activity in the cell wall by inhibiting the catalytic cycle of peroxidase and converting the enzyme to an inactive state. This would have the effect of decreasing cell wall lignification catalysed by peroxidases and increasing food quality. However, peroxidases are non-specific towards the nature of their reductant. The study conducted by Preis (2010) in order to elucidate the likely impact of the activity of plant peroxidases on the quality and safety of agricultural

food products, showed that a model plant peroxidase (horseradish peroxidase) was able to catalyse the oxidation of a model xenobiotic compound (naphthol). Furthermore, naphthol was able to deregulate the control exerted by NADH by converting the enzyme from an inactive state to an active state. Reactivation of peroxidase activity would have the effect of increasing cell wall lignifications (Preis et al., 2010, manuscript in preparation). Increased cell wall thickenings modify the cell wall to a hydrophobic and transfer-reduced network, restricting the expansion of the cell as plants do not possess a mechanism to degrade cell walls (Rogers & Campbell, 2004).

No significant differences were observed in the size of stele between control and HC-treated tall fescue, but noticeably smaller cells were observed in the stele of 14 months old HC-treated tall fescue. In phenanthrene-treated 21 days old *Arabidopsis* plants, the transcript levels of expansins (EXP8), genes which have known roles in cell wall loosening and cell enlargement, were found to be reduced in the reverse-transcription (RT) PCR experiments (Alkio et al., 2005). This could lead the way to smaller cells. As environmental stimuli can motivate changes in genes of an organism, and as the older plant roots were exposed to higher environmental influence over a longer period of time, the noticeably smaller cells inside root stele in older, HC-treated tall fescue roots could have been caused due to changes in transduction pathways. Increased thickening in cell walls associated with peroxidase activities may also be responsible for the small size of the treated cells.

A decrease in the xylem volume due to narrower bore of xylem vessels were observed in HC-treated tall fescue roots ($p < 0.001$). Smaller xylem vessels were also observed in HC-treated beetroot roots. Similarly, Barcelo et al. (1988) showed that smaller xylem vessels were produced in bush bean stems exposed to Cd- toxicity. Hence, the smaller xylem vessels may indicate a plant response to toxicity. Additionally, Huang et al. (1991) demonstrated smaller and fewer metaxylem vessels in seminal wheat roots exposed to higher temperature (40°C), suggesting modifications in xylem vessels are motivated due to adverse environmental conditions. The differences in xylem volume were more dramatically pronounced in tall fescue roots grown in HC-treated sand for 14 months. Kubo et al. (2005) reported that the formation of xylem vessels is controlled by transcription factors, suggesting a genetic control over the

production of xylem vessels in plants. As, environmental influences could have impacts on the expression of genes of an organism, the dramatic influence of exposure to HC-contamination for a long period of time (14 months), on the xylem volume of tall fescue roots, indicate changes in genetic composition/ transduction pathways. The reduced diameter of xylem vessels in treated tall fescue roots may also be due to increased cell wall lignifications.

Whilst growth in HC-treated sand promoted untimely death and stunted growth in carrot and beetroot, tall fescue plants, after an acclimation period of ~3months, elongated without restrictions in both shoot ward and root ward directions and lived long, perhaps due to the metabolic diversity of the plants. This highlighted the importance of understanding the metabolic picture of tall fescue grown in soils contaminated with potentially toxic organic xenobiotics (e.g. naphthalene).

The gas chromatography-mass spectrometric studies revealed subtle indications of the presence of conjugated naphthol in the root tissues of tall fescue at negligible levels. The plant cell wall represents the front line of defence against xenobiotics. Plants can isolate xenobiotics from the metabolic powerhouse by incorporation of their xenobiotic metabolites into cell wall material (Meagher, 2000). In the process of cell wall formation peroxidases generate cell xenobiotic metabolite radicals which can bind to cell wall components. Xenobiotic metabolites are polymerised into the cell wall and therefore bound irreversibly (Sterling et al., 2006). Moreover, the metabolic profiles of plant root shoot extracts showed greatly reduced concentrations or absence of a compound speculated to be indole acetic acid (IAA) ($p < 0.001$) in naphthalene-treated tall fescue tissues, suggesting degradation of IAA and associated detoxification (Machackova et al., 1988) of naphthol and other polar naphthalene metabolites within plant roots. IAA degradation may be also associated with strengthening structural defences such as higher lignification and suberisation (Gaspar et al., 1991 and references therein). The naphthalene-treated tall fescue roots possessed well-formed Casparian banding and suberin lamellae depositions in both the endodermis and hypodermis (when well-developed Casparian band structures are present in the hypodermis, it is called exodermis), evidenced by our epi-fluorescent microscopic study. IAA degradation could account for the well-formed endodermis and exodermis observed in naphthalene-treated tall fescue, but peroxidase catalysed

activities could also be responsible for the increased lignification and suberisation in cell walls (Preis et al., 2010, manuscript in preparation; Harvey et al., 2001).

PAHs could enter plant tissues from contaminated growth mediums, and affect plants at tissue and cellular levels. In a study carried out on *Arabidopsis*, cell death was demonstrated in leaves of the plants grown on Murashige and Skoog (MS) medium supplemented with 0.5mM phenanthrene (Fig.6.1 E) (Alkio et al., 2005). Here, the detached leaf was taken and photographed after staining with trypan blue (n>6). Cell death was quantified as ion leakage expressed as a percentage of the total ion content (Fig.6.1 F). To determine total ion content, samples were autoclaved to kill the tissue and the conductivity was measured again (Alkio et al., 2005). Also, the exposure of *Arabidopsis* leaves to phenanthrene was shown to induce localized hydrogen peroxide (H_2O_2) production, expressed as the polymerisation of 3, 3'-diaminobenzidine (DAB) which is visible as a brown precipitate in the presence of H_2O_2 . As H_2O_2 is known to mediate cell death, it further supports the idea that phenanthrene exposure promoted cell death in *Arabidopsis* leaf tissues.

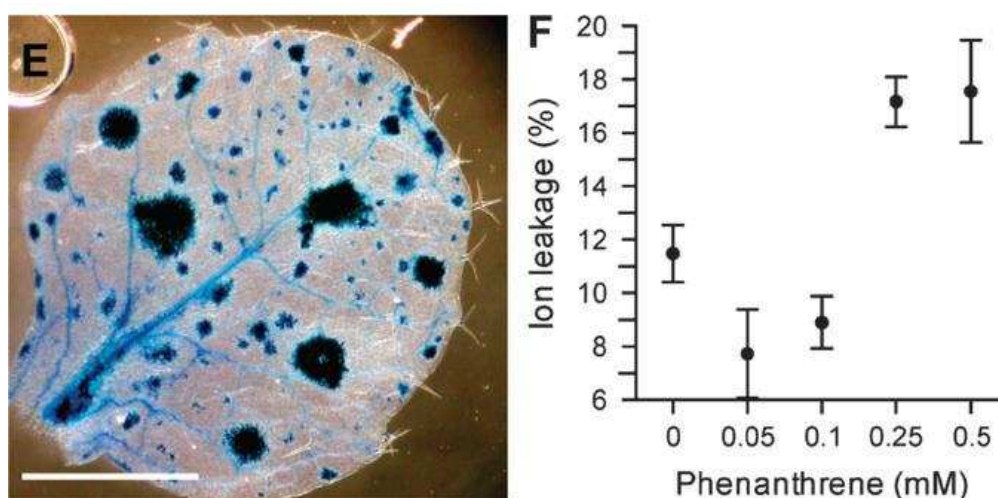


Fig.6.1: (E) Leaf of a plant grown continuously on 0.5 mM phenanthrene for 60 d before staining with trypan blue. Dark blue spots indicate dye accumulation in dead cells. (F) Ion leakage (as the percentage of total ion content) into distilled water during 20 h of incubation at room temperature in 26-d-old plants grown on 0–0.5 mM phenanthrene. Data points show mean and standard deviation; n=4 for 0, 0.05, and 0.1 mM phenanthrene, n=3 for 0.25 and 0.5 mM phenanthrene. Scale bar in E = 1 mm (Presented directly as in Alkio et al., 2005).

The results of the investigation conducted by Alkio et al. (2005) showed oxidative stress in *Arabidopsis thaliana* exposed to the three-ring PAH, phenanthrene. The need for oxygen for the efficient production of the molecular energy currency, ATP, is in balance with the necessity of controlling the level of reactive oxygen species

(ROS), which are produced in the presence of oxygen and particularly under stress. Evolving effective antioxidant defence responses is critical in resisting oxidative stress that inversely correlates with lifespan in a variety of organisms (Bolouri-Moghaddam et al., 2010 and references therein).

Stress-induced redox reactions in cells could either directly or indirectly cause a drain on reducing equivalents such as NADPH and NADH, reducing the cellular capacity to reduce O_2 to water, causing the concentration of intracellular O_2 and consequently reactive oxygen species (ROS) such as hydrogen peroxide H_2O_2 to rise and an unstable hyperoxidant state to develop. In an attempt to reduce the concentration of ROS and to compensate the hyperoxidant state, lignifications and depositions in the cell wall can be induced in cells (Harvey et al., 2001). The enhanced thickening in the root endodermis, perhaps due to increased lignification and the quantity of 'bound' residues in tall fescue grown in naphthalene-treated sand in our study could have been triggered due to the increased concentrations of ROS under stress conditions.

Glucose has been documented as an important regulator of cytosolic ROS, taking a central position in the sugar signalling and antioxidant network scheme in plants (Bolouri-Moghaddam et al., 2010 and references therein). Higher abundance of glucose ($p < 0.01$) was found in the root tissues of tall fescue grown in naphthalene-treated sand. Also, generally higher concentrations of sugars and sugar-like compounds are associated with ROS scavenging (Bolouri-Moghaddam et al., 2010 and references therein). The metabolic profiles of plant roots and shoots showed higher abundance of sugars and sugar-like compounds (ribose, glucose, fructose, galactose, sucrose, trehalose and UDP-glucose) in the root tissues of plants grown in naphthalene-treated sand than their control counterparts, whereas an opposite effect was observed in the shoot tissues: the treated shoots had a lower concentration of sugars and sugar-like compounds. Furthermore, the root: shoot ratio of abundance of sucrose was much higher in naphthalene-treated roots ($p < 0.01$). Sucrose signalling appears to be associated with the production of anthocyanin, which is an antioxidant (Ritsema et al., 2009; Solfanelli et al., 2006; Weber et al., 2005). Antioxidants neutralise damaging chemicals, called free radicals, which are an unavoidable by-product of metabolism (Mattson and Calabrese, 2008). Perhaps, antioxidants formed

as a result of changes in sucrose signalling arising from growth in naphthalene-treated sand, could have positively influenced the resistance to oxidative stress disorders in treated tall fescue in this study.

The metabolic profile of tall fescue grown in naphthalene-treated sand showed that the plant had adapted an effective antioxidant mechanism to control the level of ROS as well as an effective redox network, involving sugar-signalling and presumably IAA signalling pathways. Moreover, the results indicated that synergistic interactions of sugars and phenolic compounds may create an effective redox system in the roots of tall fescue exposed to naphthalene contamination, quenching ROS, detoxifying the PAH/PAH metabolites, promoting and strengthening structural defences, and contributing toward stress tolerance.

The passage of naphthalene/ naphthalene metabolites across root tissues was investigated using Nile red as a molecular probe. Nile red has been used to stain hydrophobic components in animal tissues (Diaz et al., 2008; Greenspan et al., 1985), but to the best of our knowledge, has not been applied in the study of plant tissues so far. Living roots were stained with Nile red and before visualisation with epifluorescent microscopic techniques, consecutively stained with berberine hemisulphate that stains Casparian band specifically (Brundrett et al., 1998). Casparian band functions as the “customs” in a “port” in withholding molecules that may be harmful to the plants from being delivered into the inner core of the roots (Berlow, 2005; Enstone et al., 2003). The results showed that the path of Nile red across the root tissues did not extend beyond the endodermis in naphthalene-treated plant roots as the treated roots possessed a well-formed exodermis and a well-developed endodermis possessing Casparian bands in the radial walls of almost all endodermal cells, lacking passage cells ($p < 0.0001$). On the other hand, uptake of Nile red into protoxylem vessels beyond the endodermis occurred in their control counterparts via the passage cells in the root hair zone as well as the branching zone. The increased cortical zone observed in treated plant roots may also have an impact on the entry of the xenobiotic compound into protoxylem vessels as suggested by Collins et al., 2006. The images of plant roots sectioned from the root tip towards the root base illustrated that a stronger apoplastic barrier system existed in plant roots grown in naphthalene-treated sand, whilst also revealing that a minute region above

the root tip of the treated roots did not possess thickened cells, allowing the action of root elongation (Fig.6.2).

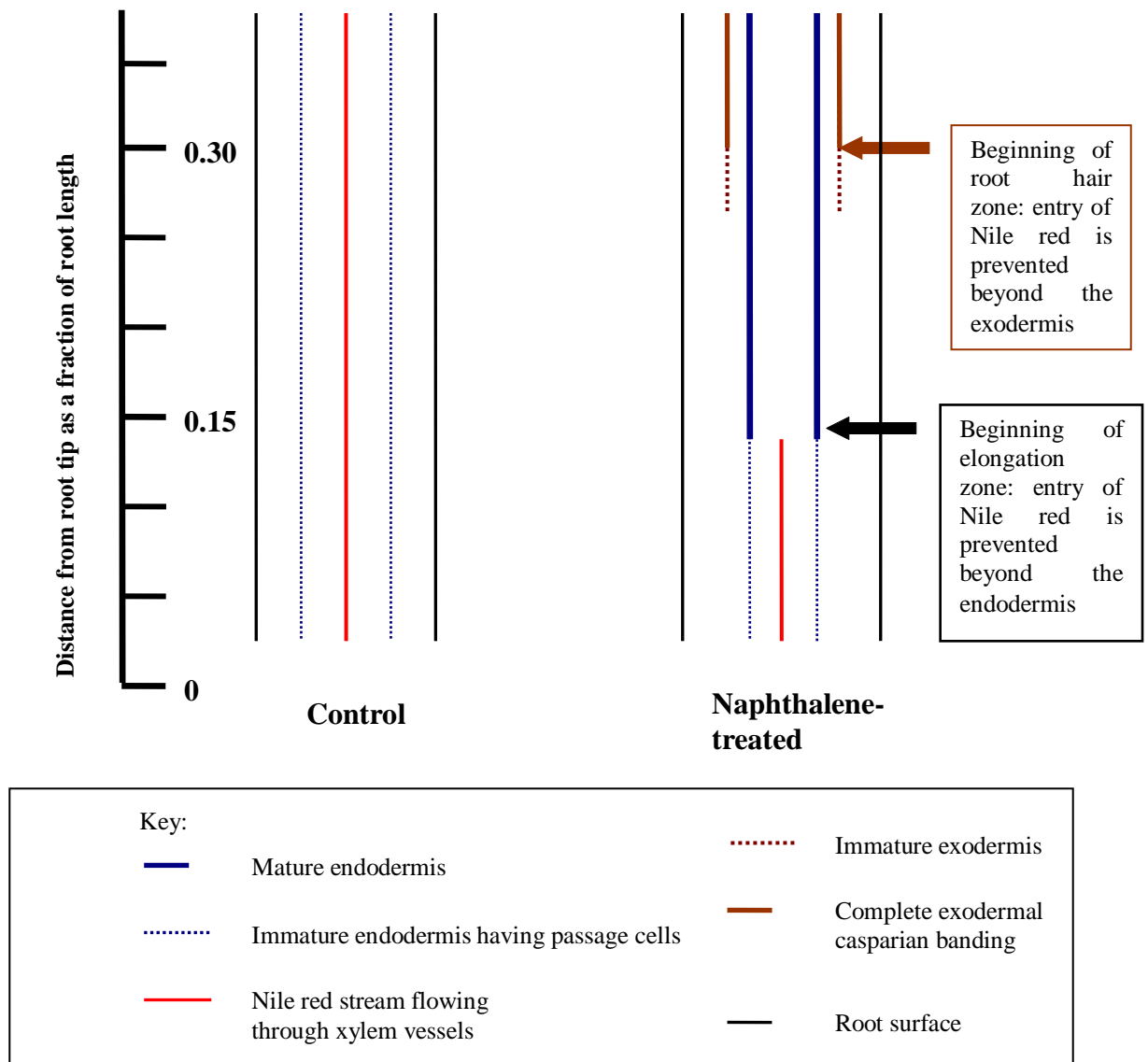


Fig.6.2: Schematic diagram of the xenobiotic uptake models for control and naphthalene-treated tall fescue roots, based on both general and initial results

Similarly Wild et al. (2005) demonstrated that anthracene and phenanthrene which entered the epidermal cells along the elongation, root hair and branching zones moved radially through the epidermal cells to enter the cortex in the root hair and branching zones of maize and wheat grown in contaminated sand medium, but did not pass beyond the endodermis to be taken up by the xylem vessels. To examine whether all species of plants grown in PAH-treated sand exhibit the same phenomenon, the roots of carrot (*Daucus carota*) and white clover (*Trifolium repens*) grown in PAH-

contaminated sand were stained with Nile red and the root sections were visualised with epi-fluorescent microscopic techniques. The epi-fluorescent micrographs showed that penetration of Nile red into xylem vessels occurred in treated carrot and white clover roots similarly as their control counterparts (see appendix 2). Wild and Jones (1991) reported that highest PAH concentrations occurred in the peel tissues, but that detectable levels of PAH compounds were found in the core section of carrot as well. This shows the responses of plants to PAH contamination and PAH uptake into the root core vary across the plant species, whilst illustrating the ability of tall fescue adapted to growth in PAH-contaminated environment to restrict the uptake of xenobiotic substances into the inner core of the root and thus to prevent the long distance translocation of xenobiotic substances towards the shoots in transpiration stream.

Furthermore, naphthol or other polar naphthalene metabolites were not detected in the shoot tissues of tall fescue grown in naphthalene-treated sand, indicating the metabolite(s) was not translocated in the transpiration stream to plant aerial parts. This finding is in agreement with the results as regards the effect of growth in naphthalene-treated sand on Nile red-staining profile. Similarly, Wild et al. (2005) showed localisation and metabolism of anthracene and phenanthrene and longitudinal movement of the xenobiotic compounds toward the shoots within the cortex cells of maize and wheat roots, but also reported that no detectable levels of the xenobiotic compounds were found in the shoots throughout the 56 day-duration.

The plant shoots were not directly exposed to naphthalene contamination, but some of the stress responses of roots, particularly the lower concentration of the putative IAA associated with IAA degradation and presence of fructans which have the function of stabilising membranes under stress were illustrated in the shoot tissues of plants grown in naphthalene-treated sand. Perhaps, the plant root cells sensed cellular stress and activated genes that code for protective molecules, some of them acting as messengers to alert other cells which were not exposed to the stress/ danger directly. Salicylic acid, which is a phenolic phytohormone, in particular, is involved in endogenous signalling, mediating against plant defence against pathogens (Hayat and Ahmad, 2007), and perhaps toxic xenobiotics as well. It plays a role in the resistance to pathogens by inducing the production of pathogenesis-related proteins (Hooft Van

Huijsduijnen et al., 1986). It is involved in the systemic acquired resistance (SAR) in which a pathogenic attack (or toxic effect) on one part of the plant induces resistance in other parts. The signal can also move to nearby plants by salicylic acid being converted to the volatile ester, methyl salicylate (Taiz and Zeiger, 2002). Also, the shift in photosynthetic sugars, a higher portion being translocated to the roots as expressed in the metabolic profiles of naphthalene-treated tall fescue could have caused sugar depletion in the aerial parts of the plants, perhaps triggering a stress response.

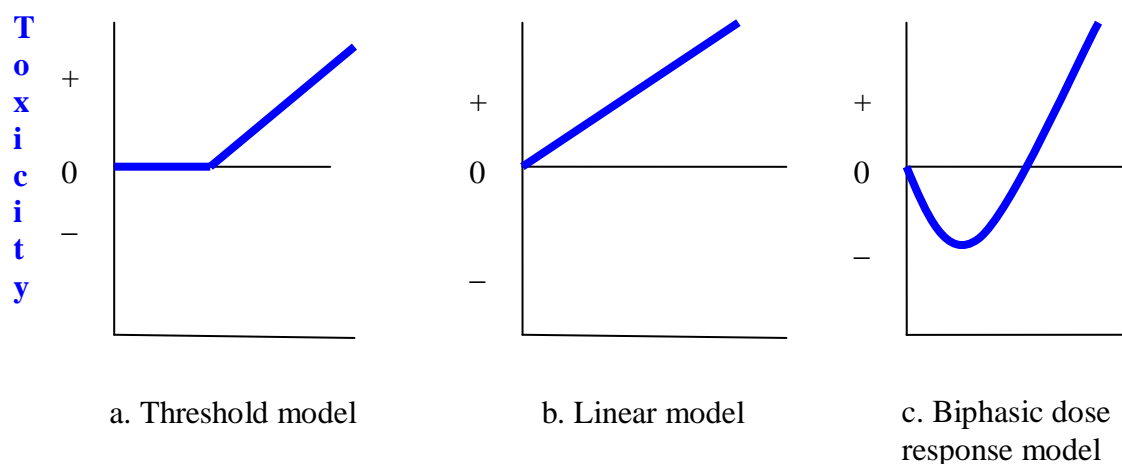
HC/naphthalene -treated tall fescue roots exhibited partial collapse /distortions in the cortical zone, a symptom documented by Enstone et al. (2003) as a feature of water stress. So, the root structural and ultrastructural modifications observed in plant roots grown in HC-treated sand showed not only symptoms of phytotoxicity but symptoms akin to water stress as well.

Naphthalene-treated sand possessed stronger (more negative) matrix potential than the clean, agricultural sand, at similar soil moisture content levels, as recorded with dielectric water potential sensors under both well-watered and water deficit conditions. Since the stronger matrix potential exhibits soil water stress (Taiz and Zeiger, 1998; Slatyer, 1967), it strengthens the notion that the partial collapse in HC/naphthalene-treated tall fescue roots indicates soil water stress. When control plants were exposed to drought conditions, partial collapse was induced in the cortical zone of the control roots, confirming that partial collapse in the cortical zone is a water stress symptom and that growth in PAH-contaminated soils stimulates drought stress in plant roots.

Tall fescue roots grown in HC/naphthalene-treated sand possessed an increased cortical zone due to the arrangement of isodiametrically shaped cortex cells, in contrast to the longitudinal arrangement of cortex cells observed in control roots ($p < 0.001$). Similarly, Barcelo et al. (1988) demonstrated an increased cortical zone due to isodiametrically shaped cortex cells in bush bean stems exposed to Cd-toxicity. The root diameter of treated plants was also increased, due to the increase in cortical zone ($p < 0.01$). Merkl et al., 2005, Bengough, 2003, Bouma et al., 2000 and Boot et al., 1990 also reported an increased root diameter in plants exposed to petroleum

hydrocarbon-contamination. The increased cortical zone and root diameter may be an adaptive response of the plants to protect the tissues against toxicity, but could have also been caused due to water stress as well. There were no significant differences in either the distance from epidermis to stele or the root diameter between control and naphthalene-treated plants subjected to water stress. Remarkably, when subjected to water stress, tall fescue grown in HC/naphthalene-treated sand survived drought stress better than the control plants, suggesting a ‘hormetic’ response. Trehalose which has protective functions against drought stress (Higashiyama, 2002) was expressed in naphthalene-treated roots 8 times as much as in control roots ($p < 0.001$), and could be accountable for the drought resilience effect observed in treated tall fescue. Furthermore, the well-formed exodermis observed in naphthalene-treated tall fescue could have been useful in preventing the efflux of water from the root tissues, when the soil solution became hypertonic, as suggested by Jupp et al. (1987), contributing positively toward the drought resilience effect observed in treated plants.

Permeating all of biology, “hormesis” has been accepted as the fundamental principle of biology as well as of biomedicine. It was first recognised in the 16th century by the Swiss physician and alchemist Paracelsus, who wrote that “all things are poison and nothing is without poison, only the dose makes something not a poison”. The defining characteristic of hormesis is the “biphasic dose response”, in which high doses of a substance are toxic but low doses are beneficial (see Fig.6.3).



Concentration of toxins or other stress factors

Fig.6.3: Dose response models used in toxicology (Source: Mattson and Calabrese, 2008)

Biphasic responses have been reported in organisms ranging from bacteria to human, but to date, 'hormesis' has been primarily associated with only human toxins. Low levels of toxins or other stressors produce beneficial effects by triggering the production of defence molecules within the organism. Once formed, these defence molecules not only deal with the immediate threat but also increase resistance to other threats. They can even repair existing damage. The way hormetic toxins or other stressors affect an organism differ according to the way they are used. Dose is critical when deciding whether a stressor is beneficial or damaging (Mattson and Calabrese, 2008). When the contaminant dose was increased above the concentration of either ~ 11 g total DCM extractable hydrocarbons kg^{-1} sand dw or 0.8 g naphthalene kg^{-1} sand dw in growth mediums, tall fescue did not show growth stimulation in our study. Timing is also a deciding factor. Cells must have time to recover in order to accrue the benefits of stress. During the recovery period, any cell damage caused by the stress is repaired, and the cells also increase the production of stress-resistance proteins (Mattson and Calabrese, 2008). Here, tall fescue plants needed an acclimatisation period of ~ 3 months, before illustrating beneficial effects of stress caused due to the exposure to HC (>10.8 g TEH kg^{-1} sand dw) / naphthalene (>0.8 g kg^{-1} sand dw) contamination. Perhaps, in this particular case, the tall fescue plants needed an acclimation period of ~ 3 months to produce an efficient apoplastic barrier system to prevent the uptake of the potentially harmful components into the root xylem which represent the fast and predominant route of transport for solutes and water from roots toward shoots. Furthermore, the genetic composition, i.e. the species of plant may also be crucial in taking advantage of hormesis in phytoremediation, as the dose of HC contamination that triggered adaptive/stimulatory responses in tall fescue (after the acclimation period of ~ 3 months), was damaging for parsnip, carrot, beetroot and brown top bent. Similarly the concentration of anthracene that stimulated the growth of tall fescue was damaging for brown top bent. The results also suggest that the presence of literally water-insoluble PAHs such as anthracene and B(a)P in soil may expose the plants to stressors other than toxins, whereas relatively water soluble, LMW PAHs such as naphthalene and the presence of HC that contains many water-soluble, xenobiotic components expose plants to stress factors among which toxicity is a major problem.

Tall fescue grown in HC/ naphthalene-contaminated sand showed remarkably well-expressed hormetic responses throughout our study such as resilience to drought stress and restrictions to the entry of xenobiotic uptake, indicating promising applications of ‘hormesis’ to the fields of phytoremediation and agrochemistry.

The observations and results of this investigation are summarised as follows:

- ❖ The presence of petroleum crude oil (HC)/ naphthalene contamination in soil creates a number of challenges for the establishment and development of plants (i.e. water scarcity, mineral and oxygen deficiency, phytotoxicity, possible temperature stress and unfavourable pH) (Merkl et al., 2005). Toxicity and water scarcity were the key stress factors in HC/ naphthalene-treated soils.
- ❖ The ability of seeds to germinate in petroleum hydrocarbon-contaminated soils depends on seed type (seeds with or without sufficient food reserves), type and amount of the contaminant. Tall fescue (*Festuca arundinacea*) germinated well when sown directly in naphthalene-treated sand (0.8 g kg^{-1} sand dw), after an initial delay in germination ($p < 0.01$). This plant species germinated well in HC-treated sand ($10.8 \text{ g TEH kg}^{-1}$ sand dw), when a layer of clean sand was used as a seed bed.
- ❖ In contrast to carrot (*Daucus carota*), beetroot (*Beta vulgaris*), parsnip (*Parsnica sativa*), and brown top bent (*Agrostis capillaries* L.) which failed to survive the HC-contamination, tall fescue established well in HC-contaminated sand, perhaps owing primarily to its root features. Tall fescue demonstrated morphological plasticity to the changes in its growth environment and once past the initial acclimatisation period of ~3 months, possessed an increased root mass ($p < 0.01$) and a well spread, deep root system, demonstrating a potential of this species for phytoremediation.
- ❖ Exposure to HC ($10.8 \text{ g TEH kg}^{-1}$ sand dw) contamination induced structural and ultrastructural disorders in beetroot and tall fescue roots. Enhanced cell wall thickenings and smaller xylem vessels suggested evidence of stress especially xenobiotic stress as well as a variety of strategies and mechanisms to survive the stress conditions.

- ❖ Growth conditions, such as sowing seeds directly in contaminated sand and the presence of organic matter in contaminated growth mediums had impacts on plant growth patterns. However, prolonged contact with HC/naphthalene-contamination stimulated similar root ultrastructural modifications such as enhanced thickening in the endodermal cell walls in tall fescue, regardless of plant growth conditions.
- ❖ Partially collapsed cortex cells which are akin to the effects of drought described by Enstone et al. (2003) were observed in HC/ naphthalene-treated tall fescue roots. The root ultrastructural modifications of treated tall fescue also exhibited symptoms of phytotoxicity described by Barcelo et al. (1988), such as isodiametrically shaped cortex cells rather than the normal elongated shape, and an increased cortex zone. These could imply that the modifications in structural and ultrastructural features of the roots of tall fescue exposed to HC/ naphthalene contamination were synergistic responses of the plants to water scarcity and phytotoxicity. These changes in root ultrastructure provided restrictions to the entry of hydrophobic xenobiotics, exemplified by the path of Nile red, into the inner core of the treated root via apoplastic fluxes while effectively preventing the efflux of water when the soil solution becomes hypertonic.
- ❖ There were subtle indications of the presence of further oxidised or glycosylated/ malonylated naphthol in tall fescue roots grown in naphthalene-treated sand, suggesting that opening of the aromatic ring and insertion of oxygen into the substrate had occurred, presumably in the rhizosphere and that the compound had been taken up by the plant roots. Naphthol or any other naphthalene metabolites were not detected in the aerial parts of the plants grown in naphthalene-treated sand, suggesting the xenobiotic compound was not translocated to the shoots in transpiration stream.
- ❖ A compound speculated to be indole acetic acid (IAA) was either absent or subdued in the root, shoot tissues of tall fescue grown in naphthalene-treated sand, suggesting IAA degradation and associated detoxification of xenobiotic compounds as well as the existence of an effective structural defence system within treated plant tissues.
- ❖ Tall fescue grown in naphthalene-treated sand possessed an increased root: shoot ratio of the concentration of sugars, including glucose, sucrose and

trehalose. This demonstrates that tall fescue plants were able to resist the oxidative stress due to the overproduction of ROS caused by naphthalene contamination, by allocating more sugars, more glucose in particular, to its root tissues ($p < 0.01$) and controlling the damages via sugar signalling and ROS scavenging.

- ❖ The HC/ naphthalene-treated tall fescue showed resilience to drought stress, especially after the acclimatisation period of up to 3 months, perhaps enhanced by the modifications in root ultrastructural features such as a well-formed exodermis and adaptations at molecular levels such as higher root: shoot concentration of trehalose.

Research implications

Abandoned, potentially harmful old gas work sites as well as other soils with low to medium concentrations of PAH burden could be transformed into aesthetically pleasing sites with a well-established vegetative cover to minimise soil erosion and pollution spread, when appropriate plant species that suit the environmental conditions are selected. The risk of the movement of toxic PAH molecules into wildlife food chains could be minimised by the appropriate choice of plants used in phytoremediation. The resistance to drought stress shown by tall fescue grown in HC/ naphthalene-treated sand could be applied in the interest of making crop plants more resistant to drought, through genetic engineering techniques. The research implications of this study are listed as follows:

1. Tall fescue demonstrates a good potential for use in restoring sites polluted with petroleum crude oil (< 10.8 g total extractable hydrocarbons kg^{-1} sand dw) and naphthalene (< 0.8 g kg^{-1} sand dw).
2. Further investigation using a stable isotope labelled naphthalene is required in assessing the uptake of naphthalene/ naphthalene metabolites within plant tissues. Still, the investigations carried out so far implies that tall fescue withstands the inflow of xenobiotic substances towards the inner core of the roots. An initial study suggested that foliar accumulation of PAHs via gaseous exchange or particulate deposition was also negligible in tall fescue (see

appendix 3). Hence using this plant species for remediation of PAH-contaminated sites would not cause a major concern over food chain transfers of the PAH.

3. The fact that tall fescue withstood enhanced water deficit conditions after adapted to growth in HC/ naphthalene-contaminated sand could be explored further in the interest of making crop plants more drought resistant.

Further work recommendations

1. A scanning electron microscopic study on the root ultrastructural features of plant species that did not show adaptability to growth in crude oil/ PAH-treated sand such as brown top bent.
2. Obtaining direct evidence for the incorporation of naphthol and or other naphthalene metabolites into plant metabolism, using stable isotope labelled naphthalene.
3. Obtaining evidence for the unambiguous identification of the putative IAA, which exhibited absence or much subdued signal in the tissues of tall fescue grown in naphthalene-treated sand, in the interest of developing the event to obtain complete positive conclusions regarding the connection between IAA degradation and detoxification/ defence pathways in plant tissues exposed to organic xenobiotics.
4. Investigations into stress related proteins and alterations of the gene expressions in PAH-treated tall fescue.

References

- Adam, G. and Duncan, H., 1999. The effect of diesel fuel on growth of selected plant species. *Environmental Geochemistry and Health*, 21, pp. 353-357.
- Adriano, D., 2011. Opinion on sustainability. *TE News: Communication is the language of Science*, 2(1)
- Agarwal, U.P., 2006. Raman imaging to investigate ultrastructure and composition of plant cell walls: distribution of lignin and cellulose in black spruce wood (*Picea mariana*) *Planta*, 224, pp. 1141-1153.
- Alexander, M., 1995. How toxic are chemicals in soil? *Environmental Science and Technology*, 29, pp.2713-2717.
- Alkio, M., Tabuchi, T.M., Wang, X., et al., 2005. Stress responses to polycyclic aromatic hydrocarbons in *Arabidopsis* include growth inhibition and hypersensitive response-like symptoms. *Journal of Experimental Botany*, 56 (421), pp. 2983-2994.
- Alkorta, I. and Garbisu, C., 2001. Phytoremediation of organic contaminants in soils. *Bioresource Technology*, 79, pp. 273-276.
- Anderson, J.W., Neff, J.M., Cox, B.A., et al., 1974. Characteristics of dispersions and water soluble extracts of crude and refined oils and their toxicity to estuarine crustaceans and fish. *Marine Biology*, 27, pp. 75-88.
- Anderson, T.A., Guthrie, E.A., Walton, B.T., 1993. Bioremediation in the rhizosphere. *Environmental Science & Technology*, 27(13), pp.2630-2636.
- Aprill, W. and Sims, R., 1990. Evaluation of the use of prairie grasses for stimulating polycyclic aromatic hydrocarbon treatment in soil. *Chemosphere*, 20, pp. 253-265.
- Atkinson, D., 2000. Root characteristics: Why and what to measure. In: A.L.Smit, A.G.Bengough, C.Engels, M.van Noordwijk, S.Pellerin, S.C.van de Geijn, eds. 2000. *Root Methods. A Handbook*. Berlin Heidelberg: Springer-Verlag, pp.1-13.
- Baker, J.M., 1973. Growth stimulation following oil pollution. In: E.B. Cowell, ed. 1973. *The ecological effects of oil pollution on Littoral Communities*. Essex: Applied Science Publishers, pp. 72-77.
- Bandurski, R.S., Schulze, A., Leznicki, A., et al., 1988. Regulation of the amount of IAA in seedling plants. In: M. Kutacek, R.S. Bandurski, J. Krulek, eds. 1988. *Physiology and biochemistry of auxins in plants*. Acad Praha, pp. 21-32.
- Barcelo, J., V'azquez, M.D. and Poschenrieder, Ch., 1988. Cadmium-Induced structural and ultrastructural changes in the vascular system of bush bean stems. *Botanica Acta*, 101, pp. 254-261.

Barnett, J.R., Ed. 1981. Xylem Cell Development. Kent: Castle House Publications Ltd.

Beck, A.J., Johnson, D.L., Jones, K.C., 1996. The form and bioavailability of non-ionic organic chemicals in sewage sludge-amended agricultural soils. *Chemosphere*, 58, pp. 321-328.

Benegough, A.G., 2003. Root growth and function in relation to soil structure, composition, and strength. In: H. DeKroon, E.J.W. Visser, Eds. 2003. *Root ecology*, Heidelberg: Springer, Chapter 6.

Bell, R.M., 1992. Higher plant accumulation of organic pollutants from soils. EPA/600/R-92/138. Cincinnati: United States Environmental Protection Agency.

Berlow, S., 2005. Roots exposed! [online] Maximum Yield-Indoor Gardening. Available at :< <http://www.MaximumYield.Com>.> [Accessed 20 November 2011].

Bernards, M.A., 2002. Demystifying suberin. *Canadian Journal of Botany* ,80,pp.227-240.

Bernards, M.A., Fleming, W.D., Llewellyn, D.B. et al.,1999. Biochemical characterisation of the suberization-associated anionic peroxidase of potato. *Plant Physiology*, 121, pp. 135-145.

Better Soils. [online] Available at: <<http://www.soilwater.com.au>> [Accessed 10 October 2011].

Binet, P., Portal, J.M. and Leyval, C., 2001. Application of GC-MS to the study of anthracene disappearance in the rhizosphere of ryegrass. *Organic Geochemistry*, 32(2), pp.217-222.

Bolouri-Moghaddam, M.R., Roy, K.L., Xiang, L., et al., 2010. Sugar signalling and antioxidant network connections in plant cells. Review Article. *FEBS Journal*, 277, pp. 2022-2037.

Boot, R.G.A. and Mensink, M., 1990. Size and morphology of root systems of perennial grasses from contrasting habitats as affected by nitrogen supply. *Plant and Soil*, 129, pp. 291-299.

Boudet, A.M., 2000. Lignins and lignifications: Selected issues. *Plant Physiology and Biochemistry*, 38, pp. 81-96.

Bouma, T.J., Broekhuysen, A.G.M., Veen, B.W., 1996. Analysis of root respiration of *Solanum tuberosum* as related to growth, ion uptake and maintenance of biomass. *Plant Physiology and Biochemistry*, 34(6), pp. 795-806.

Bouma, T.J., Nielsen, K.L., Koutstaal, B., 2000. Sample preparation and scanning protocol for computerised analysis of root length and diameter. *Plant and soil*, 218, pp.185-196.

Brady, J.D., Sadler, I.H. and Fry, S.C., 1986. Di-isodityrosine, a novel tetrameric derivative of tyrosine in plant cell wall proteins: a new potential cross-link. *Biochemical Journal*, 315, pp. 323-327.

Brandt, R; Merkl, N; Schultze-Kraft, R. et al., 2006. Potential of vetiver (*Vetiveria zizanioides* (L.) Nash) for phytoremediation of petroleum hydrocarbon-contaminated soils in Venezuela. *International journal of phytoremediation*, 8(4), pp.273-284.

Brett, T.C. and Waldron, W.K., 1990, 1996. The cell wall and intercellular transport. In: M.Black, B.Charlwood, Eds. 1996. *Physiology and Biochemistry of Plant Cell Walls*. London: Chapman & Hall, pp.151-172.

Briggs, G., Bromilow, R., Evans, A. et al., 1983. Relationships between lipophilicity and the distribution of non-ionised chemicals in barley shoots following uptake by the roots. *Pesticide Science*, 14, pp. 492-500.

Briggs, C.L. and Morris, E.C., 2008. Seed - coat dormancy in *Grevillea linearifolia*: Little Change in Permeability to an Apoplastic Tracer after Treatment with Smoke and Heat. *Annals of Botany*, 101, pp. 623-632.

Brundrett, M., 2008, 1999. *Mycorrhizal Associations: Structure of Roots*. Version 2. [online] Available at <<http://mycorrhizas.info/root.html>> [Accessed 10 October 2011].

Brundrett, M.C., Enstone, D.E. and Peterson, C.A., 1988. A berberine-aniline blue fluorescent staining procedure for suberin, lignin, and callose in plant tissue. *Protoplasma*, 146, pp.133-142.

Cairney, J.W.G. and Ashford, A.E., 1989. Reducing activity at the root surface in *Eucalyptus pilularis*-*Pisolithus tinctorius* ectomycorrhizas. *Australian Journal of Plant Physiology*, 16, pp. 99-105.

CCME (Canadian Council of the Ministers of the Environment). 2010. *Canadian Soil Quality Guidelines for Carcinogenic and Other Polycyclic Aromatic Hydrocarbons (Environmental and Human Health Effects)*. Scientific Criteria Document (revised). ISBN 978-1-896997-94-0

Chaineau, C.H., Morel, J.L., Oudot, J., 2000. Biodegradation of fuel oil hydrocarbons in the rhizosphere of maize. *Journal of Environmental Quality*, 29(2), pp. 569-578.

Chen, Yen-Chih., Banks, M.K. and Schwab, A.P., 2003. Pyrene degradation in the rhizosphere of tall fescue (*Festuca arundinacea*) and switchgrass (*Panicum virgatum* L.). *Environmental science & technology*, 37, pp. 5778-5782.

Chiou, C.T., Sheng, G.Y., Manes, M., 2001. A partition-limited model for the plant uptake of organic contaminants from soil and water. *Environmental science & technology*, 35, pp. 1437-1444.

Collins, C., Martin, I. and Fryer, M., 2006. Evaluation of models for predicting plant uptake of chemicals from soil. (Science Report- SC050021/SR) Bristol: Environment Agency.

Couee, I., Sulmon, C., Gouesbet, G., et al., 2006. An involvement of soluble sugars in reactive oxygen species balance and responses to oxidative stress in plants. *Journal of Experimental Botany*, 57, pp. 449-459.

Coutts, M.P., 1989. Factors affecting the direction of growth of tree roots. *Annals Science Forum*, 46(Suppl), pp. 277-287.

Crowe, A.U., Han, B., Kermode, A.R., et al., 2001. Effects of oil sands effluent on cattail and clover: photosynthesis and the level of stress proteins. *Environmental Pollution*, 113(3), pp. 311-322.

Crowley, D.E., 1996. Physiological status of rhizosphere bacteria in relation to phyto-remediation of xenobiotic soil contaminants. Abstracts of papers of the American Chemical Society Part 1. 212, p. 90-AGRO

Crnkovic', D., Ristic, M., Antonovic, D., 2006. Distribution of heavy metals and arsenic in soils of Belgrade (Serbia and Montenegro). *Soil and Sediment Contamination*, 15(6), pp. 581-589.

Currier, H.B. and Peoples, S.A., 1954. Phytotoxicity of hydrocarbons. *Hilgardia*, 23, pp. 155-160.

Decagon Devices Inc., 2007. Manual, Water potential probe.

de Hoffmann, E. and Stroobant, V., 2002. *Mass Spectrometry: Principles and Applications*. 2nd ed. Ontario: John Wiley & Sons, Ltd.

De Maagd, P.G.-J., ten Hulscher, T.E.M., Van den Heuvel, H., et al., 1998. Physicochemical properties of polycyclic aromatic hydrocarbons: aqueous solubilities, n-octanol/water partition coefficients, and Henry's law constants. *Environmental Toxicology and Chemistry*, 17, pp. 252-257.

Department of Agriculture Bulletin, 462, 1960.

Dettmer, K., Aronov, P.A. and Hammock, B.D., 2007. Mass spectrometry-based metabolomics. *Mass Spectrometry Reviews*, 26(1), pp. 51-78.

Diaz, G., Melis, M., Batetta, B. et al., 2008. Hydrophobic characterisation of intracellular lipids in situ by Nile Red red/yellow emission ratio. *Micron*, 39, pp.819-824.

Dinkelaker, B., Hengeler, C., Neumann, G., et al., 1996. Root exudates and mobilization of nutrients. In: H. Rennenberg, W. Eschrich, Eds. 1996. *Trees-contributions to modern tree physiology*. Amsterdam: SPB Academic Publishing, pp. 3-14.

Dinkelaker, B., Hahn, G., Romheld, V., et al., 1993a. Non-destructive methods for demonstrating chemical changes in the rhizosphere 1. Description of methods. *Plant Soil*, 155(156), pp. 67-70.

Dinkelaker, B., Hahn, G., Marschner, H., 1993b. Non-destructive methods for demonstrating chemical changes in the rhizosphere 11. Application of methods. *Plant Soil*, 155(156), pp. 71-74.

Downard, K., 2004. *Mass Spectrometry. A Foundation Course*. Cambridge: The Royal Society of Chemistry.

Dragan, C., Mirjana, R., Anka, J., et al., 2007. Levels of PAHs in the soils of Belgrade and its environs. *Environmental Monitoring Assessment*, 125, pp. 75–83.

Du, H., Wang, Z., Yu, W., et al., 2011. Differential metabolic responses of perennial grass *Cynodon transvaalensis* × *Cynodon dactylon* (C₄) and *Poa Pratensis* (C₃) to heat stress. *Physiologia Plantarum*, 141, pp. 251-264.

Dubey, R.S., 1997. Photosynthesis in plants under stressful conditions. In: M. Passarakli, Ed. 1997. *Handbook of photosynthesis*. New York: Marcel Dekker, pp. 859-875.

Ehrlich, G.G., Goerlitz, D.F., Godsy, E.M., et al., 1982. Degradation of phenolic contaminants in ground water by anaerobic bacteria: St. Louis Park, Minnesota. *Ground Water*, 20(6), pp. 703-710.

Engels, Ch., Neumann, G., Gahoonia, T.S., et al., 2000. Assessing the ability of roots for nutrient acquisition. In: A.L.Smit, A.G.Bengough, C.Engels, M.van Noordwijk, S.Pellerin, S.C.van de Geijn, Eds. 2000. *Root Methods. A Handbook*. Berlin Heidelberg: Springer-Verlag, pp. 405-449.

Enstone, D.E., Peterson, C.A. and Ma, F., 2003. Root endodermis and exodermis: structure, function, and responses to the environment. *Journal of plant growth regulation*, 21, pp.335-351.

Environment agency. 2004. Update on estimating vapour intrusion into buildings, CLEA Briefing Note 2. Bristol: Environment Agency.

Esau, K., 1977. *Anatomy of seed plants*. New York: John Wiley.

Esau, K., 1965. *Plant anatomy*, 2nd edition. New York: John Wiley and Sons, p. 767.

Esau, K., 1953. *Plant Anatomy*. Second Edition. New York, London, Sidney: John Wiley & Sons, Inc., p. 767.

Farrell-Jones, J., 2003. Petroleum hydrocarbons and polyaromatic hydrocarbons. In: C.K. Thompson, P.C. Nathanail, Eds. 2003. Chemical analysis of contaminated land. Oxford: Blackwell Publishing Ltd.

Fismes, J., Perrin-Ganier, C., Empereur-Bissonnet, P., et al., 2002. Soil-to-root transfer and translocation of polycyclic aromatic hydrocarbons by vegetables grown on industrial contaminated soils. *Journal of Environmental Quality*, 31, pp. 1649-1656.

Fitter, A.H., 1996. Characteristics and functions of root systems. In: Y. Waisel, A. Eshel, and K. Kafkaki, Eds. 1996. Plant roots, the hidden half. New York: Marcel Dekker, pp. 1-20.

Forbes, J.C. and Watson, R.D., 1992. Plants in Agriculture. The Press Syndicate of the University of Cambridge. ISBN: 0 521 417554 hardback; ISBN: 0 521 427916 paperback. pp. 82-108.

Frick, C.M., Farrell, R.E. and Germida, J.J., 1999. Assessment of phytoremediation as an in situ technique for cleaning oil-contaminated sites. Calgary: Petroleum Technology Alliance of Canada.

Fry, S.C., 1986. Cross-linking of matrix polymers in the growing cell walls of angiosperms. *Annual Review of Plant Physiology*, 37, pp.165-186.

Fry, S.C. and Miller, J.G., 1987. H₂O₂ –dependent cross-linking of feruloyl-pectins in vivo. *Food hydrocolloids*, 1, pp. 395-397.

Gahoonia, T.S. and Nielsen, N.E. 1998. Direct evidence on participation of root hairs in phosphorus (32 P) uptake from soil. *Plant Soil*, 198, pp.147-152.

Gang, D.R., Costa, M.A., Fujita, M. et al., 1999. Regiochemical control of monolignol radical coupling: a new paradigm for lignin and lignan biosynthesis. *Chemistry & Biology*, 6, pp.143-151.

Gao, Y., Ren, L., Ling, W. et al., 2010. Desorption of phenanthrene and pyrene in soils by root exudates. *Bioresource Technology*, 101, pp. 1159-1165.

Gao, Y. and Zhu, L., 2004. Plant uptake, accumulation and translocation of phenanthrene and pyrene in soils. *Chemosphere*, 55, pp. 1169-1178.

Gaspar, Th., Penel, C., Hagege, D., et al., 1991. Peroxidases in plant growth, differentiation and development processes. In: J. Lobarzewski, H. Greppin, C. Penel, and Th. Gaspar, Eds. 1991. Biochemical, molecular and physiological aspects of plant peroxidases. Geneva: University of Geneva, Switzerland, pp. 249-280.

Glisic, B.S., Mistic, R.D., Stamenic, D.M. et al., 2007. Supercritical carbon dioxide extraction of carrot fruit essential oil: Chemical composition and antimicrobial activity. *Food Chemistry* (Article in press).

Gonzalez-Mendoza, D., Quiroz-Moreno, A. and Zapata-Perez, O., 2008. An improved method for the isolation of total RNA from *Avicennia germinans* leaves. *Verlag der Zeitschrift für Naturforschung*, 63(1-2), pp. 124-126.

Grambow, H.J., 1986. Pathway and mechanism of the peroxidase catalyzed degradation of indole-3-acetic acid. In: H. Greppin, C. Penel, Th. Gaspar, Eds. 1986. *Molecular and physiological aspects of plant peroxidases*. Geneva: University of Geneva, Switzerland, pp. 31-41.

Grayston, S.J., Vaughan, D., Jones, D., 1996. Rhizosphere carbon flow in trees, in comparison with annual plants: the importance of root exudation and its impact on microbial activity and nutrient availability. *Applied Soil Ecology*, 5, pp. 29-56.

Greenspan, P. and Fowler, S.D., 1985. Spectrofluorometric studies of the lipid probe, Nile red. *Journal of Lipid Research*, 26, pp. 781-789.

Greenspan, P., Mayer, E.P. and Fowler, S.D., 1985. Nile red: a selective fluorescent stain for intracellular lipid droplets. *The Journal of Cell Biology*, 100, pp. 965-973.

Gromova, M. and Roby, C., 2010. Toward *Arabidopsis thaliana* hydrophilic metabolome: assessment of extraction methods and quantitative ¹H NMR. *Technical Focus. Physiologia Plantarum*, 140, pp. 111-127.

Halliwell, B., 2006. Reactive species and antioxidants. Redox biology is a fundamental theme of aerobic life. *Plant Physiology*, 141, pp. 312-322.

Harms, H., Dehnen, W., Monch, W., 1977. Benzo (a) pyrene metabolites formed by plant cells. *Z. Naturforsch*, 32c, pp.321-326.

Harms, H.H., 1996. Bioaccumulation and metabolic fate of sewage derived organic xenobiotics in plants. *Science of the Total Environment*, 185, pp.83-92.

Harms, H.H., 1992. In-vitro systems for studying phytotoxicity and metabolic fate of pesticides and xenobiotics in plants. *Pesticide Science*, 35 (3), pp. 277-281.

Harmsen, J. and Frintrop, P., 2003. Non-halogenated organic compounds including semi-volatile organic compounds (SVOCs) in Chemical analysis of contaminated land. In: C.K. Thompson, P.C. Nathanail, Eds. 2003. *Chemical analysis of contaminated land*. Oxford: Blackwell Publishing Ltd.

Harvey, P.J., Campanella, B.F., Castro, P.M.L., et al., 2001. Phytoremediation of Polyaromatic hydrocarbons, Anilines and Phenols. *Review Articles: Phytoremediation. ESPR-Environmental Science and Pollution Research*, pp. 1-19.

Hayat, M.A., 1986. *Basic Techniques for Transmission Electron Microscopy*. London: Academic Press Inc. ISBN: 0-12-333925-1 (alk. paper), ISBN: 0-12-333926-X (paperback).

Hayat, S. and Ahmad, A., 2007. Salicylic acid-A Plant Hormone. Springer. ISBN: 1402051832.

Heitkamp, M.A., Freeman, J.P. and Cerniglia, C.E., 1987. Naphthalene Biodegradation in Environmental Microcosms: Estimates of Degradation Rates and Characterization of Metabolites. *Applied and Environmental Microbiology*, 53 (1), pp.129-136.

Heitzer, A., Webb, O.F., Thonnard, J.E., et al., 1992. Specific and quantitative assessment of naphthalene and salicylate bioavailability by using a bioluminescent catabolic reporter bacterium. *Applied and Environmental Microbiology*, 58, pp.1839-1846.

Hether, NH., Olsen, RA., Jackson, LL , 1984. Chemical identification of iron reductants exuded by plant roots. *Journal of Plant Nutrition*, 7, pp. 667-676.

Higashiyama, T., 2002. Novel functions and applications of trehalose. *Pure and Applied Chemistry*, 74 (7), pp. 1263–1269.

Hoffland, E., Findenegg, G.R., Nelemans, J.A., 1989. Solubilization of rock phosphate by rape. II. Local root exudation of organic acids as a response to P-starvation. *Plant Soil*, 113, pp. 161-165.

Hooft Van Huijsduijnen, R.A.M., Alblas, S.W., De Rijk, R.H., et al., 1986. Induction by Salicylic Acid of Pathogenesis-related Proteins and Resistance to Alfalfa Mosaic Virus Infection in Various Plant Species. *Journal of General Virology*, 67, pp. 2135-2143.

Howard, P.H., 1989. Handbook of environmental fate and exposure data for organic chemicals. Vol. 1. Lewis Publishers, pp. 408-421.

Huang, B.R., Taylor, H.M. and McMichael, B.L., 1991. Effects of temperature on the development of metaxylem in primary wheat roots and its hydraulic consequence. *Annals of Botany*, 67, pp.163-166.

Huang, X.D., El-Alawi, Y., Penrose, D.M., et al., 2004. Response of three grass species to creosote during phytoremediation. *Environmental Pollution*, 130, pp. 453-463.

Huckelhoven, R., Schuphan, I., Thiede, B., et al., 1997. Biotransformation of pyrene by cell cultures of soybean (*Glycine max* L.), wheat (*Triticum aestivum* L.), jimsonweed (*Datura stramonium* L.), and purple foxglove (*Digitalis purpurea* L.). *Journal of Agricultural and Food Chemistry*, 45, pp.263-269.

IARC., 1983. Monographs on the evaluation of the carcinogenic risk of chemicals to humans. *Polynuclear Aromatic Hydrocarbons*, 32, Lyon: WHO.

Janska, M., Hajslova, J., Tomaniova, M., et al., 2006. Polycyclic aromatic hydrocarbons in fruits and vegetables grown in the Czech Republic. *Bulletin of Environmental Contamination and Toxicology*, 77(4), pp.492-499.

Jenkins, R.O., 1992. Catabolism of organics and man made chemicals. In: G.D.Weston, Ed. 1992. *Energy Sources for Cells*. Oxford: Butterworth Heinemann Limited, pp. 107-134.

Johnson, D.L., Maguire, K.L., Anderson, D.R., et al., 2004. Enhanced dissipation of chrysene in planted soil: the impact of a rhizobial inoculum. *Soil biology and biochemistry*, 36(1), pp. 33-38.

Joner, E.J., Johansen, A., Loibner, A.P. et al., 2001. Rhizosphere effects on microbial community structure and dissipation and toxicity of polycyclic aromatic hydrocarbons (PAHs) in spiked soil. *Environmental Science and Technology*, 35, pp. 2773-2777.

Joner, E.J. and Leyal, C., 2001. Arbuscular mycorrhizal influence on clover and ryegrass grown together in a soil spiked with polycyclic aromatic hydrocarbons. *Mycorrhiza*, 10, pp. 155-159.

Joner, E.J., Leyval, C., van Colpaert.,J., 2006. Ectomycorrhizas impede phytoremediation of polycyclic aromatic hydrocarbons (PAHs) both within and beyond the rhizosphere. *Environmental Pollution*, 142, pp. 34-38.

Jones, D.L., Shaff, J.E., and Kochian, L., 1995. Role of calcium and other ions in directing root hair tip growth in *Limnobium stoloniferum*. I. Inhibition of tip growth by aluminium. *Planta*, 197 (4), pp. 672-680.

Jones, K.C., Stratford, J.A., Waterhouse, K.S., et al., 1989. Organic compounds in Welsh soils: polynuclear aromatic hydrocarbons. *Environmental Science and Technology*, 23, pp.540-550.

Jordahl, J.J., Foster, L., Schnoor, J. L., et al., 1997. Effect of Hybrid Poplar Trees on Microbial Population Important to Hazardous Waste Bioremediation. *Environmental Toxicology and Chemistry*, 16, pp.1318–1321.

Jupp, A.P. and Newman, E.I., 1987. Morphological and anatomical effects of severe drought on the roots of *Lolium-perenne* L. *New Phytologist*, 105(3), pp. 393-402.

Kanaly, R.A. and Harayama, S., 2000. Biodegradation of high-molecular weight polycyclic aromatic hydrocarbons by bacteria. *Journal of bacteriology*, 182, pp. 2059-2067.

Karickhoff, S.W., 1981. Semi-empirical estimation of sorption of hydrophobic pollutants on natural sediments and soils. *Chemosphere*, 10(8), pp.833-846.

Kechavarzi, C., Pettersson, K., Harrison, P.L., et al., 2007. Root establishment of perennial ryegrass (*L.perenne*) in diesel contaminated subsurface soil layers. *Environmental pollution*, 145, pp.68-74.

Kipopoulou, A.M., Manoli, E., Samara, C., 1999. Bioconcentration of polycyclic aromatic hydrocarbons in vegetables grown in an industrial area. *Environmental Pollution*, 106, pp.369-380.

Kmentova', E., 2003. Response of plant to fluoranthene in environment. Ph.D. Masaryk University.

Kolattukudy, P.E., 2001. Polyesters in higher plants. *Advances in Biochemical Engineering/ Biotechnology*, 71, pp. 1-49.

Kolb, M. and Harms, H., 2000. Metabolism of fluoranthene in different plant cell cultures and intact plants. *Environmental Toxicology and Chemistry*, 19, pp. 1304-13010.

Kolek, J. and Kozinka, V., 1991. Physiology of the plant root system. 1991. *Developments in Plant and Soil Sciences*, 46. Dordrecht/Boston/London :Kluwer Academic Publishers.

Kubo, M., Udagawa, M., Nishikubo, N. et al., 2005. Transcription switches for protoxylem and metaxylem vessel formation. *Research Communication. Genes and Development*, 19, pp. 1855-1860.

Kyveryga, P.M., Blackmer, A.M., Ellsworth, J.W., et al., 2004. Soil pH Effects on Nitrification of Fall-Applied Anhydrous Ammonia. *Soil Science Society of America Journal*, 68, pp. 545–551.

Lamb, C. and Dixon, R.A., 1997. The oxidative burst in plant disease resistance. *Annual Review of Plant Physiology and Molecular Biology*, 48, pp.251-275.

Lasat, M.M., 2001. The use of plants for the removal of toxic metals from contaminated soils. *American Association for the Advancement of Science*.

Lee, C.H., Lee, J.Y., Cheon, J.Y., et al., 2001. Attenuation of Petroleum Hydrocarbons in Smear Zones: A Case Study. *Journal of Environmental Engineering*, 127, pp. 639–647.

Leggo, P.J. and Ledesert, B., 2008. Chapter 10. Organo-Zeolitic-Soil System: A new approach to plant nutrition. In: L.R. Elsworth et al., Eds. *Fertilisers, Properties, Applications and Effects*. Nova Science Publishers, Inc. ISBN 978-1-60456-483-9.

Liste, H.H., and Alexander, M., 2000 a. Accumulation of phenanthrene and pyrene in rhizosphere soils. *Chemosphere* ,40, pp. 11-14.

Liste, H.H., and Alexander, M., 2000 b. Plant promoted pyrene degradation in soil. *Chemosphere* ,40, pp. 7-10.

Liu, S.L., Luo, Y.M., Cao, Z.H. et al., 2004. Degradation of benzo [a] pyrene with arbuscular mycorrhizal alfalfa. *Environmental Geochemistry and Health*, 26, pp.285–293.

- Lynch, J. M., 1990. *The Rhizosphere*. New York: Wiley.
- Machackova, I., Ullmann, J., Krekule, J. and Opatrny, Z., 1988. Comparison of in vivo IAA decarboxylation rate with in vitro peroxidase, IAA oxidase activities. In: R. Kutacek, R.S. Bandurski, J. Krekule, eds. 1988. *Physiology and biochemistry of auxins in plants*. Acad Praha, pp. 87-91.
- Mackay, D., Shiu, W. and Ma, K., 2000. *Physical-chemical and environmental fate handbook*. CRC Press LLC.
- Mackay, D., Shiu, W.Y., Ma, K.C., et al., 2006. *Handbook of physical-chemical properties and environmental fate for organic chemicals*. Taylor & Francis Group, LLC.
- Marschner, H., Romheld, V., Kissel, M., 1986. Different strategies in higher plants in mobilization and uptake of iron. *Journal of Plant Nutrition*, 9, pp. 695-713.
- Mattson, M. and Calabrese, E., 2008. When a little poison is good for you, *NewScientist*, [online] Available at: <<http://www.NewScientist.com>> [Accessed 06 August 2008].
- McCann, H.J., Greenberg, M.B., Solomon, R.K., 2000. The effect of creosote on the growth of an axenic culture of *Myriophyllum spicatum* L. *Aquatic Toxicology*, 50, pp. 265-274.
- McCully, M.E. and Boyer, J.S., 1997. The expansion of root cap mucilage during hydration: III. Changes in water potential and water content. *Physiologia Plantarum*, 99, pp.169–177.
- McCutcheon, S.C. and Schnoor, J.L., 2003. Overview of phytotransformation and control of wastes. In: S.C.McCutcheon, J.L.Schnoor, Eds. 2003. *Phytoremediation: transformation and control of contaminants*. New Jersey: John Wiley & Sons Inc., pp. 3-58.
- McFarlane, J.C., 1995. Plant transport of organic chemicals. In: S.Trapp, J.C.McFarlane, Eds. 1995. *Plant contamination: Modelling and simulation of organic chemical processes*. Boca Raton: Lewis.
- Meagher, R.B., 2000. Phytoremediation of toxic elemental and organic pollutants. *Current Opinion in Plant Biology*, 3, pp. 153-162.
- Merck, 1989. *The Merck Index: An Encyclopedia of Chemicals, Drugs, and Biologicals*. New Jersey: Merck & CO., Inc.
- Merkl, N., Schultze-Kraft, R., and Infante, C., 2005a. Phytoremediation in the tropics-influence of heavy crude oil on root morphological characteristics of graminoids. *Environmental Pollution*, 138, pp. 86-91.

Merkl, N., Schultze-Kraft, R., and Infante, C., 2005b. Assessment of tropical grasses and legumes for phytoremediation of petroleum-contaminated soils. *Water, Air and Soil Pollution*, 165, pp. 195-209.

Meudec, A., Dussauze, J., Deslandes, E., et al., 2006. Evidence for bioaccumulation of PAHs within internal shoot tissues by a halophytic plant artificially exposed to petroleum-polluted sediments. *Chemosphere*, 65, pp.474-481.

Meudec, A., Dussauze, J., Jourdin, M., et al., 2006. Gas chromatographic-mass spectrometric method for polycyclic aromatic hydrocarbon analysis in plant biota. *Journal of Chromatography A*, 1108, pp. 240-247.

Meulenberg, R., Rijnaarts, H.H.H.M., Doddema, H.J., et al., 1997. Partially oxidised polycyclic aromatic hydrocarbons show an increased bioavailability and biodegradability. *FEMS Microbiology Letters*, 152, pp. 45-49.

Miller, R.M. and Jastrow, J.D., 1992. The application of VA mycorrhizae to ecosystem restoration and reclamation. In: M.F.Allen, Ed. 1992. *Mycorrhizal functioning*. New York: Chapman and Hall, pp. 438-467.

Molina, I., 2010. Plant lipid biochemistry. Biosynthesis of plant lipid polyesters. The AOCs Lipid Library, [online] Available at: <<http://www.lipidlibrary.aocs.org/plantbio/polyesters/index.htm>> [Accessed 06 October 2011].

Morel, J., Habib, L., Plantureux, S., et al., 1991. Influence of maize root mucilage on soil aggregate stability. *Plant Soil*, 136, pp. 111-119.

Morris, C., 1992. In: C.Morris, Ed. 1992. *Academic press dictionary of science and technology*. Toronto: Academic Press. p. 2432.

Mueller, J.G., Chapman, P.J., Pitchard, P.H., 1989. Creosote-contaminated sites: their potential for bioremediation. *Environmental Science and Technology*, 23, pp. 1197-1201.

Nakajima, D., Yoshida, Y., Suzuki, J., et al., 1995. Seasonal-changes in the concentration of polycyclic aromatic-hydrocarbons in azalea leaves and relationship to atmospheric concentration. *Chemosphere*, 30(3), pp.409-418.

Nassau, P.M., Martin, S.L., Brown, R.E., et al., 1996. Galactofuranose Biosynthesis in *Escherichia coli* K-12: Identification and Cloning of UDP-Galactopyranose Mutase. *Journal of Bacteriology*, 178 (4), pp. 1047-1052.

Neergaard, E.de., Lyshede, O.B., Gahoonia, T.S., et al., 2000. Anatomy and histology of roots and root-soil boundary. In: A.L.Smit, A.G.Bengough, C.Engels, M.van Noordwijk, S.Pellerin, S.C.van de Geijn, Eds. 2000. *Root Methods. A Handbook*. Berlin Heidelberg: Springer-Verlag.

Newman, L.A. and Reynolds, C.M., 2004. Phytodegradation of organic compounds. *Current opinion in Biotechnology*, 15, pp. 225-230.

- Ober, E.S. and Sharp, R.E., 2007. Regulation of root growth responses to water deficit. In: Matthew A. Jenks, Paul M.Hasegava, S.Mohan Jain, Eds. 2007. *Advances in molecular breeding toward drought and salt tolerant crops*. Springer, pp. 33-53.
- Okoh.A.L. and Trejo-Hernandez, M. R., 2006. Remediation of petroleum hydrocarbon polluted systems: Exploiting the bioremediation strategies. *African Journal of Biotechnology*, 5(25), pp.2520-2525.
- Orfánus, T. and Eitzinger, J., 2010. Factors influencing the occurrence of water stress at field scale. *Ecohydrology*, 3(4), pp. 478-486.
- Pages, L., Asseng, S., Pellerin, S., et al., 2000. Modelling root system growth and architecture. In: A.L.Smit, A.G.Bengough, C.Engels, M.van Noordwijk, S.Pellerin, S.C.van de Geijn, Eds. 2000. *Root Methods. A Handbook*. Berlin Heidelberg: Springer-Verlag.
- Parrish, Z.D., White, J.C., Isleyen, M., et al., 2006. Accumulation of weathered polycyclic aromatic hydrocarbons (PAHs) by plant and earthworm species. *Chemosphere* ,64, pp. 609-618.
- Passioura, J.B., 1991. Soil structure and plant-growth. *Australian Journal of Soil Research* ,29, pp. 717-728.
- Pego, J.V., Kortstee, A.J., Huijser, C., et al., 2000. Photosynthesis, sugars and the regulation of gene expression. *Journal of Experimental Botany* ,51, pp. 407-416.
- Peter, H. R. and George, B.J., 1995. Carol J. Mills, Ed. 1995. *Understanding Biology* .3rd edition. WM C. Brown, p. 203.
- Phillips, L.A., Greer, C.W., and Germida, J.J., 2006. Culture-based and culture-independent assessment of the impact of mixed and single plant treatments on rhizosphere microbial communities in hydrocarbon contaminated flare-pit soil. *Soil Biology & Biochemistry* ,38, pp.2823-2833.
- Postek, M.T., Howard, K.S., Johnson, A.H., & M^CMichael, K.L , 1980. *Scanning Electron Microscopy-A Student's Handbook*.
- Preis, M., 2010. Analysis of the peroxidase-catalysed oxidation of hydroxamic acids. Ph.D. University of Greenwich.
- Rademacher, T.W., Parekh, R.B. and Dwek, R.A., 1988. Glycobiology. *Annual Review of Biochemistry*, 57, pp. 785-838.
- Ramon, M., Rolland, F. and Sheen, J., 2008. Sugar sensing and signalling. *The Arabidopsis Book*. American Society of Plant Biologists. doi: 10.1199/ tab.0117.
- Raven, P.H., Evert, R.F., and Eichhorn, S.E., 1999. *Biology of plants*, 6th ed. New York: Freeman Co.

- Reilley, K.A., Banks, M.K., Schwab, A.P., 1996. Dissipation of polycyclic aromatic hydrocarbons in the rhizosphere. *Journal of Environmental Quality*, 25, pp. 212-219.
- Rentz, J.A., Chapman, B., Alvarez, P.J., et al., 2003. Stimulation of hybrid poplar growth in petroleum-contaminated soils through oxygen addition and soil nutrient amendments. *International Journal of Phytoremediation*, 5(1), pp. 57-72.
- Ritsema, T., Brodmann, D., Diks, S.H., et al., 2009. Are small GTPases signal hubs in sugar –mediated induction of fructan biosynthesis? *PLoS ONE*, 4(8), e6605, doi:10.1371/journal.pone.0006605.
- Rogers, L. and Campbell, M.M., 2004. Tansley Review: The genetic control of lignin deposition during plant growth and development. *New Phytologist* ,164, pp.17-30.
- Rolland, F, Winderickx, J. and Thevelein, J.M., 2001. Glucose sensing mechanisms in eukaryotic cells. *Trends in Biochemical Sciences*, 26, pp. 310-317.
- Romheld, V., 1991. The role of phytosiderophores in acquisition of iron and other micronutrients in graminaceous species: an ecological approach. *Plant Soil*, 130, pp.127-134.
- Rougier, M. and Chaboud, A., 1985. Mucilages secreted by roots and their biological function. *Israel Journal of Botany*, 34, pp.129-146.
- Ryan, J.A., Bell, R.M., Davidson, J.M. , et al., 1988. Plant Uptake of Non-ionic organic chemicals from soils. *Chemosphere*, 17, pp. 2299-2323.
- Ryser, U. and Keller, B., 1992. Ultrastructural localisation of a bean glycine-rich protein in unligified primary walls of protoxylem cells. *The Plant Cell*, 4, pp.773-783.
- Sandermann Jr, H., 1994. Higher plant metabolism of xenobiotics: the “Green Liver” concept. *Pharmacogenetics*, 4, pp. 225-241.
- Scheer, C.E, 2006. Adaptations of tall fescue to petroleum crude oil-polluted soils. Unpublished manuscript. University of Greenwich.
- Schnoor, J.L., Lich, L.A., McCutcheon, S.C., 1995. Phytoremediation of organic and nutrient contaminants. *Environmental Science and Technology*, 29, pp. 318-323.
- Schreiber, L., 1996. Chemical composition of Casparian strips isolated from *Clivia miniata* Reg. roots: evidence for lignin. *Planta*, 199, pp.596-601.
- Schreiber, L., Breiner, H.W., Riederer, M. et al., 1994. The Casparian strip of *Clivia miniata* Reg. roots: isolation, fine structure and chemical nature. *Botanica Acta* ,107, pp. 353-361.
- Schröder, P., Harvey, P.J., and Schwitzgöbel, J.P., 2002. Prospects for the Phytoremediation of Organic Pollutants in Europe. *Environ Soil & Pollution Research*, 9(1), pp. 1-3.

- Schulz, H., 2008. Oxidation of fatty acids in eukaryotes. In: D.E.Vance and J.E. Vance, eds. 2008. *Biochemistry of lipids, lipoproteins and membranes*, Fifth edition, Elsevier, B.V. pp. 131-154. ISBN: 978-0-444-53219-0
- Scott, M.G. and Peterson, R.L., 1979. The endodermis in *Ranunculus acris*. I. Structure and ontogeny. *Canadian Journal of Botany*, 57, pp.1040–1062.
- Shann, J. R. and Boyle, J. J., 1994. Influence of plant species on in situ rhizosphere degradation. In: T.A. Anderson, J.R.Coats, Eds. 1994. *Bioremediation Through Rhizosphere Technology*. Washington, DC : ACS Symposium Series 563. ACS. pp. 70–81.
- Siciliano, S.D., Germida, J.J., Banks, K., et al., 2003.Changes in microbial composition and function during a polyaromatic hydrocarbon phytoremediation field trial. *Applied and Environmental Microbiology*, 69, pp. 483-489.
- Simonich, S.L., and Hites, R.A., 1994. Vegetation-atmosphere partitioning of polycyclic aromatic hydrocarbons. *Environmental Science and Technology*, 28, pp. 939-943.
- Slatyer, R.O., 1967. *Plant-water relationships*. London: Academic Press Inc.
- Smith, M.J., Flowers, T.H., Duncan, H.J. et al., 2006. Effects of polycyclic aromatic hydrocarbons on germination and subsequent growth of grasses and legumes in freshly contaminated soil and soil with aged PAHs residues. *Environmental pollution*, 141(3), pp. 519-525.
- Sobotik, M. and Haas, D., 2009. The importance of anatomical structure of roots for physiological processes. International Symposium “Root Research and Applications”
- Sohal, R.S. and Weindruch, R., 1996. Oxidative stress, caloric restriction, and aging. *Science*, 273, pp.59-63.
- Solfanelli, C., Poggi, A., Loreti, E., et al., 2006. Sucrose-specific induction of the anthocyanin biosynthetic pathway in *Arabidopsis*. *Plant Physiology*,140, pp. 637-646.
- Soukup, A., Mala, J., Hrubcova, M., et al., 2004. Differences in anatomical structure and lignin content of roots of pedunculate oak and wild cherry-tree plantlets during acclimation. *Biologia Plantarum*, 48 (4), pp. 481-489.
- Stankovic, B., Volkmann, D. and Sack, F.D., 1998. Autonomic straightening after gravitropic curvature of cress roots. *Plant Physiology*, 117, pp. 893-900.
- Sterling, J.D., Atmodjo, M.A., Inwood, S.E. et al., 2006. Functional identification of an *Arabidopsis* pectin biosynthetic homogalacturonosyltransferase. *PNAS* ,103(13), pp. 5236-5241.
- Stintzi, A. and Browse, J., 2000. The *Arabidopsis* male-sterile mutants, *opr3*, lacks the 12-oxophytodienoic acid reductases required for jasmonate synthesis. *Proceedings of*

the National Academy of Sciences of the United States of America, 97, pp.10625-10630.

Stotz, H.U., Pittendrigh, B.R., Kroymann, J. et al., 2000. Induced plant defence responses against chewing insects. Ethylene signalling reduces resistance of Arabidopsis against Egyptian cotton worm but not diamondback moth. *Plant Physiology*, 124, pp. 1007-1018.

Sutherland, J.B., 1992. Detoxification of polycyclic aromatic hydrocarbons by fungi. *Journal of Industrial Microbiology*, 9, pp.53-62.

Taguchi, G., Ubukata, T., Nozue, H. et al., 2010. Malonylation is a key reaction in the metabolism of xenobiotic phenolic glucosides in Arabidopsis and tobacco. *Plant Journal*, 63 (6), pp. 1031-1041.

Taiz, L. and Zeiger, E., 1998. *Plant Physiology*. 2nd ed. Massachusetts: Sinauer Associates.

Taiz, L. and Zeiger, E., 2002. *Plant physiology*. 3rd ed. Massachusetts: Sinauer Associates, p.306.

Taylor, V.F., March, R.E., Longerich, H.P., et al., 2005. A mass spectrometric study of glucose, sucrose, and fructose using an inductively coupled plasma and electrospray ionisation. *International Journal of Mass Spectrometry*, 243, pp. 71-84.

Thomas, J.M., Yordy, J.R., Amador, J.A., et al., 1986. Rates of dissolution and biodegradation of water-insoluble organic compounds. *Applied and Environmental Microbiology*, 52(2), pp. 290-296.

Trolldenier, G., 1988. Visualization of oxidizing power of rice roots and of possible participation of bacteria in iron deposition. *Z Pflanzenernahr Bodenkd*, 151, pp.117-121.

Troquet, J., Larroche, C., Dussap, CG., 2003. Evidence for the occurrence of an oxygen limitation during soil bioremediation by solid-state fermentation. *Biochemical Engineering Journal*, 13, pp.103-112.

Uren, N.C. and Reisenauer, H.M., 1988. The role of root exudates in nutrient acquisition. *Advanced Plant Nutrition*, 3, pp. 79-114.

U.S. Department of health & human services. [online] Available at: <<http://householdproducts.nlm.nih.gov/cgi-bin/household/brands?tbl=brands&id=3012004>> [Accessed 17 April 2010].

U.S. Department of Health and Human Services, 2005. Toxicological profile for naphthalene, 1-methylnaphthalene, and 2-methylnaphthalene. [pdf] Georgia: Agency for Toxic Substances and Disease Registry. Available at: <<http://www.atsdr.cdc.gov/toxprofiles/tp67.pdf>> [Accessed 16 April 2012]. USEPA, 1985

- US EPA, 1999. Phytoremediation Resource Guide. EPA 542-B-99-003. Office of solid waste and emergency response. Washington, D.C: EPA
- Vamerali, T., Bandiera, M., Mosca, G., 2010. Field crops for phytoremediation of metal-contaminated land. A review. *Environmental chemistry letters*, 8(1), pp. 1-17.
- VandenBosch, K.A., Bradley, D.J.I., Knox, J.P. et al., 1989. Common components of the infection thread matrix and the intercellular space identified by immunocytochemical analysis of pea nodules and uninfected roots. *The EMBO Journal*, 8(2), pp.335 – 342.
- Van den Ende, W. and Valluru, R., 2009. Sucrose, sucrosyl oligosaccharides, and oxidative stress: scavenging and salvaging? *Journal of Experimental Botany*, 60, pp. 9-18.
- Vandevivere, P. and Verstraete, W., 2001. Environmental applications. In: C. Ratledge, B. Kristiansen, Eds. *Basic biotechnology*. Second edition. Cambridge University Press. pp. 531-557.
- Vangronsveld, J., Colpaert, J., Van Tichelen, K., 1996. Reclamation of a bare industrial area contaminated by non-ferrous metals: physico-chemical and biological evaluation of the durability of soil treatment and revegetation. *Environ Pollution*, 94, pp. 131-140.
- Vangronsveld, J. and Cunningham, S.D., 1998. Introduction to the concepts. In: J. Vangronsveld, S.D.Cunningham, Eds. *Metal-contaminated soils: In-situ inactivation and phytoremediation*. Berlin Heidelberg: Springer Verlag, pp.1-15.
- Vangronsveld, J., Sterckx, J., Van Assche, F., et al., 1995b. Rehabilitation studies on an old non-ferrous waste dumping ground: effects of revegetation and metal immobilization by beringite. *Journal of Geochemical Exploration*, 52, pp. 221-229.
- Vangronsveld, J., Van Assche, F., Clijsters, H., 1995a. Reclamation of a bare industrial area contaminated by non ferrous metals-in situ metal immobilization and revegetation. *Environmental Pollution*, 87, pp. 51-59.
- Váňová, L., 2009. The use of in vitro cultures for effect assessment of persistent organic pollutants on plants. Ph.D. Masaryk University.
- Vazquez, M.D., Poschenrieder, C. and Barcelo, J., 1989. Pulvinus structure and leaf abscission in cadmium-treated bean plants (*Phaseolus vulgaris*). *Canadian Journal of Botany*, 67, pp.2756-2764.
- Verdin, A., Sahraoui, ALH., Fontaine, J., et al., 2006. Effects of anthracene on development of an arbuscular mycorrhizal fungus and contribution of the symbiotic association to pollutant dissipation. *Mycorrhiza*, 16(6), pp. 397-405.
- Walker, T.S., Bais, H.P., Halligan, K. M., et al., 2003. Metabolic profiling of root exudates of *Arabidopsis thaliana*. *Journal of Agricultural and Food Chemistry*,

51(9), pp. 2548-2554.

Wallace, T., 1943. The diagnosis of mineral deficiencies in plants by visual symptoms, [online] Available at: < (<http://www.hbci.com/~wenonah/min-def/index.html>). > [Accessed 12 August 2009].

Walton, B.T., Guthrie, E.A. and Holyman, A.M., 1994. Toxicant degradation in the rhizosphere. In: T.A. Anderson, J.R. Coats, Eds. Bioremediation through rhizosphere technology. Columbus, Ohio: American Chemical Society, pp. 11-26.

Watanabe, K., Futamata, H., Harayama, S., 2002. Understanding the diversity in catabolic potential of microorganisms for the development of bioremediation strategies. *Antonie Van Leeuwenhoek*, 81(1-4), pp. 655-663.

Watt, M., McCully, M.E., Canny, M.J., 1994. Formation and stabilization of rhizosheaths of *Zea mays* L.: effect of soil water content. *Plant Physiology*, 106, pp. 179-186.

Weaver, J.E., 1926. Root development of field crops. New York: McGraw Hill. [online] Available at: <<http://www.soilandhealth.org/01aglibrary/010139fieldcroproots/010139toc.html>.> [Accessed 23 February 2010].

Weber, A.P., Schwacke, R. and Flugge, U.I., 2005. Solute transporters of the plastid envelope membrane. *Annual Review of Plant Biology*, 56, pp. 133-164.

Weissenfels, W.D., Klewer, H.J. and Langhoff, J., 1992. Adsorption of polycyclic aromatic hydrocarbons (PAHs) by soil particles: influence on biodegradability and biotoxicity. *Applied Microbiology and Biotechnology*, 36, pp.689-696.

Wenzel, W.W., Adriano, D.C., Salt, D., et al., 1999. Phytoremediation: a plant-microbe-based remediation system. In: D.C. Adriano, J.M. Bollag, W.T. Frankenberger Jr., R.C. Sims, Eds. Bioremediation of contaminated soils. American society of agronomy, Crop science society of America, Soil science society of America, pp. 457-508.

Werck-Reichhart, D. and Feyereisen, R., 2000. Cytochrome P450-A success story. *Genome Biology*, 1(6), reviews:3003.1-3003.0

Wild, E., Dent, J., Thomas, G.O. and Jones, K.C., 2005. Direct observation of organic contaminant uptake, storage and metabolism within plant roots. *Environmental Science and Technology*, 39(10), pp. 3695-3702.

Wild, S.R. and Jones, K.C., 1995. Polynuclear aromatic hydrocarbons in the United Kingdom environment. A preliminary source inventory and budget. *Environmental Pollution*, 88 (1), pp.91-108.

- Wild, S.R. and Jones, K.C., 1992. Polynuclear aromatic hydrocarbons uptake by carrots grown in sludge-amended soil. *Journal of environmental quality*, 21, pp.2217-2225.
- Wild, S.R. and Jones, K.C., 1991. Studies on the polynuclear aromatic hydrocarbon content of carrots (*Daucus carota*). *Chemosphere*,23(2), pp.243-251.
- Wilkins, B.M., 1999. Light-and gravity-sensing guidance systems in plants. *Proceedings of the Royal Society London B*, pp.513-524.
- Wilson, S. and Jones, K., 1993. Bioremediation of soil contaminated with polynuclear aromatic hydrocarbons (PAHs): a review. *Environmental Pollution*, 81, pp. 229-249.
- Wu, G., Shao, H.B., Chu, L.Y., et al., 2007. Insights into molecular mechanisms of mutual effect between plants and the environment. A review. *Agronomy for Sustainable Development*, 27(1), pp. 69-78.
- Xing, W. Q., Luo, Y. M., Wu, L. H., et al., 2006. Spatial distribution of PAHs in a contaminated valley in Southeast China. *Environmental Geochemistry and Health*, 28, pp. 89–96.
- Xu, J.G. and Johnson, R.L., 1995. Root growth, microbial activity and phosphate activity in oil-contaminated, remediated and uncontaminated soils planted to barley and field pea. *Plant and soil*, 173, pp.3-10.
- Yanai, R.D., Fahey, T.J., and Miller, S.L., 1995. Efficiency of nutrient acquisition by fine roots and mycorrhizae. In: W.K.Smith, T.M.Hinckley, Eds. *Resource physiology of conifers: Acquisition, allocation and utilisation*. San Diego, CA: Academic Press, pp. 75-103.
- Young, I.M., 1995. Variation in moisture contents between bulk soil and the rhizosheath of *Triticum aestivum* L. cv. *New Phytologist*, 130, pp.135–139.
- Zacchi, L., Morris, I. and Harvey, P.J., 2000. Disordered ultrastructure in lignin-peroxidase-secreting hyphae of the white-rot fungus *Phanerochaete chrysosporium*. *Micobiology*, 146, pp. 759-765.
- Zeier, J., Goll, A., Yokoyama, M., et al., 1999. Structure and chemical composition of endodermal and rhizodermal/ hypodermal walls of several species. *Plant, Cell and Environment*, 22, pp. 271-279.
- Zeier, J. and Schreiber, L., 1998. Comparative investigation of primary and tertiary endodermal cell walls isolated from the roots of five monocotyledonous species: Chemical composition in relation to fine structure. *Planta* ,206, pp. 349-361.
- Zohair, A., Salim, A., Soyibo, A.A., et al., 2006. Residues of polycyclic aromatic hydrocarbons (PAHs), polychlorinated biphenyls (PCBs) and organochlorine pesticides in organically-farmed vegetables. *Chemosphere*, 63, pp. 541-553.

Appendix 1

Spectrum interpretation and identification of compounds

Note: Apart from methylated, 1 TMS indole acetic acid, the structures for the derivatised compounds are not shown here.

TMS derivative of further oxidised or glycosylated/ malonylated Naphthol (MW of Naphthol=144Da)



The high molecular weight ion peak (~m/z 500) in treated roots (Fig A1-1) may be due to further oxidation or glycosylation/ malonylation of naphthol. The presence of the peak at m/z 216 would be consistent with a trimethylsilylated (TMS) naphthol component, whilst the peak at m/z 143 would be consistent with loss of the TMS component from trimethylsilyl naphthol. The ion at m/z 144 may correspond to the molecular weight of naphthol. The base peak at m/z 142 could be due to loss of one H atom from the ion at m/z 143. Loss of HCO[•] from the ion at m/z 143 followed by loss of a H atom, would give rise to a peak at m/z 113. The unstable bond in the aliphatic branch and weakening of the bond in benzene ring of the ion at m/z 113 would lead to opening of benzene ring and further fragmentations and rearrangements, and might produce fragment ions at m/z 80, 70, 68, 55 and 43 due to losses of neutral C, H, saturated and unsaturated hydrocarbon chains (Fig. A1-1). However, whilst the possibility of naphthol cannot be ruled out, naphthol is very rapidly oxidised (Preis, 2010) and unlikely to be detected as free naphthol.

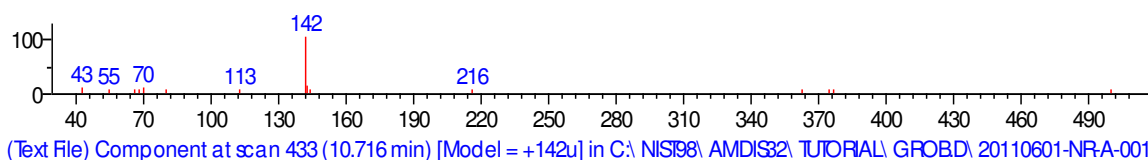
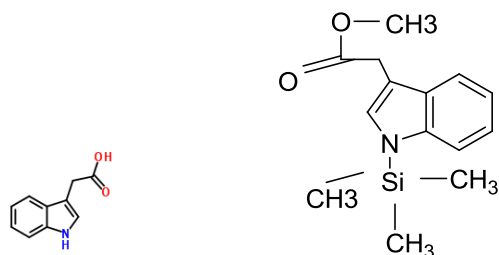


Fig. A1-1: The extracted mass spectrum for the compound tentatively identified as further oxidised or glycosylated/ malonylated naphthol (RT 10.72 min) from treated root extract

Methyl, TMS derivative of Indole acetic acid (IAA) (MW of IAA= 175Da)



The ion at m/z 216 would be consistent with the loss of 3 methyl groups from the molecular ion of methylated 1 TMS IAA (261Da). Loss of a methyl group (15Da) from methyl, 1 TMS IAA followed by loss of a H atom would give rise to an ion at m/z 245. The loss of another methyl group from the ion at m/z 245 would give rise to an ion peak at m/z 230. Each of these ion peaks is visible in the spectrum in Fig.A1-2. The fragment ions at m/z 73 $[(CH_3)_3Si]^+$ and m/z 75 $[(CH_3)_2Si-OH]^+$ reveal the presence of a hydroxyl group. An ion mass of 147 Da shows the molecule contains more than one $(CH_3)_3SiO$ -group. The presence of an acidic group is indicated by the fragment ion of medium-intensity at m/z 45. The weakly observed ion at m/z 173 would be consistent with the fragment ion which would result from elimination of $[(CH_3)_3Si]$ followed by NH^0 from the molecular derivative at m/z 261. The base peak at m/z 142 would be consistent with the loss of CH_3O^0 (31Da) from the ion at m/z 173. The presence of benzylum ion is indicated by the peak at m/z 77 (see Fig.A1-2).

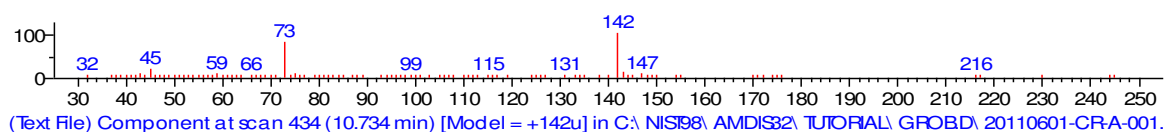
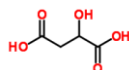


Fig. A1-2: The extracted mass spectrum for the compound tentatively identified as IAA (RT 10.73 min) from control root extract

TMS derivative of Malic acid (MW of malic acid= 134 Da)



The fragment ion at m/z 335 is due to the loss of CH_3 from the molecular ion at m/z

350 (not observed). The ion at m/z 261 is due to the loss of $[(CH_3)_3Si]$. The fragment ion at m/z 232 is due to the loss of $[(CH_3)_3SiOC=OH]$ from the molecular ion and m/z 245 is due to the loss of $(CH_3)_3SiOH$ from m/z 335. The fragment ions at m/z 73 $[(CH_3)_3Si]^+$ and m/z 75 $[(CH_3)_2Si-OH]^+$ reveal the presence of a hydroxyl group. An ion at m/z 147 is due to cleavage between the CH_2 and the $CHOH$ to form the ion $[(CH_3)_3SiOC=OCHOH]$. The presence of acidic group is indicated by the fragment ion at m/z 45 (medium-intensity fragment). The loss of 18 Da (H_2O molecule) from the ion at m/z 134 (molecular ion of malic acid), is indicated by the peak at m/z 116 and is derived from the fragmentation process specific for an alcohol. The 116 Da ion due to a rearrangement reaction in the ion source produces the fragment ion at m/z 117. This ion loses 18 Da (H_2O molecule), and yields the fragment ion at m/z 99 which splits up to form a $COOH$ ion at m/z 45 and propenone ion at m/z 56. The spectrum shows intensive fragmentation due to aliphatic nature of the molecule (see Fig. A1-3).

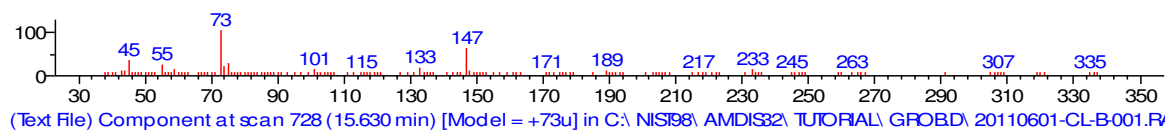
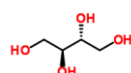


Fig. A1-3: The extracted mass spectrum for the compound identified as malic acid (RT 15.63 min) from control shoot extract.

TMS derivative of Erythritol (MW of erythritol= 122 Da)



The fragment ions at m/z 73 $[(CH_3)_3Si]^+$ and m/z 75 $[(CH_3)_2Si-OH]^+$ reveal the presence of a hydroxyl group. An ion at m/z 147 is due to cleavage between the $CHOH$ and the $CHOH$ to form the ion $[(CH_3)_3SiOC=OCHOH]$. The fragmentation resulting from elimination of $[(CH_3)_3Si]$ groups is weakly observed at m/z 118. An ion at m/z 119 due to a rearrangement reaction in the ion source is observed, but the molecular ion at m/z 122 is not observed. The ion at m/z 118 loses 31 Da (CH_3O^0) to produce the fragment ion at m/z 87. The fragment ion at m/z 87 loses 18 Da (H_2O molecule) to form the ion at m/z 69. The ion at m/z 119 loses 31 Da (CH_3O^0)

followed by 18 Da (H₂O molecule) to form the weak ion at m/z 70 (see Fig. A1-4).

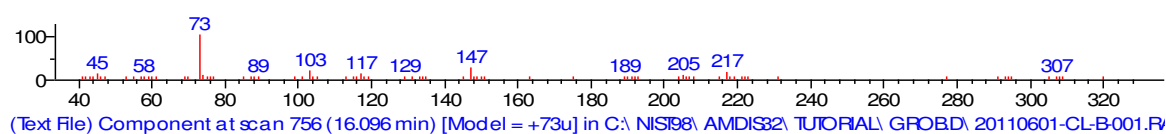
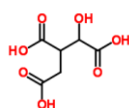


Fig. A1-4: The extracted mass spectrum for the compound identified as erythritol (RT 16.10 min) from control shoot extract

TMS derivative of Isocitric acid (MW of isocitric acid= 192 Da)



The fragment ions at m/z 73 [(CH₃)₃Si]⁺ and m/z 75 [(CH₃)₂Si-OH]⁺ reveal the presence of a hydroxyl group. An ion at m/z 147 is due to cleavage between the CHOH and the CHOH to form the ion [(CH₃)₃SiOC=OCHOH]. The presence of acidic group is indicated by the medium-intensity fragment, appearing at m/z 45. The loss of 18 Da (H₂O molecule) from the molecular ion at m/z 192, is indicated by the high-intensity fragment, appearing at m/z 174 and is derived from the fragmentation process specific for an alcohol. McLafferty rearrangement creates a loss of 55 Da (C⁺OHC=CH₂) from the ion at m/z 174, and is observed in the spectrum. The spectrum shows intensive fragmentation due to many patterns of fragmentations (see Fig. A1-5).

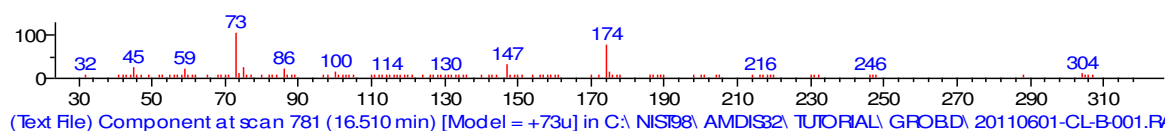
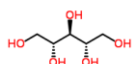


Fig. A1-5: The extracted mass spectrum for the compound identified as isocitric acid (RT 16.51 min) from control shoot extract

TMS derivative of Ribitol (MW of ribitol= 152 Da)



The fragment ions at m/z 73 $[(\text{CH}_3)_3\text{Si}]^+$ and m/z 75 $[(\text{CH}_3)_2\text{Si-OH}]^+$ reveal the presence of a hydroxyl group. An ion at m/z 147 is due to cleavage between the CHOH and the CHOH to form the ion $[(\text{CH}_3)_3\text{SiOC=OCHOH}]$. The ions formed due to recombination with H^+ ions in the ion source are observed at m/z 148, 149 and 150, but the underivatised molecular ion at m/z 152 is not observed. The ion at m/z 205 is due to $[\text{OTMSCH}_2\text{CHOTMS}]^+$ (see Fig. A1-6).

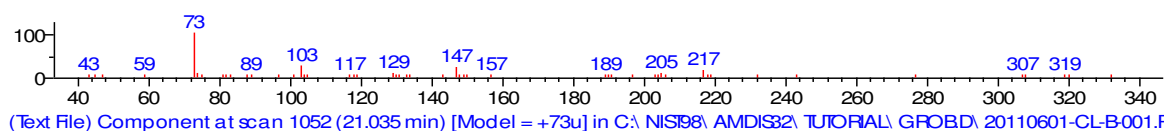
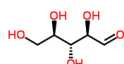


Fig. A1-6: The extracted mass spectrum for the internal standard, ribitol (RT 21.04 min) extracted together with control shoots

Methyloxime-, TMS derivative of Ribose (MW of ribose=150 Da)



The fragment ions at m/z 73 $[(\text{CH}_3)_3\text{Si}]^+$ and m/z 75 $[(\text{CH}_3)_2\text{Si-OH}]^+$ reveal the presence of a hydroxyl group. An ion at m/z 147 is due to cleavage between the CHOH and the CHOH to form the ion $[(\text{CH}_3)_3\text{SiOC=OCHOH}]$. The fragmentation resulting from elimination of $[(\text{CH}_3)_3\text{Si}]$ and $[\text{CH}_3\text{O}]$ groups is detected at m/z 144. The ions formed due to re-protonation and rearrangement are observed at m/z 147, 148, 149 and 150 (original underivatised molecular ion). The ion at m/z 149 loses 18 Da (H_2O molecule), and produces a fragment ion at m/z 131, whilst the molecular ion at m/z 150 loses 31 Da (CH_3O) to produce a fragment ion at m/z 119. The ion at m/z 119 loses 18 Da (H_2O molecule) and produces an ion at m/z 101, which consecutively loses 31 Da (CH_3O) to produce a fragment at m/z 70 (see Fig.A1-7).

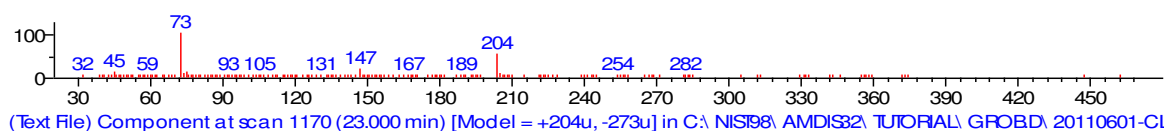
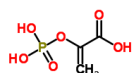


Fig. A1-7: The extracted mass spectrum for the compound identified as ribose (RT 23.00 min) from control shoot extract

TMS derivative of Phosphoenolpyruvic acid (MW of phosphoenolpyruvic acid=168 Da)



The fragment ions at m/z 73 $[(CH_3)_3Si]^+$ and m/z 75 $[(CH_3)_2Si-OH]^+$ reveal the presence of a hydroxyl group. An ion at m/z 147 is due to cleavage between the $CHOH$ and the $CHOH$ to form the ion $[(CH_3)_3SiOC=OCHOH]$. The ion at m/z 255 arises from the phosphate end of the molecule and is due to $[(CH_3)_3SiO]_2P=OOCH_2^+$. The spectrum shows intense fragmentation due to the aliphatic nature of the compound (see Fig. A1-8).

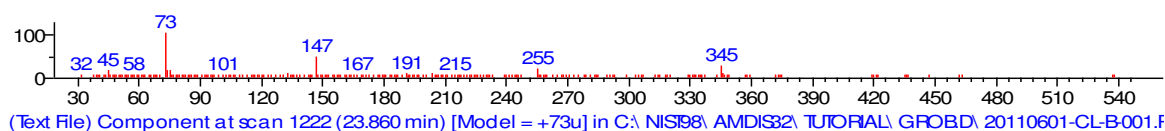
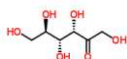


Fig. A1-8: The extracted mass spectrum for the compound identified as phosphoenolpyruvic acid (RT 23.86 min) from control shoot extracts

Methyloxime-, TMS derivative of Fructose (MW of fructose=180 Da)



An ion at m/z 147 is due to cleavage between the $CHOH$ and the $CHOH$ to form the ion $[(CH_3)_3SiOC=OCHOH]$. The ions formed due proton transfer and rearrangements are observed at m/z 174, 176, 177, 178, 179 and 180 (original underivatised molecular ion of fructose; only weakly observed). The ion at m/z 179 loses 18 Da (H_2O molecule) and forms the fragment ion at m/z 161, which consecutively loses 30 Da

(CH₂O) to produce a fragment ion at m/z 131. The ion at m/z 131 loses 30 Da (CH₂O) which loses 31 Da (CH₃O), yielding successively the ions at m/z 101 and m/z 70. The 101Da ion recombines with 2 H atoms and produces a fragment ion at m/z 103 (most abundant ion). The fragment ion at m/z 161 also loses 2 H₂O molecules and one H atom and produces an ion at m/z 124. This 5-membered ring species undergoes ring cleavage and loses 18 Da (H₂O molecule) to form the primary alcohol at m/z 106. The ion at m/z 179 also loses 30 Da (CH₂O) and produces an ion at m/z 149 which consecutively loses 30 Da (CH₂O) and produces an ion at m/z 119. The ion at m/z 119 loses 30 Da (CH₂O) and produces a fragment ion at m/z 89. The ion at m/z 89 loses 2 H atoms and produces the m/z 87 fragment. The ion at m/z 179 loses 2 H₂O molecules to produce an ion at m/z 143 which in turn loses CH₂O and produces an ion at m/z 113. The spectrum shows intense fragmentation mainly due to neutral losses of H₂O and CH₂O (Fig. A1-9).

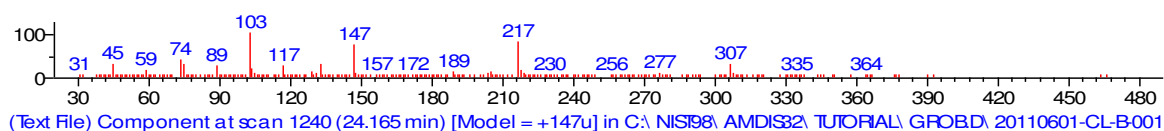
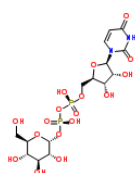


Fig. A1-9: The extracted mass spectrum for the compound identified as fructose (RT 24.17 min) from control shoot extract

Methyloxime-, TMS derivative of UDP-glucose (MW of UDP-glucose=566 Da)



The fragment ion appearing at m/z 292 (ribose sugar + 2 phosphate groups) loses 30 Da (CH₂O) and forms a fragment ion at m/z 262. The fragment ion at m/z 111 indicates the scission of the bond cleavage to release uracil. The ions at m/z 133 (after recombination with an H⁺ ion in the ion source), 144 and 179 show the bond cleavages to release ribose, phosphate groups and glucose. The molecular ion of glucose at m/z 180 is weakly observed. The glucose ion at m/z 180 loses 31 Da (CH₃O) and produces an ion at m/z 149. The uracil ion at m/z 111 loses 17 Da (NH₃) and forms the ion at m/z 94. The bi-phosphate group fragments to produce the ions at

m/z 80 as well as m/z 96 (see Fig. A1-10).

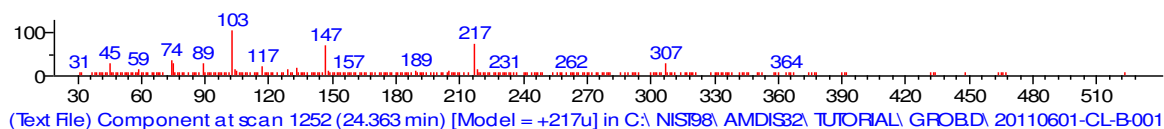
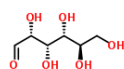


Fig. A1-10: The extracted mass spectrum for the compound identified as UDP-glucose (RT 24.36 min) from control shoot extract

Methyloxime-, TMS derivative of Glucose (MW of glucose =180Da)



The fragment ions at m/z 73 $[(\text{CH}_3)_3\text{Si}]^+$ and m/z 75 $[(\text{CH}_3)_2\text{Si-OH}]^+$ reveal the presence of a hydroxyl group. An ion at m/z 147 is due to cleavage between the CHOH and the CHOH to form the ion $[(\text{CH}_3)_3\text{SiOC=OCHOH}]$. The ion at m/z 178 loses 18 Da (H_2O molecule) and forms the fragment ion at m/z 160, which is of medium intensity. The ion at m/z 179 loses 18 Da (H_2O molecule) and forms the fragment ion at m/z 161, which consecutively loses another H_2O molecule and produces the ion at m/z 143. The ion at m/z 143 loses 30 Da (CH_2O) to produce a fragment ion at m/z 113. The ion at m/z 179 also loses 30 Da (CH_2O) and produces an ion at m/z 149. The ion at m/z 149 loses 30 Da (CH_2O) to produce an ion at m/z 119 or loses 18 Da (H_2O molecule) and forms an ion at m/z 131 (Fig.A1-11).

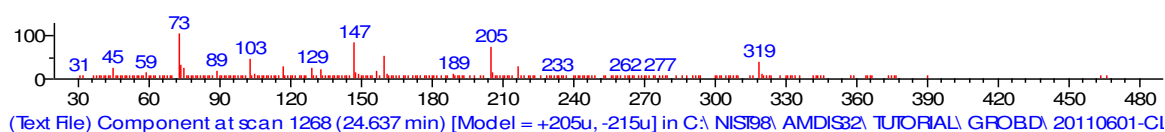
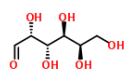


Fig. A1-11: The extracted mass spectrum for the compound identified as glucose (RT 24.64 min) from control shoot extract

Methyloxime-, TMS derivative of Galactose (MW of galactose=180)



The fragment ions at m/z 73 $[(\text{CH}_3)_3\text{Si}]^+$ and m/z 75 $[(\text{CH}_3)_2\text{Si-OH}]^+$ reveal the

presence of a hydroxyl group. An ion at m/z 147 is due to cleavage between the CHOH and the CHOH to form the ion $[(CH_3)_3SiOC=OCHOH]$. (see Fig. A1-12). Fragmentation patterns are similar to that of glucose.

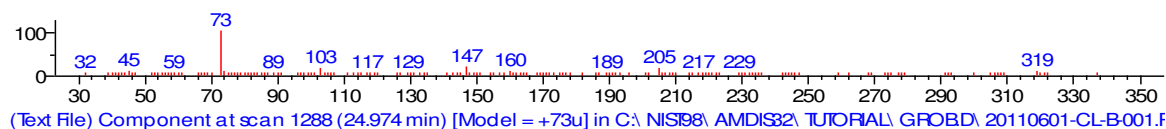
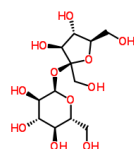


Fig. A1-12: The extracted mass spectrum for the compound identified as galactose (RT 24.97 min) from control shoot extract

TMS derivative of Sucrose (MW of sucrose=342)



The fragment ions at m/z 73 $[(CH_3)_3Si]^+$ and m/z 75 $[(CH_3)_2Si-OH]^+$ reveal the presence of a hydroxyl group. An ion at m/z 147 is due to cleavage between the CHOH and the CHOH to form the ion $[(CH_3)_3SiOC=OCHOH]$. The ion at m/z 437 is due to cleavage between the two silylated rings. The fragment ions at m/z 275, 245, 227, 209 and 191 are produced from the neutral losses of H_2O and CH_2O . The ions at m/z 119, 131, 143 and 149, which are also present in the product ion mass spectrum of glucose and fructose, are formed by neutral losses of H_2O and CH_2O (Fig. A1-13).

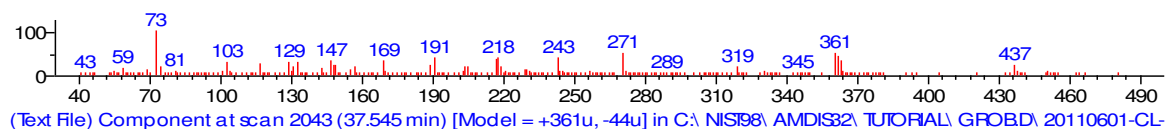
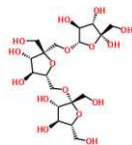


Fig. A1-13: The extracted mass spectrum for the compound identified as sucrose (RT 37.56 min) from control shoot extract

TMS derivative of Fructan (MW of fructan= 341; >341 when >2 fructose units are attached)



The fragment ions at m/z 73 $[(CH_3)_3Si]^+$ and m/z 75 $[(CH_3)_2Si-OH]^+$ reveal the presence of a hydroxyl group. An ion at m/z 147 is due to cleavage between the CHOH and the CHOH to form the ion $[(CH_3)_3SiOC=OCHOH]$. The medium-intensity fragments appearing at m/z 361, 362 and 363, and the ion observed at m/z 334 (related to molecular ion) indicate the molecule has more than one hexose unit. The ion at m/z 306 indicates loss of 2 H_2O molecules (from the disaccharide unit at m/z 342). The ion at m/z 306 loses 2 CH_2O molecules and forms an ion at m/z 246 which consecutively loses another CH_2O and recombines with an H atom to form a fragment ion at m/z 217. This 217 Th ion loses a H_2O molecule and forms a fragment at m/z 199. The fragment ions at m/z 149, 143, 131, 105, 103, 101, 89 and 71 which are present in the product ion mass spectrum of fructose indicate the molecule is fructan, and are formed by neutral losses of H_2O , CH_2O and H (see Fig. A1-14).

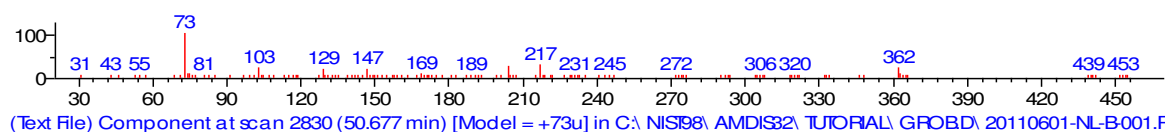
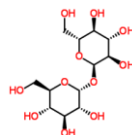


Fig. A1-14: The extracted mass spectrum for the compound identified as fructan (RT 50.68 min) from treated shoot extract

TMS derivative of Trehalose (MW of trehalose=342)



The fragmentation patterns are similar to that of sucrose, but exhibit less intensity. The fragment ions at m/z 179 and 161 indicate scission of the glycoside bond to form two $[glucose-H]^+$ and two $[glucose-H_3O]^+$. The ions at m/z 119, 131, 143 and 149, which are also present in the product ion mass spectrum of glucose, are formed by neutral losses of H_2O and CH_2O (see Fig. A1-15).

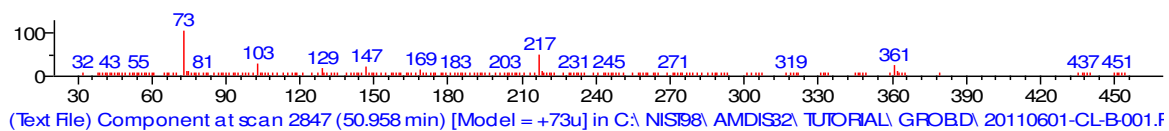


Fig. A1-15: The extracted mass spectrum for the compound identified as trehalose (RT 50.96 min) from control shoot extract

Appendix 2

Entry of xenobiotics into xylem vessels of plant roots exemplified by Nile red penetration

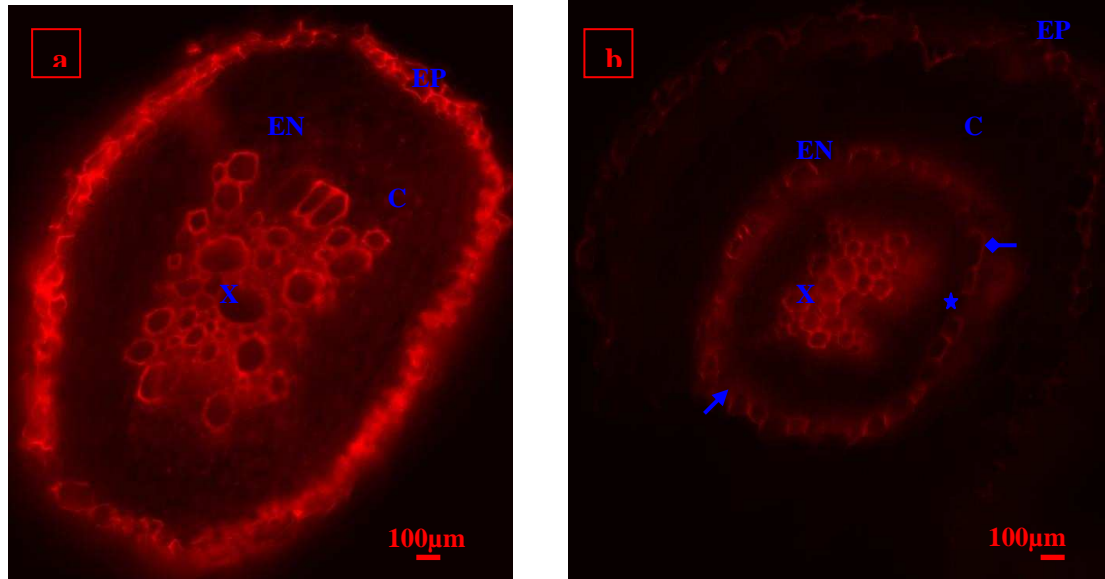


Fig. A2-1: Epi-fluorescent micrographs of transversal sections of 3 months old carrot (*Daucus carota*) roots stained with Nile red and viewed through Texas red HYQ filter cube (excitation at 589 nm; emission at 615 nm). a: The plant was grown in clean sand b: The plant was grown in fluoranthene-treated sand (1 g kg^{-1} sand dw). Arrow shows Casparian band. Diamond arrow shows suberin lamella. Star indicates passage cell. C: cortex; EN: endodermis; EP: epidermis; X: xylem vessels. Scale: $400\mu\text{m}$. A clear banding of Casparian strip and suberin lamellae was observed in the endodermis of fluoranthene-treated roots, but the root also possessed passage cells (indicated by star symbol). Nile red penetration into xylem vessels was observed in both control and fluoranthene-treated roots. Nile red uptake into xylem vessels was also observed in the roots of carrot grown in phenanthrene/ pyrene (1 g kg^{-1} sand dw)-treated sand.

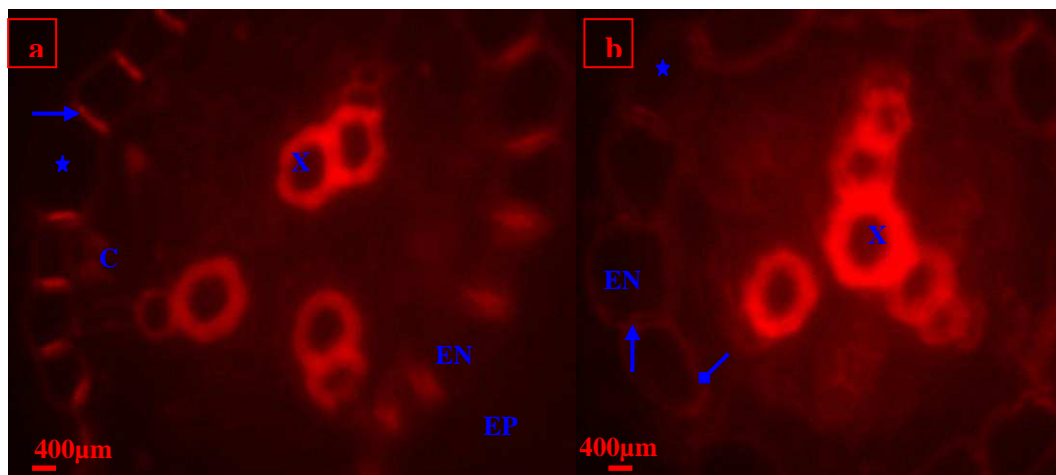


Fig. A2-2: Epi-fluorescent micrographs of transversal sections of 3 months old white clover (*Trifolium repens*) roots stained with Nile red and viewed through Texas red HYQ filter cube (excitation at 589 nm; emission at 615 nm). a: The plant was grown in clean sand b: The plant was grown in naphthalene-treated sand (0.8g kg^{-1} sand dw). Arrow shows Casparian band. Diamond arrow shows suberin lamella. Star indicates passage cell. EN: endodermis; X: xylem vessels. Scale: $400\mu\text{m}$. A clear banding of Casparian strip was observed in the endodermis of the control roots. Both Casparian strip and suberin lamellae were observed in the endodermis of naphthalene-treated roots, but the root also possessed passage cells (indicated by star symbol). Nile red penetration into xylem vessels was observed in both control and naphthalene-treated roots.

Appendix 3

Quantification of naphthalene in the root, shoot tissues of tall fescue (*Festuca arundinacea*) grown in naphthalene-treated sand (0.8g kg^{-1} sand dw) for 6 months using GC-FID technique

Table A3-1: Concentration of naphthalene detected in plant tissues grown in naphthalene-treated sand (0.8g kg^{-1} sand dw) for 6 months

Plant tissue	Naphthalene ($\mu\text{g g}^{-1}$ tissue fw) Mean (\pm SE)	No. of replicates of plant samples	No. of pooled extracts run on GC
Root tissue	0.022(\pm 0.002)	6	3
Shoot tissue	0.006 (\pm 0.005)	6	3

No. of GC runs: 2; SE = standard error of the mean